Production and characterization of alkaliphilic amylases from *Bacillus halodurans* Alk36

By

Latifa Mbwana Mrisho

MSc Thesis

Centre of Bioprocess Engineering Research

Department of Chemical Engineering

September, 2015.

Acknowledgements

I would like to express appreciation to the people who have contributed to the success of this project.

To my supervisors, Prof Sue Harrison and Dr. Caryn Fenner, thank you for giving me the opportunity to work with you. I am grateful for the encouragement, guidance, support and patience that you have showed me throughout this program.

The CeBER family, I am fortunate that I got to know and work with some of you. Thank you all for the support and assistance that you have given me, as well as the good times that we have shared.

Mrs. Sue Jobson and Miss Candice Mazzolini, for the administrative assistance and organisation of events that allowed us to get to know each other. Mrs. Fran Pocock (the former CeBER laboratory manager), Miss Sharon Rademeyer and Mr. Emmanuel Ngoma, thank you for making sure the laboratory operates smoothly and going out of your way to help with the experiments. Dr. Madelyn Johnstone-Roberston and Dr. Rob Huddy, for the valuable inputs and advice. Dr. Brandon Weber and Prof. Trevor Sewell, of the Structural Biology Unit, for the assistance in protein purification, guidance and all your valuable input.

Dr. Michael Crampton of the CSIR, for the donation of the *B. halodurans* strain investigated in this project. I am grateful for the funding and financial support provided by the National Research Foundation (NRF) and the Center of Bioprocess Engineering Research (CeBER).

To my friends, too many to mention, thank you for the support, encouragement and for being there, to listen, laugh and explore with me. You have helped me grow and evolve. To my family, even though you are all far away, thank you for all the love and support. My parents, Mr. Vincent Mrisho and Dr. Fatma Mrisho, thank you for giving me the freedom of choice, the guidance, support and unconditional love.

Last but not least, I thank God, for giving me the strength, patience and wisdom that has guided me through this project.

Declaration

I, **Latifa Mbwana Mrisho,** hereby declare that the work on which this thesis is based is my original work (except where acknowledgements indicate otherwise) and that neither the whole work nor any part of it has been, is being, or is to be submitted for another degree in this or any other university. I authorise the University to reproduce for the purpose of research either the whole or any portion of the contents in any manner whatsoever.

Signed by candidate

Signature Removed

Date: 30/09/2015

Abstract

Amylases are hydrolytic enzymes that cause the breakdown of starch and related polysaccharides to simple sugars. Amylases are applied in brewing, food, detergent and textile industries. Most commercial amylases are derived from fungi or bacteria. Bacterial amylases are desired for commercial use, due to their thermo-stability and faster production rates. Bacteria of the genus, *Bacillus*, are considered to be a good source of extracellular proteins because they have high growth rates and have a naturally high capacity for secretion of extracellular proteins.

Bacillus halodurans Alk36 is an alkaliphilic, thermotolerant isolate that can grow over a wide pH and temperature range. Preliminary studies have shown that *B. halodurans* Alk36 can grown in EnBase® medium (at pH 8.5) containing starch as the carbon source, without the addition of a commercial amylase. The ability to grow on starch, in the absence of an external amylase, indicated that this strain produces endogenous alkaliphilic amylases, which may be exploited for a number of industrial applications. In the present study, the physiological and biochemical characterisation of *B. halodurans* Alk36 and its endogenous amylases were investigated.

Growth of *B. halodurans* Alk36 in EnBase® medium lead to an improved biomass and amylase production compared to growth in complex LB medium. Amylase production was observed throughout growth but the maximum activity was obtained during the early stationary phase. Six potential amylases were obtained from the culture supernatant based on starch-zymography. Of the six potential amylases, two amylases were identified by Peptide Mass Fingerprinting as an alpha- amylase G-6 (105 kDa) and a polysugar-degrading enzyme (37 kDa). According to the starch zymographs of the culture supernatant, most of the observed activity was due to the alpha amylase G-6. Based on the difference in the amylase activities obtained by the DNS and the starch-iodine assays, it was predicted that the alpha amylase G-6 was an endo-acting amylase.

The specific amylase activity of the culture supernatant at early stationary phase was 61 U/mg protein, where 1 U of activity is equivalent to 1 mg of starch hydrolysed per minute, under assay conditions. The specific amylase activity obtained by the DNS assay (61 U/mg protein) was higher than that of other alkaliphilic amylases found in literature. However, the

amount of reducing sugars released from starch hydrolysis (0.5 g/L) was lower than that expected (10 g/L). The observed low concentration of reducing sugars suggested that the amylases from *B. halodurans* Alk36 were endo-acting, which usually produce reducing sugars at a lower rate than the rate the amylases hydrolyse starch. Alternatively, the products of starch hydrolysis by amylases from *B. halodurans* Alk36 could have been non-reducing sugars. Hence, it was recommended that the mode of action, as well as the types of products released form starch hydrolysis by the amylases from *B. halodurans* Alk36 should be determined in future work

Bacillus halodurans Alk36 grew optimally at pH 7 - 8.5 and temperature of 45˚C - 50 °C, with maltose as the carbon source. The specific amylase activity under these conditions (158 U/mg protein) was increased by 2.5-folds, compared to the cultures grown at 30˚C using dextrin as the carbon source. The optimal pH and temperature for growth of *B. halodurans* Alk36 was similar to the pH and temperature of the optimal amylase activity, i.e. 8.5 and 50˚C. The amylase was active at the pH range between 7 - 10 and temperature range between 30 - 60˚C. Hence, *B. halodurans* Alk36 was thought to produce moderate alkaline amylases, which may not be effective in detergent formulations at pH above 8.5. Since detergent formulations contain oxidizing agents, it was suggested that further studies should be done to determine the activity and stability of *B. halodurans* Alk36 amylases in presence oxidizing agents used in detergent formulations, to describe effective activity of the amylases under these conditions.

Amylase recovery and purification achieved by ammonium-sulphate precipitation followed by liquid chromatography using anion exchange, hydrophobic interaction and size-exclusion separation techniques, resulted in poor recovery. Poor recoveries were thought to be due to protein denaturation and interference of amylase activity caused by Tris molecules present in the buffer used for chromatography i.e. Tris/HCl buffer. Hence, it was recommended that further investigations should be done to establish a purification method for effective separation and purification of the six proteins that showed amylolytic activity on the starch-zymographs in future work. This would enable identification of the 4 protein bands that could not be identified by Peptide Mass Fingerprinting and determination of the activity of the individual amylases.

Table of Contents

List of Tables

List of Figures

Nomenclature

C_L	Oxygen concentration in the liquid (mMols/L)
C_{Sat}	Saturation oxygen concentration in the liquid (mMols/L)
C_x	Concentration of biomass (g/L)
C_0	Oxygen concentration at t=0 (mMols/L)
t_0	Time at inoculation
D_A	Diffusivity of gas in the at the gas-liquid interface layer
F_{O2}	Mole flow rates of oxygen
k_La	volumetric mass transfer coefficient
Lo_2	Henry's law constant for solubility of oxygen at a given temperature and pressure.
pO_2	Partial pressure of oxygen
Q_{O2}	Specific oxygen utilisation rate coefficient
V_L	Volume of liquid
V_s	Gas superficial velocity.
v^f	Volumetric flow rate
vvm	Volume of air per volume of medium per minute
w/v	Weight per volume
Ho_2	Henry's law constant representing solubility of oxygen at a given temperature and Pressure
I	Elemental iodine
S	Elemental sulphur
O	Elemental oxygen

Symbols

μ	Specific microbial growth rate h^{-1}
μ_{max}	Maximum specific microbial growth rate h^{-1}
δ	Thickness of the gas-interface layer

Abbreviations

AZCL	Azo-colour cross-linked amylose
BSA	Bovine serum albumin
BPNPG7	Blocked *p*-nitrophenolmaltoheptaose
DO	Dissolved oxygen
DNS	Dinitrosalicylic acid assay
HPLC	High pressure liquid chromatography
LB	Luria broth
PAGE	Polyacrylamide gel electrophoresis
PMF	Peptide mass fingerprinting
PNP	Para-nitrophenol
PNPG5	P*ara*-nitrophenolmaltopentaose
OTR	Oxygen transfer rate
OUR	Oxygen utilisation rate
SDS	Sodium dodecyl sulphate

Chapter One

Introduction

1.1 Scope

Industrial biotechnology used living cells or cell components such as enzymes in production of starch-based food materials, beverages, fine chemicals, antimicrobials, biodegradable plastics, as well as in the biomass refinery, waste-water treatment, biofuel production and biomining.

Enzymes are biological catalysts i.e. they reduce the activation energy of metabolic reactions, speeding them up. Most enzymes are proteins with a complex structure; they are highly specific with respect to the reactions they catalyse and the molecules used as substrates for these reactions (Horton et al., 1993).

The use of living cells or enzymes in industrial processes has potential for modifying industrial processes to reduce environmental impact through green chemistry, as well as enabling discovery of new products. Due to the highly selective nature of enzymes, the use of enzymes in bioprocesses allows for reduction of the number of production processes and by-product formation. Moreover, enzymes are biodegradable and require mild reaction conditions (moderate temperatures, atmospheric pressure and an aqueous environment). Hence, enzymes can be used to replace toxic organic solvents and hazardous reagents in bioprocesses (Rozell, 1999; Alcalde et al., 2006; Woodley, 2008).

The application of enzymes in industrial processes was practiced long before the nature and function of enzymes were understood. For instance, the use of barley malt in brewing and application of dung in leather making (Underkofler et al., 1958). Once the enzymes responsible for the desired biochemical reaction were known, methods for production of the enzymes were established (Underkofler et al., 1958). Ongoing research seeks better sources and less expensive methods for the production of different enzymes, along with expanded operating regions for the bioconversions.

According to the 'bcc research market forecasting', the global market for industrial enzymes was estimated to be $ 3.9 billion in 2011 and is expected to rise to $ 6 billion in 2016 (bcc Research Market Forecasting - March, 2012). A large percentage of the market for industrial enzymes is in the production of foods and beverages, followed by enzymes used in technical processes, such as in detergent formulations, textile and paper production, in addition to fuel production (bcc Research Market Forecasting - March, 2012). Hydrolytic enzymes such as proteases, amylases and cellulases form the majority of industrial enzymes currently used (Kirk et al., 2002). Proteases are protein-degrading enzymes, while amylases are starch-degrading enzymes and cellulases are enzymes that degrade cellulose (polysaccharide found in the cell-wall of green plants, most algae and some other eukaryotes (Duedahl-Olesen et al., 2000)).

The hydrolytic enzymes have replaced the use of chemicals such as phosphates, acids, alkali and emulsifiers in detergent formulations, and in the food, beverages, textile, and paper industries (Kirk et al., 2002). The largest demand (in volume and value) of hydrolytic enzymes is in detergent formulations. Here enzymes are used to improve the performance of detergents; hence, identification of new and improved enzymes is of high significance (Kirk et al., 2002).

Enzymatic detergent formulations are more cost effective, since they can facilitate effective washing at low temperatures, saving energy (Kirk et al., 2002; Sarethy et al., 2011). However, the enzymes used in detergent formulations must remain stable in alkaline environments and tolerate the oxidizing agents (such as surfactants, bleaches and chelants) present in most detergent formulations (Sarethy et al., 2011; Souza, 2010). For removal of starch-based dirt, alkaline amylases are usually used in detergent formulations, because they retain activity at high pH (pH 8 to 11) (Chaplin & Bucke, 1990). However, the majority of alkaline amylases identified so far (e.g. glucoamylases, α-glucosidases , β-amylases and maltohydrolases) are exo-acting and therefore, are used in combination with endo-acting and debranching amylases (e.g. pullulanases), for effective removal of stains (Sarethy et al., 2011).

Commercial enzymes that are currently used in detergent formulations have originated from *Bacillus* and *Aspergillus* species, i.e. BAN and Fungamyl, respectively

(Novozymes). The optimal pH range for the activity of these enzymes is pH 4 to 7 for Fungamyl, and pH 5 to 8 for BAN, as illustrated in Table 1.1 (Aehle, 2008).

Table 1.1: Commercial amylases from Novozymes (adapted from Aehle, 2008)

Product name	Microorganism	pH range	Temperature range (˚C)
Amyloglucosidase	*Aspergillus niger*	2 – 7	25- 70
Fungamyl	*Aspergillus oryzae*	4 – 7	15 – 60
BAN	*Bacillus amyloliquefaciens*	5.5 – 6.0	70 – 90
Termamyl	*Bacillus licheniformis*^{GM}	6 – 11	25 – 100
Duramyl	*Bacillus* species^{GM}	6 – 10	25 – 100
Natalase	*Bacillus* species^{GM}	5 – 10	25 – 100

GM – Genetically modified strain

Developments in molecular biology techniques (through screening and rational protein engineering) have led to the identification and development of novel enzymes with enhanced activity and stability in detergent formulations (Cherry & Fidantsef, 2003; Kirk et al., 2002). For instance, genetic modification of *Bacillus* species have resulted in amylases with increased resistance towards bleach (Duramyl) and oxidative stability, plus increased pH and temperature ranges (Termamyl and Natalase) as illustrated in Table 1.1 (Lin et al., 200; Aehle, 2008). Researchers have isolated an alpha-amylase with high stability in the presence of chelating reagents and chemical oxidants from the alkaliphilic Bacillus, as well as a cold-active detergent-stable extracellular alpha-amylase from *Bacillus cereus* (Hagihara et al., 2001; Roohi et al., 2013).

This thesis focuses on the production and characterization of naturally-occurring alkaliphilic amylases from an alkaliphilic bacterium, *Bacillus halodurans* Alk36. The investigation was done to determine the types of amylases produced by *B. halodurans* Alk36 and the potential use of the amylases in industrial processes, including detergent formulation, as well as in bioprocesses involving the use of EnBase® media, which requires an amylase for controlled release of glucose from a polysaccharide polymer (Krause et al., 2010).

1.2 Thesis structure

In Chapter 2, relevant literature pertaining to industrial production of alkaliphilic alpha-amylases is presented. A general background on amylases, their function and application, together with the known sources of amylases is discussed. The methods reported for determination of amylase activity and the factors to consider when developing a production process for alkaliphilic amylases are discussed. The latter includes the growth conditions (pH and temperature), mixing and mass transfer in agitated and shaken bioreactors, along with the methods for the determination of oxygen transfer rates and the volumetric mass transfer coefficient. Furthermore, the modes of operation of the bioreactors and the criteria for scaling-up small scale studies are also discussed. The chapter concludes by stating the rationale and objectives of the study as well as describing the research approach.

Description of the experimental apparatus and the materials and methods used in this study are presented in Chapter 3 as are all analytical methods.

In Chapter 4, the growth profiles of *B. halodurans* Alk36 cultivated in stirred tank bioreactors containing complex LB medium compared to EnBase® medium is presented. The carbon utilisation and biomass yields in the two media are compared. Factors associated with entry into stationary phase for cultures grown in EnBase® medium are also discussed. Moreover, the relationship between amylase production and growth of *B. halodurans* Alk36 in EnBase® medium is determined. The types of amylases obtained from *B. halodurans* Alk36 and their mode of action are discussed. Lastly, the amylase activity obtained from *B. halodurans* Alk36 is compared to that of amylases from other alkaliphilic bacteria as described in literature.

The conditions required for optimal growth and amylase production by *B. halodurans* Alk36 are discussed in Chapter 5. This included the characterisation of the reaction vessels used for the optimisation studies, in terms of the oxygen transfer rates (OTR) and the volumetric mass transfer coefficient (k_La). Thereafter, the effect of pH, temperature and carbon sources, on growth and amylase production, is examined.

The partial purification of amylases from *B. halodurans* Alk36 culture supernatant is detailed in Chapter 6. Partial purification and concentration of the amylases by ammonium sulphate precipitation and activated charcoal fractionation was investigated. Moreover, further amylase purification to separate the amylases from each other by liquid chromatography is also discussed. The chapter ends by examining the characteristics of the partially purified amylase solution, in terms of pH and temperature optima.

In Chapter 8, the conclusions and recommendations for future work are presented.

Chapter Two
Literature review

This chapter describes the different types of amylases, their sources and applications. Thereafter, the cultivation conditions used for amylase production, the reactor types and configuration for effective cultivation of aerobic bacteria are discussed. In combination these reviews inform critical aspects of this study, which is focused on the production and characterisation of alkaliphilic amylases from aerobic bacteria, *Bacillus halodurans* Alk36.

2.1 Amylases

2.1.1 Types of Amylases

Amylases belong to a group of enzymes known as hydrolases, i.e. enzymes that catalyse hydrolysis of chemical bonds (Bernfeld, 1955). There are several classes of hydrolases including phosphatases, peptidases, glycosidases and esterases. Amylases are glycosidases which catalyse hydrolysis of glycosidic linkages in starch and related oligosaccharides to form sugars (Bernfeld, 1955).

Starch is a heterogeneous polysaccharide composed of amylose (75% to 85%) and amylopectin (French, 1973; Van Hung, 2008). Amylose is an insoluble polymer composed of linear chains of 200 to 700 glucose residues linked by α-1,4 glycosidic linkages (Figure 2.1.A). Amylopectin is soluble and has a branched structure containing short chains of 17 to 35 glucose residues, linked by α-1,6 glycosidic linkages as shown in Figure 2.1.B (French, 1973; Manners, 1979). Amylose has a molecular weight of about 10^5 – 10^6 g.Mol^{-1} while amylopectin has a molecular weight of 10^7 - 10^9 g.Mol^{-1} (French, 1973; Manners, 1979).

Amylose consists of one reducing end containing an anomeric carbon (a carbonyl carbon with a ketone or aldehyde group) and one non-reducing end (Duedahl-Olesen et al., 2000). Amylopectin consist of one reducing end and several non-reducing ends due

to its branched structure as illustrated in Figure 2.1.B (Duedahl-Olesen et al., 2000). The presence of the anomeric carbon determines the chemistry of the starch molecule and the types of enzymes that can act upon the starch molecule, due to stereo-specificity of metabolic enzymes (Duedahl-Olesen et al., 2000).

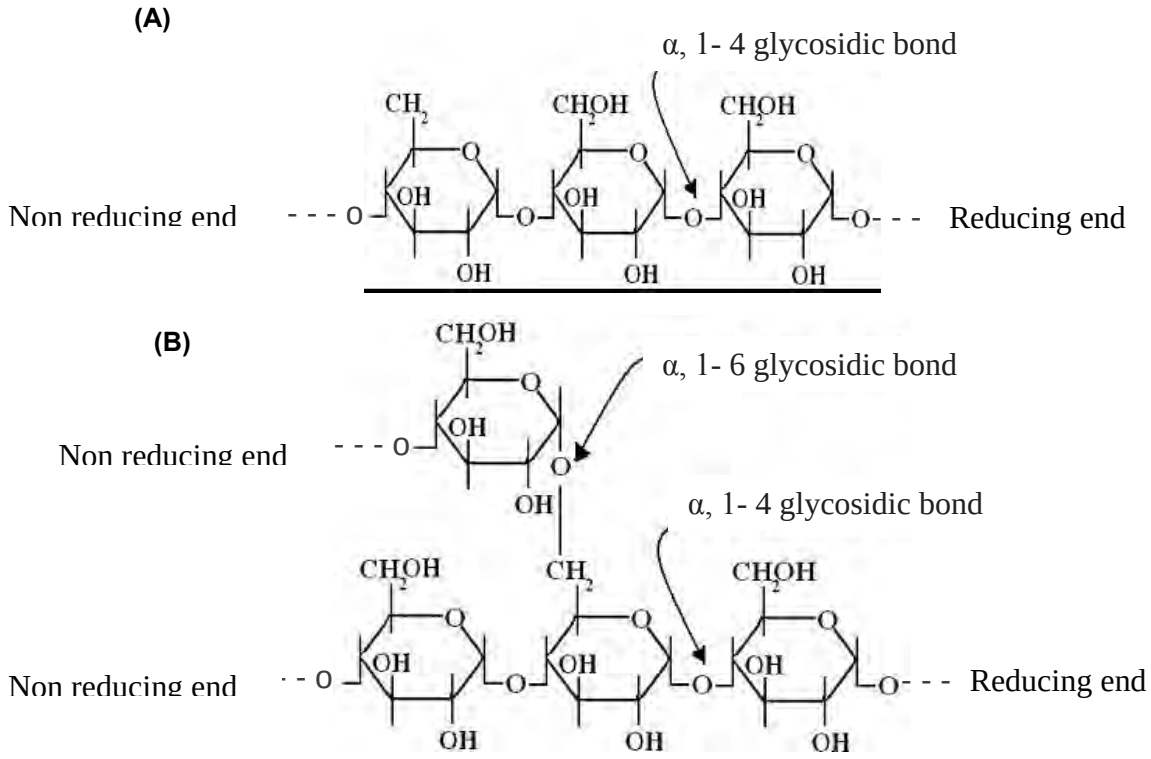

Figure 2.1: Structure of a starch molecule showing the amylose (A) and amylopectin (B) components, and the glycosidic linkages involved in the formation on the starch molecules (adapted from El-Fallal, 2012).

Amylases can be divided into two groups based on their mode of action on starch: the endo-acting and the exo-acting amylases. The endo-acting amylases hydrolyse the α-1, 4 glycosidic linkages in the interior of the polysaccharide molecule, resulting in the formation of linear and branched oligosaccharides of various chain lengths, including glucose, maltose, maltotriose, maltotetraose, maltopentaose, and maltohexaose (Van Der Maarel, et al., 2002). The endo-acting amylases include the α-amylase, isoamylase

and pullulanase. The isoamylase and pullulanase are debranching amylases which hydrolyse the α-(1, 6) linkages (Van Der Maarel et al., 2002).

The exo-acting amylases hydrolyse α-(1, 4) glycosidic linkages, resulting in short end products such as maltose (Van Der Maarel et al., 2002). Glucoamylase, α-glucosidase, β-amylase and the exo-maltohydrolase are exo-acting amylases. The glucoamylases can also hydrolyse the α-(1, 6) linkages to a limited extent (Bijttebier et al., 2008).

The α-amylases tend to be faster-acting than the β-amylases, because they can act anywhere on the polysaccharide chain. Table 2.1 gives the summary of the different types of amylases, their mode of action, the bonds they cleave and the products formed.

Table 2.1: Starch hydrolysing enzymes and their mode of action on starch
(Adapted from Duedahl-Olesen et al., 2000)

Enzyme name (Entry number on ExPASy enzyme database)	Mode of action	Glycosidic linkages attacked	Main product(s) formed
α-Amylase (E.C. 3.2.1.1)	Endo	α-D-(1→4)	mixture of malto oligosaccharides with α-configuration
β-Amylase (E.C. 3.2.1.2)	Exo	α-D-(1→4)	β-maltose
α-Glucosidase (E.C. 3.2.1.20)	Exo	α-D-(1→4)	α-glucose
Glucoamylase (E.C. 3.2.1.3)	Exo	α-D-(1→4) and α-D-(1→6)	β-glucose
Isoamylase (E.C. 3.2.1.68)	Endo	α-D-(1→6)	linear malto-oligosaccharides up to 25 glucose units without branches
Pullulanase (E.C. 3.2.1.41)	Endo	α-D-(1→6)	various linear malto-oligosaccharides
Exo-maltotetraose-hydrolase (E.C. 3.2.1.60)	Exo	α-D-(1→4)	Maltotetraose
Exo-maltohexaose-hydrolase (E.C. 3.2.1.98)	Exo	α-D-(1→4)	Maltohexaose

2.1.2 Application of amylases

2.1.2.1 General application of amylases

Amylases are used in many processes that involve hydrolysis of starch including food processing, detergent formulations, alcohol production and textile making as well as in the paper and pharmaceutical industries (Aiyer, 2005; Gupta et al., 2003a).

In the food industry, amylases are used in brewing to increase the rate of saccharification, yeast growth and alcohol yield (Aiyer, 2005). Amylases are used in liquefaction of starch to bring about a reduction in viscosity and partial hydrolysis of starch (Van Der Maarel et al., 2002; Aiyer, 2005; Gupta et al., 2003a). Amylases are also used in baking to give volume and soften bread, as well as in the production of sweeteners and syrups (Van Der Maarel et al., 2002; Gupta et al., 2003a).

Amylases are added in detergent formulations for the removal of starch stains from clothes. In the textile industry, amylases are used to remove the starch-paste wrapping, which is usually applied to threads during weaving to give the threads strength (Van Der Maarel et al., 2002; Gupta et al., 2003a; Aiyer, 2005). In the paper-making industry, amylases are used to remove the starch-coating and to degrade starch, in pulp from printed papers, during the de-inking process (Sakaguchi et al., 1999; Gupta et al., 2003a). Amylases are also used as a digestive aid during pre-treatment of animal feed (Van Der Maarel et al., 2002; Gupta et al., 2003a; Aiyer, 2005). In the pharmaceutical industry, amylases are incorporated in diagnostic devices used for detection of high molecular weight oligosaccharides (Van Der Maarel et al., 2002; Gupta et al., 2003a; Aiyer, 2005). Amylase is also used in biological cultures to provide the carbon-source for growth from a starch polymer, e.g. in EnBase® medium, which is selected for controlled glucose release (Krause et al., 2010).

In South Africa, amylases are mainly used in starch liquefaction during brewing, in sugar refining and in treatment of raw fruit juice, where amylases are used for the removal of unwanted starch (Bruijn & Jennings, 1968; AEB Africa).

2.1.2.2 Application of alkaliphilic amylases

Amylases used in the processes mentioned in Section 2.1.2.1 operate optimally in an acidic to neutral pH range (pH 4 to 7), except for detergent formulations where the enzymes are required to withstand an alkaline environment (pH 8 to 10.5) (Chaplin & Bucke, 1990). The high pH in detergent formulation is due to the presence of surfactants, soaps, oxidants, bleaching agents and chelating agents as summarised in Table 2.2 (Kumar et al., 2008; Sarethy et al., 2011; Souza, 2010a).

Table 2.2: Composition of powder and liquid enzyme detergents

(Adapted from Kumar et al., 2008)

Ingredient	Powder (% wt)*	Liquid (% wt)*
Anionic surfactants	2 – 10	8 - 10
Non-ionic surfactants	0.5 – 6	18 – 20
Soap	1 – 5	7 – 12
Sequestrants	30 – 60	-
Ethylenediaminetetracetic acid	-	1
Bleach + activator	20 – 30	-
Triethanolamine	-	7 – 13
Ethanol	-	4 – 6
Enzymes	1 – 5	1 – 5
Perfume	0.2	0.4
Optical brighteners	0.4 - 0.8	0.2
Sodium sulphate	To make 100%	-
Water	-	To make 100%

* (% wt) represents g of ingredient per 100 g of the detergent

Termamyl® 300L Type DX (Novozymes) is one of the α-amylases commonly used in detergent formulations. It is a formulation produced from *Bacillus licheniformis* and has an activity of 300 KNU/g protein at pH 5.6 and 37°C , where an activity of 1KNU results in 1 mg of starch being hydrolysed per hour (Bravo Rodríguez et al., 2006). This value corresponds to 0.005 mg starch hydrolysed per minute per mg protein. Since the optimal activity of Termamyl® 300L is obtained at near neutral pH, it is foreseeable that the activity in alkaline conditions, characteristic of detergent formulations, may be reduced. Hence, amylases that are highly stable in alkaline conditions would be of greater value in the detergent industry. Moreover, alkaliphilic amylases that exhibit activity at lower temperatures are more cost-effective in terms of energy requirements, since they do not require high temperatures to facilitate effective washing (Sarethy et al., 2011). Thus, determination of pH and temperature stability, as well as stability in the presence of oxidising agents is necessary for identification of amylases with potential use in detergent formulations. Furthermore, endo-acting amylases are not currently available for use under alkaline conditions, such as in detergent formulations. In most detergent formulations exo-acting amylases are used in combination with endo-acting and debranching amylases for effective removal of stains (Sarethy et al., 2011). Thus availability of suitable endo-acting amylases may reduce the cost of detergents by reducing the number and the amount of enzymes added.

Recently, a new application for alkaliphilic amylases in bioprocess systems with EnBase® technology has been realized (Glazyrina et al., 2012). The EnBase® technology (Biosilta OY, Oulu, Finland) offers a novel fed-batch approach that allows the slow and controlled release of glucose from a polysaccharide polymer by addition of a hydrolytic enzyme, amylase. The rate of glucose release and hence, the growth rate, oxygen-utilisation rate and pH of the medium are controlled by the amount of enzyme added. The EnBase® system employs a commercial amylase (Novozymes, Denmark) derived from a fungus, *Aspergillus niger*. The commercial amylase is active at neutral and acidic pH, which inhibits the use of this system in alkaline conditions. Thus, the development of an alkaline amylase for application with the EnBase® system could enable its use for growing alkaline microorganisms.

2.1.3 Microbial sources of alkaliphilic amylases

2.1.3.1 Bacteria and fungi as sources of alkaliphilic amylases

Plants, animals and microorganisms all produce amylases. However, microbial amylases are preferred for industrial use, because they are highly stable compared to those from plants and animals (Souza, 2010b). Moreover, microbial enzymes can be manipulated easily to obtain desired characteristics and can be produced, economically in bulk (Gupta et al., 2003b).

Commercially-available microbial amylases are obtained from bacteria and fungi, which secrete amylases to the extracellular environment (Souza, 2010b). The extracellular enzymes are favoured over intracellular or membrane-bound enzymes because the extracellular enzymes can be extracted from the growth medium, reducing downstream processing and increasing yields. Bacterial and fungal amylases usually have high thermal stability and can be produced fast, since the growth rates of most bacteria and fungi are naturally faster than that of other microorganisms (Sarethy et al., 2011; Saxena et al., 2007).

2.1.3.2 Bacilli as a source of alkaliphilic amylases

Bacilli are a good source of extracellular proteins, because they have high growth rates and naturally have a high capacity for secretion of extracellular proteins (Schallmey et al., 2004; Terpe, 2006; Simonen & Palva, 1993). Several amylases have been isolated from *Bacillus* species. These amylases vary in size, pH range and temperature range as shown in Table 2.3.

Bacilli species are appealing for use in the production of endogenous extracellular enzymes due to availability of efficient expression systems. The expression systems include the use of strains with deficient or low extracellular proteinase activity, as well as strains with native amylase promoters (Schallmey et al., 2004).

Table 2.3: Alkaliphilic amylases isolated from different *Bacillus* species

Organism	Size of amylase (kDa)	Optimal pH	pH range	Optimal temperature	Temperature range[a, b]	Reference
Bacillus sp. IMD 370	159	10	8.5 – 10.5	40°C	20°C - 40°C	Mc Tigue et al. (1995)
Bacillus sp. GM8901	97	11 -12	6 – 13	50°C	40°C – 50°C	Kim et al. (1995)
Bacillus sp. TS-23	150 and 42	9	8 – 10	70°C	ND[c]	Lin et al. (1998)
Bacillus sp. KSM-1378	53	8 – 8.5	7.5 – 9	55°C	50°C – 60°C	Igarashi et al. (1998)
Bacillus sp. KSM-K38	55	8 – 9.5	ND	55°C - 60°C	ND	Hagihara et al. (2001)
Bacillus subtilis DM-03	42	8 – 8.5	ND	55°C	ND	Das et al. (2004)
Bacillus sp. A3-15	86 and 60.5	11	9.5 – 12.5	70°C	60°C - 90°C	Arikan et al. (2008)
Bacillus sp. PN5	ND	10	4 – 12	90°C	ND	Saxena et al. (2007)
Bacillus sp. AB68	66	10.5	6 – 11.5	50°C	20°C - 90°C	Aygan et al. (2008)
B. halodurans 38C-2-1	100 75	10 – 11	7 – 11.5	50°C - 60°C	10°C - 55°C 10°C - 40°C	Murakami et al. (2007)
B. halodurans MS-2-5	90	10 – 11	6 – 11	60°C - 65°C	30°C - 55°C	Murakami et al. (2008)
B. cereus	42	8	7.5 – 11	65°C	ND	Annamalai et al. (2011)
B. alcalophilus	ND	9	7 – 11	50°C	30°C - 50°C	Yang et al. (2011)
Bacillus sp. SI-136	26	10	4 – 12	80°C	35˚C - 100˚C	Sarethy et al. (2012)

a - The range at which amylase stability was above 80%

b - The incubation time ranged between 30 minutes and 24 hours, depending on the study

c - ND stands for ‘not determined’

Moreover, systems for efficient production of recombinant proteins have been developed (Lam et al., 1998; Schallmey et al., 2004; Terpe, 2006; Wong, 1995). These include a multiple vector system for the production and export of recombinant affinity-tagged proteins in *Bacillus megaterium* (Biedendieck et al., 2007) and the use of a strong vegetative promoter, as well as an induction system based on the regulatory region in *Bacillus subtilis* (Lam et al., 1998; Terpe, 2006). The surface display of chimeric gene products on the *Bacillus halodurans* flagella system has also been shown to be an effective system for over-production of recombinant proteins (Crampton, 2007). *Bacillus subtilis* is most commonly used for heterologous protein production, because it has been well characterised (Terpe, 2006).

2.1.4 Alkaliphilic amylases from *Bacillus halodurans*

Bacillus halodurans, formerly known as *Bacillus brevis*, is an aerobic, gram-positive bacterium with straight, motile rods, rounded ends and peritrichous flagella (Louw et al., 1993). It has been reported to require a pH between pH 8 and 10 and temperatures between 48°C and 50 °C for optimal growth and morphology. *Bacillus halodurans* produces extracellular enzymes that can hydrolyse polysaccharides and proteins (Louw et al., 1993). Examples include thermostable alkaline enzymes such as xylanases, alpha-amylases and malto-oligosaccharide forming amylases (Hashim et al., 2005; Mamo et al., 2006; Murakami et al., 2007).

Some *B. halodurans* strains can produce multiple alkaliphilic, thermotolerant amylases. Two alkaline amylases with molecular weight of 105 kDa and 75 kDa were isolated from *B. halodurans* strain 38C-2-1; these amylases were named *amy* I and *amy II* (Murakami et al., 2007). Five alkaline amylases with molecular weight of 90 kDa, 85 kDa, 70 kDa, 65 kDa and 58 kDa were isolated from *B. halodurans* strain MS-2-5 (Murakami et al., 2008). However, the internal amino acid sequence of all five amylases was similar to that of *amy I* from *B. halodurans* strain 38C-2-1, suggesting that the five amylases were encoded by a single gene.

Studies have attempted to improve amylase production through the use of recombinant DNA technology. Genes encoding amylases from *B .halodurans* have been cloned into

bacteria with well-established expression systems, such as *E. coli,* to increase enzyme yield and productivity (Hashim et al., 2005; Murakami et al., 2007; Murakami et al., 2008). The expression of *amy I* from *B. halodurans* strain MS-2-5 in *E. coli* improved the amylase yield by four-fold, while productivity was increased by two-folds (Murakami et al., 2008). However, the expression of *amy I* from *B. halodurans* strain 38C-2-1 in *E. coli* was not successful in improving the protein yield (Murakami et al., 2007). The latter was suggested to be due to toxicity of the α-amylase signal peptide to the *E. coli* cells. The signal peptide was responsible for ensuring stability of the recombinant protein in *E. coli* cultures. Thus, further investigations are required to establish expression systems for effective production of amylases as recombinant proteins.

Even though expressing amylase genes in *E. coli* may be able to improve amylase yield, not much is known about the thermal and pH stability of the expressed amylases, particularly since *E. coli* is grown under neutral conditions (Murakami et al., 2008). Moreover, protein stability may be affected by the culture pH by changing the charge of the amino acid side chains that are responsible for electrostatic interactions required for folding of the proteins (Scholtz et al., 1993; Kumar et al., 2002; Osváth et al., 2007). Further, amylases from only two *B. halodurans* strains, 38C-2-1and MS-2-5, have been characterised to data. Hence, characterisation of amylases from *B. halodurans* Alk36 will add to the pool of knowledge on alkaliphilic amylases, particularly from *B. halodurans*. The determined characteristics may enable the verification of the expression systems to be used for enhanced production of amylases, comparison of amylases from *B. halodurans* Alk36 to other alkaliphilic amylases and assessment of the potential uses of the amylases.

2.1.5 Amylase activity assays

Several methods are reported to determine amylase activity. These include the saccharogenic, chromogenic and amyloclastic methods, described in Table 2.4.

The amyloclastic assays measure the residual starch concentration after enzymatic hydrolysis. These are subdivided into iodometric, turbidometric and viscometric methods. The iodometric method measures the decrease in the blue-colour complex formed by the

interaction between starch and iodine (Pimstone, 1964). The turbidometric method measures the reduction in light scattering ability of starch due to the decrease in the size of starch molecules brought about by amylase hydrolysis (Virolle et al., 1990). The viscometric method measures the reduction in the viscosity of the starch solution due to starch hydrolysis by amylases (Benfeld, 1955). The amyloclastic assays are substrate-based and do not inform the types of hydrolysis products formed. Moreover, amyloclastic assays are not very accurate because they do not directly measure the amount of starch present and may result in an over- or under-estimation of the amylase activity.

The saccharogenic assays measure the products of hydrolysis, by determining the amount of reducing sugars released. These assays are based on the oxidation of the anomeric carbon atom, at the reducing end of the hydrolysis product, by using oxidizing agents such as copper, ferricyanide and 3,5-dinitrosalicylic acids (Duedahl-Olesen et al., 2000). The saccharogenic assays are product-based and assume that uniform hydrolysis products are formed; hence, they cannot accurately determine the activity of endo-acting amylases. Therefore, when assessing the activity of endo-acting amylases, the types of hydrolysis products need to be determined to enable identification of a suitable standard for use in the assay.

The chromogenic assays involve the use of dye-labelled starch or starch-like substrates and measuring the amount of dye released from starch hydrolysis or the chromogenic products formed upon hydrolysis by amylases (Klein et al., 1970; Lorentz, 2000). The chromogenic assays are substrate-based, hence do not inform on the types of hydrolysis products. These assays may not be cost effective since some of the substrates are expensive. Furthermore, the chromogenic assays may be susceptible to interference by chemicals that can interact with the chromogenic compounds.

The choice of amylase activity assay usually depends on the type of amylase and the availability of reagents and equipment. The starch-iodine and the DNS assays are commonly used, facilitating comparison of results found in literature (Miller, 1959; Pimstone, 1964). However, variation in the assay conditions, dependent on the type of enzyme analysed, makes it difficult to compare these amylase activities.

The DNS assay quantifies the brown-coloured complex formed on reaction between DNS and reducing sugars spectrophotometrically at 575 nm (Miller, 1959) and correlates A_{575} to reducing sugar concentration using standards (glucose or maltose) of known concentrations. As the types of products released from starch hydrolysis depend on the type of amylase, the amount and types of reducing sugars released also depend on the type of amylase. Endo-acting amylases, e.g. alpha-amylases, release products of varying chain length, while the maltogenic alpha amylase and the exo-acting glucoamylases release maltose and glucose, respectively (Bijttebier et al., 2008; Van Der Maarel et al, 2002). The activity of the endo-acting amylases is not determined accurately using the DNS assay, since a fully representative standard of mixed- chain length sugars is not available.

Table 2.4: Methods for determination of amylase activity (Adapted from Duedahl-Olesen et al., 2000)

Amyloclastic methods- measures residual starch after hydrolysis			
Method	**Substrate**	**Reaction principle**	**Detection**
Iodometric	starch or amylase	Amylose-I_3^- complex (blue) hydrolysis decreases the complex and the blue colour	Spectrophotometric
Viscometric	starch in high concentrations	hydrolysis results in a decrease of the solution viscosity	viscosity measurement
Saccharogenic methods – measures reducing sugars released from starch hydrolysis			
Method	**Substrate**	**Reaction principle**	**Detection**
Ferricyanide	native or soluble starch	alkaline ferricyanide(III) reduced to ferricyanide (II), a blue-coloured compound	Spectrophotometric
Somogyi-Nelson	native or soluble starch	alkaline cupri (II) ions reduced to cupro (I) ions, which is reduces arsenomolybdate to a blue-coloured compound	Spectrophotometric
DNS[a]	native or soluble starch	alkaline 3,5-dinitrosalicylic acid reduced to 3-amino-5-nitrosalicylic acid, a brown coloured compound	Spectrophotometric
$CuSO_4$–biquinoline	native or soluble starch	alkaline cupri (II) ions reduced to cupro (I) ions, which is reduces 4,4′-dicarboxy-2,2′-biquinoline to a blue-coloured compound	Spectrophotometric
Chromogenic methods- measures chromogenic products released from starch hydrolysis			
Method	**Substrate**	**Reaction principle**	**Detection**
Cerealpha™	BPNPG7 [b]	endo-attack followed by glucoamylase/α-glucosidase action on *p*-NP[c] part release *p*-NP	Spectrophotometric
Betamyl™	PNPG5[d]	exo-attack and α-glucosidase action on *p*-NP part releases *p*-NP	Spectrophotometric
Dyed-starch	AZCL[e] amylose	release of blue colour when amylose is hydrolysed	visually or spectrophotometric
Turbidometric	starch or amylase	hydrolysis results in a decrease of the turbidity of solution	turbidity measurement

a - Dinitrosalicylic acid assay b - Blocked *p*-nitrophenolmaltoheptaose c - paranitrophenol

d - *p*-nitrophenolmaltopentaose e - Azo-colour cross linked amylose

Alternatively, the starch-iodine assay can be used to determine the activity of endo-acting amylases. The starch-iodine assay is based on the reaction between starch and iodine, to form a blue-coloured complex that can be detected at 580 nm (Huggins & Russell, 1948; Pimstone, 1964). However, the assay is limited by the nature of the starch-iodine complex; only starch chains containing 18 or more glucose residues can interact with iodine to form blue complexes measurable by spectrophotometry (Swanson, 1948). Therefore, the starch-iodine assay tends to overestimate the amount of hydrolysed starch and hence, amylase activity.

Even though the starch-iodine assay cannot be compared to the DNS assay when determining the activity of endo-acting amylases, the two assays may be used to infer the type of amylase being investigated. Xiao (2006) showed that the activity of endo-acting amylases obtained by the starch-iodine assay was higher than that obtained by the DNS assay. Since endo-acting amylases are fast-acting, they can act anywhere on the polysaccharide chain resulting in a reduction of starch chain length. Consequently, the rate of formation of blue complexes with the iodine solution will be faster than the rate of production of the reducing end products, such as glucose or maltose (Xiao et al., 2006). Hence, for an unknown amylase, if the DNS and the starch-iodine assays give the same activity, then the investigated amylase is most likely an exo-acting amylase; possibly a glucoamylase or a maltogenic amylase. On the other hand, if the amylase is an endo-acting amylase, such as the alpha-amylase, then the activity obtained with the starch-iodine assay will be higher than that obtained by the DNS acid assay.

2.2 Development of production processes for alkaliphilic amylases.

Successive bacterial growth and production of protein products usually depends on the growth conditions, such as pH, temperature and availability of oxygen, for aerobic bacteria. Hence, the identification of the optimal conditions required for growth and production of products of interest is important for the design and development of production processes.

2.2.1 Effect of pH on growth of alkaliphilic Bacilli

Alkaliphilic bacteria can grow well at pH values above 7, often between 10 and 12, but cannot grow or grow slowly at the near-neutral and slightly acidic pH, i.e. pH 6 (Horikoshi, 1999).

Alkaliphilic bacteria can be classified into obligate and facultative alkaliphiles. Obligate alkaliphiles (e.g. *B. alcalophilus* and *B. pseudofirmus* RAB) grow optimally at pH values above 11, while facultative alkaliphiles (e.g. *B. pseudofirmus* OF4, *B. halodurans* C-125, and *Bacillus cohnii* YN2000) can grow optimally at moderate pH (pH 7– 8.5) but can survive at high pH (Horikoshi, 1999; Krulwich & Guffanti, 1989). Alkaliphilic *Bacillus* species that could grow and produce amylases optimally at a pH range of 8 to 10 have been isolated by several research groups, as illustrated in Table 2.5.

Table 2.5: Optimal pH for growth of different *Bacillus* strains.

Organism	*Optimum pH*	pH range	*References*
Bacillus sp. IMD 370	10	nd*	McTigue et al. (1995)
Bacillus sp. GM8901	10.5	nd	Kim et al. (1995)
Bacillus sp. TS-23	8.5	nd	Lin et al. (1997)
Bacillus sp. KSM-1378	10	nd	Igarashi et al. (1998)
Bacillus sp. KSM-K38	10	nd	Hagihara et al. (2001)
Bacillus subtilis DM-03	8	nd	Das et al. (2004)
Bacillus sp. A3-15	9	6 -11	Arikan et al. (2008)
Bacillus sp. PN5	10	5 – 12	Saxena et al. (2007)
Bacillus sp. AB68	9	7 – 12	Aygan et al. (2008)
B. halodurans 38C-2-1	10	nd	Murakami et al. (2007)
B. halodurans MS-2-5	10	nd	Murakami et al. (2008)
B. cereus	7	5 – 9	Annamalai et al. (2011)
Bacillus sp. SI-136	4 – 12	nd	Sarethy et al. (2012)
Bacillus halodurans LBK 34	10	nd	Hashim et. al., (2005)

* nd - not determined

Alkaliphilic *Bacillus* can grow over wide ranges of pH, including far from their optima, because they have mechanisms that maintain their internal pH close to neutral. These mechanisms include (i) increasing production of acids through fermentation of sugars and deamination of amino acids (ii) increased ATP synthesis through methods that couple entry of hydrogen ions (H^+) to production of ATP; (iii) modification of cell surface properties; and (iv) increasing expression and activity of monovalent cation/proton antiporters (Padan et al., 2005).

2.2.2 Effect of temperature on growth of alkaliphilic Bacilli

The optimal growth temperature for most *Bacillus* species is reported to lie between 30°C and 60°C while that of *B. halodurans* is reported between 50 and 55 ˚C (Table 2.5). The reported optimal temperatures suggests that *Bacillus* species are either mesophiles or thermophiles since the optimum growth temperature for mesophiles is between 15 and 45 °C, and that of thermophiles is between 42 and 113 °C (Prescott et al., 2005).

Thermophiles have heat-stable enzymes and protein-synthesis systems that function well at high temperatures. Their membrane lipids have high molecular weights and are highly saturated and highly branched (Prescott et al., 2005). These properties increase the melting point of the membrane proteins and hence, allow thermophiles to survive at high temperatures.

Bacillus halodurans has been reported to produce thermostable alkaline enzymes, such as xylanase, amylases and malto-oligosaccharide-forming amylases, stable at 75°C, 60°C and 60°C, respectively (Hashim et al., 2005; Mamo et al., 2006; Murakami et al., 2007). Thermostable amylases are preferred for use on industrial scale, owing to reduced reaction time, reduced cooling duty and reduced contamination (Nigam & Singh, 1995).

Table 2.5: Optimal temperatures for growth of different *Bacillus* strains.

Organism	Optimum temperature(°C)	Temperature range range (°C)	References
Bacillus sp. IMD 370	30	nd*	McTigue et al. (1995)
Bacillus sp. GM8901	50	nd	Kim et al. (1995)
Bacillus sp. TS - 23	55	nd	Lin et al. (1997)
Bacillus sp. KSM - 1378	30	nd	Igarashi et al. (1998)
Bacillus sp. KSM - K38	30	nd	Hagihara et al. (2001)
Bacillus subtilis DM - 03	55	nd	Das et al. (2004)
Bacillus sp. A3 - 15	60	20 -65	Arikan et al. (2008)
Bacillus sp. PN5	37	30 - 70	Saxena et al. (2007)
Bacillus sp. AB68	60	25 - 40	Aygan et al. (2008)
B. halodurans 38C - 2 - 1	50	nd	Murakami et al. (2007)
B. halodurans MS - 2 - 5	50	nd	Murakami et al. (2008)
B. cereus	37	30 -50	Annamalai et al. (2011)
Bacillus sp. SI - 136	35 - 100	nd	Sarethy et al. (2012)
Bacillus halodurans LBK 34	55	nd	Hashim et. al., (2005)

* nd - not determined

2.2.3 Mixing and mass transfer in bioreactors

Mixing is and mass transfer required to ensure a homogenous culture solution where nutrients and by products are equally distributed throughout the culture. Oxygen mass transfer is one of the most important parameters in aerobic bioprocesses, because oxygen is typically the limiting nutrient. Hence, adequate mixing is required to ensure that sufficient oxygen mass transfer is achieved in the system.

2.2.3.1 Oxygen mass transfer in aerobic cultures

Oxygen utilisation is directly proportional to the consumption rate of the carbon source, while oxygen transfer is directly proportional to the mass transfer coefficient and the concentration driving force of oxygen in the culture medium. Oxygen supply may become insufficient if the consumption rate of the carbon source is high, at high cell densities. Insufficient oxygen supply may result in the slowdown of metabolism, switching to anaerobic metabolism, production of secondary products, inhibition or formation of recombinant products and cell death (Büchs, 2001; Clark & Bushell, 1995; Losen et al., 2004).

The amount of dissolved oxygen (C_L) in culture broths is determined by solubility of oxygen which sets the maximum concentration driving force, the volumetric mass transfer rate coefficient which is influenced by resistance to mass transfer and gas-liquid interfacial area for transfer and the rate of consumption of oxygen by metabolic pathways of cells (Çalik et al., 1997).The relationship between the rate of change of oxygen concentration in the culture, the oxygen transfer rate (OTR) and the oxygen utilisation rate (OUR) of the growing culture is shown in *Equation 2.1* (Tribe et al., 1995).

$$\frac{dC_L}{dt} = OTR - OUR \qquad Equation\ 2.1$$

Transfer of oxygen molecules from a gas bubble into the cells involves diffusion through the liquid film surrounding the gas bubble, movement through the bulk liquid by convection and diffusion through the liquid film surrounding the cells as illustrated in Figure 2.2 (Enfors & Häggström, 2000).

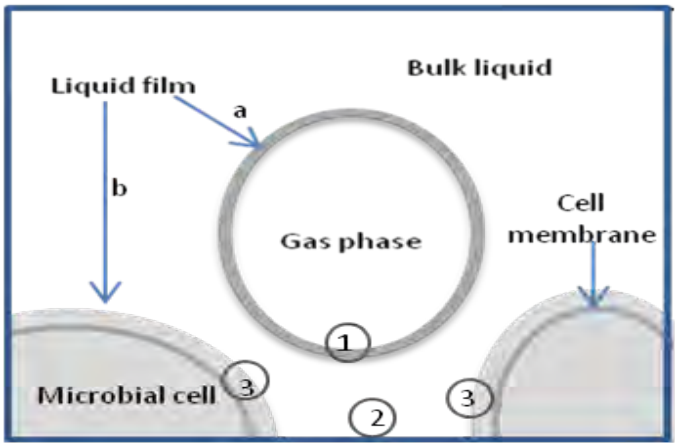

Figure 2.2: Schematic representation of an air bubble in a reactor showing the pathway of gas molecules from the gas bubble through the liquid film surrounding the gas bubble (1), movement through the bulk liquid (2) and diffusion through the liquid film surrounding the cells (3). The stagnant liquid films surrounding the gas and microbial cells are represented as the gas-liquid interface (a) and the liquid-solid interface (b), respectively (adapted from Doran, 1995).

The gas-liquid interface layer is the stagnant liquid film surrounding the air bubble. It provides the main resistance to oxygen transport from the gas bubble to the cell (Enfors & Häggström, 2000). Hence, the oxygen transfer rate is proportional to the volumetric mass transfer coefficient (k_La) and the concentration gradient between the saturation oxygen concentration at the air-liquid and the residual dissolved oxygen concentration in solution (C_{sat}- C_L) as illustrated in *Equation 2.2* (Tribe et al., 1995).

$$OTR = k_L a\,(C_{sat} - C_L) \qquad Equation\ 2.2$$

The volumetric mass transfer coefficient (k_La) represents the mass transfer per unit area (k_L) and the transfer area per unit volume (a) (Enfors & Häggström, 2000). The mass transfer per unit area (k_L) is dependent on the diffusivity of gas at the gas-liquid interface layer (D_A) and the thickness of the gas-interface layer (δ), as demonstrated in *Equation 2.3* (Enfors & Häggström, 2000).

$$k_L = \frac{D_A}{\delta} \qquad Equation\ 2.3$$

Since the saturation concentration of oxygen in liquid solutions is dependent on its partial pressure in the gas, *Equation 2.2* can be presented using the oxygen solubility (Lo_2) and its partial pressure (pO_2) as illustrated in *Equation 2.4* (Hermann et al., 2001).

$$OTR = k_L a \,.\, Lo_2 \left(pO_{2,gas} - pO_{2,liquid}\right) \quad Equation\ 2.4$$

Therefore, adequate mixing and gas dispersion is required to ensure that sufficient oxygen mass transfer can be achieved in the system. Further, oxygen mass transfer can be augmented by aeration with gas containing a high oxygen partial pressure.

2.2.3.2 Mixing in agitated bioreactors

The stirred tank reactor is the most commonly used biological reactor for aerobic cultures. Mixing in stirred tank bioreactors is achieved through the agitator system, which usually consists of baffles and standard Rushton-turbine type impellers for dispersion; these are controlled by a motor that can operate at different speeds (Bryant, 1977). The rate of mixing should be fast enough to prevent sedimentation and “dead zone” formation but slow enough to avoid foam formation and excess turbulence that may cause high shear stress to the microorganisms, inhibiting growth and metabolism (Toma et al., 1991; Lin & Lee, 1997).

If the oxygen transfer rate (OTR) is lower than the oxygen utilisation rate (OUR), the aeration rate can be increased to ensure that the OTR rises above the OUR. However, there is a limit to which an increase in aeration rate can lead to increase in DO, before impeller flooding will occur (Lin & Lee, 1997). Impeller flooding occurs when the amount of air introduced into the reactor is higher than the gas handling capacity of the stirrer, causing the gas bubbles to rise axially though the liquid, limiting the movement of the gas bubbles around the liquid as illustrated in Figure 2.3 (Warmoeskerken & Smith, 1985). Thus, the agitation rate should be high enough to promote gas recirculation in the

media, so as to lengthen the duration the air bubbles spend in the media and allow for oxygen transfer from the gas bubble to the liquid.

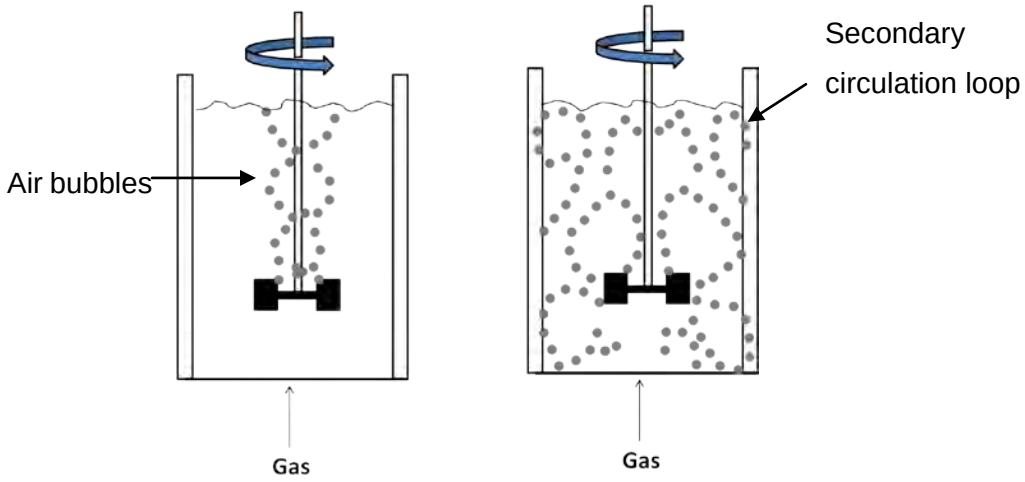

Figure 2.3: The flow pattern of gas bubbles in stirred tank bioreactors showing impeller flooding when the effect of aeration surpasses the effect of agitation (a), and when the agitation rate is high enough to cause bubble recirculation (b) indicated by secondary circulation loops (adapted from Doran, 1995).

The characteristics of gas bubbles in stirred tank bioreactors strongly affect the k_La value. Small bubbles are preferred, because they create large interfacial area (in relation to the volume of the gas) and high gas hold-up, which results in high mass transfer (Doran, 1995). However, bubbles with diameter less than 1 mm results in low mass transfer, by reducing the concentration gradient of oxygen, since the concentration of oxygen in the bubbles rapidly equilibrates with that in the medium (Doran, 1995). Moreover, bubbles with diameter less than 2 or 3 mm are associated with immobile surfaces and no gas circulation, due to high surface tension (Doran, 1995). Thus, the design of the sparger and the impeller is important in choosing bioreactors for aerobic cultures, due to the effect of the impeller in breaking up and dispersion of gas bubbles (Doran, 1995). Moreover, the expense of running the reactor must be considered, since energy input is required for agitation and sparging of air. The energy input in a mechanically stirred bioreactor is directly proportional to the agitation rate; hence, k_La

can be presented in form of the power input per unit volume $\left(\frac{P}{V_L}\right)$ and the superficial gas velocity (V_s), as illustrated in Equation 2.5 (Doran, 1995; Özbek & Gayik, 2001).

$$k_L a = A\left[\frac{P}{V_L}\right]^{\alpha}[V_S]^{\beta} \qquad Equation\ 2.5$$ (where A, α and β are constants)

The effect of oxygen limitation on growth of different bacteria and protein production in stirred tank bioreactors has been discussed by many groups (e.g. Bandaiphet & Prasertsan, 2006; Ducros et al., 2009; Feng et al., 2003; Hwang et al., 1999). Ducros et al. (2009) demonstrated that growth of *Staphylococcus aureus* in stirred-tank bioreactor was dependent on oxygen supply and protease production was growth associated. The maximum specific growth rate increased with an increase in k_La, while the maximum production of protease by *S. aureus* was observed at a specific k_La value of 175.75 h^{-1}. An increase or decrease in this k_La value resulted in a decrease in protease activity (Ducros et al., 2009). The decrease in protease production at k_La values above 175.75 h^{-1} was thought to be due to shear stress, caused by high agitation rates (Ducros et al., 2009). The decrease in protease production at k_La values below 175.75 h^{-1} could have been due to poor mixing regimes that led to insufficient supply of oxygen or nutrients required for protease production. Feng et al. (2003) also showed that production of a growth-related protein, β-mannanase, in *B. licheniformis* was dependent on oxygen availability. The dissolved oxygen concentration, specific growth rate, as well as β-mannanase activity increased with an increase in agitation (Feng et al. 2003). Agitation rates above 600 rpm were associated with shear stress that led to decrease in cell density and β-mannanase activity (Feng et al., 2003).

As a result, in aerobic bioprocesses, the agitation and aeration rates need to be optimised to ensure that the system delivers sufficient oxygen to avoid oxygen limitations without damaging the cells and proteins by shear stress.

2.2.3.3 Mixing and mass transfer in shaking reactors

Shaken bioreactors have been widely used for screening studies and bioprocess development experiments. These reactors include conical flasks, multiwell plates, TubeSpin®- bioreactors and cylindrical- or square-shaped tanks. Shaken bioreactors are the most common vessels for small-scale bioprocesses. They vary in size, from microliters (in multiwell plates) to 6 L tanks.

Shaken bioreactors are easier to make due to their mechanical design and inexpensive to operate, hence usually used for small culture volumes (Hermann et al., 2001; Buchs & Zoels et al., 2001). The energy input in shaken bioreactors is lower than that required for mechanically stirred bioreactors due to the lack of impeller or sparging. Thus, oxygen transfer is limited to surface aeration and the interfacial area between the liquid and the flask walls (Maier & Büchs et al., 2001).

However, shaken bioreactors may be associated with oxygen limitation, since gas-liquid mass transfer is not only influenced by the resistance at the gas–liquid interface but also the resistance of the vessel's closure, which reduces the partial pressure of oxygen within the flask (Hermann et al., 2003; Zimmermann et al., 2003).

Several studies showed that the interfacial area and hence, OTR in shaken reactors can be improved through vessel construction (flask shape, size, surface properties of the flask material and the types of closure material) and altering the operating conditions (shaking frequency, shaking diameter and filling volume) (Doig et al., 2005; Duetz & Witholt, 2001; Hermann et al., 2001; Hermann et al., 2003).

a. Effect of vessel construction on OTR

The construction of shaken bioreactors for improved oxygen transfer rates involves the use of vessel materials that are hydrophilic, addition of baffles and choosing appropriate vessel closure material.

Vessels with hydrophilic walls (glass flasks) have been shown to have higher OTR compared to those with hydrophobic walls (plastic flasks), due to the formation of a liquid film on the flask wall in which oxygen is primarily absorbed (Hermann et al., 2003; Maier

& Büchs, 2001; Maier et al., 2004). Thus, shake flasks made of glass material are preferred over those made of hydrophobic plastic material.

As in agitated bioreactors, the presence of baffles in shaken reactors has been shown to improve mixing and oxygen transfer rates, as well as overcome the effect of wall material-type due to improved mixing regimes (Funke, 2010; McDaniel et al.1965). However, the presence of baffles in shaken reactors may introduce splashing and out-of-phase phenomena, which limit their use (McDaniel 1969, Busch 2001).

In multiwell plates, the use of square-shaped wells has been shown to mimic the presence of baffles (Duetz & Witholt, 2001; Funke, 2010; Hermann et al. 2003). The corners of the square-shaped multiwell plates act as baffles by increasing the cross-sectional area available for oxygen transfer by causing additional turbulence (Hermann et al., 2003). Funke (2010) investigated the oxygen transfer capacity, filling volume and liquid height at the centre of the wells, across 30 microwell geometries during orbital shaking. This investigation revealed that a multiwell plate consisting of a six-petal flower-shaped well geometry can be used with higher filling volumes than normal round multiwell plates (Funke, 2010). The six-petal flower-shaped plates provided the same oxygen transfer rates as normal round plates at higher filling volumes and hence were less affected by evaporation of the culture liquid (Funke, 2010).

Vessel closures are required to reduce evaporation rates by retaining moisture in the bioreactor and to prevent contamination of the culture from the airborne microorganisms, as well as cross-contamination between wells in multiwell plates. The closures should allow venting, prevent excessive evaporation and maintain high levels of oxygen in the headspace such that the air in the headspace is saturated with oxygen by 75% or more (Duetz & Witholt, 2001). The amount of ventilation depends on the rate of oxygen transfer through the closure material. This is affected by the thickness, width and porosity of the closure material (Doran, 1995). High evaporation rates is one of the main problems associated with the use of microwell plates, due to small culture volumes. The acceptable evaporation rate should be ≤ 5% of culture volume per day (Duetz & Witholt, 2001). For microwell and multiwell plates, low evaporation rates can be achieved by the use of ‘sandwich covers’, which limits the evaporation rate to 2% of the culture volume per day (Duetz & Witholt, 2001). Other types of closure materials available for multiwell

plates include the breathable rayon sealing film and the aeroporous membranes (Alpha Laboratories). For shake flasks, cotton plugs, filter membranes or silicone sponge are used as closings (Doran, 1995; McDaniel & Bailey, 1969).

b. Effect of operation conditions on OTR

The operation conditions used for growing cultures in shake flasks (shaking frequency, filling volume and shaking diameter) can be altered to increase the interfacial surface area and hence, OTR.

The OTR increases with a decrease in filling volume, due to a decrease in the liquid film thickness distributed on the flask wall (Maier et al., 2004). The decrease in the liquid film thickness results in an increased k_La and hence OTR, since k_La is directly proportional to the reciprocal of the thickness of the interfacial layer as discussed in Section 2.2.3 (Enfors & Häggström, 2000).

In shake flasks, the increase in shaking frequency also leads to an increase in mass transfer area of the liquid surface, due to the liquid film distributed on the flask wall (Maier & Büchs, 2001). However, high shaking frequencies may lead to formation of foam, which reduces gas exchange at the surface of the culture and aggravates shear forces that can damage cells and proteins (Holmes et al., 2006). In multiwell plates, shaking frequencies tolerated are limited by spilling of the media due to an ‘out-of-phase’ condition (Duetz & Witholt, 2001). The out-of-phase condition is caused by relatively strong adhesive and capillary forces compared to the gravitational forces in small vessels. The maximum value for oxygen transfer rate (OTR_{max}) is limited by the maximum shaking frequency for a specific shaking diameter (Duetz & Witholt, 2001; Hermann et al. 2003). Under these conditions, increasing the shaking diameter and thereby surface area, increases the OTR because the ratio of gravitational forces to adhesive and capillary forces increases (Duetz & Witholt, 2001).

2.2.4 Methods of determining OTR and k_La

Several methods for determination of the oxygen transfer rate (OTR) and the volumetric oxygen mass transfer coefficient (k_La) have been reported. The volumetric mass transfer coefficient is mostly used to characterise mass transfer of a system because the interfacial area (a) of a system cannot be easily determined (Bailey, 2009).

The methods used to determine k_La and OTR include physical methods involving analysis of the inlet and outlet gas streams, as well as the determination of the dissolved oxygen transfer concentration using the dynamic gassing in-gassing out method (Tribe et al., 1995). Chemical methods such as the sulphite oxidation, enzymatic oxidation of glucose, bio-oxidation of catechol and the rate of oxygen formation from hydrogen peroxide have also been used (Hermann et al., 2001; Duetz & Witholt, 2004; Ortiz-Ochoa et al., 2005; Villadsen et al., 2011).

The dynamic gassing in – gassing out and the sulphite oxidation method are commonly used for the determination of OTR and k_La due to ease and availability of the required equipment.

2.2.4.1 The dynamic gassing in – gassing out method

In the dynamic method, the change in dissolved oxygen concentration with time and microbial oxygen demand of actively growing microorganisms is determined by using electrochemical probes with an oxygen-permeable membrane (Tribe et al., 1995).

The oxygen utilization rate is determined during the gassing-out phase when the dissolved oxygen concentrations (DO) decrease in the absence of gas supply as shown in Figure 2.4.

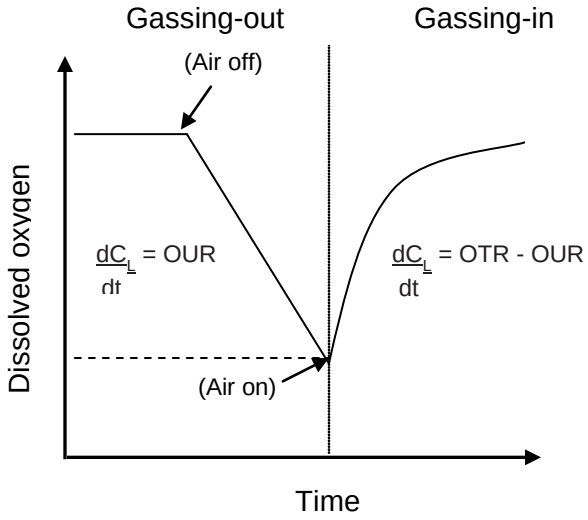

Figure 2.4: Dissolved oxygen profile obtained in a stirred tank bioreactor with active microbial culture during the dynamic gassing-out and gassing-in phase (adapted from Tribe et al., 1995).

The rate of change of DO during the gassing-out phase is equal to the rate of oxygen consumption by the respiring microorganism (OUR) as illustrated in *Equation 2.6.*

$$\frac{dC_L}{dt} = OUR \equiv -Qo_2 C_X \qquad Equation\ 2.6$$

where Q_{O2} is the specific oxygen-utilisation rate coefficient (mg O_2 per g dry biomass weight per second), C_X is the biomass concentration (g dry weight per L), C_L is the dissolved oxygen concentration (mMols.L^{-1}) and *t* is the time (seconds).

During the gassing-in phase, aeration is turned on and the dissolved oxygen concentration increases in response to the oxygen driving force, until it reaches steady state, as shown in Figure 2.4. Taking into account the estimated OUR, the k_La can be determined from the measured profile of dissolved oxygen concentration with time, using *Equation 2.7.*

$$\frac{dC_L}{dt} = k_L a\,(C_{sat} - C_L) - Qo_2\,X \qquad Equation\ 2.7$$

where C_L (mMols.L^{-1}) is the concentration of oxygen in the liquid phase, C_{sat} is the saturation concentration of oxygen in the liquid under the given temperature and pressure (mMols.L^{-1}), k_La is the volumetric mass transfer coefficient of the system (h^{-1}), Q_{02} is the specific oxygen utilisation rate of the organism (mMols.g^{-1}.h^{-1}) and C_x is the biomass concentration at time *t* (g.L^{-1}).

Equation 2.7 can be rearranged to give Equation 2.8, from which the k_La can be determined from the slope of C_L as a function of $\left(\frac{dC_L}{dt} + Qo_2X\right)$.

$$C_L = \frac{-1}{k_L a}\left(\frac{dC_L}{dt} + Qo_2X\right) + C_{sat} \qquad Equation\ 2.8$$

For meaningful determination of k_La, the probe response time must be sufficiently rapid. The probe response time is the time taken for the probe to reach 63% of the saturation concentration when transferred from the solution without oxygen to the solution saturated with oxygen (Tribe et al., 1995). The probe response time increases as the probe's membrane ages. For accurate results, the probe response time should be less than the reciprocal of the k_La; otherwise the obtained DO values must be corrected to account for the probe's response time (Mueller et al., 1967; Tribe et al., 1995; Doran, 1995).

Electrochemical sensors are fast and efficient; however, the sensors perform best at high oxygen concentrations and actively consume oxygen since their action is based on interaction between oxygen and a sensor to generate a current proportional to the gas concentration (Taylor & Schultz, 1996; Harms et al., 2002). Furthermore, these electrodes can easily be contaminated by sample contents and can be intrusive to small cultures, making miniaturization of the sensors necessary. Miniaturization of such devices requires microscale electrodes, which are expensive and require electrical

connection between the sensor electrodes and the measurement infrastructure for online measurements (Grist et al., 2010; John et al., 2003).

2.2.4.2 The sulphite oxidation method

The sulphite method is commonly used in systems where direct measurement cannot be made, such as in the small-scale reactors (shake flasks and multiwall plates). In the sulphite method, the rate of oxygen consumption during oxidation of sulphite, in the presence of a cobalt catalyst, is measured (Hermann et al., 2001). When the reaction rates are oxygen-limited, the rate of sulphite oxidation is equal to the oxygen transfer rate (Hermann et al., 2001). The experimental conditions are kept within certain limits to avoid overestimation of OTR and k_La values since the oxygen absorption rate may be enhanced by fast chemical reactions in the liquid phase (Garcia-Ochoa & Gomez, 2009).

The rate of sulphite oxidation is determined by reacting the unoxidised sulphite solution with iodine and then titrating the residual iodine with a sodium thiosulphate solution (Schultz & Gaden, 1956). The amount of sodium thiosulphate solution required to react with the residual iodine is used to calculate the amount of iodine reacted with the unoxidised sulphite and hence, the amount of oxidised sulphite based on stoichiometry as shown in Equation 2.9 to 2.11.

$$I_2 + 2S_2O_3^{2-} \rightarrow 2I^- + S_4O_6^{2-} \qquad Equation\ 2.9$$

$$I_2 + SO_3^{2-} + H_2O \rightarrow 2I^- + SO_4^{2-} + 2H^+ \qquad Equation\ 2.10$$

$$SO_3^{2-} + \frac{1}{2}O_2 \rightarrow SO_4^{2-} + H^+ \qquad Equation\ 2.11$$

The OTR is given by the rate of sulphite oxidation (Equation 2.12) and k_La can be calculated from the OTR using Equation 2.13 since the concentration of oxygen in the sulphite solution ($C_{L)}$ is assumed to be zero.

$$OTR = \frac{Rate\ of\ oxidation\ of\ sulphite}{2} \qquad Equation\ 2.12$$

$$OTR = k_L a\,(C_{sat} - C_L) \equiv k_L a\,.Ho_2\,.pO_2 \qquad Equation\ 2.13$$

where C_L is the concentration of oxygen in the liquid phase, C_{sat} is the saturation concentration of oxygen in the liquid under the given temperature and pressure, Ho_2 is the Henry's law constant, representing solubility of oxygen at a given temperature and pressure and pO_2 is the partial pressure of oxygen.

Duetz (2000) showed that the OTRs determined by the sulphite method are slightly lower than those derived from the direct oxygen measurement in biological systems. This is probably due to the reduced oxygen solubility caused by the high salt content in the sulphite solution (Duetz & Witholt, 2001). Hence, it is necessary to take the effects of the culture media into account before using the sulphite model system, by determining the OTR in the culture media (Maier et al., 2004; Duetz et al., 2000; Duetz & Witholt, 2004; Hermann et al., 2001).

The sulphite method is time-consuming and the kinetics of the reactions are complex. Kensy (2005) modified the method by using bromothymolblue, as an indicator, to monitor the colour change associated with acid formation. This simplified the method, since the colour change was monitored using a digital camera and the OTR value was calculated using the time taken for the colour shift to occur, instead of using a series of calculations based on titration volumes.

The sulphite oxidation method is not recommended for determination of the volumetric mass-transfer coefficient in sparged bioreactors, due to the changes in physicochemical properties of liquids, such as bubble coalescence, caused by the salts (Garcia-Ochoa & Gomez, 2009).

2.3 Mode of bioreactor operation

Industrial bioprocesses usually involve large-scale fed-batch cultivations, characterised by the controlled addition of the nutrients, without removal of culture; hence the volume of the culture increases with time (Doran, 1995). Fed-batch cultivations allow for temporal variation of nutrients and tight control of cellular metabolism. Thus, high productivity can be achieved (Doran, 1995). Moreover, fed-batch cultivation can be used to prevent overflow metabolism (i.e. formation of by-products due to high rates of glycolysis), as well as mutation of the microbial strain through control of metabolism (Korz et al., 1995; Reynders et al., 1996; Villadsen et al., 2011).

Carbon-source is the limiting factor in most fed-batch processes where the rate of consumption of the carbon source is balanced by the feeding rate of the carbon substrate (Doran, 1995). This allows culture to grow at the maximum specific growth rate. Therefore, the residual dissolved oxygen concentration in the reactor depends on the rate of consumption of the carbon substrate (Šiurkus et al., 2010). As the biomass concentration increases, a pseudo-steady state where the oxygen-utilisation rate equals the oxygen-transfer rate is reached. Therefore, the rate of biomass production is usually kept constant to ensure that the culture is not oxygen limited as it enters the steady state (Korz et al., 1995; Reynders et al., 1996; Villadsen et al., 2011; Šiurkus et al., 2010). Therefore, the maximum biomass concentration supported during the steady state is determined by the oxygen-transfer capacity of the bioreactor, the substrate concentration in the feed solution and the amount of substrate required for cellular maintenance (Šiurkus et al., 2010). Consequently, by controlling the substrate concentration at a constant value, high growth rates and high cell densities can be reached, while avoiding oxygen limitation.

Fed-batch conditions cannot be attained by liquid feeding in small-scale reactors due to volume limitations and the difficulty of maintaining volume control in the absence of robotics. Therefore, reactions in small-scale vessels are usually done in batch mode. Microbial physiology and protein production in the batch process is dynamic, whereas pseudo steady-state conditions can be maintained under fed-batch conditions (Doran, 1995; Reynders et al., 1996). Moreover, batch fermentations are associated with

overflow metabolism, medium acidification and oxygen limitation, owing to the high initial concentration of the carbon source (Büchs, 2001; Losen et al., 2004). Overflow metabolism occurs when the rate of carbon assimilation into biomass exceeds the rate of oxygen utilisation (Xu et al., 1999). Consequently, cellular metabolism is shifted towards the production of organic acids by fermentation, which causes medium acidification and inefficient use of the carbon source (Xu et al., 1999).

The EnBase® system (Biosilta OY, Oulu, Finland) was established to mimic fed-batch conditions in small-scale reactors. The system consists of a glucose-free mineral salt medium, supplemented with thiamine and trace elements, a booster component containing complex nitrogen, and the polysaccharide polymer (starch) (Krause et al., 2010). The EnBase® system allows for slow and controlled release of glucose by the addition of the hydrolytic enzyme, amylase. The amount of enzyme added controls the rate of glucose released and hence, the growth rate, oxygen utilisation rate and pH of the medium, through preventing overflow metabolism and medium acidification (Hortsch & Weuster-Botz, 2011; Krause et al., 2010). The EnBase® system employs a commercial amylase (Novozyme, Denmark) derived from *Aspergillus niger*. This enzyme is active at neutral and acidic pH, reducing its effectiveness under alkaline conditions (Norouzian et al., 2006). The EnBase® technology provides controlled cultivation conditions in small-scale experiments and has been used for screening processes and optimization studies in reactors of different scale (deep-well plates, 3 L and 150 L reactors), since it produces similar growth patterns and high yields of recombinant proteins (Grimm et al., 2012; Šiurkus et al., 2010; Glazyrina et al., 2012).

When using small-scale bioreactor systems to derive process information or to screen for optimal performance, it is important to use a representative system. Oxygen mass transfer is usually used as a representative system for aerobic processes, since ensuring sufficient oxygen mass transfer is a well-recognized requirement for aerobic processes (Büchs, 2001; Kensy et al., 2005; Maier & Büchs, 2001; Maier et al., 2004). Following screening, it is recognized that rigorous scale-up/scale-down experiments are required (Islam et al., 2008; Micheletti et al., 2006). Hence, oxygen transfer rates and the volumetric mass transfer coefficient are usually used as scale-up criteria for aerobic processes. Engineering characteristics such as power per unit volume, mixing time,

superficial gas velocity and reactor geometry are also recognized as important scale-up criteria (Schmidt, 2004).

2.4 Rationale of the research

The literature reviewed in this study has described the importance of amylases in industry, particularly, in detergent formulations. The use of alkaline amylases in detergent formulation enables more effective removal of starch-stains, since alkaline amylases remain stable for longer in the alkaline environment. The alkaline amylases that have been identified so far have not been well characterised, in terms of their applicability in detergent formulations. In addition, the potential use of alkaline amylases with the EnBase® medium in alkaline bioprocesses depends on the stability and activity of the amylases. Thus, characterisation of the alkaliphilic amylases from *B. halodurans* Alk36 will allow evaluation of its application in detergent formulations as well as with the EnBase® system.

2.4.1 Objectives

Based on the gaps identified in the critical review of the literature, the objectives of this study are as follows:

i. To determine the types of amylases produced by *B. halodurans* Alk36.

ii. To validate the use of multiwell plates and shake flasks as small-scale reaction vessels for bioprocess optimization.

iii. To optimize the culture conditions for improved biomass yield and amylase production, using EnBase® medium to achieve pseudo fed-batch conditions.

iv. To characterise the amylases from *B. halodurans* Alk36, in terms of the pH and temperature optima, as well as stability profiles.

2.4.2 Key questions

To guide the research programme, he following key questions will be addressed:

i. What are the types of amylases produced by *B. halodurans* Alk36?

ii. At what stage during growth are the amylases produced?

iii. Does the medium used and its carbon source influence the growth of *B. halodurans* and its amylase production?

iv. What are the oxygen transfer rates and the volumetric mass transfer coefficients provided by the shake flasks and multiwell plates at different operating conditions?

v. How is growth of *B. halodurans* Alk36 affected by operating pH, temperature and oxygen supply?

vi. Can conventional protein purification methods be used to recover and purify the amylases from *B. halodurans* Alk36?

vii. What is the mode of action of the amylase produced?

viii. What is the pH and temperature stability of the amylase produced by *B. halodurans* Alk36?

ix. Do the amylases from *B. halodurans* Alk36 have potential for commercial applications?

2.5 Research approach

The aim of this study was to produce and characterise amylases from *B. halodurans* Alk36 with the purpose of assessing commercial application of the amylases. This was done through identifying the types of amylases produced by *B. halodurans* Alk36, characterising them and by identifying the optimal growth conditions required for improved production of the amylases.

For the identification study, *B. halodurans* Alk36 cultures were grown in a bioreactor for bulk production of biomass and amylases. The use of complex LB medium and EnBase® medium was investigated to determine the medium that resulted in high biomass and hence, amylase production, since production of amylases was shown to be biomass-dependent.

Since *B. halodurans* secreted the amylases to the extracellular environment, ammonium sulphate precipitation and activated charcoal fractionation were investigated as methods of concentrating and partially purifying the amylases from the culture supernatant. The amylases present in the concentrate were identified by peptide mass fingerprinting and further purified by liquid chromatography to remove non-amylolytic proteins and separate the amylases from each other..

The optimal conditions (i.e. pH, temperature and carbon source) for growth of *B. halodurans* Alk36 were studied to determine conditions for enhanced biomass production and amylase activities. The optimisation studies were done in shake flasks and multiwell plates; hence, the operating conditions (i.e. shaking frequency, filling volume and evaporation rate), that could result in high biomass yields, were investigated.

The *B. halodurans* Alk36 amylases were characterised based on size, mode of action, as well as pH and temperature stability. These characteristics were used to establish the potential for commercial application of the amylases.

Chapter Three

Materials and Methods

3.1 Microorganisms, inoculation and growth conditions

3.1.1 Maintenance of cultures

Bacillus halodurans Alk36 strain was obtained from Dr. Michael Crampton of the Council for Scientific and Industrial Research (Pretoria, South Africa). The strain was isolated from a soil sample in South Africa (Louw et al., 1993).

Bacterial colonies were grown on Luria Bertani (LB) agar containing 5 g/L yeast extract, 10 g/L tryptone, 10 g/L NaCl, 15 g/L agar supplemented with10 µg/mL chloramphenicol and 5 µg/mL erythromycin. The antibiotics were added to select for the *B. halodurans* Alk36 mutant strain containing the surface dispay flagellin system and to eliminate contamination from other bacteria (Crampton et al., 2007). The agar plates were incubated overnight at 30 ˚C.

A single colony, from the LB agar plates, was inoculated into LB broth at pH 8.5. The pH of the broth was adjusted using 5M NaOH, prior to sterilization. The culture was grown at 30 ˚C at 200 rpm for 8 hours. The 8 hour-culture was used to prepare 40% glycerol stocks by adding 500 µL sterile glycerol (80% v/v) into 2 mL Eppendorf tubes containing 500µL of the culture. The glycerol stock cultures were stored at -60 °C. Plate cultures were prepared monthly from the glycerol stocks for growth experiments. The plate cultures were sub-cultured weekly to maintain the viability of the colonies.

3.1.2 Liquid growth media

Bacterial cultures were grown in LB medium and EnBase® medium (Biosilta, Oulu Finland). The LB medium contained yeast extract, tryptone and NaCl as stated above (Section 3.1.1), while the EnBase® medium contained 30 g/L starch polymer, macroelement solution, trace elements, thiamine and a booster solution (Glazyrina et al.,2012). Both the LB and EnBase® media were supplemented with 10 µg/mL chloramphenicol and 5 µg/mL erythromycin, prior to inoculation.

3.1.3 Preparation of pre-cultures

Inocula for the cultures grown in EnBase® media were prepared in two stages, the pre-inoculum and the inoculum. The pre-inoculum was used to grow a sizeable starter culture while the inoculum was used to adapt the cells for amylase production by enabling the expression of amylase genes. Thus, the pre-inoculum cultures were prepared in EnBase® medium containing a booster solution that supplied the culture with easily utilizable carbon and nitrogen sources as well as growth factors and vitamins, while the inoculum was prepared in EnBase® medium without booster solution i.e. a defined medium. The sequence of cultivation volumes and conditions used for the preparation of the pre-cultures is illustrated in Figure 3.1.

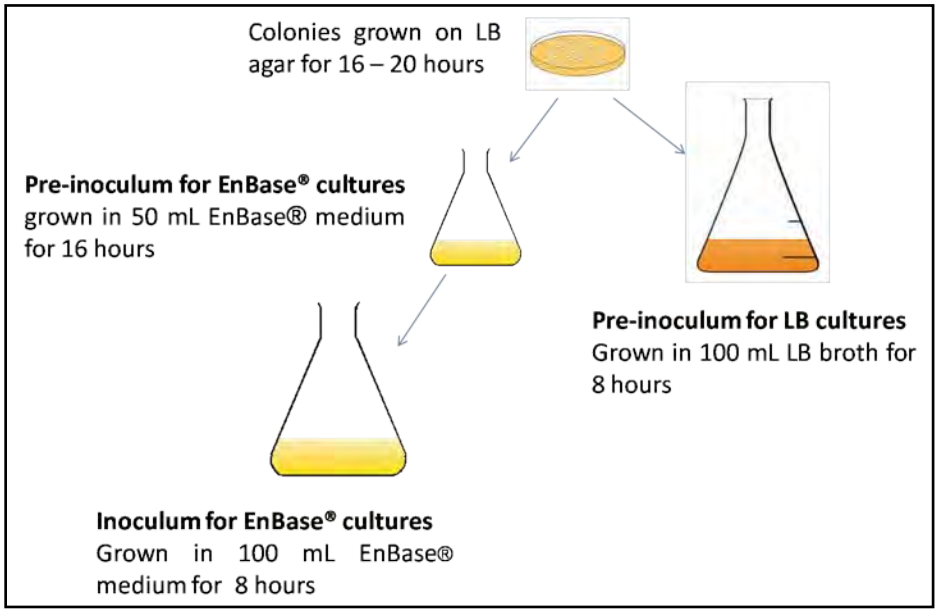

Figure 3.1: The sequence of cultivations used to prepare the pre-cultures of *B. halodurans* Alk36.

The LB pre-cultures were prepared in 500 mL Erlenmeyer flasks filled with LB medium to 10% of the flask volume capacity. The EnBase® pre-inoculum cultures were prepared in 250 mL Erlenmeyer flasks, while the inoculum cultures were prepared in 500 mL Erlenmeyer flasks. The flasks were filled with culture media to 20% of the flask volume

capacity, sealed with cotton wool bungs and then sterilized by autoclaving at 121˚C for 20 minutes. The media was inoculated with fresh colonies grown on LB agar overnight (16 to 20 hours). The colonies were scraped from the LB agar plate, suspended in 1 mL culture media and the optical density (OD) of the solution was measured using a spectrophotometer at 600nm. The bacterial solution was used to inoculate pre-inoculum media (EnBase® medium) to a starting OD_{600} of 0.2. The pre-inoculum was grown for 16 hours and used to inoculate the inoculum medium to OD_{600} of 0.2. The inoculum cultures were grown in for 8 hours at 30˚C on an orbital shaker at 200 rpm.

3.1.4 Cultivation methods

3.1.4.1 Shake flask cultivations

Erlenmeyer flasks of 500 mL capacity were used to grow cultures in small volumes (100 mL), representing 20% of the flask volume. The flasks were sealed with cotton-wool bungs to allow gas transfer and sterilized at 121˚C for 20 minutes. LB or EnBase® media (50 mL) was prepared as described in Section 3.1.2 and the pH of the medium was maintained at the desired range using a 0.1 M phosphate buffer (Na_2PO_4/$NaHPO_4$), for cultures maintained at pH 7, 8 and 8.5, or a 0.1 M carbonate buffer (Na_2CO_3/$NaHCO_3$), for cultures maintained at pH 9 (since the carbonate buffer can only buffer between pH 9 and 10). The buffer solutions were made and sterilized separately and added to the media prior to inoculation. The culture medium was inoculated under aseptic conditions, with inoculum prepared as described in Section 3.1.3, to a starting OD_{600} of 0.2. The volume of the inoculum (≤ 5 mL) was less than 10% of the culture volume. The cultures were grown at 30˚C with 200 rpm, unless stated otherwise. The samples (1 mL) were taken at 3 hour intervals and used to measure the culture pH and optical density.

3.1.4.2 New Brunswick bioreactor cultivations

The New Brunswick BioFlo 110 stirred-tank bioreactor system (New Brunswick Scientific, USA), with 7 L capacity and 5 L working volume shown in Figure 3.2, was used to investigate the growth of *B. halodurans* Alk36 in LB and EnBase® medium. The

stirred-tank bioreactor system was also used for bulk production of amylases for characterisation purposes.

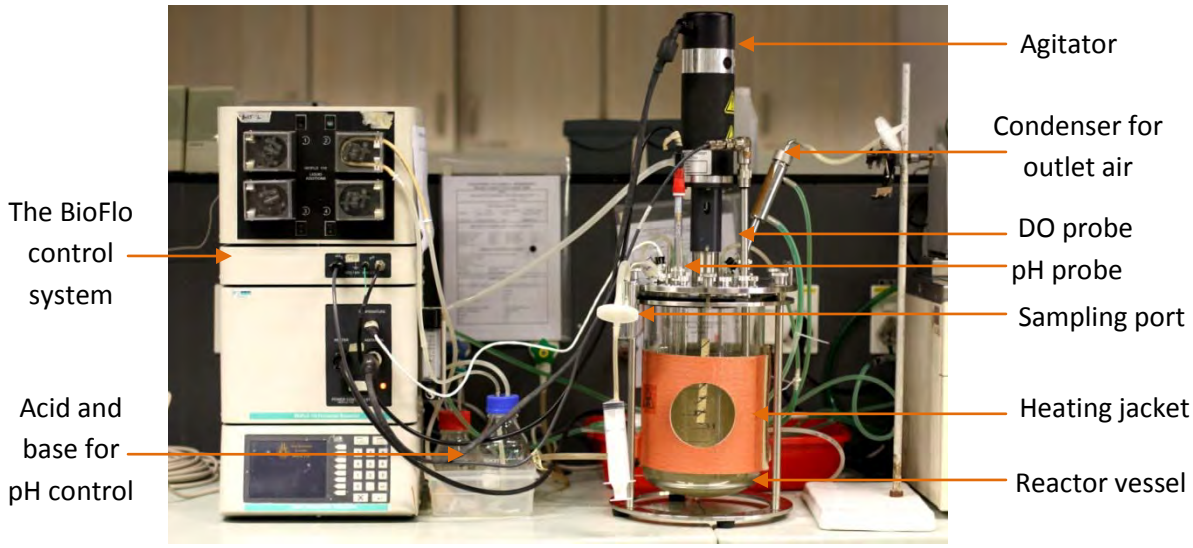

Figure 0.2: The New Brunswick BioFlo 110 stirred- tank bioreactor system.

The reactor and culture media (2.7 L) were sterilized at 121°C for 20 minutes . When EnBase® medium was used, a 2.4 L solution containing the starch polymer was autoclaved in the reactor and the other components of the EnBase® medium (macroelements, trace elements, $MgSO_4$ and thiamine) were autoclaved separately and added into the reactor, prior to inoculation, followed by the antibiotics (chloramphenicol and erythromycin) to a volume of 2.7 L. The culture medium was heated to and maintained at 30ºC through the use of a heating jacket or circulating cooling liquid through the internal cooling coil. The pH was monitored using a pressurizable gel-filled pH probe (Serial no. 6474132, Mettler Toledo) and was adjusted and maintained at pH 8.5 using 5 M NaOH. The reactor system was supplied with oxygen through sparging of filtered, compressed air at 1 vvm. Mixing and mass transfer were achieved by using baffles and a six-blade Rushton impeller. The impeller was fixed such that its distance from the bottom of the reactor is equal to its diameter. The speed of the impeller was controlled by an agitator to increase in a cascade mode between 200 and 1200 rpm to maintain the dissolved oxygen concentration at 40% or above and hence, ensure that

the culture was not oxygen limited. The dissolved-oxygen concentration was measured with a polarographic dissolved oxygen probe fitted with a Teflon membrane (Part number P/N 52201019, Mettler Toledo).

The culture media was then inoculated with 300 mL inoculum, prepared as described in Section 3.1.3, to achieve a final working volume within the reactor of 3L. The cultures were grown at 30˚C and pH was maintained at 8.5, unless stated otherwise. The growth conditions (pH, temperature, agitation) were monitored and controlled with the BioCommand software (New Brunswick Scientific, USA). Culture samples (5 mL) were taken at 2 hours intervals till the cultures entered stationary phase. The samples were used to determine the culture's growth and amylase production. Cell growth was determined by both spectrophotometry (optical density (OD) at 600 nm) and gravimetric analysis.

3.1.4.3 Sixfors bioreactor cultivations

The Sixfors bioreactor system (Infors HT, Switzerland), with a capacity of 400 mL, was used for the determination of optimal pH for growth of *B. halodurans* Alk36. The system consists of six reactors that can each be operated at different growth conditions in parallel as illustrated in Figure 3.3.

The Sixfors reactor has online monitoring and control of pH, temperature, dissolved oxygen concentration and agitation. The pH of the cultures was monitored using a pressurizable gel-filled pH probe (Serial number 1362454, 0230633, 1331007, 1492552, 1490532 and 0230647, Mettler Toledo) and the dissolved oxygen concentration was measured with a polarographic dissolved oxygen probe fitted with a Teflon membrane (Serial number 6298103, 6128119, 5488218, 6298102, 6178000 and 6348018, Mettler Toledo). The pH was maintained at the desired range by titrating with 5 M NaOH, while the temperature was maintained at the desired range by heating supplied through the heater block, which holds the reactors in place and cooling through a water-cooled heat exchanger.The reactors were supplied with oxygen through sparging with filtered, compressed air.

Mixing and mass transfer were achieved by baffles and a magnetically rotated stirrer shaft, fitted with two three-blade marine propellers.

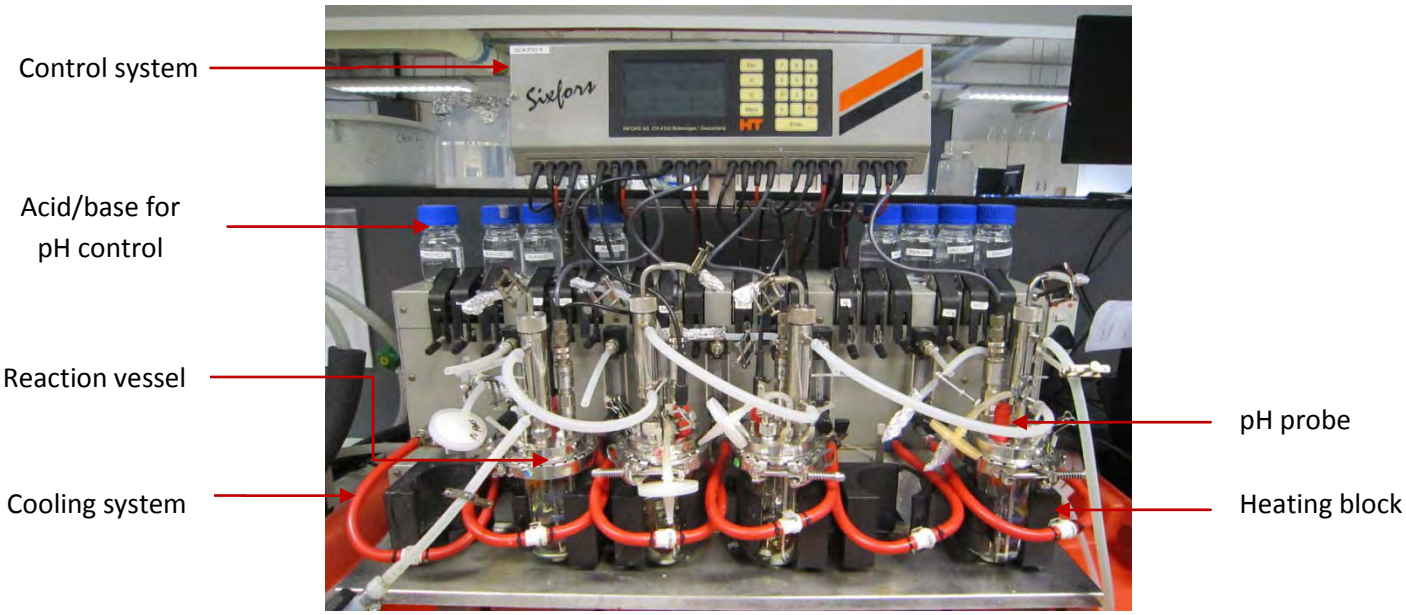

Figure 0.3: The Sixfors bioreactor system (Infors, version 3.01, Switzerland).

The reactors were sterilized with 200 mL starch solution and the other components of the EnBase® medium (macroelements, trace elements, MgSO4 and thiamine), as well as the antibiotics (chloramphenicol and erythromycin) were added to the reactors prior to inoculation. The medium pH and temperature were adjusted to the desired range using 5 M NaOH. The media was inoculated with 25 mL inoculum (prepared as described in Section 3.1.3) at 10 % (v/v) to achieve a final culture volume of 250 mL. The inoculum was grown in media at five different starting pH's, so that pH at its time of inoculation, was closer to that of the culture media to be inoculated. The reactor was controlled at 30˚C aerated at 1 vvm and the agitation speed was set to cascade between 200 rpm and 1000 rpm to maintain the dissolved oxygen concentration at 40% or above. The cultures were inoculated with inoculum at appropriate pH and grown at 30˚C. The pH of the cultures was maintained at pH 7, 8, 8.5, 9 or 10 and the growth conditions were monitored and controlled with the Iris software (Infors HT, Switzerland).

Bacterial growth was monitored by determining the optical density of the culture using the samples (2 mLs) taken at regular intervals (every 2 hours).

3.2 Experimental procedures

3.2.1 Determination of growth profile of *Bacillus halodurans* Alk36

3.2.1.1 Comparison of growth in shake flasks using LB and EnBase® media

Bacillus halodurans Alk36 was grown in a batch culture using EnBase® media and LB broth in shake flasks to determine the growth profiles in the given media. The shake flasks and culture media were prepared as described in Section 3.1.4.1. The culture media was inoculated with 5 mL inoculum prepared as described in Section 3.1.3 to achieve a final working volume within the shake flasks of 100 mL. The cultures were grown at 30˚C, pH 8.5 with shaking at 200 rpm. Culture samples (2 mL) were taken at 2 hour intervals until the cultures entered stationary phase. Optical density and pH were measured. The raw data can be found in Appendix 1.2.

3.2.1.2 Comparison of growth in stirred-tank bioreactor using LB and EnBase® media

Bacillus halodurans Alk36 was grown in a batch culture using EnBase® media and LB broth in the BioFlo reactor (New Brunswick Scientific, USA). The reactor and culture media were prepared as described in Section 3.1.4.2. The culture media was inoculated with 300 mL inoculum prepared as described in Section 3.1.3 to achieve a final working volume within the reactor of 3 L. The cultures were grown at 30˚C, pH 8.5 with cascade agitation to maintain the dissolved oxygen concentration at 40%. The growth conditions (pH, temperature as well as agitation) were monitored and controlled with the BioCommand software (New Brunswick Scientific, USA) as described in Section 3.1.4.1. Culture samples (5 mL) were taken at 2 hour intervals until the cultures entered stationary phase. The samples were used to determine the culture's growth, amylase production, concentration of starch, glucose, organic acids as well as proteins. The raw data can be found in Appendix 1.2.

3.2.1.3 Determination of the oxygen transfer rates, the volumetric mass transfer coefficient and the oxygen utilization rate of *Bacillus halodurans Alk36* culture the stirred-tank bioreactor.

The oxygen-transfer rate (OTR) and the volumetric mass transfer coefficient (k_La) of the system were determined using the dynamic gas-in gas-out method prior to inoculation. Nitrogen gas was sparged into the system to remove the dissolved oxygen prior to the addition of air. Once aeration commenced, the dissolved oxygen concentration and the time to reach oxygen saturation was measured and used to determine the k_La and the OTR of the system. The oxygen utilization rate (OUR) was determined in exponential phase cultures. The air supply was turned off (at about 10 hours post-inoculation) and the dissolved oxygen (DO) concentration in the culture was recorded. The rate of change of the dissolved oxygen concentration (i.e. the decrease in dissolved oxygen concentration with time) due to bacterial metabolism represented the OUR. When the DO concentration reached 40%, the air supply was turned on to ensure the culture was not oxygen-limited. The biomass concentration of the culture, at the time when the OUR measurement was taken, was used to determine the specific oxygen utilization rate. The raw data can be found in Appendix 1.7.

3.2.2 Optimisation of growth conditions for improved biomass and amylase production by *Bacillus halodurans* Alk36

3.2.2.1 Determination of the oxygen transfer rate and the volumetric mass transfer coefficient in shake flasks

Mass transfer in the shake flasks was investigated to allow for the determination of operating conditions that ensure maximum oxygen transfer into the systems and hence the comparison of the cultures grown in shake flasks to those grown in the bioreactors. Mass transfer was investigated by determining the oxygen transfer rates and the volumetric mass transfer coefficient (k_La) at 200 rpm shaking frequencies with 10% and 20% filling volumes.

The sulphite-oxidation method was used to determine OTR in shake flasks due to unavailability of miniature probes required for direct measurement of the dissolved oxygen concentration on such a small scale. The method is based on the oxidation of sulphite by oxygen in the medium (Hermann et al., 2001).

Sulphite solution (1 M) was made in 0.1 M phosphate buffer and added into shake flasks at filling volumes of 10% and 20%. The catalyst ($CoSO_4$) was added to a final concentration of 10^{-7} M. The flasks were sealed with cotton wool bungs and incubated at 30˚C with shaking at 200 rpm. Samples (1 mL) were taken at regular intervals, added into acidified Iodine solution (deep brown in colour) and titrated with sodium thiosulphate (5 mM) solution until the solution turned colourless. The OTR of the system was determined from the rate of sulphite oxidation as described in Appendix 2.

3.2.2.2 Determination of the optimal pH for growth of *Bacillus halodurans* Alk36 in shake flasks using EnBase® media.

Bacillus halodurans cultures were grown in shake flasks using EnBase® media buffered at different pH to determine the optimal growth pH. The effectiveness of the buffer solutions to maintain the desired pH during growth in shaken reactors was also assessed.

The cultures were prepared as described in Section 3.1.4.1, however, the concentration of the carbon-source in the medium was reduced by three fold to mimic the bioreactor conditions where the cultures enters the stationary phase prior to becoming oxygen limited. Therefore, the results obtained from shake-flasks experiments could be compared to those obtained from the bioreactor experiments. The pre-inoculum and inoculum cultures used in these experiments were grown at different pH (pH 7 to 9) to ensure that the inoculum pH was closer to that of the culture medium to be inoculated and hence reduce the lag phase. Inoculum culture grown at pH 9 was used to inoculate the medium maintained at pH 10 and pH 11 since *B. halodurans* Alk36 did not grow above pH 9.

The flasks were sealed with cotton bungs and cultures were grown at 30°C while shaking at 200 rpm. Samples (1 mL) were taken at 2 hour intervals and used to measure the culture pH and optical density. The raw data can be found in Appendix 2.2.

3.2.2.3 Determination of the optimal pH for growth of *B. halodurans* Alk36 in EnBase® medium using the stirred-tank bioreactor system.

The Sixfors reactor system (Infors HT, Switzerland) was used for the determination of optimal pH for growth. The reactors were used to investigate culture growth at pH 7, 8, 8.5, 9, 10 and 11 in EnBase® media. The medium and reactors were prepared as described in Section 3.1.2 and 3.1.4.3, respectively. The pre-inoculum and inoculum cultures used in these experiments were grown at different pHs (pH 7 to 9) ensure that the inoculum pH is closer to that of the culture media to be inoculated and hence reduce the lag phase. Culture samples (5 mL) were taken at 2 hour intervals until the cultures entered stationary phase. The samples were used to determine the bacterial growth through measuring the optical density of the culture. Raw data can be found in Appendix 2.3.

3.2.2.4 Determination of the temperature for optimal growth of *Bacillus halodurans* Alk36

Shake flasks (500 mL volume) were filled with 50 mL water and sealed with cotton bungs. The vessels were weighed and incubated at 30°C, 37˚C, 42˚C and 50 ˚C with shaking at 200 rpm. The vessels were re-weighed every two or three hours (for about 9 to 12 hours) and the rate of water loss was used to calculate the evaporation rate. Raw data can be found in Appendix 2.3.

Bacillus halodurans Alk36 cultures, at pH 8.5, were grown in 500 mL Erlenmeyer flasks at five different temperatures i.e. 30˚C, 37˚C, 45˚C, 50˚C and 60˚C with shaking at 200 rpm in a humidified incubator shaker.

The cultures were prepared as described in Section 3.1.4.3. Sterile distilled water, equivalent to the amount of water loss from the culture, was added to the culture at 2 hours intervals to correct for evaporation. Samples were taken from the cultures every two hours post inoculation, following correction for evaporation, and used to determine pH of the culture and optical density. Raw data can be found in Appendix 2.3.

3.2.2.5 Determination of the effect of carbon-source on growth and amylase production

Bacillus halodurans cultures were grown in shake flasks with EnBase® media containing dextrin, soluble starch and maltose as carbon sources. The medium was prepared as described in Section 3.1.2. The cultures were grown at the optimal temperature and pH (determined from the above experiments) with 200 rpm shaking. Samples were taken at 2 hours intervals (until the cells entered stationary phase) to determine the pH, optical density and the growth rates as well as the amylase activity of stationary phase culture. Raw data can be found in Appendix 2.4.

3.2.3 Recovery, purification and characterisation of amylases

3.2.3.1 Protein concentration by ultra-filtration

Pierce™ protein concentrator units (Catalogue # 87739, Thermo Scientific) with a volume capacity of 20 mL and molecular weight cut-off of 9 kDa were used to concentrate the proteins within the *B. halodurans* Alk36 culture supernatants by filtration. Centrifugation is used to generate pressure which forces small molecules and proteins (< 9 kDa) to pass through the membrane while macromolecules such as polysaccharides and proteins larger than 9 kDa are retained in by the membrane. *Bacillus halodurans* Alk36 culture supernatant (50 mL) was added into the spin columns and centrifuged at 4000 x g for 40 to 60 minutes to concentrate the protein approximately 10-fold. The culture supernatant was obtained from shake flask cultures grown on EnBase® medium containing dextrin as the carbon source, at pH 8.5 and 30°C, with shaking at 200 rpm. The concentrated proteins were re-suspended in a buffer solution (5 mL) and stored at 4˚C in a sterile Eppendorf tube for further analysis.

3.2.3.2 Protein concentration by ammonium sulphate precipitation

Ammonium sulphate precipitation is commonly used to concentrate and purify proteins from solutions. The method involves saturating the protein solution with ammonium sulphate salt to remove the water required for solubilisation of proteins, causing the protein to aggregate, a phenomenon known as 'salting out' (Chick & Martin 1913; Foster et al., 1971). 'Salting out' divides the solution into two phases, the supernatant and the precipitate, which can be separated by centrifugation.

Preliminary experiments were done on the *B. halodurans* Alk36 culture supernatant to determine the optimal ammonium sulphate concentration required for fractionation and partial purification of the amylases. The culture supernatant was obtained from the bioreactor cultures grown on EnBase® medium at 30°C and pH 8.5. The culture supernatant was centrifuged at 17,664 g for 20 minutes at 4°C; the cell pellet was discarded and the supernatant was collected. The extracellular proteins in the supernatant were precipitated at 4°C by adding increasing amounts of solid ammonium sulphate in a stepwise fashion, from 0 to 80%, in 10% increments, in order to achieve the desired ammonium sulphate saturation in the amylase-containing supernatant. The amount of salt required to achieve a given saturation was calculated using the ammonium sulphate calculator (EnCor Biotechnology, 2013).

The solid ammonium sulphate was dissolved by gentle stirring for 12 hours at 4˚C to prevent denaturation of proteins. The protein precipitate fraction, at each ammonium sulphate saturation were collected by centrifugation at 17,664 g for 15 minutes at 4 °C. The supernatant obtained from centrifugation was retained and sequentially treated with solid ammonium sulphate in a step-wise fashion, as described above. The precipitate was re-suspended in 10 to 20 mL 0.1 M phosphate buffer (pH 8) and dialysed using cellulose membrane tubing (D9777, Sigma-Aldrich), to remove the ammonium salts. The concentrated protein solution was dialysed with 1 L phosphate buffer (0.1 M) at pH 8 for 6 to 12 hours, then stored at 4°C. Fractions containing high amylase activity were pooled and analysed by polyacralyrimide gel electrophoresis (PAGE) to determine the types of proteins present. Raw data can be found in Appendix 3.2.

3.2.3.3 Partial protein purification by activated charcoal

Activated charcoal was used to remove unwanted proteins from the culture supernatant containing amylases, according to the method by Kareem (2011). The culture supernatant of *B. halodurans* Alk36 grown in bioreactors with EnBase® medium at pH 8.5 and 35°C was partially purified by adding activated charcoal of 4 to 8 mesh particle size (C2764, Sigma-Aldrich) to a final concentration of 1% w/v. The solution was incubated at 4˚C with continuous stirring for 24 hours. The samples were then filtered to remove the charcoal using 0.45 µm filter membranes. The filtrate was analysed to determine the protein content and amylase activity. Raw data can be found in Appendix 3.2.

3.2.3.4 Partial purification of amylases by liquid chromatography

Liquid chromatography was used to further purify the partially purified amylase solution obtained from ammonium sulphate precipitation to obtain a solution containing one type of amylase for characterisation. Amylase in the *B. halodurans* Alk36 culture supernatant was concentrated by ammonium sulphate precipitation as described in Section 3.2.3.2. Fractions containing high amylase activity were pooled and purified based on charge, hydrophobicity and size. The total protein concentration and amylase activity of the samples obtained from the different purification stages were determined to assess the effectiveness of the purification step. Raw data can be found in Appendix 3.3.

a) Desalting and buffer exchange

Prior to chromatography, the protein sample was subjected to buffer exchange to replace the phosphate buffer with Tris buffer at pH 8 and concentrate the proteins. The phosphate buffer was removed to prevent interference caused by phosphate ions in the subsequent anion exchange chromatography. The desalting and buffer exchange processes use the principle of gel filtration to separate molecules based on size (Porath & Flodin 1959; Lindquist, 1962).

A HiPrep 26/10 desalting column and the AKTA explorer system (GE Healthcare Life Sciences) were used for buffer exchange. The HiPrep 26/10 column contains cross-linked Sephadex G-25 beads which form a matrix with an exclusion limit of 5 kDa. Hence the matrix allows small molecules (< 5 kDa) such as salt ions to pass through the pores while proteins and larger molecules are retained in the column (Porath, 1962; Gjessing & Lee, 1967).

The method described in the GE Healthcare Gel filtration handbook (2007a) was followed. The protein solution obtained from ammonium sulphate precipitation was loaded onto the column where the phosphate buffer (0.1 M) was replaced by 50 mM Tris buffer containing 200 Mm NaCl. The protein solution in Tris buffer was stored in ice for further analysis.

b) Anion exchange chromatography

A HiTrap Q HP 16/10 column (GE Healthcare Life Sciences) was used for anion exchange. The column contains a sepharose matrix made from highly cross-linked agarose particles (Cuatrecasas, 1970). The Q sepharose matrix contains a quaternary amine group carrying a positive charge, which interacts with negatively charged amino-acid residues of proteins in the solution (Cuatrecasas, 1970). Since proteins have different amino acid composition and hence net charges, their interaction with the column matrix varies. The method described in the GE Healthcare Ion Exchange Chromatography & Chromatofocusing handbook (2007b) was followed.

The protein solution obtained after desalting and buffer exchange was loaded into HiTrap Q HP 16/10 column (GE Healthcare Life Sciences) previously equilibrated with 50 mM Tris buffer (containing 200 mM NaCl) at pH 8. The column was equilibrated to ensure that the amine groups on the sepharose matrix were negatively charged and pH of the column was maintained at pH 8. At this pH the alpha amylases were negatively charged and expected to bind to the column since pH 8 is above the isoelectric point (IEP) of the alpha amylases (IEP≈5.4. The isoelectric point used in this study (pI of 5.4) was derived from the amino acid sequences of *B. halodurans* amylases obtained from the UniProt protein sequence database. The use of isoelectric point allows for the

separation of the amylases from proteins with net positive charge, which will not interact with the column matrix, or weak negative charge, which will interact weakly with the column matrix (Yamamoto et al., 1988; Kenney, 1992).

The proteins that bind to the column matrix were eluted depending on the strengths of their interaction with the column. Since protein with high negative charge binds strongly to the column, a linear gradient of 0.2 to 1.0 M NaCl salt solution (in 50 Mm Tris buffer) was used to elute the proteins that were bound to the column. The increase in salt concentration decreased the strength of the interactions between the protein and the matrix by reducing the net negative charge in the column (Yamamoto et al., 1988; Kenney, 1992). Protein elution was monitored by determining the absorbance at 280 nm, which is the absorbance maxima for proteins due to the presence of aromatic amino acids (Layne, 1957). Samples containing protein peaks observed from the chromatograms were pooled and concentrated using Amicon Ultra-filtration discs with 10 kDa cut-off (Merck Millipore). Starch-zymography was used to analyse the concentrated protein samples to determine samples containing amylases using the method that will be described later (3.3.5.2).

c) Hydrophobic interaction chromatography

The protein solution containing the amylases was further purified by hydrophobic interaction chromatography using a HiPrep Phenyl HP 16/10 column (GE Healthcare Life Sciences). The HiPrep Phenyl HP 16/10 column consists of highly cross-linked agarose beads containing phenyl groups bound to the matrix via ether linkages. The method described in the GE Healthcare hydrophobic interaction and reverse-phase chromatography handbook (2006) was followed.

The column was equilibrated with 50 mM Tris buffer containing 2 M NaCl prior to protein loading. The protein solution, containing amylases, obtained from anion exchange chromatography was added into the column. In the presence of the high salt concentration, the ionic interactions between the charged groups on the protein molecules and water were minimized (O'Farrell, 1996). Hence, the hydrophobic amino acids on the protein molecules become exposed to and interact with the hydrophobic

phenyl groups on the column since the salt quenches the water from the solution (O'Farrell, 1996).

The proteins were eluted with a decreasing linear gradient of 2 M NaCl salt solution, in 50 Mm Tris buffer. The reduction of salt in the buffer weakened the interactions between the hydrophobic proteins and the column matrix and facilitated the elution of the proteins, starting with proteins that were least hydrophobic to those that were highly hydrophobic (O'Farrell, 1996).Protein elution was monitored by determining the absorbance at 280 nm and samples containing protein peaks observed from the chromatograms were pooled and concentrated using Amicon Ultra-filtration discs with 10 kDa cut-off (Merck Millipore). Starch-zymography was used to analyse the concentrated protein samples to determine samples containing amylases.

Samples containing amylases were separated based on their size by gel filtration using a HiPrep 16/60 Sephacryl S-200 HR column (GE Healthcare Life Sciences). The column was equilibrated with a 50 mM Tris buffer containing 2 M NaCl (at pH 8) prior to protein loading. The proteins were eluted using the same buffer and the fractions containing eluted proteins were pooled and analysed by starch zymography to determine fractions containing amylases. The samples were stored at°C for further analysis, i.e. determination of total protein concentration and amylase activity.

d) Gel filtration chromatography

The protein fractions that contained the amylases, obtained from the hydrophobic interaction chromatography were further purified by gel filtration based on the size of the proteins. Gel filtration was done using the Sephacry S200 column (GE Healthcare Life Sciences) which consist of a hydrophilic matrix of cross linked dextran molecules. The dextran matrix can separate globular proteins of molecular weight between 5 and 250 kDa and has an exclusion limit if 400 kDa(GE Healthcare Life Sciences). The method described in the GE Healthcare Gael filtration handbook (2007a) was followed.

The protein solution obtained from hydrophobic-interaction chromatography was loaded onto the column and eluted using 20 mM Tris buffer at pH 8.5 containing 200 mM NaCl.

Protein separation was based on interaction between the proteins and the matrix pore, depending on the size and shape of the proteins. Small proteins that could fully or partially penetrate into the pores interacted with the matrix for longer and hence eluted last (Andrews, 1964; Mori & Barth, 1999). Large proteins either passed through the column or interacted briefly with the pores and hence eluted early (Andrews, 1964; Mori & Barth, 1999).

Fractions containing eluted proteins were pooled and analysed by starch zymography to determine fractions containing amylases. The samples were stored at 4°C for further analysis, i.e. determination of total protein concentration and amylase activity.

3.3 Analytical procedures

3.3.1 Biomass assays

3.3.1.1 Determination of bacterial optical density

Optical density (OD) represents the light-scattering capacity of a suspension due to the presence of particulate matter such as cells. Thus an increase in cell number leads to an increase in cell density and hence the optical density of the culture.

The Genesys 10UV spectrophotometer (Thermo Scientific) was used to measure the optical density of the culture samples (2 mL) at a wavelength of 600 nm. At this wavelength the absorbance of light by other molecules in the cell, such as flavins and carotenoids is minimal. The spectrophotometer was calibrated with the culture medium prior to taking the OD readings. The OD readings were measured in duplicate at each time point to determine reproducibility of the OD readings. Samples with OD values ≥ 1 were diluted in water because, at high cell density, the linear relationship between light absorbance and cell concentration is violated i.e. the Beer Lambert's law does not hold (Lawrence & Maier, 1977). For the diluted samples the actual culture OD was determined from the product of the absorbance of the diluted sample and the dilution factor. Raw data can be found in Appendix 1.2.

3.3.1.2 Determination of bacterial dry weight

Bacillus halodurans Alk36 culture samples (10 mL) were filtered through 0.45 µm pre-weighted filters to separate the cells from the filtrate. The filtration was done in triplicate and the filtrate/supernatant was stored at 4°C for subsequent analyses. The biomass - containing filter papers were dried in an oven at 80°C for 24 hours and then cooled in a desiccator prior to weighing of the dry biomass. The biomass dry weight was used to determine the correlation factor representing the relationship between the bacterial optical density and dry weight.

3.3.2 Carbon concentration assays

3.3.2.1 The starch-iodine assay

The concentration of starch in the culture filtrates was measured using the starch-iodine assay. The starch-iodine assay is based on the interaction between starch and iodine to form a blue-coloured complex with maximum absorption between 450 and 650 nm (Rundle et al., 1944, Baldwin et al., 1944; Rundle et al., 1944; Swanson, 1948).

Bacillus halodurans Alk36 culture filtrates (200 µL) were mixed with equal volumes of 1 M HCl to inactivate the amylase(s) and generate acidic pH conducive for the formation of the starch-iodine complex. The solution was diluted such that the starch concentration was≤ 1 g/L prior to addition of 50 mM iodine solution (50 µL). The solution was mixed by vortexing and 200 µL was transferred into a single well of 96-well microwell plates. Its absorbance was determined at 580 nm using the FLUOstar Omega microplate reader (BMG Labtech). The assay was done in triplicate and the absorbance units were converted to starch concentration using a starch standard curve prepared across the concentration range of 0 to 1 g/L at 0.2 g increments. Raw data and the standard curve can be found in Appendix 1.4.

3.3.2.2 The Dinitrosalicylic acid assay

The dinitrosalicylic acid (DNS) assay, described by Miller (1959) was used to determine the residual concentration of reducing sugars in the *B. halodurans* Alk36 culture filtrate. The culture filtrate was diluted as required in 0.1 M phosphate buffer at pH 8 such that the concentration of reducing sugars was within the linear range of the assay i.e. 0.06 g/L and 4 g/L (Goncalves et al., 2010). The DNS acid solution (500 µL) and the diluted sample (500 µL) were mixed and boiled at 90°C for 15 minutes to allow for the reduction of 3,5-dinitrosalysilic acid and hence colour formation. The solution was cooled prior to addition of 1 mL 40% (w/v) potassium tartrate salt, to stabilize the 3-amino-5-nitrosalicylic acid. The solutions were mixed by vortexing and 200 µL was transferred into a single well of a 96-well multiwell plate. The absorbance of the solution was determined at 575 nm using the FLUOstar Omega microplate reader (BMG Labtech). The assay was done in triplicate and the absorbance units were converted to glucose concentration using a standard curve, prepared with glucose solutions across a concentration range of 0 to 100 mg/L at 20 mg/L increment. Raw data and the standard curve can be found in Appendix 1.4.

3.3.2.3 High performance liquid chromatography

The presence of glucose and organic acids in the culture was determined by high performance liquid chromatography (HPLC, Spectra System LC, Thermo Scientific) using the Aminex HPX-87H column. The analysis was done at room temperature using acidified water (0.001M) as the mobile phase, at a flow rate of 0.6 mL/min. The samples were diluted such that the concentration of glucose was $\leq$ 10 g/L and sterilized by filtration using 0.22 µm Millex syringe filter units (Millipore, Corp.) prior to analysis. The ultra violet (UV) detector (set at 210 nm) and the refractive index (RI) detector were used for the detection of organic acids and glucose, respectively. The concentration of metabolites was determined by comparing the areas under the peaks on the chromatogram obtained from the samples to those obtained from the glucose and acetic acid standard samples across a concentration range of 0 to 10 g/L, at 2 g/L increment.

Both samples and standards were analysed in triplicate to indicate reproducibility. Raw data and the standard curves can be found in Appendix 1.5.

3.3.3 Determination of total protein concentration

The Bradford assay (Bradford, 1976), was used to determine the concentration of soluble protein in *B. halodurans* Alk36 culture filtrates. The BioRad microassay was used in the present study where 1 mL of Bradford solution (Bio-Rad) was added to 100 µl of the protein sample (diluted with 0.1 M phosphate buffer at pH 7 to ensure that the concentration of protein was within the detection limits). The solutions were mixed by vortexing and incubated at room temperature for 5 minutes to allow colour development, after which 200 µL was transferred into a single well of a flat bottom 96-well microtiter plate. The absorbance of the solution was determined at 595 nm using the FLUOstar Omega microplate reader (BMG Labtech). The assay was done in triplicate and the average absorbance units were converted to protein concentration using a standard curve prepared with Bovine Serum Albumin (BSA) across a concentration range of 0 to 100 mg/L at 20 mg/L increment. Raw data and the standard curve can be found in Appendix 1.10.

3.3.4 Determination of amylase activity

3.3.4.1 The Starch-Iodine assay

The method described by Fuwa (1954) was used to determine amylase activity of the culture supernatant. This method uses the starch-iodine assay to determine the amount of starch remaining after hydrolysis by amylases to establish the rate of starch hydrolysis.

Briefly, 500 µL of the sample solution containing amylase was added in five test tubes and incubated in a water bath at 50°C for 15 minutes. The amylase solution was pre-warmed to 50°C, the apparent optimal temperature for *B. halodurans* amylase activity based on literature (Hashim et al., 2005; Murakami et al., 2007). Equal volumes of 1% soluble starch, pre-warmed at 50°C, were added to the amylase solution. A high

concentration of the starch solution was used to ensure saturation of the enzyme with substrate (Eadie, 1926; Huggins & Rusels, 1948). The solution was incubated at 50°C for 10 minutes to allow for starch hydrolysis and the time course of hydrolysis was monitored by stopping the amylase reaction through the addition of 1 M HCl (200 µl) at 0, 2, 4, 6, 8 and 10 minutes (in one test-tube at a time). Immediately after addition of the acid, the test tubes were removed from the water bath, thoroughly mixed by vortexing and allowed to cool. After cooling, 200 µL iodine solution (5 mM) was added and the concentration of residual starch was determined as described in Section 3.3.2.1. The enzyme solution was diluted such that a linear rate of production of reducing sugars was obtained. Raw data can be found in Appendix 1.10.The amylase activity was calculated from the linear rate of starch hydrolysis as illustrated by the following equation:

$$\text{Amylase activity}\left(\text{U.mg}^{-1}\text{ protein}\right) = \frac{\text{Rate of starch hydrolysis}\left(\text{g.L}^{-1}\text{.min}^{-1}\right)}{[\text{protein}]\left(\text{mg.L}^{-1}\right)} \qquad \text{Equation 3.1}$$

Where 1 U of activity is equivalent to the mg of starch hydrolyse per minute under assay conditions.

3.3.4.2 The Dinitrosalicylic acid assay

The DNS assay was also used to determine amylase activity though measuring the reducing sugars produced from starch hydrolysis by amylases. The amylase solution was incubated with starch solution to allow for starch hydrolysis as described above (Section 3.11). Briefly, 500 µL of the sample solution containing amylase was added in five test tubes and incubated in a 50°C water bath for 15 minutes after which 500 µL of pre-warmed 1% soluble starch was added. The solution was incubated at 50°C for 10 minutes to allow for starch hydrolysis and the amylase reaction was stopped by the addition of DNS acid solution (1 mL) at 0, 2, 4, 6, 8 and 10 minutes (in one test-tube at a time). The amount of reducing sugars was determined as described in Section 3.3.2.2. The enzyme solution was diluted such that a liner rate of production of reducing sugars was obtained. Raw data can be found in Appendix 1.10. The amylase activity was

calculated from the linear rate of production of reducing sugars using the following equation:

$$\text{Amylase activity}\left(\text{U.mg}^{-1}\text{ protein}\right) = \frac{\text{Rate of formation of reducing sugars}\left(\text{g.L}^{-1}\text{.min}^{-1}\right)}{[\text{protein}]\left(\text{mg.L}^{-1}\right)} \quad \text{Equation 3.2}$$

Where 1 U of activity is equivalent to the amount of mg of glucose released per minute under assay conditions.

3.3.5 Determination of the presence of amylases in the culture supernatant by Polyacrylamide gel electrophoresis (PAGE)

Polyacrylamide gel electrophoresis (PAGE) was used to determine the different types of proteins present in the culture supernatant and concentrated protein solution based on their size. The method relies on the migration of protein through a porous polymer across an electric field; hence protein migration is based on electrophoretic mobility i.e. the size and charge of the protein (Ornstein, 1959; Clarke, 1959, Weber & Osborne, 1969). Small proteins migrate further through the gel than large proteins since small proteins can diffuse through the gel pores more easily than large proteins (Mauer, 1978; Scopes 1994). The size of the pores can be altered by increasing or decreasing the concentration of acrylamide in the gel, so as to enhance or reduce protein resolution, respectively (Mauer, 1978; Scopes, 1994). An electric field applied across the gel forces the negatively charged proteins to migrate towards the positively charged anode; hence speeds up the diffusion of proteins through the gel (Mauer, 1978l; Scopes, 1994). Three forms of PAGE analysis were performed, namely denaturing SDS-PAGE, native or non-denaturing PAGE and substrate PAGE or zymographs.

3.3.5.1 Denaturing PAGE

Denaturing PAGE was done, according to the method described by Laemmli (1970), using 12% acrylamide gels. Sample buffer (30 µL) containing β-mercaptoethanol,

sodium dodecyl sulphate (SDS), Tris buffer at pH 8 and glycerol was added into 10 µL protein samples. Beta-mercaptoethanol was used to reduce the covalent disulphide bonds that stabilize protein's tertiary and quaternary structure (Weber & Osborne, 1969). The SDS was used to unfold the proteins, by breaking up the two- and three-dimensional structures of the proteins, and give the protein strand a uniform negative charge per unit length (Dunker & Rueckert, 1969; Scopes, 1994). Tris buffer was added to maintain the pH of the solution while glycerol was added to increase the density of the samples, allowing the sample to sink to the bottom of the wells during gel loading. The samples were heated at 90C for 10 minutes for further denaturation of proteins (Weber & Osborne, 1969) and 35 µL was loaded into the gel together with Page Ruler prestained protein ladder (Pierce Biotechnology, USA). The samples were electrophorised for 180 minutes at a constant voltage of 200 V in SDS-PAGE running buffer containing 1 g/L SDS, 3.03 g/L Tris and 14.41 g/L Glycine. Thereafter, the polyacrylamide gels were removed from the electrophoresis apparatus and stained for a minimum of two hours at room temperature with Coomassie staining solution containing 0.25% (w/v) Coomassie Brilliant Blue-R250 10% (v/v), glacial acetic acid and 50% (v/v) methanol. Protein bands were visualized after removing excess Coomassie stain from the polyacrylamide gels using the destaining solution [made up with 10% (v/v) glacial acetic acid and 50% (v/v) methanol] until the protein bands were clearly visible. The approximate size of the protein bands was estimated by comparing their relative mobilities to that of the molecular weight marker that had been electrophorised on the same polyacrylamide gel.

3.3.5.2 Native PAGE

Native PAGE was performed under non-denaturing conditions to maintain the protein's structure and activity. The gels and samples were prepared similarly to that for SDS-PAGE, except that SDS and beta-mercaptoethanol were omitted from the loading buffer and the protein samples were not heated åC 90 prior to loading into the gels. Moreover, electrophoresis was done in a running buffer without SDS. The gels were

stained with Coomassie staining solution and the bands were visualized as described above, in Section 3.4.5.1.

3.3.5.3 Starch-zymography

Starch-zymography is a common tool for characterisation of enzyme-substrate specificity (Ayrapaa & Nihlen, 1954; Hunter & Burstone, 1960). Starch zymography involves electrophoresis of samples using a gel containing starch and then staining the gel with iodine to identify bands containing active proteins i.e. proteins that can hydrolyse starch (Ayrapaa & Nihlen, 1954; Smithies, 1955). The iodine will interact with starch to form blue coloured complex which will turn the gel blue except for regions where starch has been hydrolysed (Ayrapaa & Nihlen, 1954; Smithies, 1955). These regions appear white and hence proteins present in the white zones are identified as active bands.

Starch-zymography was done in a similar manner as the native PAGE (Section 3.4.5.2); except that soluble starch was added to the gel to a final concentration of 10 g/L. Further, after electrophoresis, the gels were stained with 50 mM iodine solution and excess iodine was removed by washing the gel with distilled water.

3.3.6 Protein identification by Peptide Mass Fingerprinting (PMF)

Peptide Mass Fingerprinting (PMF) was used to identify protein bands that showed amylase activity on zymographs by comparing their peptide sequences to those of known proteins in databases (Pappin, Hojrup & Bleasby, 1993). PMF analysis was done to confirm if the protein bands that showed activity on starch zymography were amylases since several proteins can interact with starch in the zymographs.

PMF analysis was done at the Centre for Proteomic and Genomic Research (South Africa) using active bands excised from the zymographs. The bands were dried with acetonitrile (500 µL) for 2 hours after which the acetonitrile was removed and the bands were air dried to remove the residual acetonitrile.

The proteins in the gel pieces were treated with reducing and alkylation reagents to break down the disulphide bonds by reducing cystines or cysteines in the proteins (Wedemeyer et al., 2000). Thereafter, the proteins were digested with Trypsin, which cleaves protein molecules at the carbonyl side of Lysine or Arginine, when the amino acids are not found next to Proline (Davie & Neurath, 1955). The resulting peptide fragments were extracted from the gels, purified and concentrated prior to analysis by mass spectrometry, using the matrix-assisted laser desorption/ionisation (MALDI).

The experimental mass values obtained from the mass spectrometry were then compared with peptide mass values calculated by applying Trypsin cleavage rules to the entries in the MSDB protein database. The Mascot algorithm (Matric Science) was used to determine the closest match or matches.

Chapter Four

Amylase production by *B. halodurans* Alk36

4.1 Introduction

Bacillus halodurans, initially known as *Bacillus brevis,* is an alkaliphilic bacterium that can grow between pH 8 and 10 (Louw et al., 1993). It produces endogenous amylase(s) active in alkaline conditions ((Louw et al., 1993; Hashim et al., 2005; Murakami et al., 2007; Murakami et al., 2008). The aim of this study was to investigate the production and characterisation of amylase(s) by a locally isolated strain, *B. halodurans* Alk36.

To determine the types of amylase(s) produced by *B. halodurans* Alk36, the strain was grown in a commercial medium called EnBase® and compared to the complex Luria broth (LB) media. The EnBase® medium is a minimal salt medium containing starch, trace elements and a booster solution containing complex carbon and nitrogen sources (Krause et al., 2010). Typically, glucose is released from the starch through the addition of a commercial glucoamylase (Krause et al., 2010). In this study, the commercial amylase was omitted so that any growth in the EnBase® medium would be attributed to the activity of the endogenous amylase(s) produced by *B. halodurans* Alk36.

In this section the growth kinetics and biomass production in EnBase® and LB media were compared to determine the best medium for growth and the production of amylase(s). The relationship between amylase production and the growth cycle was identified. The amylase(s) produced by *B. halodurans* Alk36 were identified and compared to alkaliphilic amylases described in literature based on the amylase activities.

4.2. Growth of *B. halodurans* Alk36 in shake-flask cultures

Preliminary growth studies were done in shake-flasks to determine the growth profile of *B. halodurans* Alk36 in EnBase® and LB media. The cultures were grown as described in Section 3.1.4.1 (page 46); pH and optical density were monitored throughout growth until the cultures entered stationary phase. The raw data is presented in Appendix 1.1.

The growth profiles of the culture in EnBase® medium and LB medium were similar in shape, as shown in Figure 4.1, with LB medium presenting faster growth. This growth of *B. halodurans* Alk36 in EnBase® medium without addition of commercial amylase indicated that *B. halodurans* Alk36 produced endogenous amylase(s) that can hydrolyse starch to produce simple sugars (such as glucose) that can be assimilated for growth.

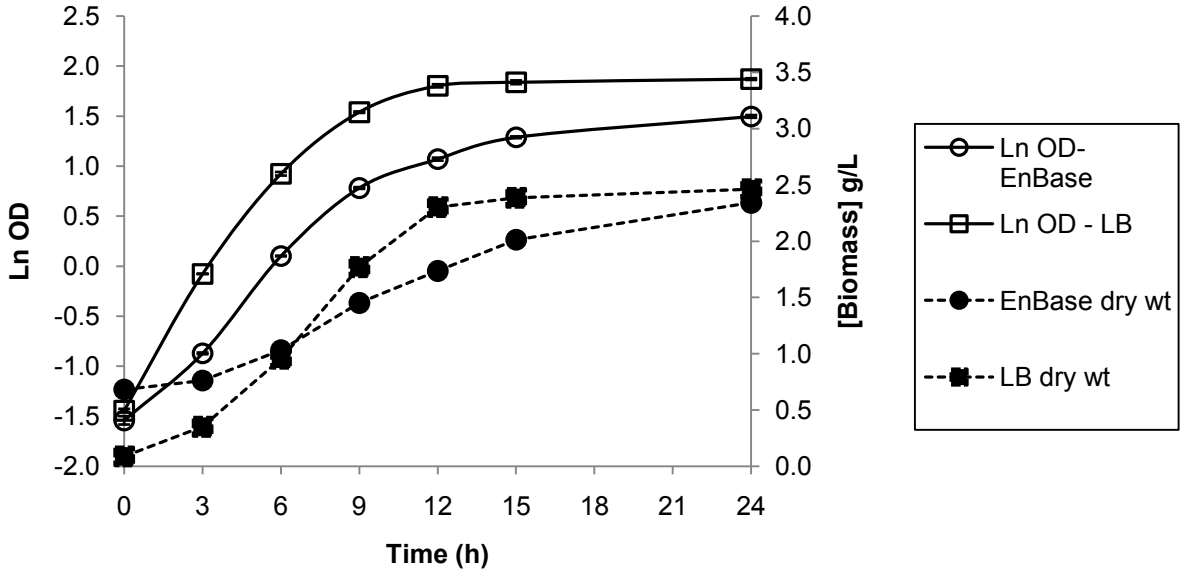

Figure 4.1: Growth profile of *B. halodurans* Alk36 culture grown in shake-flasks using EnBase® and LB media at 30°C with shaking at 180 rpm. The values presented were calculated from the averages from triplicate experiments and the error bars were derived from the standard deviation of the values obtained from the triplicate experiments. Where error bars are not visible, they are within the dimensions of the symbols.

The maximum specific growth rate was calculated according to the Monod equation using exponential phase data from the slope of the plot of ln(OD) as a function of time. The maximum specific growth rate achieved in EnBase® medium (0.27± 0.02 h^{-1}) was lower than that achieved in LB medium (0.39 ± 0.04h^{-1}), probably due to the readily available carbon-source and amino acids in LB medium as shown in Figure 4.1. In EnBase®, the growth rate may be expected to be constrained by the availability and activity of amylase. The biomass concentration was determined through the construction of a standard curve correlating dry cell weight (DCW) and optical density,

where 1 OD at 600nm was corresponded to 0.38 g/L DCW as illustrated in Appendix 1.2.At stationary phase, the biomass concentration attained by the culture grown in LB medium (2.46 ± 0.01 g/L) was similar to that attained by cultures grown in EnBase® medium (2.34 ± 0.62 g/L). The biomass concentration obtained in the EnBase® culture was lower than expected, considering that the concentration of the carbon in the EnBase® medium (1.56 M Carbon) was three and a half times higher than that in the LB medium (0.44 M Carbon, assuming that all the carbon present as amino acids could be utilised by the bacterium) (Appendix 1.6). Thus, the lower biomass concentration observed in the EnBase® cultures could be due to the limitation of a nutrient other than carbon, e.g. nitrogen or oxygen. The pH of the EnBase® culture decreased from about pH 8.38 to pH 6.87, while that of the culture grown in LB medium decreased from pH 8.36 to pH 7.81 and then increased to pH 8.78 after 24 hours, as shown in Figure 4.2. The increase in pH is a characteristic of LB medium, owing to the production of alkaline amines through catabolism of peptides in the medium (Sezonov et. al, 2007).

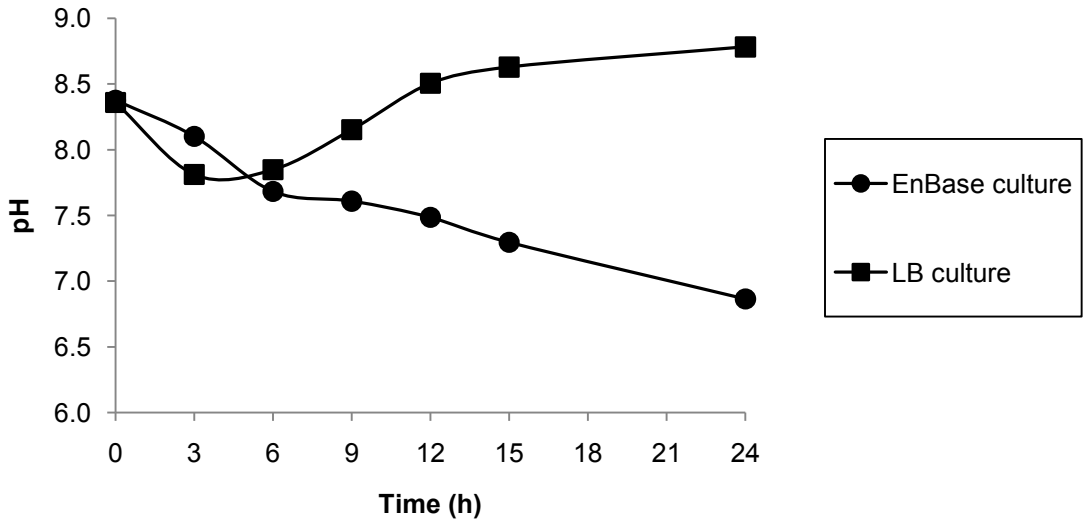

Figure 4.2: Change in pH with time in *B. halodurans* Alk36 cultures grown in shake-flasks with EnBase® and LB media at 30°C with shaking at 180 rpm. The values presented were calculated from the average of triplicate experiments and the error bars were derived from the standard deviation of triplicate values. The error bars are not visible because they are within the dimensions of the symbols.

The decrease in pH in cultures grown in EnBase® medium was probably due to

utilisation of the nitrogen source i.e. $(NH_4)_2SO_4$. Even though the pH of the EnBase® medium was adjusted to pH 8 (starting pH), the pH of the culture decreased throughout growth to pH 7. The decrease in pH could have been due to the fact that the EnBase® medium is constructed to buffer at pH 7. Hence, it was suggested that the medium should be re-constructed (following this experiment) to improve the buffering capacity at pH 8. Since *B. halodurans* requires pH 8 to10 for optimal growth (Louw et al., 1993; Murakami et al., 2007; Murakami et al., 2008), the decrease in pH may have resulted in the lower biomass concentration observed in the EnBase® cultures compared to that expected from nutrients provided.

The shake flask system did not allow control of some factors important for growth of *B. halodurans* Alk36, such as pH discussed above. Further, it was not known if the amount of oxygen provided in the shake flask system was sufficient to ensure that the *B. halodurans* Alk36 culture was not oxygen limited. In order to minimise factors limiting growth and to maintain steady conditions such as oxygen transfer rates and pH, *B. halodurans* Alk36 was cultivated in a stirred tank bioreactor to enable a fair comparison of growth based on medium composition alone.

4.3 Growth of *B. halodurans* Alk36 in a stirred-tank bioreactor

The *B. halodurans* cultures were grown in a stirred-tank bioreactor where pH, temperature and dissolved oxygen concentration were controlled and monitored for 24 hours as described in Section 3.1.4.1. Biomass concentration, at different time points, was measured and the data for these experiments is presented in Appendix 1.3.

As shown in Figure 4.3, the culture grown in LB medium had a higher growth rate and entered stationary phase earlier than the culture grown in EnBase® medium. The LB culture entered stationary phase at about 8 hours, while the EnBase® culture entered stationary phase at about 16 hours. The maximum specific growth rate in LB broth (0.52 h^{-1}) was higher than that in EnBase® medium (0.41 h^{-1}). Two-phase growth was observed in cultures grown in EnBase® medium, where the initial growth rate was 0.40 h^{-1} for the first 8 hours (post inoculation) and then decreased to 0.23 h^{-1}.

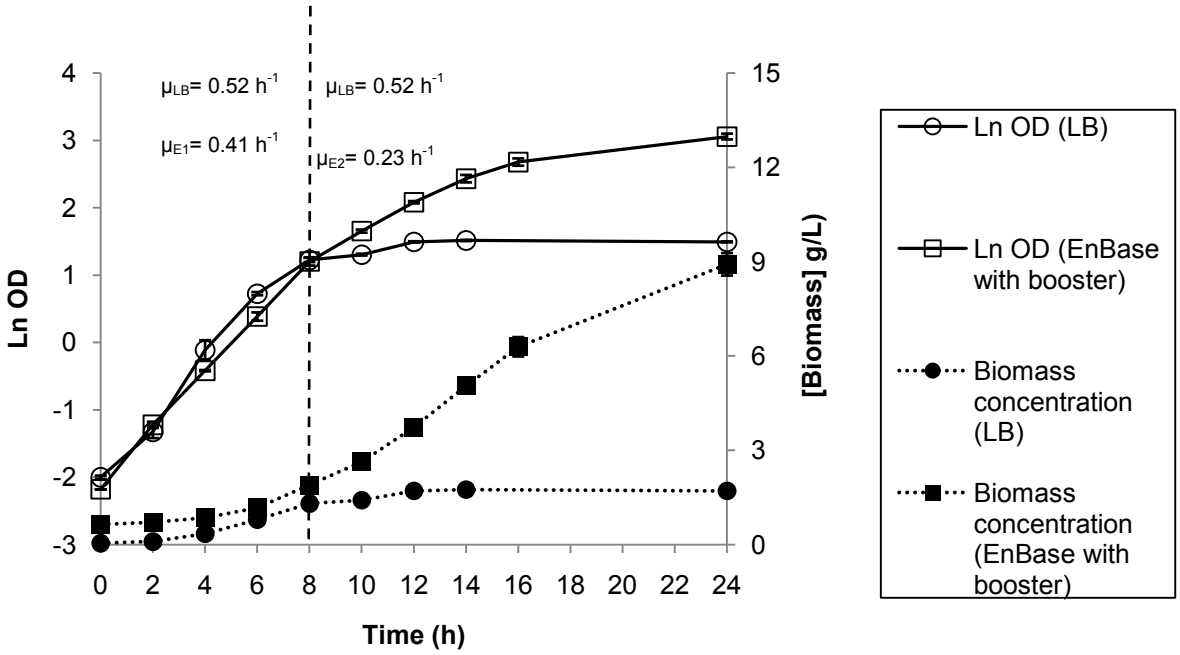

Figure 4.3: Growth profile of *B. halodurans* Alk36 in LB and EnBase® media. The cultures were grown in a stirred tank bioreactor at 30°C , pH 8 to 8.5 and cascade agitation between 200 and 1000 rpm. The growth rates in EnBase® medium, during the two-phase growth period, are represented by μ_{E1} and μ_{E2} while that in LB medium is represented by μ_{LB}. The plots represent averages from duplicate experiments and the error bars were derived from the standard error of the mean. Where the error bars are not visible, they are within the dimension of the symbols.

The two-phase growth observed in the cultures grown in EnBase® medium did not display a typical biphasic shape of diauxic growth with two sigmoidal branches associated with the change in metabolism of one substrate to another (Narang & Pilyugin, 2007). The absence of transitional lag phase associated with the diauxic growth suggested that the culture had become nutrient limited or had changed the metabolic pathway. Hence, the diauxic growth observed in the EnBase® culture could have been due to initial growth on complex carbon and nitrogen sources in the booster solution. Once the booster solution was depleted and/or a sufficient amount of amylase had been produced (by virtue of there being more biomass), the metabolism switched

to starch utilisation or became dependent on starch utilisation only, where the growth rate was dependent on the rate of glucose released from the starch polymer. The absence of transitional lag phase associated with diauxic growth also suggested that *B. halodurans* Alk36 constitutively expressed amylases.

The maximum biomass concentration in the EnBase® culture (8.92 g/L) was about 5 times higher than that achieved by the LB culture (1.72 g/L), as shown in Figure 4.3. Similar results were observed by Krause et al. (2010), where *E. coli* cultures grown in EnBase® medium attained higher biomass concentrations compared to cultures grown in minimal salt, LB and Terrific Broth media. The improved biomass production in EnBase® medium was due to the higher content of carbon source and the controlled release of glucose (Krause et al., 2010). In the present study, the biomass yield (on carbon) obtained from cultures grown on EnBase® medium (0.24 moles biomass per moles carbon) was also higher than that of the cultures grown in LB broth (0.16 moles biomass per mole carbon) as illustrated in Table 4.1.

Table 4.1: The biomass concentrations, maximum growth rate (μ_{max}) and biomass yields achieved by the cultures grown in LB and EnBase® media in a stirred-tank bioreactor (based on the amount of carbon added into the medium).

Media	Amount of carbon in the media (moles/L)	μ_{max} (h^{-1})	Average maximum biomass concentration (g/L)	Maximum carbon concentration in the biomass (moles/L) [a]	Biomass yield on carbon (moles biomass per moles carbon)
LB	0.44	0.51	1.72	0.071	0.16
EnBase®	1.56	0.41[b] 0.23[c]	8.92	0.368	0.24

a - The carbon concentration in the biomass was calculated using the general empirical formula for aerobic bacteria i.e. $CH_{1.8}O_{0.5}N_{0.2}$ (Bailey & Ollis, 1986).

b - The initial growth rate in EnBase®, from t_0 to t_8, suspected to be based on utilisation of nutrients provided by the booster solution.

c - The growth rate in EnBase® after t_8, suspected to be based on the rate of glucose released from starch by endogenous amylase/s.

The yield calculated for LB cultures may be underestimated since it was assumed that all carbon was consumed for biomass production. The residual carbon content in LB broth was not measured nor was overflow metabolism considered. From the improved biomass yield for cultures grown in EnBase® medium, it is thus postulated that *B. halodurans Alk36* has the ability to utilize starch more efficiently than it can utilize the carbon sources in LB medium. To determine the amount of residual carbon in EnBase® cultures, the starch hydrolysis by amylase(s) from *B. halodurans* Alk36 was investigated (Table 4.4).

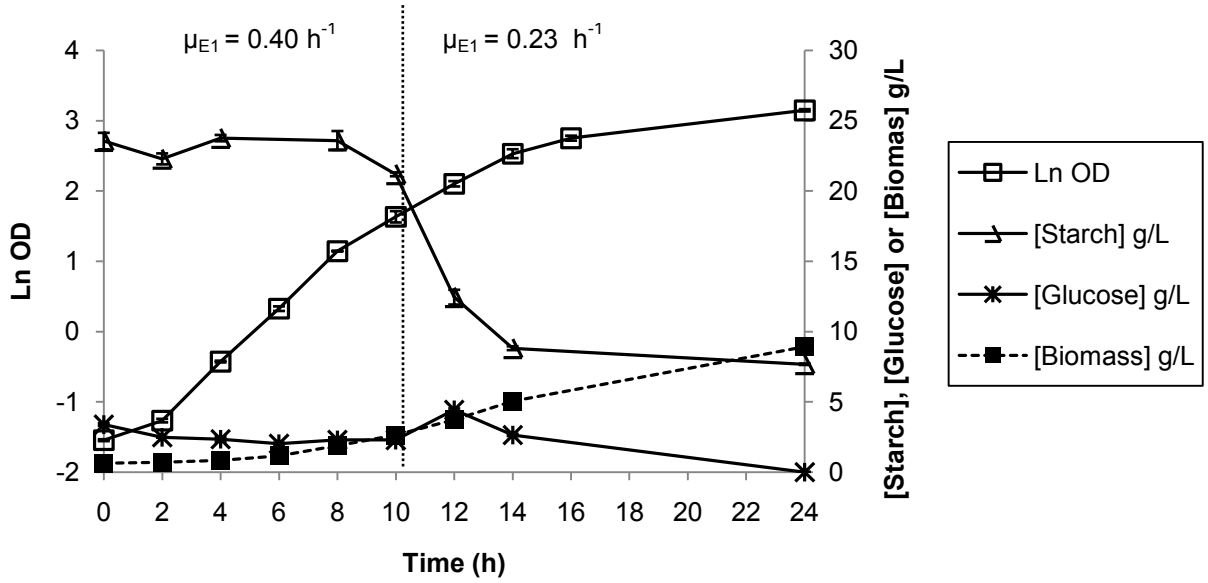

Figure 4.4: The starch utilisation profile of *B. halodurans* Alk36 culture grown on EnBase® medium with booster solution in a stirred tank bioreactor at 30C and pH 8.5. The dotted line distinguishes the two growth stages represented by the specific growth rates (μ). The starch and glucose values presented were calculated from the averages of triplicate readings of the same samples and their standard deviation. The growth profiles represent averages from duplicate experiments and the error bars were derived from the standard error of the mean. Where error bars are not shown, these are within the dimension of the symbols.

The concentration of starch in the EnBase® culture showed little change, about 23.54 g/L, during the first 8 hours post inoculation (Figure 4.4). The relatively constant starch concentration, during this period, suggested that growth was due to the presence of complex nutrients provided by the booster solution. The starch concentration decreased to about 8 g/L as the cells entered stationary phase.

The residual glucose concentration in solution lay between 2 and 3 g/L between 0 and 8 hours, peaked at 3.75 g/L at 12 hours post inoculation, and reduced to 0 g/L by 24 hours (as illustrated in Figure 4.4). The observed free glucose in the medium, at the start of the cultivation, may have resulted from starch hydrolysis during medium sterilization. The increase in glucose concentration at 12 hours post inoculation could have been due to a higher rate of glucose released (enzymatically) than the utilisation rate, owing to increasing cell number and the contribution of complex media components to nutrient provision. From this point onwards, it is postulated that the cells shifted their metabolism to utilising the glucose released from starch, hence the residual glucose concentration decreased.

The change in carbon metabolism coincided with the change in the growth rate assumed to be due to the initial utilization of complex additives in the booster solution, followed by utilization of starch. For this reason, the effect of booster solution on growth of *B. halodurans* Alk36 was assessed by omitting the booster solution from EnBase® medium. The growth profile of the culture grown in conventional EnBase® medium was compared to that grown in the absence of booster solution (Figure 4.5).

The cells grown in EnBase® medium without booster grew more slowly than the cells grown with booster solution. The culture grown without booster solution grew linearly (the average growth rate was 0.26 h^{-1}) until the cultures entered stationary phase. The growth rate in EnBase® medium without booster solution (0.26 h^{-1}) was similar to that of the cells grown in EnBase® medium with booster solution following the assumed depletion of the booster solution i.e. 8 hours post inoculation (0.23 h^{-1}) as shown in Figure 4.5.

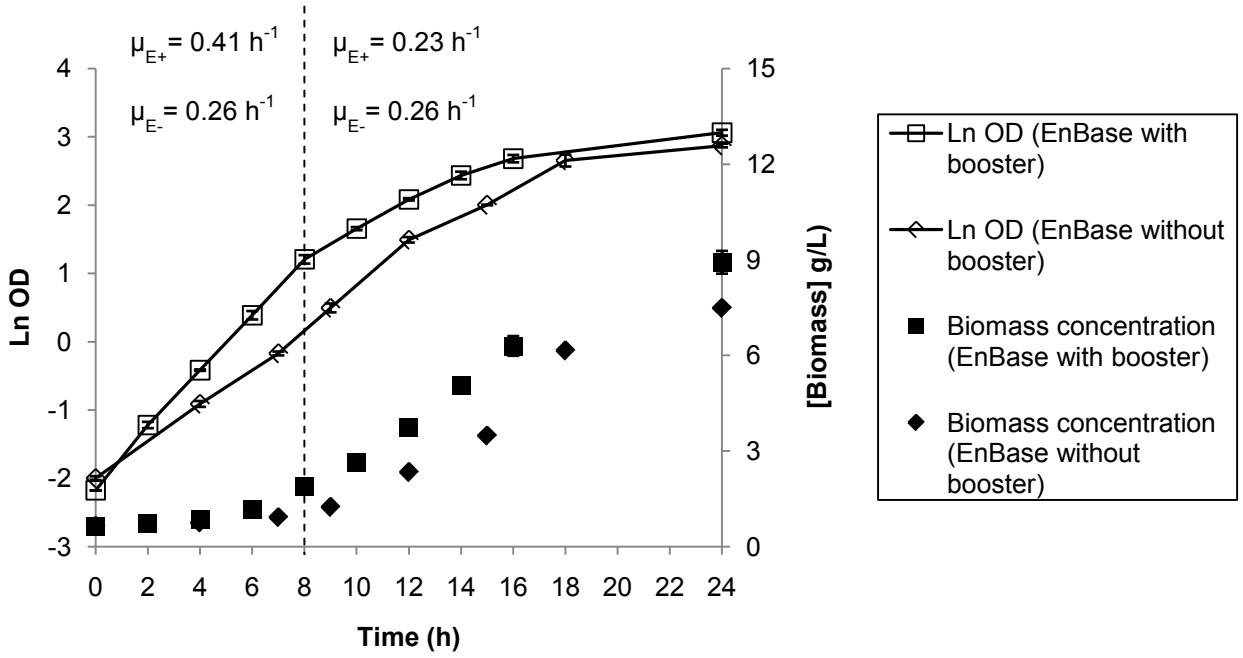

Figure 4.5: Growth profile of *B. halodurans* Alk36 cultures in EnBase® medium in the presence and absence of booster solution. The growth rates of cultures grown in the presence of booster solution are indicated by (μ_{E+}) while that of the cultures grown in absence of booster solution are indicated by (μ_{E-}). The plots represent averages from duplicate experiments and the error bars were derived from the standard error of the mean. Where error bars are not shown, these are within the dimension of the symbols.

In cultures grown without booster solution, the starch concentration (26 g/L) was constant during the first 7 hours post inoculation. The cells could have been growing on the glucose already present in the medium following heat-based hydrolysis or on the residual media components transferred with the inoculum (Figure 4.6).

A low concentration of glucose (between 3.97 and 5.45 g/L) was observed in the medium in the first 4 hours post inoculation, decreasing to about 2.00 g/L as shown in Figure 4.6. The residual starch concentration in the culture at stationary phase was about 4.97 ± 0.04 g/L, which was slightly less than that observed in the culture grown in EnBase® with booster (7.68 ± 0.00 g/L) (Figure 4.4).The presence of residual starch in the EnBase® medium, with or without booster, when the cultures entered stationary phase indicated that the carbon source was not the growth-limiting factor.

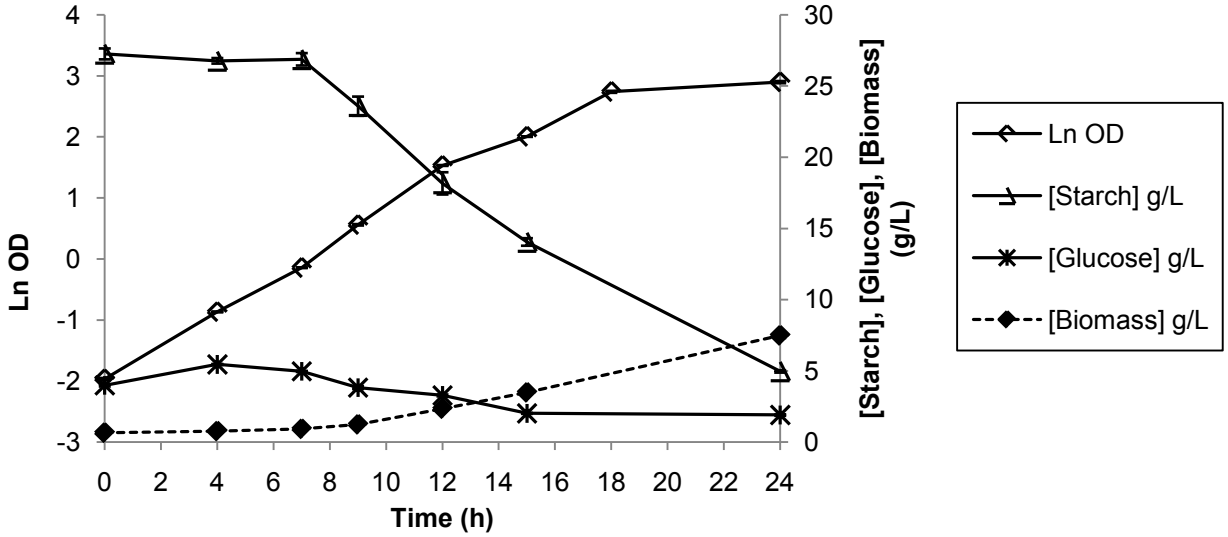

Figure 4.6: The starch utilisation profile of *B. halodurans* Alk36 growing in EnBase® medium in the absence of booster in a stirred tank bioreactor at 30°C and pH 8.5. The starch and glucose values presented were calculated from the averages of triplicate readings of the same sample and their standard deviation. The growth profiles represent averages from duplicate experiments and the error bars were derived from the standard error of the mean. Where error bars are not shown, these are within the dimension of the symbols.

Thiamine, $MgSO_4$ and trace elements were added into the culture when the optical density of the culture reached an absorbance of 10 (equivalent to 3.85 g/L biomass). No change in the growth profile was observed upon addition of thiamine, $MgSO_4$ and trace elements, indicating that these were not limiting nutrients. High performance liquid chromatography (HPLC) was used to investigate the production of organic acids such as acetic acid. No organic acids were detected in either culture (results shown in Appendix 1.7) indicating that most of the hydrolysed starch was used by the cells for growth and biomass production and that there was no overflow metabolism.

The biomass yield, on carbon-source, obtained from cultures grown in EnBase® medium containing booster solution (0.30 ± 0.04 moles biomass per moles carbon) was similar to that of the cultures grow without booster solution (0.37 ± 0.01 moles biomass

per moles carbon) as illustrated in Table 4.2. However, the yield obtained from the culture grown in presence of the booster solution could have been underestimated since it was calculated assuming that all the carbon present and amino acids present in the booster solution could be utilised by the bacterium.

Table 4.2: Comparison of yields of *B. halodurans* Alk36 cultures grown in EnBase® medium with and without booster in stirred-tank bioreactors(based on the measured amount of carbon in the medium).

Media	Amount of carbon in media (moles/L)	Residual carbon content (moles/L)	Concentration of carbon used (moles/L)	Average Biomass[a] concentration (moles/L)	Biomass yield on carbon (moles biomass per moles carbon)
EnBase® (with booster)	1.46 ± 0.05	0.26 ± 0.02	1.20 ± 0.13	0.36 ± 0.01	0.30 ± 0.04
EnBase® (without booster)	1.04 ± 0.00	0.23 ± 0.00	0.81 ± 0.00	0.30 ± 0.01	0.37 ± 0.01

a - The carbon concentration in the biomass was calculated using the general empirical formula for aerobic bacteria i.e. $CH_{1.8}O_{0.5}N_{0.2}$ (Bailey &Ollis, 1986).

For cultures grown in EnBase® medium containing booster solution, the biomass yield, on carbon-source (0.30 ± 0.04 moles biomass per moles carbon) presented in Table 4.2 seemed to be slightly higher than that presented in Table 4.1 (0.24 moles/L). The discrepancy could have been due to the different methods used to determine the concentration of the content in medium. The yield quoted on Table 4.2 (0.24 moles/L) was calculated from the weight of the carbon-source added into the medium while that quoted on Table 4.2 (0.30 ± 0.04 moles biomass per moles carbon) was calculated from the amount of carbon-source measured by the starch-iodine assay, with tends to overestimate the amount of hydrolysed starch and hence the carbon-source present in the medium (Swanson, 1948).

4.4 Factors associated with entry into stationary phase

Bacterial cultures usually enter stationary phase because of nutrient depletion, accumulation of waste products that may be toxic to the bacteria, product inhibition or changes in growth conditions such as temperature or pH (El-Mansi et al., 2006). The residual starch concentration in *B. halodurans* Alk36 cultures at stationary phase (Figure 4.4 and 4.6) suggested that inhibitory conditions or the depletion of macronutrients or micronutrient (other than the carbon-source) occurred.

The dissolved oxygen profile of the cultures grown in EnBase® medium shows that the cultures were not oxygen limited, since the dissolved oxygen concentration was between 50% and 60% as the cultures entered the stationary phase, as illustrated in Figure 4.7 and 4.8. Further, owing to the ongoing supply of oxygen, its limitation would not cause the onset of stationary phase but rather limit the growth rate.

Entry into stationary phase was associated with an increase in dissolved oxygen concentration, attributed to the slowing of cell metabolism resulting in a decrease in the oxygen-utilisation rate. The oxygen-transfer rate obtained in the bioreactor at the operational conditions used (30˚C, pH 8.5, 1 vvm aeration and agitation between 400 – 1000 rpm) was between 11 to 47 mMols.L^{-1}.h^{-1} (Appendix 1.5). The oxygen transfer rates exceeded the oxygen utilisation rate of *B. halodurans* Alk36 growing in EnBase® medium at 30°C (3.48 mMol.L^{-1}.h^{-1}) (Appendix 1.7). Therefore, the cultures were not oxygen-limited.

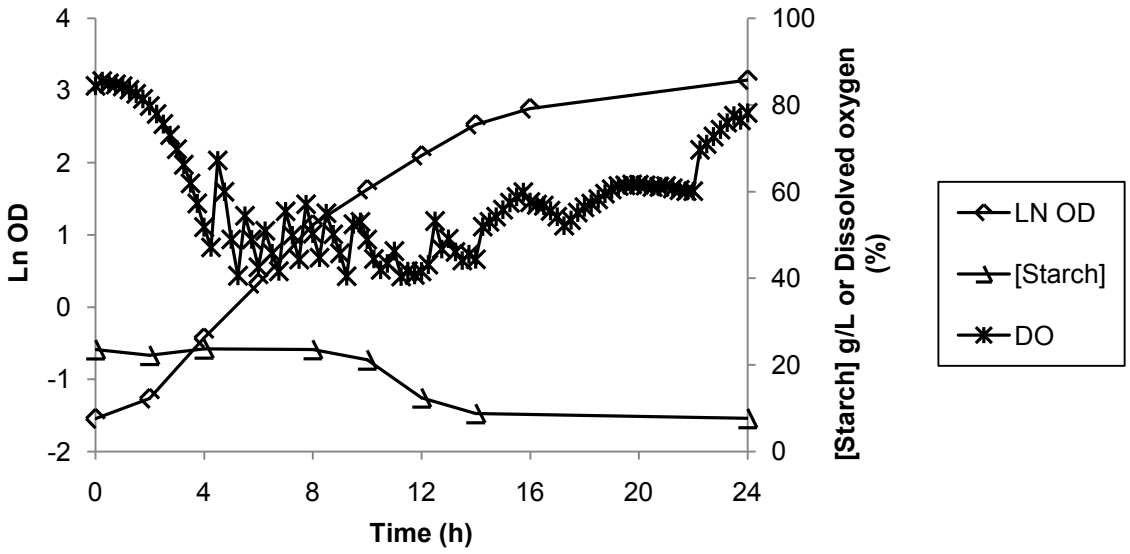

Figure 4.7: The dissolved oxygen concentration (DO), residual starch concentration and optical density (Ln OD) of *B. halodurans* Alk36 culture grown in EnBase® medium with of booster.

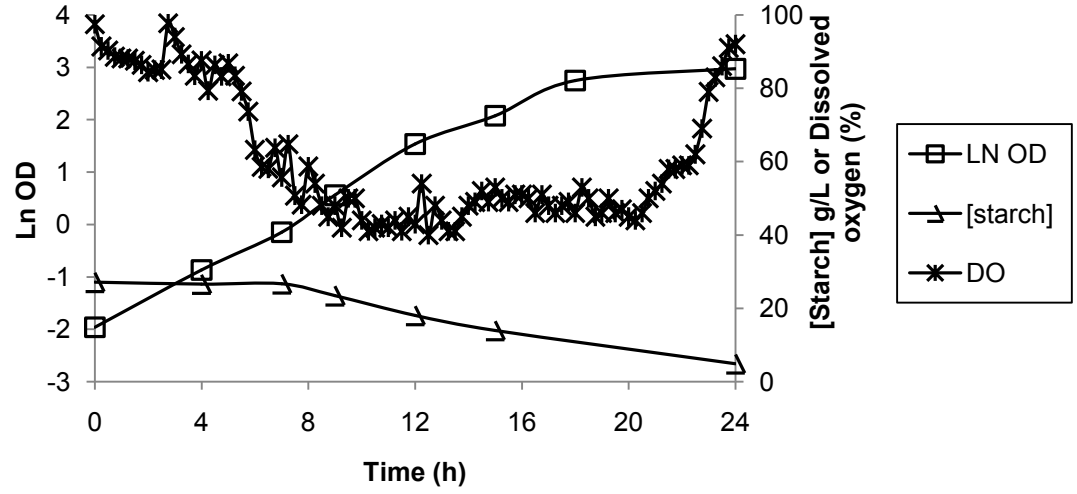

Figure 4.8: The dissolved oxygen concentration (DO), residual starch concentration and optical density (Ln OD) of *B. halodurans* Alk36 culture grown in EnBase® medium without booster.

To determine whether nitrogen could be the limiting nutrient, causing the culture to enter stationary phase prematurely, *B. halodurans* Alk36 was grown in EnBase® medium in the absence of booster, and additional ammonium sulphate was added at early stationary phase (i.e. about 22 hours post inoculation). The amount of ammonium sulphate added was such that the concentration of the salt in the medium was 46 mM. The addition of ammonium sulphate did not lead to recovery in growth but led to cell death, as demonstrated by the decrease in the optical density (OD) of the culture after addition of ammonium salt, while the OD of the culture that was not supplemented with the ammonium salt remained constant as shown in Figure 4.9.

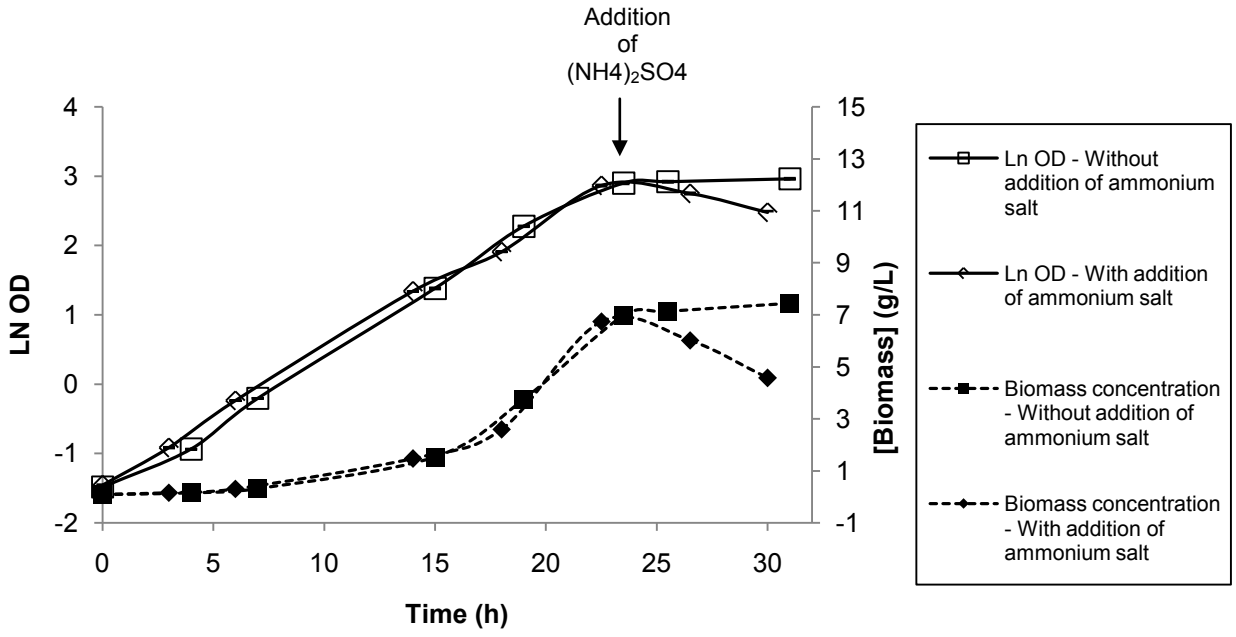

Figure 4.9: Growth profile of *B. halodurans* Alk36 in EnBase® medium showing the effect of ammonium sulphate addition at early stationary phase. The values presented were calculated from the average of the triplicate readings of the same sample and their standard deviation. Where error bars are not shown, these are within the dimension of the symbols.

Even though these experiments were not replicated, the two experiments showed reproducibility since the growth profiles and average biomass concentration, up to the point of addition of the ammonium salt, were similar.

The cell death caused by addition of ammonium salt was unexpected because the biomass concentration of the growth phase did not differ much between supplementation with the ammonium salt, and without. Further, the addition of ammonium sulphate (at about the same concentration as the initial concentration) has been shown to increase the biomass concentration of *E. coli* cultures grown on EnBase® medium in the study done in96-well plates (Panula-Perälä, et al., 2008). However, the pH of the *E. coli* culture in the study done by Panula-Perälä et al. (2008) was not controlled, while that of the *B. halodurans* Alk36 culture (investigated in this study) was controlled and maintained at pH 8 through the addition of concentrated sodium hydroxide solution. Hence, the detrimental effect of the ammonium sulphate, observed in the present study, could have been due to changes in culture osmolality due to the addition of the ammonium salt in the culture. Changes in culture osmolarity have been shown to affect the growth rate and growth profile of bacteria (Csonka, 1989). Thus, addition of a lower concentration of ammonium sulphate should be investigated and the resultant conductivity measured.

4.5 Determination of the activity of *B. halodurans* Alk36 amylase(s)

The starch-iodine and the dinitrosalicylic acid (DNS) assays were used to determine the consumption of reactant (starch) and production of product (reducing sugars), respectively, in the measurement of the amylase activity of the *B. halodurans* Alk36 culture supernatant as described in Section 3.3.4. The activities obtained from the two assays were compared to infer the mode of action of the amylases, i.e. endo-acting or exo-acting amylases as described in Section 2.1.5.

Preliminary assays were done using both the starch-iodine and the DNS assays, at different dilutions of a commercial amylase with known activity i.e. amylase from *Bacillus licheniformis* (A455A-Sigma Aldrich) (raw data in Appendix 1.9)

The activities obtained with the DNS assay (Table 4.3) were similar to those given by

the manufacturers (which were also determined by the DNS assay). However, the activities obtained with the starch-iodine assay were slightly higher than those determined by the DNS assay (Table 4.3).The higher activity obtained with the starch-iodine assay was not surprising since the starch iodine assay is recognised to overestimate the amount of hydrolysed starch, and hence amylase activity (Saenger, 1984). Overestimation of the amount of starch hydrolysed results from the ability of iodine to only form blue-coloured complexes with starch molecules containing more than eighteen glucose residues (Swanson, 1948). Hence, starch molecules containing less than eighteen glucose residues were assumed to be hydrolysed to glucose.

Table 4.3. Comparison of amylase activities from *B. licheniformis* obtained with the starch-iodine and DNS acid assays.

Activity given by the manufacturer (Units/mg)[a]	Activity with DNS assay (Units/mg)[a]	Activity with starch-iodine assay (Units/mg)[b]	% activity based on the manufacturer assay	
			DNS assay	Starch-Iodine assay
1	1.03 ± 0.05	1.14 ± 0.03	103	114
5	4.38 ± 0.14	6.68 ± 0.20	88	134
10	9.66 ± 0.05	11.45 ± 0.02	97	115

a - One unit of activity as determined by the DNS assay is defined as the average of 1 mg of maltose equivalents liberated from starch in 3 min at 20˚C and pH 6.9.

b - One unit of activity as determined by the starch-iodine assay is defined as the average of 1 mg of starch hydrolysed in 3 min at 20˚C and pH 6.9.

The culture supernatant (filtered through 0.22 µM filters) obtained from *B. halodurans* Alk36 grown in a stirred-tank bioreactor for 24 hours using EnBase® medium (without booster solution) was analysed by the starch-iodine and the DNS assays to determine activity of the amylase(s) present. The concentration of proteins in the culture supernatant, determined by Bradford assay as described on Section 3.3.3 (page 63) was 75 mg/L (Appendix 1.9).

The activity obtained with the starch-iodine assay (339 Units/mg protein) was five times

higher than that obtained by the DNS assay (64 Units/mg protein). This ratio of amylase activities obtained by the starch-iodine assay and by the DNS assay was also reported as five fold by Xiao et al. (2006), where the activity. The observed differences in amylase activity in the present study suggested that *B. halodurans* Alk36 produces an endo-acting α- amylase, which cleaves the starch molecules at random positions releasing products of different sizes including glucose, maltose and oligosaccharides containing 3 to 6 glucose residues(Van Der Maarel, et al., 2002). This would result in an inconsistency between the reducing ends produced for interaction with the DNS reagent and the hydrolysis events, resulting in low activities. However, the amount of reducing sugars produced when almost all the starch was hydrolysed was very low (0.5 g/L). Since 10 g/L starch was used in these assays, the obtained concentration of reducing sugars (0.5 g/L) was about 5% of the expected amount of reducing sugars (9.25 g/L) Figure 4.10.

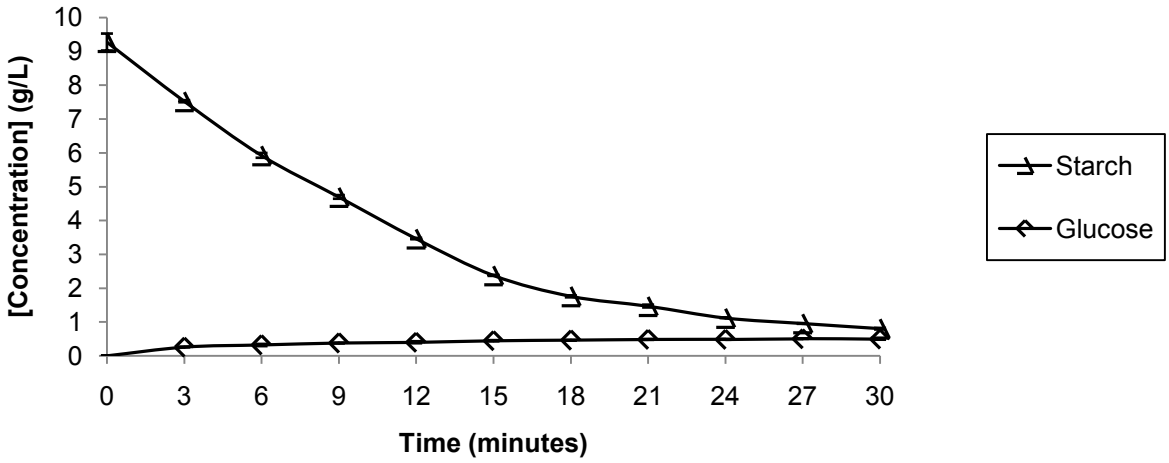

Figure 4.10: The starch hydrolysis profile obtained from the amylase activity assay. The average concentration of residual starch (Δ) obtained by the starch-iodine assay is compared to the average concentration of reducing sugars(◊) obtained by the DNS assay. The values presented were calculated from the average of the triplicate experiments and the error bars were derived from the standard error of the mean. Where error bars are not detectable, these are within the dimension of the symbols.

The low concentration of reducing sugars released from starch hydrolysis by *B.*

halodurans Alk36 amylases could be due to slow hydrolysis of intermediate products or non-reducing sugar products such as cyclodextrins. Cyclodextrins are cyclic oligosaccharides formed in presence of a glycosyltransferase enzyme, which has been isolated in some *Bacillus* strains (Del Valle, 2004). Thus, it is recommended that the hydrolysis products be analysed in future work to determine the chain lengths of sugars produced, which will enable further characterisation of *B. halodurans* Alk36 amylase(s), and hence, confirmation of the mode of action of the amylase(s). Furthermore, it was concluded that the DNS assay was not an appropriate assay for determination of amylase activity of *B. halodurans* Alk36 amylase(s) since the hydrolysis products obtained were not all reducing sugars. However, it was extremely useful in confirming mechanism of amylase action. Hence, the starch-iodine assay was used for the determination of the amylase activity in the subsequent experiments.

4.6 Amylase production in relation to growth of *B. halodurans* Alk36

In this section, amylase production from both the bioreactor experiments and the shake flask experiments is measured and compared. In the bioreactor experiments, amylase activity is considered in exponential and stationary phase. Activities are then compared between experimental systems in the early stationary phase.

The culture supernatant obtained from *B. halodurans* Alk36 grown in the stirred-tank bioreactor at 30°C and pH 8.5 on EnBase® medium (without booster) was analysed to determine the total protein concentration and the amylase activity. The Bradford assay (Bradford, 1976) was used to determine the protein concentration while the starch-iodine assay (Fuwa, 1954) was used to determine the amylase activities as described in Chapter 3 (Section 3.3.3 and 3.3.4).

The total protein concentration of the culture supernatant samples collected at different time points during growth increased in accordance with the increase in biomass (Figure 4.11). There was approximately 109.51 ± 0.04 mg/L protein in the culture supernatant at early stationary phase (21hours post inoculation),as shown in Figure 4.11.

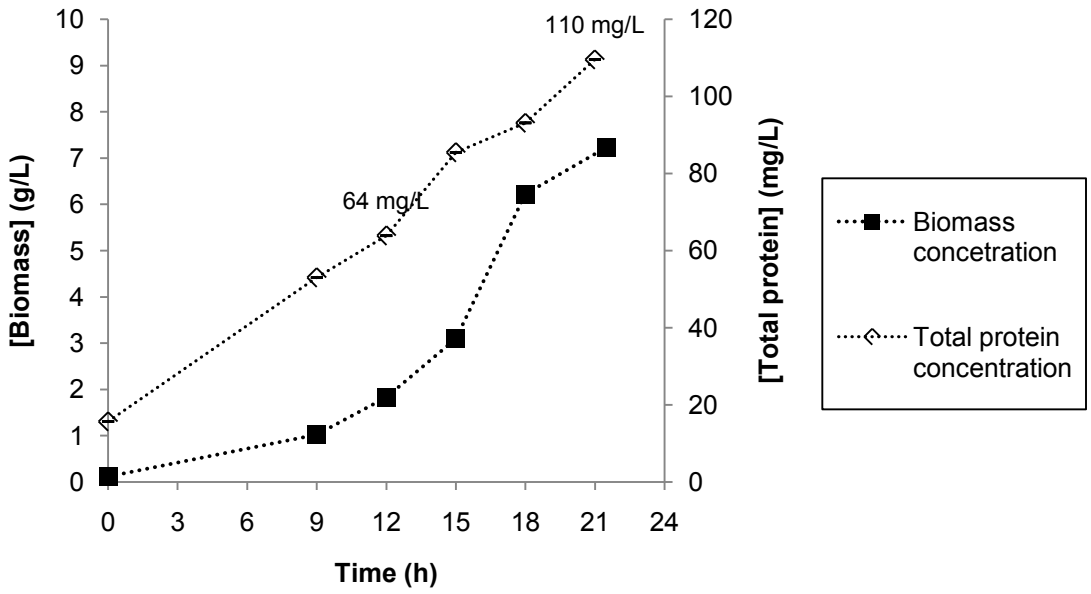

Figure 4.11: Total protein profile of *B. halodurans* Alk36 culture grown on EnBase® medium in stirred tank bioreactor at 30C and pH 8.5 showing the growth profile (o) and the average protein concentration (♦) at different time points during growth. The values presented were calculated from the average of the triplicate readings of the same sample and the error bars were derived from the standard deviation of the values. Where error bars are not shown, these are within the dimension of the symbols.

The specific amylase activity of the culture supernatant, based on protein present, obtained from exponential phase (2.48 ± 0.10 Units/g protein) was approximately 20times lower than that of the culture from early stationary phase (44.64 ± 0.85 Units/g protein) as shown in Table 4.4. The activity of the culture supernatant, based on biomass, obtained from exponential phase (0.08 ± 0.01 Units/g biomass) was also lower than that of a culture from early stationary phase (0.68 ± 0.01 Units /L biomass) as shown in Table 4.4. The higher specific amylase activity at stationary phase may be due to the lower concentration of the carbon source at early stationary phase. Since the concentration of starch and hence, available glucose was low, the bacterium may have secreted more amylase/s to meet the demand for carbon, resulting in increased production and accumulation of amylase/s in the culture medium. Thus, for bulk

production of amylase/s, the enzyme/s was extracted from cultures at early stationary phase.

Table 4.4: Amylase activities of culture supernatant obtained from exponential and stationary phase cultures of *B. halodurans* Alk36 grown in EnBase® media at 30˚C and pH 8.5.

Culture sample	Exponential phase (12 hours culture)	Early stationary phase (21.5 hours culture)
Amylase activity (U/L)	0.16 ± 0.02	4.91 ± 0.09
Total protein concentration (mg/L)	63.85 ± 0.03	109.51 ± 0.04
Specific amylase activity (U/g of protein)*	2.50 ± 0.10	44.84 ± 0.85
Culture biomass (g/L)	1.83 ± 0.03	7.25 ± 0.00
Activity per unit biomass (U/g biomass)	0.08 ± 0.01	0.68 ± 0.01

Note:

* One unit (U) of amylase activity is defined as the amount of enzyme that hydrolyses 1 g of starch per minute under the assay conditions. The amylase activity assays were done at 50˚C in phosphate buffer at pH 8.5.

The biomass concentration and activities of the amylases obtained from the cultures grown in shake flasks were compared to those obtained in cultures grown in the bioreactor. The specific amylase activity obtained from the culture grown in the shake-flasks at early stationary phase (2.61 ± 0.11 U/g protein) was 17-times lower than that of the culture grown in the bioreactor (44.84 ± 0.85 U/g protein) (Table 4.5). Hence it was apparent that the use of EnBase® medium and the stirred-tank bioreactor system resulted in improved growth conditions and amylase production as indicated by high biomass yields and amylase activity. The EnBase® medium allowed the use of high concentration and controlled release of the carbon source (starch), which minimised

overflow metabolism (evidenced by absence of acetic acid, analysed by HPLC (see Appendix 1.7), resulting in high biomass production and, hence, amylase activity. Further, the use of the stirred-tank bioreactor system allowed for better pH control and provided better mixing ensuring that the cultures were not oxygen limited, as discussed in Section 4.4.

Table 4.5: Amylase activities obtained from *B. halodurans* Alk36 culture grown on EnBase® medium in shake-flasks and stirred-tank bioreactor.

Sample source	Total protein (mg/L)	Amylase activity (mg/L/min)	Specific amylase activity (U/g protein)*	Biomass concentration (g/L)
Bioreactor culture	109.51 ± 0.04	4.91 ± 0.09	44.84 ± 0.85	7.25 ± 0.00
Shake-flask culture	23.01 ± 4.93	0.06 ± 0.00	2.61 ± 0.11	2.01 ± 0.01

∗ where1 unit (U) is equivalent to 1 g of starch hydrolysed per minute under assay conditions.

4.7 Identification of types of amylases produced by *B. halodurans* Alk36

Bacillus halodurans Alk36 culture supernatants from the exponential and early stationary phase of growth obtained from the stirred tank bioreactor were analysed by starch-zymography (Section 3.3.5.3) to determine whether different types of amylases were produced during exponential and stationary phase of the growth cycle. The proteins in the culture supernatant were concentrated by ammonium sulphate precipitation at 80% salt saturation prior zymography analysis as described on Section 3.2.3.2.

A total of six bands exhibiting amylase activity were observed on the zymograms of protein samples obtained from *B. halodurans* Alk36 cultures in exponential phase, as well as that in stationary phase (Figure 4.12).

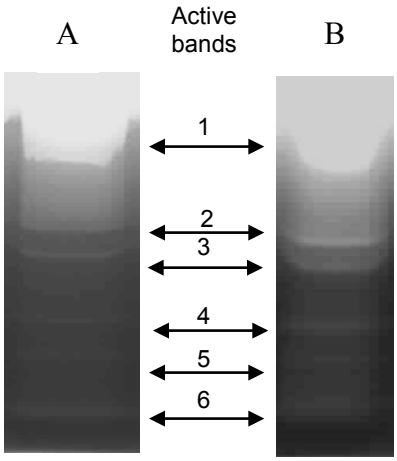

Figure 4.12: Starch zymograms showing active bands obtained from protein samples obtained from the culture in exponential (A) and stationary phase (B).

Peptide mass fingerprinting (PMF) was used to identify the proteins that showed activity on starch zymograms. Out of the six active bands identified by starch-zymography, only two bands (the 1st and 4th band) were identified as amylases by peptide-mass fingerprinting (PMF) with high confidence intervals (>95%), as shown in Table 4.6.

The rest of the bands were not identifiable, possibly due to impurities in the protein samples or the presence of novel proteins that have no homologous sequences in the NCBI protein database. The impurities in the protein samples could have resulted in peptide fragments that do not completely match with fragments obtained from known proteins in the database. Hence, further purification and possibly determination of amino acid sequence of the four proteins could enable identification which was not possible by PMF analysis.

Table 4.6: PMF Identification of protein corresponding to active bands obtained from starch-zymograms of a sample from *B. halodurans* Alk36 culture grown in EnBase® medium.

Band #	Protein identified	Protein Score[1]	% confidence interval[2]	Size (kDa)*
1	**Alpha-amylase G-6 precursor BH0413 [imported] - *Bacillus halodurans* (strain C-125)**	**174**	**100**	**107**
2	2-deoxy-D-gluconate 3-dehydrogenase kduD [imported] - *Bacillus halodurans* (strain C-125)	62	89.0	
3	Two-component response regulator.- *Clostridium tetani.*	52	0	
4	**Polysugar degrading enzyme (alpha-amylase) BH3007 [imported] - *Bacillus halodurans*(strain C-125)**	**69**	**97.6**	**37**
5	Polysugar degrading enzyme (alpha-amylase) BH3007 [imported] - *Bacillus halodurans* (strain C-125)	50	0	
6	Conserved hypothetical protein yogG [imported] - *Lactococcuslactis* subsp. *lactis* (strain IL1403)	47	0	

1. Protein score is the probability that the observed match is a random event.
2. The percentage confidence interval indicates the percentage similarity between the obtained sequences to the matching sequence in the database.

* The sizes of the proteins were calculated using the amino acid sequences of the predicted proteins.

The first and fourth bands that showed amylase activity on starch zymograms, were identified as an α-amylase precursor and a polysugar-degrading alpha-amylase from *B. halodurans* strain C-125, respectively. The alpha-amylase precursor (accession number BH0413) consists of 958 amino acids and has a molecular weight of 107 kDa, while the polysugar-degrading α-amylase (accession number BH3007) consists of 336 amino acids and has a molecular weight of 37 kDa. The presence of two amylases in *B. halodurans* cultures have also been reported by Murakami et al.(2007). These amylases were isolated from *B. halodurans* 38C-2-1 and had molecular weight of 100kDa and 75 kDa.

In the present study, the amino acid sequence of the 107 kDa-amylase from *B. halodurans* Alk36 was compared to the amino acid sequence of other Bacillus species using the UniProt database. The amino acid sequence of the 107 kDa-amylase from *B. halodurans* Alk36 showed 100% homology to the amino acid sequence of amylases isolated from *B. halodurans* strain C-125, 38C-1,MS-2-5 and LBK 34(Table 4.7). It was also similar to the α-amylase sequence obtained from *Bacillus* clausii (99% sequence homology) as shown in Table 4.7. The similarity in amino acid sequences indicated that these amylases are the same.

Table 4.7: The amino acid sequences similarity between the α-amylase G-6from *B. halodurans* C-125 and the amylase sequences found in the UniProt protein database.

Protein description	Organism	Length of amino acid sequence	% similarity
Alpha-amylase G-6 precursor	*Bacillus halodurans* (strain C-125)	958	100
Alkaline and thermostable amylase	*Bacillus halodurans* (strain 38C-2-1)	958	100
Alkaline, thermotolerant, and maltotetraose-producing amylase	*Bacillus halodurans*(strain MS-2-5)	958	100
Maltohexaose-producing alpha-amylase	*Bacillus halodurans*(strain LBK 34)	958	100
Alkaline amylase	*Bacillus clausii*	955	99

Based on the similarities in the amino acid sequences and the starch-degrading capabilities, it can be concluded that the 107 kDa amylase was an active amylase, even though it was identified as an amylase precursor. Further, the overall amylase activity of *B. halodurans* Alk36 was attributed to the activity of the alpha-amylase G6, with a smaller contribution by the polysugar-degrading amylase, as observed by the difference in intensity of the corresponding bands in the starch zymograms (Figure 4.12).

The amino acid sequence of the polysugar-degrading α-amylase has been predicted from the genomic sequence of several *Bacillus* species, however, there is no record of the isolated protein or the activity of a 37 kDa amylase from *Bacillus* species in literature. The smallest amylase that has been identified is approximately 26 kDa in size (Saxena, 2012). Unfortunately, to date, the 26 kDa amylase has not been sequenced hence its sequence cannot be compared to that of the polysugar-degrading amylase from the present study. The 37 kDa protein could have resulted from the truncation of a portion of the 75 kDa amylase identified by Murakami (2007). Unfortunately, the sequence of the 75 kDa amylase was not available in the database to enable comparison.

According to the NCBI Conserved Domain Database (CDD), the α-amylase G-6contain three conserved domains, namely AmyAc_family, the CHB_HEX_C and the CBM_25 domains (Figure 4.13). The AmyAc_family domain is the α-amylase catalytic domain, while the CHB_HEX_C domain is the carbohydrate binding module (CBM). The α-amylase catalytic domain is found in enzymes that can degrade starch, glycogen, and related oligo- and polysaccharides. These enzymes includeα-amylase, maltosyltransferase, cyclodextringlycotransferase, maltogenic amylase, neopullulanase, isoamylase, 1,4-alpha-D-glucan maltotetrahydrolase, 4-alpha-glucotransferase, oligo-1,6-glucosidase, amylosucrase, sucrose phosphorylase, and amylomaltase.

On the other hand, the polysugar-degrading enzyme consists of the NlpC/P60 family domain as shown in Figure 4.14. The function of the NlpC/P60 is not yet known but it is present in several lipoproteins and hydrolases. The NlpC/P60 family domain is present in most bacteria peptidases with a wide spread role in dynamics of bacterial cell wall. In Bacillus, the NlpC/P60 family are endopeptidases that hydrolyze the D-γ-glutamylmeso-diaminopimelate linkage in the cell-wall peptides (Anantharaman & Aravind, 2003).

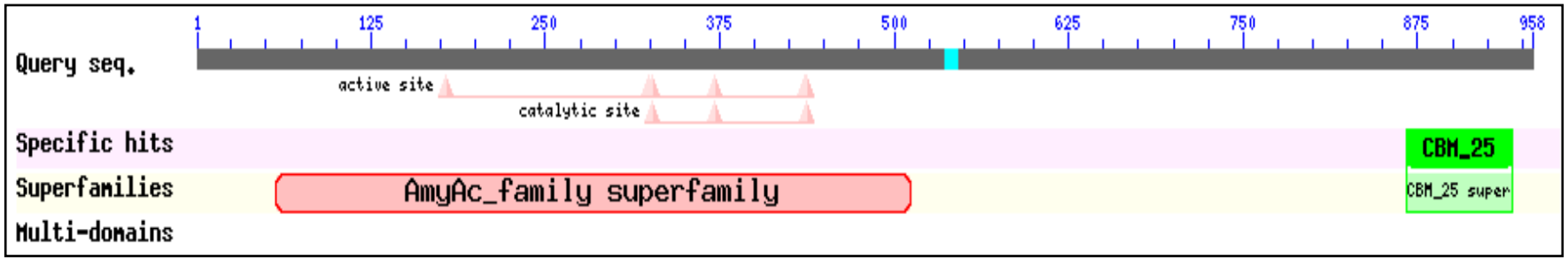

Figure 4.13: **Graphical representation of the conserved domains found in the α-amylase G-6 protein from *Bacillus halodurans* strain C-125 (accession number BH0413) (reproduced from the NCBI Conserved Domains Database).**

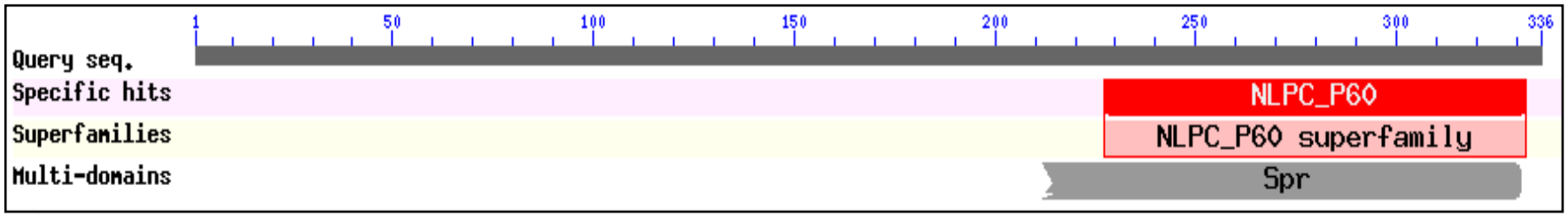

Figure 4.14: **Graphical representation of the conserved domains found in the polysugar-degrading amylase from *Bacillus halodurans* strain C125 (accession number BH3007) (reproduced from the NCBI Conserved Domains Database).**

The amino acid sequence of the polysugar-degrading amylase and the α-amylase G-6, both from the present study, only showed 38% similarity to one another. The sequence similarity was observed in four different areas including part of the catalytic sites of the α-amylase G-6, as shown in Figure 4.15. Sequence similarities at the catalytic site might confer the ability to degrade starch to the polysugar-degrading enzyme. Thus, it appeared reasonable to conclude that the amylases identified from *B. halodurans* strain Alk36 are different, based on their sizes and sequence homology.

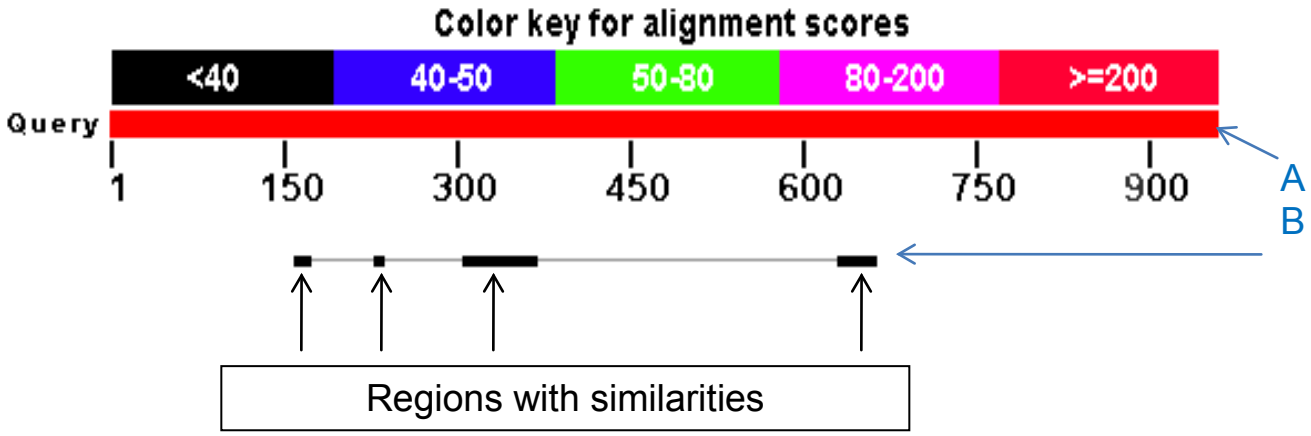

Figure 4.15: Sequence alignment showing similarities between (A) the α-amylase G-6 precursor (accession number BH0413) and(B) the polysugar degrading α-amylase sequences (accession number BH3007) from *B. halodurans* strain C-125 (reproduced from NCBI Basic Local Alignment Search Tool (BLAST)).

4.8 Comparison of amylase activities obtained from *B. halodurans* Alk36 to amylase activities reported in literature.

The activity of the amylase/s identified in the present study and of alkaliphilic amylases obtained from other *B. halodurans* strains as well as other alkaliphilic *Bacillus* strains reported in literature are reported in Table 4.8. These could not be effectively compared due to the differences in assay conditions used (Table 4.8).

Table 4.8: Overview of activities of the alkaliphilic amylases reported in literature.

Source	Protein size (kDa)	Growth conditions	Amylase activity(U[a]/mg protein)	Assay	Assay conditions	Reference
B. halodurans Alk36	107	EnBase media with 30 g/L starch in ST-Bioreactor	64	DNS	0.1 M Phosphate buffer at pH 8.5 and 50 ˚C	The present study
B. halodurans LBK 34	107	LB media in shake-flasks (recombinant expressed in *E.coli*)	117	DNS	0.1 M Glycine-NaOH buffer at pH 10 and 55˚C	Hashim et al. (2005)
B. halodurans 38C-2-1	100 75	Minimal salts medium with 5 g/L starch in shake-flasks	0.22	Somogyi Nelson[b]	0.1 M Glycine-NaOH buffer at pH 10 and 50˚C	Murakami et. al. (2007)
B. halodurans MS-2-5	90	Minimal salts medium with 5 g/L starch in shake-flasks	1.00	Somogyi Nelson[b]	0.1 M Glycine-NaOH buffer at pH 10 and 50˚C	Murakami et. al. (2008)
Bacillus species *IMD 370*	159	Minimal salts medium with 10 g/L starch in shake-flasks	1.9	DNS	0.1 M Glycine-NaOH buffer at pH 10 and 40˚C	Antoinette et al. (1995)

Continuation of table 4.8 ....

Table 4.8: Overview of activities of the alkaliphilic amylases reported in literature.

Source	Protein size (kDa)	Growth conditions	Amylase activity(U[a]/mg protein)	Assay	Assay conditions	Reference
Bacillus sp. TS-23	150	Complete medium with 10 g/L starch in shake-flasks	1.3	DNS	0.1 M Tris/HCl buffer at pH 9 and 70˚C	Lin et al. (1998)
Bacillus Strain, GM8901	97	Minimal salts medium with 10 g/L starch in a jar fermenter	1.3	DNS	0.05 M Glycine-NaOH buffer at pH 10 and 50˚C	Kim et al. (1995)
Bacillus sp. KSM-1378	53	Minimal salt media with 10 g/L starch in shake-flasks	827	DNS	0.05 M Tris/HCl buffer at pH 8.5 and 50˚C	Igarashi et al. 1998
Bacillus sp. KSM-K38	55	Alkaline medium containing soluble starch, tryptone, Soytone, NaCl and Na_2CO_3 at pH 10).	5	DNS	0.05 M Glycine-NaOH buffer at pH 10 and 50˚C	Hagihara et al. 2001
Bacillus sp. PN5	nd[c]	Media containing starch 0.2% (w/v) peptone 0.5% (w/v) and beef extract 0.3% (w/v).	80	DNS	0.1 M Glycine - NaOH buffer at pH 10 and 37˚C	Saxena et al. 2007

a - One unit of amylase activity is defined as the amount of enzyme that produces 1 µMol of glucose per min under the assay conditions.

b - The assay is similar to the DNS assay, it measures the amount of reducing sugars formed through oxidation by Cu(II) ions(Nelson, 1994).

c - not determined

In the present study, the amylase activities obtained using the DNS assay were compared to those in literature as it seems to be the standard assay used for determination of amylase activities. However, the present study have shown that the DNS assay could not accurately determine the activity of *B. halodurans* Alk36 amylases since the amount of reducing sugars detected was substantially less than expected as discussed in Section 4.5. Therefore a reasonable comparison of the amylase activities could not be made. Moreover, the activity assays in the present study were performed at different conditions to those in literature due to variations of the amylases and their optimal conditions. In the present study, a phosphate buffer at pH 8.5 was used in the assays as used in the growth medium and determination of activity under growth conditions was of prime importance for the EnBase® study. The other studies used glycine buffer at pH 10. The activity assays in the present study were done at 50˚C because it was the suggested optimal temperature for amylase activity (Murakami et al., 2007; Murakami et al., 2008). Thus, the next step in the present study was to determine the optimal pH and temperature for growth of *B. halodurans* Alk36, as well as the temperature and pH required for optimal amylase activity.

For this reason an accurate comparison of amylase activities could not be made, at this stage. However, this study has highlighted the significance of having standard methods for determining amylase activities, while considering some of the properties of the amylase(s) being investigated. In further work it is recommended that amylase activities be determined under standard conditions for comparison and under growth conditions to determine the impact of the amylase in the EnBase® system.

4.9 Conclusion

Bacillus halodurans Alk36 was able to grow on the starch-based EnBase® medium (pH 8.5) without addition of an external amylase. This indicated that *B. halodurans* Alk36 produces an extracellular amylase that can hydrolyse starch under alkaline conditions.

Growth on EnBase® medium was improved when *B. halodurans* Alk36 was grown in stirred-tank bioreactor instead of in shake flasks. The improved growth in stirred-tank bioreactor was thought to be due to the provision of controlled growth environment.

Bacillus halodurans Alk36could be cultured to higher cell density in EnBase® medium than in LB medium due to the high concentration of the carbon source and the controlled delivery of the glucose into the EnBase® system. Improved growth, on the basis of biomass yield in EnBase® medium, was enhanced by the intrinsic ability of *B. halodurans* Alk36 to secrete amylase into the extracellular environment, where it hydrolysed the starch polymer to produce glucose. Hence, the rate of glucose release and the rate of cell growth were dependent on the rate of production and secretion of the amylase, as well as the amylase activity.

A two-phase growth was observed in cultures grown on EnBase® medium containing booster solution. The two-phase growth was assumed to be due to the change in metabolism of complex additives (amino acids and growth factors) provided by the booster solution. Since the presence of booster solution did not affect the final biomass concentration and the biomass yield, the booster solution was omitted from the medium.

Even though oxygen, Mg_2SO_4, trace elements or thiamine were not limiting nutrients, the cultures grown in EnBase® medium entered stationary phase prior to depletion of the carbon-source. Addition of ammonium salt in early stationary-phase culture did not lead to recovery in growth but led to cell death. The latter was thought to be due to changes in culture osmolarity, thus further investigation was suggested to determine the effect of addition of a lower concentration of ammonium sulphate.

The activity of amylases from the early stationary phase culture supernatant of *B. halodurans* Alk36 was higher than that of exponential phase culture. Thus, for bulk production of amylase/s, the enzyme/s was extracted from cultures at early stationary phase.

Based on the difference in amylase activities obtained from the starch-iodine and the DNS assays, it was concluded that *B. halodurans* Alk36 produces endo-acting amylases. It was recommended that the starch-hydrolysis products must be determined in order to confirm the mode of action of amylase(s) from *B. halodurans* Alk36.

B. halodurans Alk36 produced as many as six putative amylases, of which two were confirmed to be alpha-amylases. The identified alpha-amylases had molecular weights of 107 kDa and 37 kDa; these were designated as the α-amylase and the polysugar-degrading amylase, respectively. Even though two alpha-amylases were identified, the majority of the amylolytic activity was due to the 107 kDa α-amylase, based on the starch-zymography. Further purification was suggested to identify the other four enzymes which showed activity on starch-zymograms.

The activity of *B. halodurans* Alk36 amylases could not be directly compared to the amylases found in literature due to the difference in type of assay and assay conditions used. Thus, it was recommended that the mode of action of the amylases and/or the products of hydrolysis should be identified to enable the selection of appropriate assays that would more provide accurate activities.

Chapter 5
Optimisation of growth conditions

5.1 Introduction

Bacillus halodurans Alk36 has been shown to produce six potential amylases when grown in EnBase® medium at 30˚C and pH 8.5, as discussed in Chapter 4. Bulk production of the amylases was required to enable purification and characterisation of the individual amylases. Hence, conditions required for optimal biomass and amylase production were identified.

The optimal growth conditions were determined using small scale reactor vessels, shake flasks and multiwell plates, to reduce cost and time. Shake flasks and multiwell plates are usually used for initial proof of concept and optimisation studies because they are easy to operate and allow multiple experiments to be performed at the same time (Busch, 2001). Bioreactors are then used to provide a controlled environment, allowing data on biokinetics, mass transfer requirements and optimal bioreactor configuration to be provided (Margaritis & Wallace, 1984)and these to be further optimised. Further, bioreactors allow product samples to be prepared in bulk for design of downstream processes or evaluation of product quality.

In order to determine which small scale vessel to use for the optimisation experiments done in the present study, mixing and mass transfer in shake flasks (of 1000 mL volume capacity) and multiwell plates (of 10 mL capacity per well) were investigated. The oxygen transfer rate (OTR) and the volumetric mass transfer coefficient (k_La) were determined at different operating conditions to evaluate the mass transfer efficiency of the system. Since *B. halodurans* Alk36 is an aerobic organism, operational conditions that result in an OTR greater than the oxygen utilisation rate (OUR) were required to ensure that the cultures were not oxygen-limited. The small scale vessel of choice was then used to optimise growth conditions for improved growth and amylase production by *B. halodurans* Alk36. The growth conditions investigated included the pH and temperature, as well as the types of carbon sources required for improved amylase production.

5.2 Characterisation of shake flasks and multiwell plates based on the oxygen transfer rate (OTR) and the volumetric mass transfer coefficient (k_La).

The oxygen transfer rate (OTR) in shake flasks and multiwell plates is influenced by the shaking frequency, shaking diameter and filling volume. In the present study, the effect of the shaking frequency and filling volume on OTR and hence k_La was investigated using the sulphite model system described in Section 3.2.2.1. The effect of the shaking diameter was not investigated since the shaking orbit of the incubator shaker was a fixed parameter that could not be altered.

The OTR and k_La values in the multiwell plates varied with the filling volume and shaking frequencies (Figure 5.1 and 5.2). Both the increase in shaking frequency and the decrease in filling volume resulted in enhanced mass transfer area per unit volume and hence OTR as shown in Figure 5.1 and 5.2.

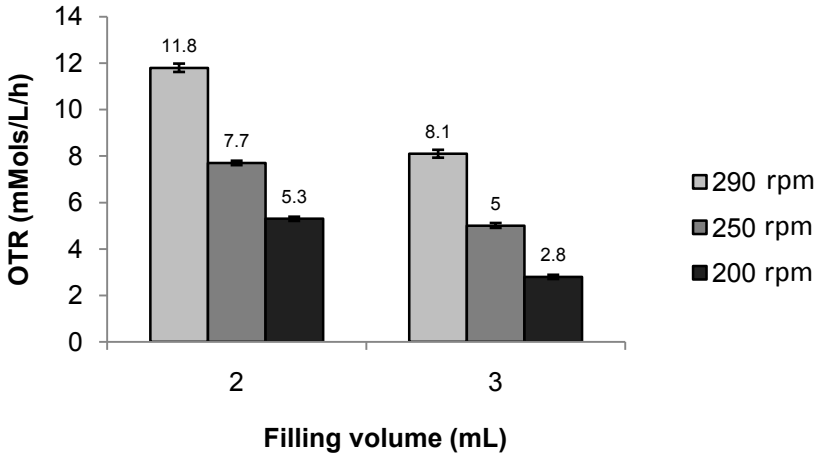

Figure 5.1: The OTR values obtained in 24-well multiwell plates at different filling volumes and shaking frequencies using the sulphite oxidation method. The OTR values presented were obtained from the average of triplicate measurements from one sample and the error bars were derived from the standard deviation of the values.

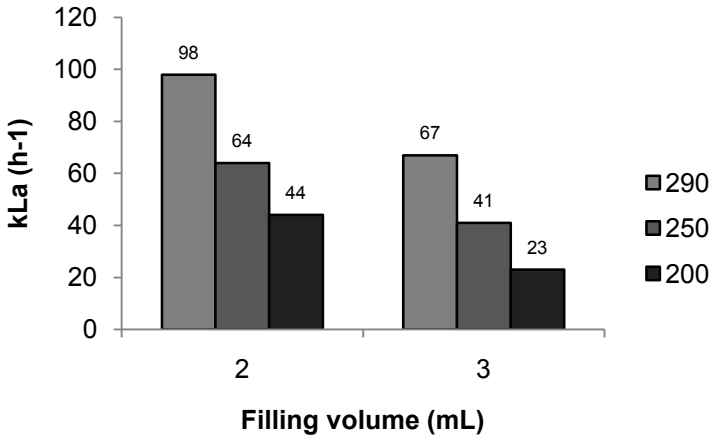

Figure 5.2: The k_La values obtained in 24-well multiwell plates at different filling volumes and shaking frequencies using the sulphite oxidation method. The kLa vales were calculated from the average OTR values.

A 1.5-fold increase in OTR was observed, when the filling volume was decreased from 3 mL to 2 mL (while the shaking frequency remains constant) for each of the shaking frequency investigated. The OTR also increased when the shaking frequency was increased by 50 rpm while the filling volume remained constant, for both filling volumes investigated i.e. 2 mL and 3 mL (Figure 5.1). Even though the experiments were not replicated, the decrease in OTR with the decrease in shaking frequency was observed for both filling volumes, indicating reproducibility. However, triplicate experiments should have been done to confirm the observed results.

Oxygen transfer rates of 35 mMols.L^{-1}.$h^{-1}$and 51 mMols.L^{-1}.h^{-1} have been reported in 24 well-multiwell plates when the shaking frequency was 220 rpm and 300 rpm, respectively, at a filling volume of 2.5 mL and 55 mm shaking diameter (Duetz & Witholt, 2004). However, these OTR values (35 to 51 mMols.L^{-1}.h^{-1}) are about four-fold higher than those attained in the present study at 2 mL filling volume, 50 mm shaking diameter and 200 rpm, as well as 300 rpm i.e. 5 mMols/L/h and 12 mMols/L/h, respectively, as shown in Figure 5.1. Even though the filling volume and shaking diameter used in the present study was slightly different from that used in the study by Duetz and Witholt (2004), the observed differences in OTR values were quite high. High OTR values attained in the study by Duetz and Witholt (2004) were thought to be due to the

difference in the methods used to determine the OTR. In the present study the sulphite-oxidation system was used, while Duetz and Witholt (2004) used an enzymatic method that coupled the oxidation of glucose by glucose oxidase and reduction of 2,2'-azino-bis(3-ethylbenzothiazoline-6-sulphonic acid ($ABTS^+$) by horseradish peroxidase.

As in the case of multiwell plates, OTR and k_La in shake flasks also increased with the decrease in filling volume. The OTR increased by two-fold when the filling volume was reduced by half, from 20 to 10%,as shown in Table 5.1.

Table 5.1: OTR and k_La values obtained using the sulphite oxidation method in 1L shake flask at different filling volumes and 200 rpm shaking frequency. The presented values are averages from triplicate experiments.

Filling volume (mL)	Filling volume (%)	OTR ($mMol.L^{-1}.h^{-1}$)	kLa (h^{-1})
100	10	13.36 ± 0.81	111
200	20	6.57 ± 0.20	54

The OTRs obtained in the shake flasks at 200 rpm, 13.36 ± 0.81 $mMol.L^{-1}.h^{-1}$ and 6.57 ± 0.20 $mMol.L^{-1}.h^{-1}$ were, (Table 5.1) higher than the OUR (3.48 $mMol.L^{-1}.h^{-1}$) when the biomass concentration was about 1.64 g/L (Appendix 1.7). This suggested that the shake-flask cultures were not oxygen limited. However, since the OTR in shake flasks was determined by the sulphite oxidation method, the obtained values are not directly representative of the conditions in the presence of culture medium.

The OTR and k_La obtained in shake flasks at 20% filling volume and shaking at 200 rpm (6.57 $mMol.L^{-1}.h^{-1}$ and 54 h^{-1}) were slightly higher than those obtained in the multiwell plates with 20% filling volume and the same shaking frequency (5.30 $mMol.L^{-1}.h^{-1}$ and 44 h^{-1}). Furthermore, the OTR obtained in the shake flask at 10% filling volume and 200 rpm shaking frequency (13.36 ± 0.35 $mMol.L^{-1}.h^{-1}$) was similar to that obtained in multiwell plates at 290 rpm with 10% filling volume. Hence, a higher shaking frequency was required when using multiwell plates in order to achieve OTRs similar to those

obtained in shake flasks when operating under the same conditions (i.e. temperature, pH and filling volume ratio). However, high shaking frequencies may cause shear stress that can damage the cells and reduce the OTR due to foam formation (Holmes et al., 2006). Shake flasks were used for optimisation studies since the OTR and k_La values obtained in shake flasks were higher than those obtained in the 24-wellmultiwell plates, under the given operational conditions.

5.3 Optimum pH for growth of *B. halodurans* Alk36

In order to ensure good growth of *B. halodurans* and hence, amylase production, the pH of the culture needed to be maintained in a range that would ensure optimal growth. To determine this pH range, *B. halodurans* Alk36 was grown in shake flasks using EnBase® medium, buffered at pH7, 8, 8.5, 9, 10 and 11,as described in Section 3.2.2.2. The pH and growth profiles of cultures are illustrated in Figure 5.3.

Cultures grown at pH 7, 8 and 8.5 had similar growth rates and attained higher optical densities than the culture maintained at pH 9 (Figure 5.3).The growth rates of the cultures grown at pH 7, 8 and 8.5 were 0.29 ±0.06 h^{-1}, 0.28 ± 0.10 h^{-1} and 0.28 ± 0.06 h^{-1}, respectively, while that of the culture grown at pH 9 was 0.20 ± 0.08 h^{-1}.

The biomass concentrations attained by the cultures grown at pH 7, 8 and 8.5 were 1.51 g/L, 1.80 g/L and 1.70 g/L, while that of the cultures grown at pH 9 was 0.94 g/L. The low growth rate and biomass yield in cultures grown at pH 9 suggested low amylase activity since amylase was responsible for the release of the carbon source required for growth. Based on these findings, the optimal pH for growth of *B. halodurans* Alk36 appears to be between pH 7 and 8.5.

The pH of the cultures, although buffered, was not maintained at the required values throughout the experiment as shown in Figure 5.4. Hence, the Sixfors bioreactor system was used to grow *B. halodurans* Alk36 cultures at different pH values to confirm the results obtained from the shake flask experiments. The reactor system provided pH control, not available in the shake flasks. The culture pH was maintained at pH 7, 8, 9, 10 and 11 as described in Section 3.2.2.

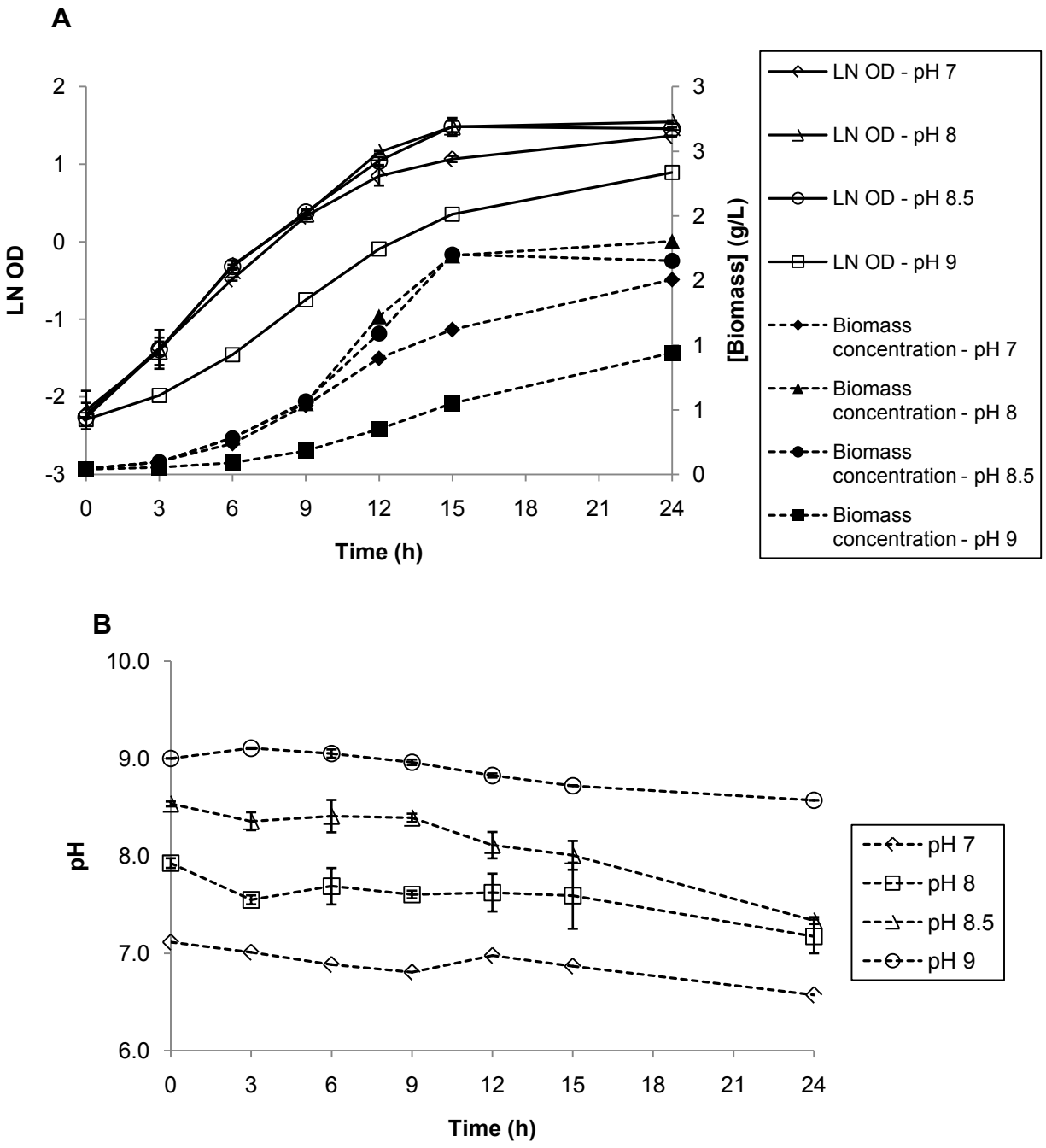

Figure 5.3: **Growth (A) and pH (B) profiles of *B. halodurans* Alk36 cultures in shake flasks using EnBase® medium maintained at different pH values using phosphate and carbonate buffers. The values presented were obtained from the averages of two experiments, where each experiment was performed in triplicate. The error bars were derived from the standard error of the mean and where error bars are not showing, they are within the dimensions of the symbols.**

The growth profiles of the cultures grown at pH 7.0, pH 8.0 and pH 8.5 in the Sixfors bioreactor system, were comparable. These cultures did not show a lag phase and gave similar specific growth rates, 0.25 h^{-1}, 0.30 h^{-1} and 0.30 h^{-1}, for pH 7, pH 8.0 and pH 8.5, respectively, as shown in Figure 5.4.

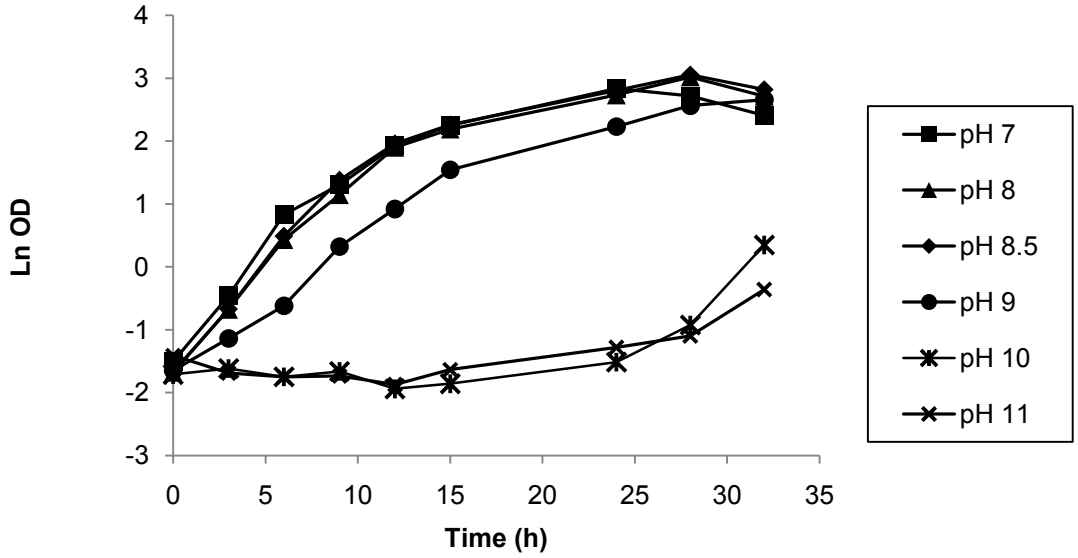

Figure 5.4: The growth profiles of *B. halodurans* Alk36 cultures grown at 30C in the Sixfors bioreactors with EnBase® medium maintained at different pH values with 5 M NaOH. The values presented were calculated from the average of the triplicate readings from one experiment and the error bars were derived from the standard deviation of the values. Where error bars are not showing, they are within the dimensions of the symbols.

The culture grown at pH 9.0 did not have any a lag phase but presented a reduced specific growth rate to 0.24 h^{-1}. Cultures grown at pH 10 and pH 11 had long lag phases; growth in culture at pH 10 was observed 24 hours post inoculation at a growth rate of 0.32 h^{-1}, while the lag phase in the culture at pH 11 lasted for more than 32 hours. The highest biomass concentration (8.16 g/L) was attained by the culture grown at pH 8.5, followed by the culture grown at pH 8 (7.89 g/L) and pH 7 (6.56 g/L), while the culture grown at pH 9 gave a biomass concentration of 5.51 g/L as illustrated in

Figure 5.5. The growth rates of the culture maintained at pH 9, in the Sixfors bioreactor, (0.24 h^{-1}) was lower than that in the shake flasks (0.16 h^{-1}) as shown in Table 5.2.

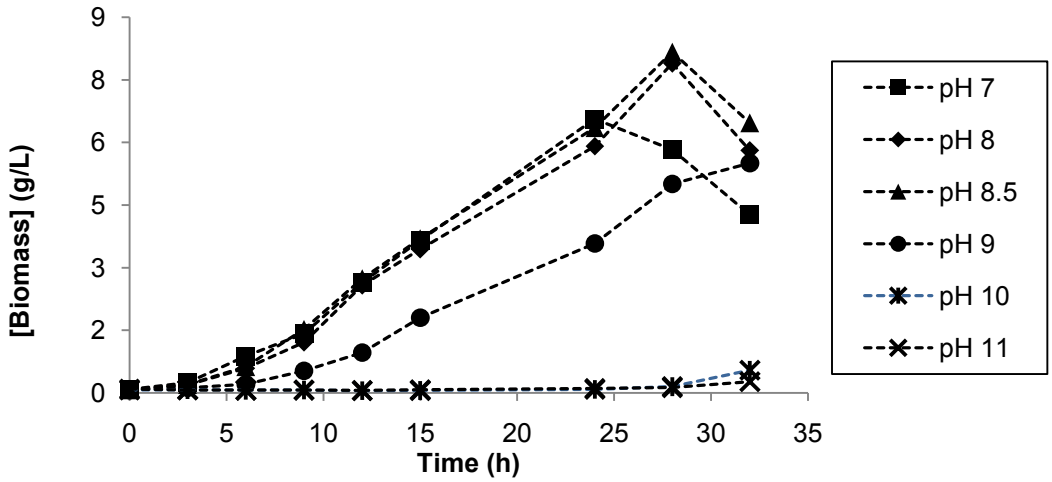

Figure 5.5: **The biomass concentration profiles of *B. halodurans* Alk36 cultures grown at 30°C in the Sixfors bioreactors with EnBase® medium maintained at different pH values with 5 M NaOH. The values presented were calculated from the average of the triplicate readings from one experiment and the error bars were derived from the standard deviation of the values. Where error bars are not showing, they are within the dimensions of the symbols.**

Table 5.2: **The maximum growth rate (μ_{MAX}) and highest optical densities (OD) attained by the cultures grown in EnBase® medium at different pH values in the Sixfors bioreactors versus shake flasks.**

Culture pH	Sixfors bioreactor		Shake flasks	
	μ_{MAX} (h^{-1})	[Biomass] (g/L)	μ_{MAX} (h^{-1})	[Biomass] (g/L)
7.0	0.25	6.56	0.28	1.51
8.0	0.30	7.89	0.30	1.80
8.5	0.30	8.16	0.29	1.70
9.0	0.21	5.51	0.16	0.94

The poor growth rate in shake flask cultures grown at pH 9.0could be due to the effect of the buffer solution (carbonate buffer) that was used to maintain pH 9 in the shake flask culture . For cultures grown at pH 7.0 and 8.0, the growth rates obtained from the Sixfors cultures were similar to those obtained in shake flask cultures (Table 5.2). It was suggested that *B. halodurans* Alk36 could be a facultative alkaliphile, since the optimal growth of *B. halodurans* Alk36 (in the range of pH 7 to 10) was observed between pH 7 and 8.5. Facultative alkaliphiles can grow optimally at moderate pH (pH 7– 8.5) (Horikoshi, 1999; Krulwich & Guffanti, 1989).

To quantify the reproducibility of the growth of *B. halodurans* in the Sixfors system, five reactors were used to grow cultures at pH 8.5. The growth profiles and pH profiles of the cultures are shown in Figure 5.6 and 5.7 (raw data presented in Appendix 2.2.2). While these profiles show similar trends, the inter-reactor variation is substantially larger than the intra-reactor variability.

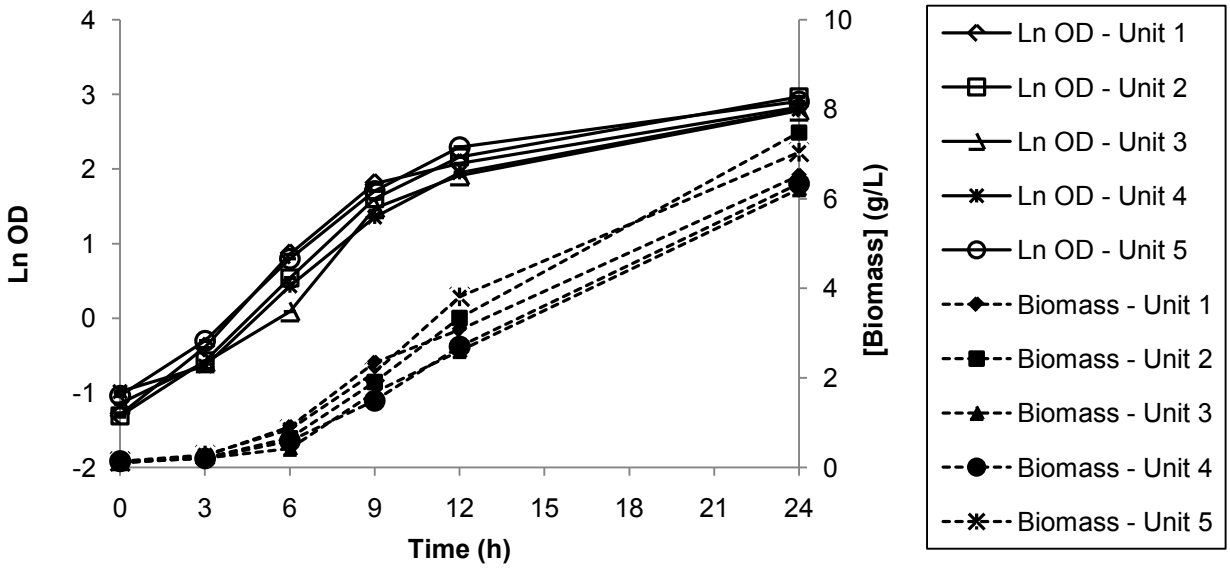

Figure 5.6: Reproducibility in the Sixfors bioreactor system. The growth profile (A) of *B. halodurans* Alk36 cultures grown in five Sixfors bioreactors using EnBase® medium at 30°C. The values presented were calculated from the average of the triplicate readings from one experiment and the error bars were derived from the standard deviation of the values. Where error bars are not showing, they are within the dimensions of the symbols.

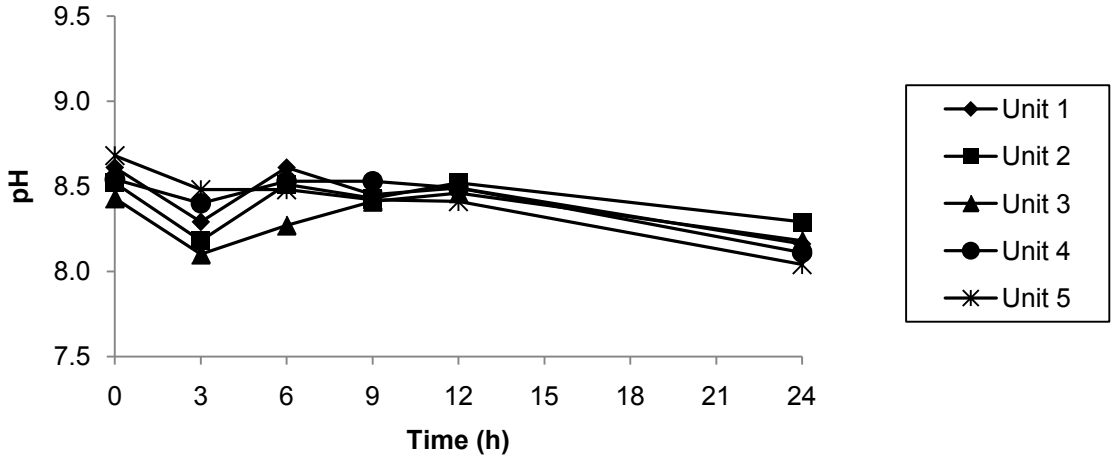

Figure 5.7: **Reproducibility in the Sixfors bioreactor system. The pH profile of *B. halodurans* Alk36 cultures grown at 30°C using the Sixfors bioreactors and the EnBase® medium. The values presented were calculated from the average of the triplicate readings and the error bars were derived from the standard deviation of the values. Where error bars are not showing, they are within the dimensions of the symbols.**

The biomass concentration at stationary phase (i.e. 24 hours post inoculation) varied between 6.2 and 7.5 g/L while the specific growth rates of the cultures varied between 0.26 and 0.35 h^{-1}., as illustrated in Table 5.3. The difference in the growth rates and the biomass concentrations attained in the different units could have been due to the inconsistency of the starter inoculum as the OD at t0 varied between 0.185 and 0.245. Alternatively, inconsistencies in operation in terms of air sparging, agitation or similar may have been experienced. The reproducibility analysis confirms that the performance in terms of growth was reduced at pH9.0 and above; however, no difference in performance can be determined between the cultures conducted in the range pH7.0 to 8.5.

Table 5.3: The optical densities and growth rates obtained from cultures grown in the Sixfors bioreactors using EnBase medium at 30˚C.

Reactor	Average biomass concentration (g/L)	Growth rate (h^{-1})
Unit 1	6.52 ± 0.10	0.35 ± 0.01
Unit 2	7.49 ± 0.03	0.30 ± 0.01
Unit 3	6.22 ± 0.01	0.28 ± 0.02
Unit 4	6.34 ± 0.01	0.26 ± 0.02
Unit 5	7.05 ± 0.01	0.29 ± 0.01

Owing to the high inter-reactor variation experienced in the Infors reactor system, it was decided to complete the experiments for the selection of optimal physicochemical conditions in shake flasks. Temperature and media requirements were thus considered in shake flasks.

5.4 Optimal temperature for growth of *B. halodurans* Alk36

Prior to the determination of the optimal temperature for growth of *B. halodurans* Alk36, preliminary studies were done to determine the evaporation rate of water from the shake flask system used at the growth temperatures being investigated (i.e. 30˚C, 37˚C, 42˚C, 45˚C and 50˚C), as described in Section 3.2.2.4. The evaporation rate increased with increase in temperature as illustrated in Table 5.4.

Table 5.4: The relationship between evaporation rate and temperature in 500 mL shake flasks at a filling volume of 100 mL.

Temperature (˚C)	30	37	42	50
Evaporation rate(µL.h^{-1})	33	83	113	213

Evaporation of water from the culture medium may lead to changes in osmolarity of the culture medium and viscosity, which may affect the growth rate and growth profile (Csonka, 1989). Further, it affects the monitoring of the experiment through affecting concentrations measured. Hence, sterile distilled water equivalent to the amount of evaporated water was added in cultures at different intervals to maintain the viscosity and osmolarity of the culture throughout its incubation and avoid the need for volume corrections.

To determine the optimal temperature for growth of *B. halodurans* Alk36, cultures were grown in shake flasks at 30C, 37˚C, 42˚C, 45˚C, 50˚C and 60˚C in EnBase ® medium, buffered with phosphate buffer at pH 8.5, as described in Section 3.2.2.5. The pH of the culture was maintained between pH 7.0 and pH 8.5, which was identified as the optimal pH range for growth of *B. halodurans* Alk36 (Section 5.3). The raw data is presented in Appendix 2.2. The growth profiles of the cultures are presented in Figure 5.8 – 5.10.

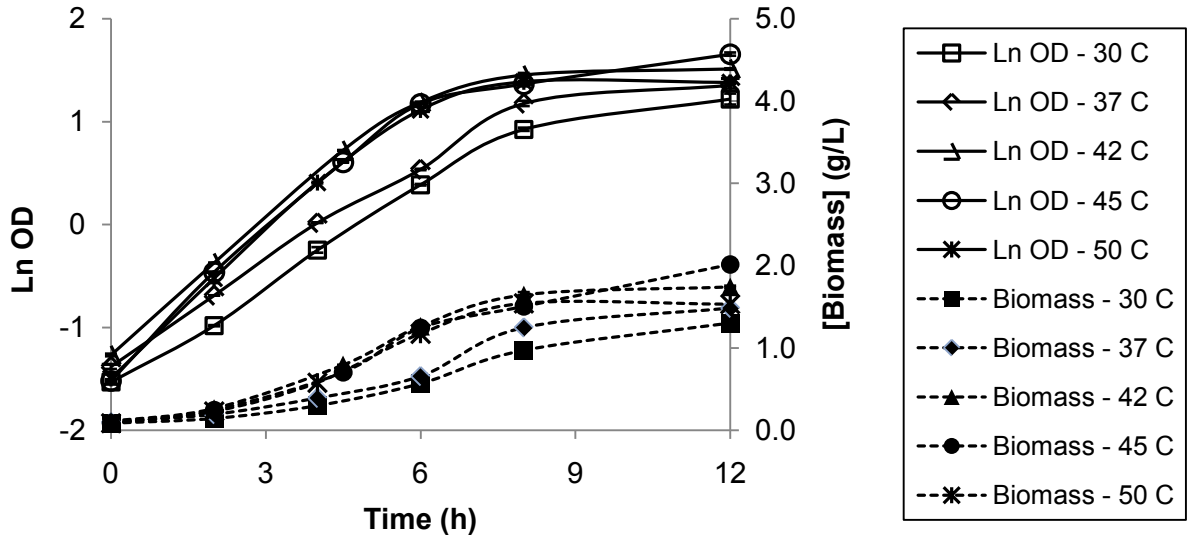

Figure 5.8: **Growth of *B. halodurans* Alk36 cultures in shake flasks containing EnBase® medium at different temperatures. The values presented were calculated from the average readings obtained from triplicate experiments and the error bars were obtained from the of the values. Where error bars are not showing, they are within the dimensions of the symbols.**

Cultures at 30 °C and 37 °C grew similarly and more slowly than the cultures grown at 42 °C, 45°C and 50°C. The growth profiles of the latter were statistically similar.

Even though the pH changed with time, it was maintained within the optimal range (i.e. between pH 7.5 and 8.5 as illustrated in Figure 5.9.

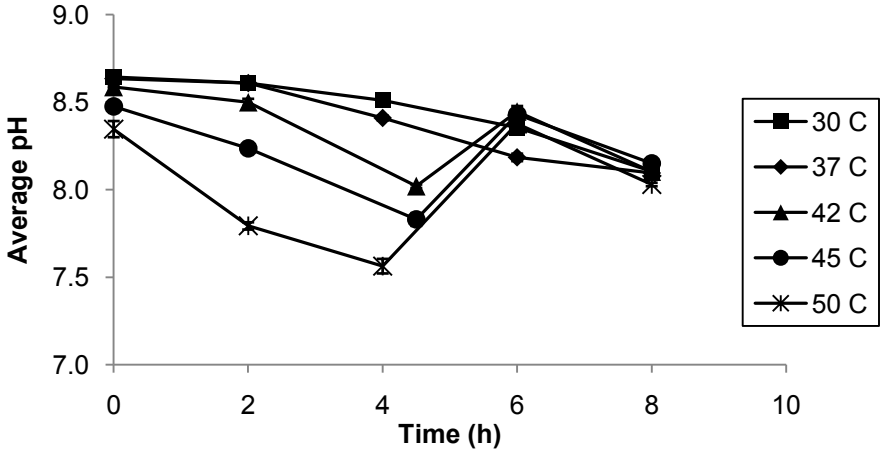

Figure 5.9: **The pH profiles of *B. halodurans* Alk36 cultures grown in shake flasks containing EnBase® medium at different temperatures. The values presented were calculated from the average of readings from triplicate experiments the error bars were obtained from the standard deviation of the values. Where error bars are not showing, they are within the dimensions of the symbols.**

The growth rate increased with increase in temperature; however, the highest specific growth rate was attained by the cultures grown at 45˚C (0.452 ± 0.05 h^{-1}) and 50˚C (0.443 ± 0.07 h^{1}) as shown in Figure 5.10. There was no growth in cultures at 60˚C, even when the inoculum used was pre-adapted to growth at 50°C. It is possible that *B. halodurans* Alk36 is a thermos-tolerant mesophile, since its optimal growth was between 45°C and 50 ˚C, while that of mesophiles is between 15°C and 45 °C and that of thermophiles is between 42 and 113 °C (Prescott et al., 2005).

The observed optimal growth temperature of *B. halodurans* Alk36 (45°C - 50˚C) was similar to that of *B. halodurans* strains MS-2-5 and 38C-2-1 isolated from Japan and Thailand, respectively (Murakami et al., 2007; Murakami et al., 2008). However, Hashim (2005) reported *B. halodurans* strains (isolated from Kenya) that could grow well at

55˚C.Hence, growth of *B. halodurans* Alk36 at 55°C should also be investigated in future work.

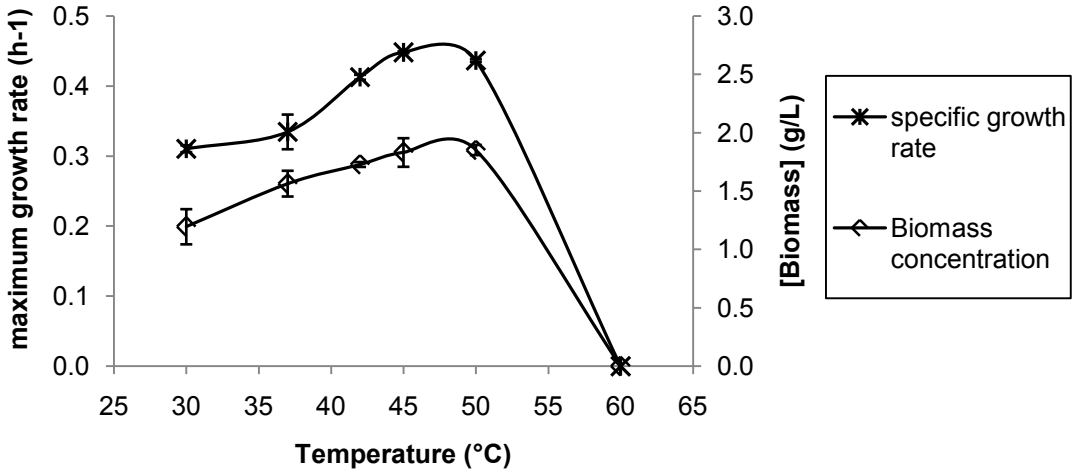

Figure 5.10: Relationship between the growth rate and growth temperature of *B. halodurans* Alk36 cultures. The values presented were obtained from the average of replicate set of experiments and the error bars were derived from the standard of error the mean of the average values. Where error bars are not showing, they are within the dimensions of the symbols.

5.5 Effect of Carbon-source on growth of *B. halodurans* Alk36

Bacillus halodurans Alk36 was grown in EnBase® medium containing dextrin (from potato starch), maltose or soluble starch as the carbon-source to determine the effect of the carbon source on growth and amylase production.

The growth profile of the cultures grown in media containing soluble starch, maltose and dextrin (polymeric substance made through partial hydrolysis of starch by thermal degradation under acidic conditions), were comparable, as shown in Figure 5.11 (Raw data in Appendix 2.4). However, the growth profile of the culture grown in EnBase® medium containing soluble starch as the carbon source was different from that of the cultures grown on maltose or dextrin. The growth rate in soluble starch decreased after four hours post inoculation and the cells stopped growing after nine hours, while the

cultures grown on dextrin and maltose only entered stationary phase at 12 hours. The poor growth in soluble starch could have been due to the formation of starch-hydrolysis products that could not be utilized by *B. halodurans* Alk36 as evidenced by the small amount of reducing sugars measured by the DNS assay (as discussed in Section 4.6).Further, formation of precipitates was observed in the cultures grown using soluble starch a few hours post inoculation. The formed precipitates were assumed to be due to starch hydrolysis products that interacted with salts in the medium.

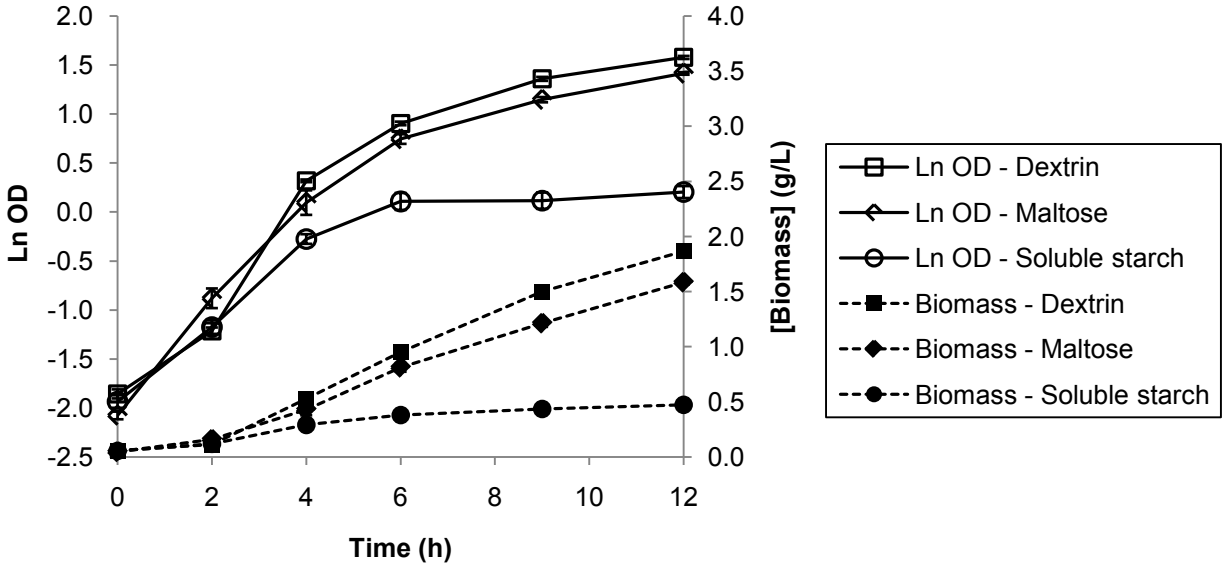

Figure 5.11: The growth profile of *B. halodurans* Alk36 strain in shake flasks with EnBase® media containing different sources of carbon at 45°C. The values presented were calculated from the average of the triplicate experiments and the error bars were derived from the standard of error the mean of the average values. Where error bars are not showing, they are within the dimensions of the symbols.

The biomass concentrations of the dextrin, maltose and soluble starch cultures at early stationary phase (12 hours post inoculation) was 1.87 ± 0.03 g/L, 1.59 ± 0.02 g/L and 0.47 ± 0.03 g/L, respectively (Figure 5.10). The culture grown on dextrin attained higher biomass concentration than that grown on maltose even though the two had similar specific growth rates while that of the culture grown in maltose was slightly lower (Table

5.5). The total protein concentration in the sample obtained from the dextrin culture (0.32 ±0.01 g/L) was slightly less than that obtained from the maltose culture (0.40± 0.11 g/L) (Table 5.5). Moreover, the amylase activity of the dextrin cultures (22.86 ± 0.90 U/mg protein) was slightly lower than that of the maltose culture (29.06 ± 1.14 U/mg protein) (Table 5.5).

Table 5.5: The effect of the type of carbon source on growth and amylase production by *B. halodurans* Alk36.

Carbon source	Dextrin	Maltose	Soluble starch
Growth rate (h^{-1})	0.46 ± 0.05	0.48 ± 0.15	0.43 ± 0.08
Biomass concentration at early stationary phase (g/L)	1.89 ± 0.05	1.60 ± 0.04	0.48 ± 0.05
Protein concentration (g/L)	0.32 ± 0.01	0.40 ± 0.11	nd¤
Specific amylase activity (U/mg protein*)	22.86 ± 0.90	29.06 ± 1.14	nd¤

* 1U is equivalent to 1mg of starch hydrolysed per minute under assay conditions.

¤ nd stands for not determined

The high amylase activity in cultures grown in maltose suggests that maltose was a better source of carbon for amylase production in *B. halodurans* Alk36, while dextrin was a better source of carbon for biomass production. The observed differences in amylase activities were initially proposed to be due to selection of a particular amylase. However, zymograms of protein samples obtained from the dextrin and maltose cultures showed that similar types of amylases were produced across the carbon sources maltose and dextrin, as shown in Figure 5.13. The presence of similar types of amylases in cultures grown in the presence of dextrin and maltose suggested that the

quantity of amylases in cultures grown on maltose was higher than that in cultures grown on dextrin.

The active bands obtained in the zymograms of supernatants from cultures grown at 45˚C using EnBase® medium with dextrin and maltose as the carbon source (Figure 5.12) were similar to those obtained from the cultures grown at 30˚C with the same media (Figure 4.11, Section 4.7, page 18). The similarity of active bands suggested that the same types of amylases were produced despite the difference in temperature and carbon source.

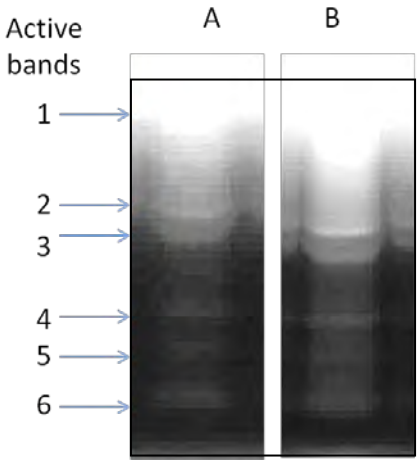

Figure 5.12: Starch-zymogram showing active bands obtained from culture grown in EnBase® medium containing dextrin (A) and maltose (B) as the carbon source.

5.6 Conclusions

The small-scale reactor vessels used in the optimisation studies were characterised in terms of mass transfer, by determining the oxygen transfer rates (OTR) and the volumetric mass transfer coefficients (k_La). Higher OTR and k_La values were attained with the shake flasks compared to the multiwell plates. Since *B. halodurans* Alk36 is an aerobic bacterium and, hence, oxygen is crucial for optimal growth, shake flasks were used for the optimisation studies.

The optimal pH for growth of *B. halodurans* Alk36, tested between pH 7 and11, was found in the range of pH 7.0 to 8.5, while the optimal temperature was between45˚C and 50˚C. The measured pH and temperature optima suggested that *B. halodurans* Alk36 is a thermotolerant, moderate alkaliphilic bacterium. Unlike other alkaliphilic *B. halodurans* strains, *B. halodurans* Alk36 grew poorly at pH values above 9.

The growth of *B. halodurans* Alk36 in medium containing dextrin as a carbon source was better than that in medium containing maltose and soluble starch. However, the amylase activity of the culture grown on maltose was higher than that grown on dextrin or starch, suggesting that maltose was a better substrate for amylase production. Additionally, the types of amylases produced by *B. halodurans* Alk36 did not appear to differ depending on temperature, pH or the type of carbon source (maltose or dextrin), supported by the similarity of patterns observed on the starch zymograms.

Chapter Six

Partial purification and characterisation of amylases from *B. halodurans* Alk36

6.1. Introduction

*Bacillus halodurans*Alk36 produced thermo-tolerant moderate alkaline amylases that enabled it to grow in EnBase® medium under alkaline conditions (pH 7 to 9) without addition of external amylase (as shown in Chapter 4 and 5). The starch-zymograms of the culture supernatant obtained from *B. halodurans* Alk36 grown in EnBase® medium indicated that *B. halodurans* Alk36 produced six potential amylases (Section 4.7).However, only two amylases were identified by Peptide-Mass Fingerprinting (PMF), the alpha amylase G-6 and the polysugar-degrading amylase (Section 4.7).

The starch-zymograms of the culture supernatant also showed that the alpha amylase G-6 had higher activity than the polysugar-degrading amylase suggesting that alpha amylase G-6 may be expressed more than the polysugar degrading amylase. Alternatively, the polysugar-degrading amylase expressed could have a lower activity or a lower selectivity for starch, or both, than the alpha amylase G-6. The low selectivity could have been due to the mode of action of the poly-sugar degrading amylase. These postulates can be confirmed by determining the activity of the individual amylases. Thus, partial purification was done to separate the six proteins that showed amylase activity on starch-zymograms to enable the determination of activity of the individual amylases, as well as for identification of the proteins that could not be identified by PMF analysis.

This section discusses the partial purification and separation as well as the characterisation of the amylases from *B. halodurans* Alk36. The purification protocol used in this study was adapted from a study done by Murakami et al. (2007), where multiple amylases from *B. halodurans* 38C-2-1 were partially purified and separated. The protocol involved partial purification and concentration of the amylases from the culture supernatant by ammonium sulphate precipitation, followed by liquid chromatography as indicated in Section 3.2.3.

6.2. Partial purification and concentration of amylases by ammonium sulphate precipitation

Ammonium sulphate precipitation was used to partially purify and concentrate the amylases from the proteins in the culture supernatant of *B. halodurans* Alk36 grown in EnBase® medium at 45˚C with maltose as the carbon source. Preliminary studies were done to determine the optimum concentration of ammonium sulphate required to achieve maximum precipitation of the amylases, with concomitant removal of unwanted proteins. Separation of the individual amylases was also considered. The proteins were precipitated using different salt concentrations, as described in Section 3.2.3.2.The precipitated protein fractions were re-solubilised in phosphate buffer at pH 8.5 and analysed by polyacrylamide gel electrophoresis (PAGE) as described in Section 3.3.5.

Precipitation at high salt concentration (60 to 80% of ammonium-sulphate saturation) resulted in recovery of a high concentration of proteins compared to precipitation at low salt saturation, as shown in Figure 6.1.

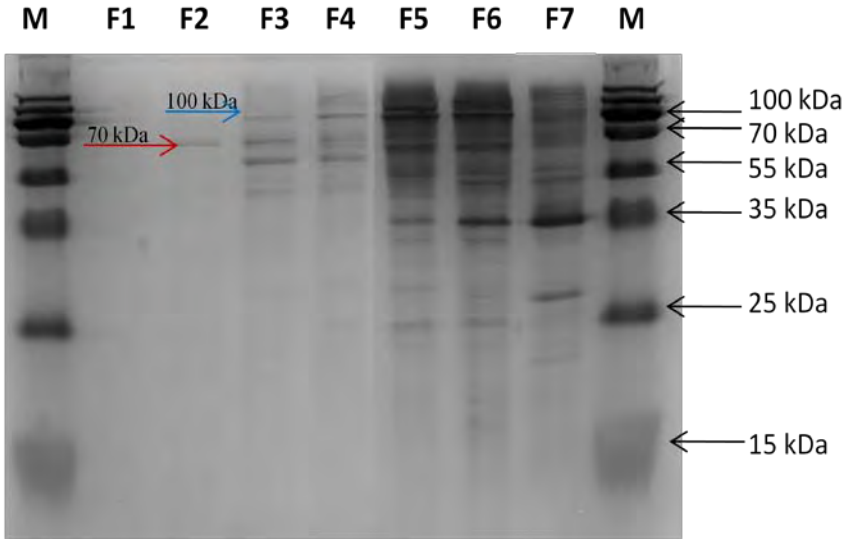

Figure 6.1: SDS-PAGE gel of protein samples obtained from ammonium sulphate (AS) precipitation test. Lane M contains the protein molecular weight marker, lanes labelled F1- F7 contain protein sample precipitated with ammonium sulphate at different saturation concentrations: F1 (0 – 20% AS), F2 (20 – 30%), F3 (30 – 40%), F4 (40 – 50%), F5 (50 – 60%), F6 (60 – 70%) and F7 (70 – 80%).

A band of approximately 70 kDa was observed from the sample precipitated with 20 to 30% ammonium sulphate, while five bands of sizes between 35 and 100 kDa were observed from sample precipitated with 30 to 40% and 40 to 50% salt. Fractions precipitated with 50 to 80% salt contained a wide range of protein bands whose sizes ranged between 15 kDa and 100 kDa.

Starch-zymograms were used to determine which of the ammonium sulphate fractions contained amylase(s). Two bands with activity on starch were observed in fractions F2, F3, F6 and F7, while six bands were observed in fractions F4 and F5 as illustrated in Figure 6.2.

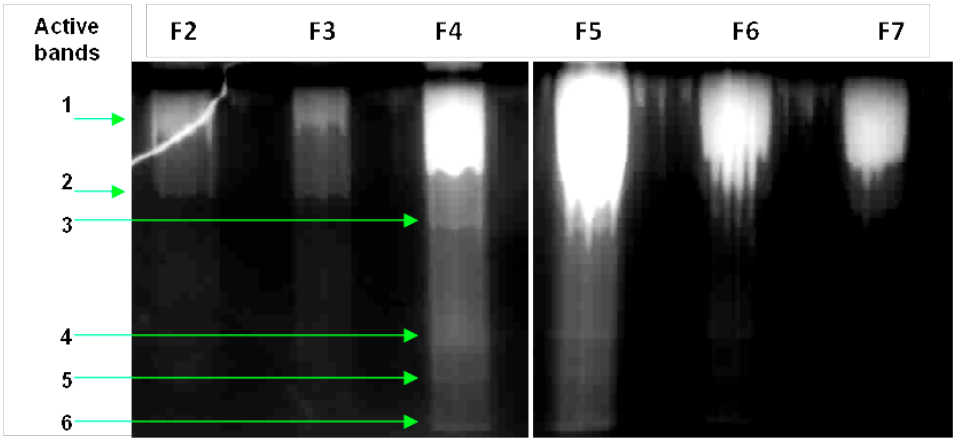

Figure 6.2: Starch-zymograms showing bands with amylase activity (white bands) obtained from proteins samples precipitated with ammonium sulphate at different saturation concentrations. F1 (0 – 20%), F2 (20 – 30%), F3 (30 – 40%), F4 (40 – 50%), F5 (50 – 60%), F6 (60 – 70%) and F7 (70 – 80%).

The protein concentrations and amylase activities of the different fractions were determined to confirm the results obtained from the zymograms. The highest amylase activities were obtained from fraction F4 (156 units/mg) and fraction F5 (225 units/mg) as shown in Table 6.1. These results substantiate the zymogram results illustrated in Figure 6.2, where band 1 in fraction F4 and F5 showed the highest amylase activity. Hence, precipitation with 50% to60% ammonium sulphate was chosen for further purification procedures, since it resulted in the highest protein and amylase recovery (31% and 27.56%, respectively).

Table 6.1: Amylase activities of protein samples obtained from different ammonium sulphate (AS) fractions.

Sample	Culture supernatant (no AS)	20 - 30% AS (F2)	30 - 40% AS (F3)	40 - 50% AS (F4)	50 - 60% AS (F5)	60 - 70% AS (F6)	70 - 80% AS (F7)
Protein concentration ($mg.L^{-1}$)	115 ± 1.56	822 ± 5.80	853 ± 5.91	1224 ± 26.17	3781 ± 27.35	4622 ± 150.4	2070 ± 9.670
Volume (mL)	3500	24	20	29	35	18	10
Total protein recovered based on Bradford assay(mg)	420	20	17	35	132	83	21
Protein recovery	100 %	5 %	4 %	8 %	31 %	20 %	5 %
Amylase activity of the fractions obtained from AS precipitates ($g.L^{-1-}.min^{-1}$)	5.55 ± 0.53	3.08 ± 0.31	2.58 ± 0.12	34.33 ± 0.72	152.98 ± 13.36	59.73 ± 3.26	42.53 ± 3.12
Total activity ($mg.min^{-1}$)	107.90	0.40	0.29	5.53	29.75	5.97	2.36
Recovered activity	100 %	0.38 %	0.27 %	5.13 %	27.56 %	5.53 %	2.19 %
Specific activity (U/mg protein*)	48.01 ± 0.00	3.75 ± 0.11	3.02 ± 0.05	28.04 ± 0.04	40.45 ± 0.09	12.92 ± 0.09	20.55 ± 0.08

* One unit of amylase activity is defined as the amount of enzyme that hydrolyses 1mg of starch per min under the assay conditions.

Although, about 73% of the protein that was present in the culture supernatant was recovered in the fractions obtained from ammonium sulphate precipitation, the amylase activity recovered from the fractions was quite low (41% of that of the culture supernatant, prior to protein concentration).However, the total amount of the activity recovered using ammonium sulphate precipitation, in this study, (41%) was within the range of yields obtained from other studies using 80% salt concentration for purifying amylases (40% to 65%) (Annamalai et al., 2011;Hagiara et al., 2001; Murakami et al., 2007). The observed low amylase activity could have been due to inactivation of amylases by removal of activator proteins during precipitation or instability of the amylases under the purification conditions used. Alternatively, low amylase activities could have also been due to inadequate precipitation of amylases byammonium sulphate. Thus, the amylase activity of the solution that remained after precipitation should have been determined.

The poor amylase recovery prompted the investigation of other concentration methods, such as the use of activated charcoal, which has been shown to be efficient in recovering proteins, particularly amylases, from dilute solutions(Kareem et al., 2011; Kumar, 2003). About 59% of the proteins were recovered from 1 litre of culture supernatant using activated charcoal, while ammonium sulphate precipitation, at 50 to 60 % salt saturation, was able to precipitate only 33% of the proteins in the culture supernatant, as shown in Table 6.2.

The amylase activity recovered from the enzyme solution after treatment with activated charcoal was 92% of that of the culture supernatant prior to purification, while only 11.4% of the amylase activity was recovered from the enzyme solution obtained from ammonium sulphate precipitation, at 50 to 60 % salt saturation as illustrated in Table 6.2. In addition, the specific amylase activity obtained from the activated charcoal filtrate (40 units/mg protein) was higher than that obtained from ammonium sulphate precipitation (9.2 units/mg protein).

Table 6.2: Protein and amylase yields obtained from partial purification of proteins from *B. halodurans* Alk36 culture supernatant by ammonium sulphate precipitation compared to activated charcoal fractionation. .

Sample	[protein] mg/L	Volume	Total protein (mg)	Protein recovery	Amylase activity (mg/L/min)	Total activity (U*)	Recovered activity	Specific amylase activity (U/mg protein)
Culture supernatant	150	1 L	150	100%	3955	3955	100 %	26
Filtrate from activated charcoal	88	1 L	88	59%	3584	3584	91 %	40
Ammonium sulphate precipitation at 50 – 60% salt saturation	2701	18 mL	49	33%	45100	812	21 %	9.2

* One unit of amylase activity is defined as the amount of enzyme that hydrolyses 1 mg starch per min under the assay conditions.

Even though the amylase yield obtained in the present study, when using activated charcoal, was higher than that obtained from ammonium sulphate precipitation, an additional concentration step was required (after the activated charcoal purification step) since the amylase remained in the bulk solution. The concentration methods that could have been used to concentrate the amylases in the filtrated obtained from activated charcoal precipitation included lyophilisation, ultra-filtration with molecular weight cut-off membrane and ammonium sulphate precipitation. However, the activated charcoal filtrate was not analysed further due to time constraints. It was, thus, recommended that further studies should be done to determine which concentration method would result in the highest amylase yields.

6.3. Partial purification of amylases by liquid chromatography

Since ammonium sulphate precipitation, using different salt concentrations, could not separate the potential amylases,liquid chromatography was used to further purify the concentrated proteins so as to separate the amylases with the purpose of identifying and then characterizing the individual amylases. The protein sample concentrated by ammonium sulphate precipitate, at 50 to 60 % salt saturation, was subjected to anion-exchange, hydrophobic interaction and size exclusion chromatography to separate the proteins according to charge, hydrophilic nature and size, respectively.The chromatographic procedures are described in Section 3.2.3.4.

Three protein peaks were obtained from the anion-exchange chromatography as illustrated in Figure 6.3. The peaks represented proteins of different charges, since proteins that contained positive charge or weak negative charge eluted first, while those with a strong negative charge eluted last. Zymograms carried out using protein fractions pooled from each of the peaks showed that only peak 2 and peak 3 contained proteins with activity on starch (Figure 6.4).

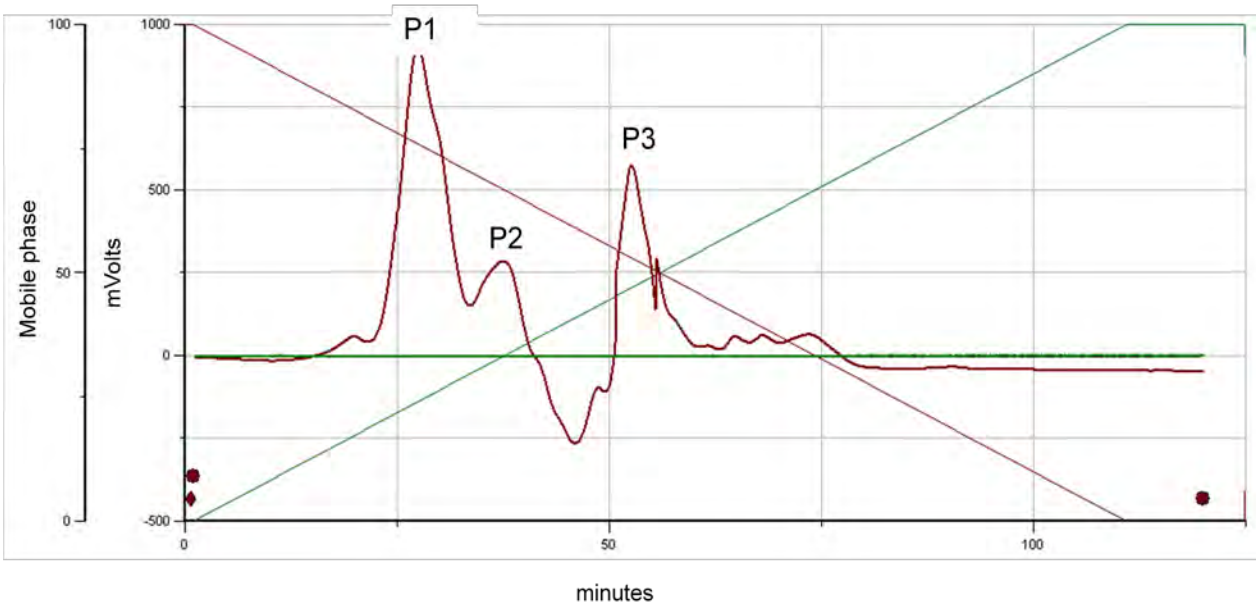

Figure 6.3: Chromatogram showing protein peaks (P1, P2 and P3) obtained from anion-exchange of culture supernatant of *B. halodurans* Alk36 using QXP Sephrose column.

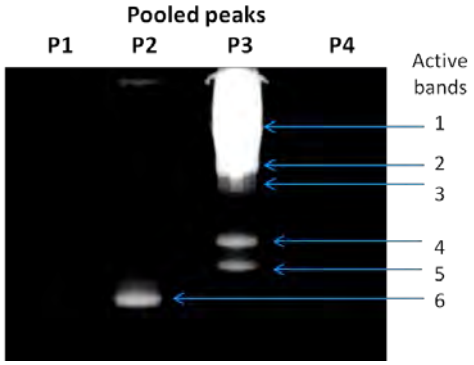

Figure 6.4: Starch-zymogram of the protein samples pooled from the fractions containing protein peaks obtained from anion exchange showing bands with activity on starch. Lane labelled P1- P4 contained protein samples containing Peak 1, Peak 2, Peak 3 and the flow-out solution.

One active band was obtained from peak 2, while peak 3 contained about five additional active bands. The absence of active bands from peak 1 indicated that this purification step has removed significant amounts of non-amylase proteins as shown in Figure 6.5.

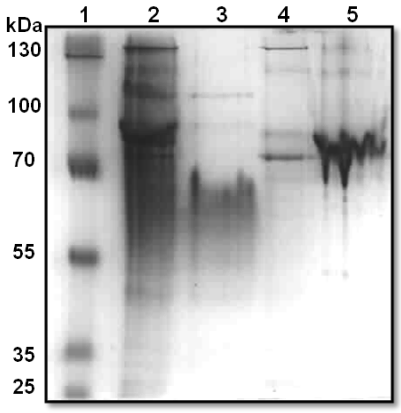

Figure 6.5: Native gel of the protein samples pooled from the fractions containing protein peaks obtained from anion exchange. Lane 1 contained the PageRuler protein molecular weight marker, Lane 2 contained the protein sample from ammonium sulphate precipitation, Lane 3 – 5 contained protein sample containing Peak 1, Peak 2 and Peak 3 from anion exchange chromatography, respectively.

The fraction that contained the five active bands (peak 3)was further purified using the hydrophobic interaction column, where hydrophilic proteins were collected in the effluent(mobile phase leaving the column prior to elution) since they did not bind to the column. The proteins bound to the column (hydrophobic proteins) required subsequent elution, using a buffer with decreasing salt concentration, such that the least hydrophobic protein eluted first and most hydrophobic proteins eluted last. Only one protein peak was obtained from the hydrophobic fraction, suggesting that the bound proteins had similar hydrophobicity as shown in Figure 6.6. Even though there was an appearance of a peak at the end of the chromatogram, no peak was observed when the chromatogram was continued.

It was suggested that the salt concentration of the mobile phase should be increased since the observed peak only appeared in the last 25 minutes of the 125 minute elution. The use of mobile phase with higher salt concentration would shorten the elution time and allow proper visualization of the evens at the end of the run.

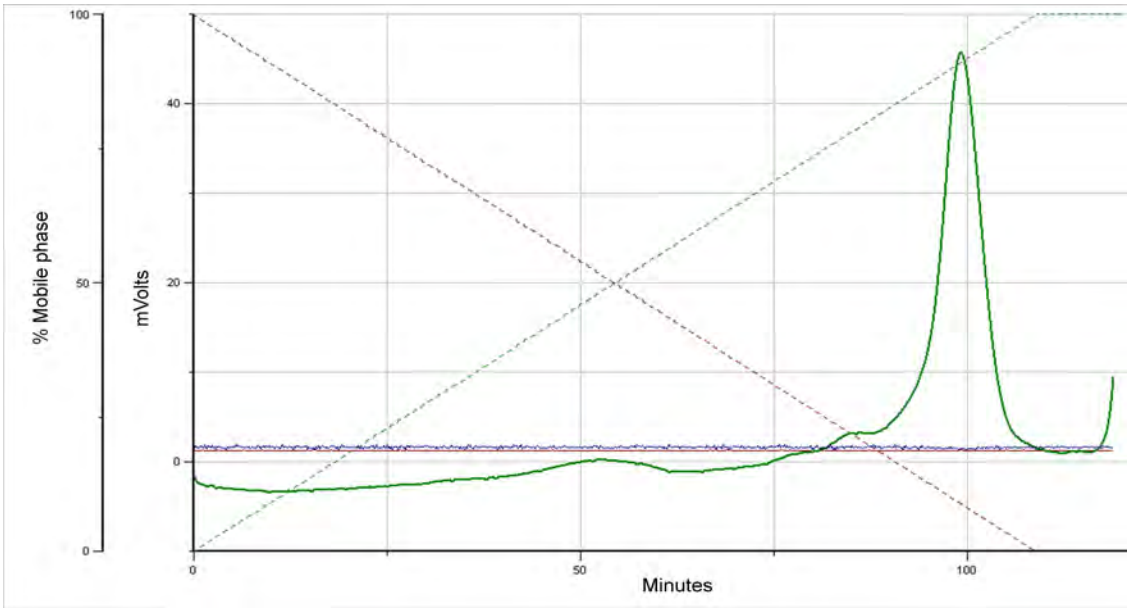

Figure 6.6: Chromatogram showing the protein peak representing proteins that bound the hydrophobic interaction column.

Zymograms of the protein sample obtained from the effluent solution (i.e. the mobile phase leaving the column prior to elution) and the proteins eluted from the hydrophobic-interaction column showed similar protein bands (with activity on starch) (Figure 6.7). Six active bands with the same relative mobility were observed in the starch-zymogram.

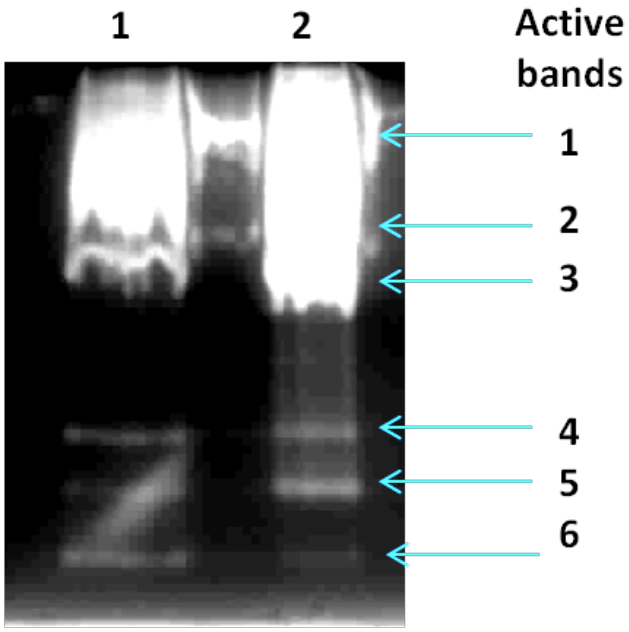

Figure 6.7: Starch-zymogram of the protein samples obtained from the effluent and proteins eluted from the hydrophobic interaction chromatography (HIC) showing amylases present in the two samples. Lane 1 contained the protein sample from the effluent solution while Lane 2 contained the protein sample from the peak eluted from the HIC column.

The presence of similar protein bands in the effluent and eluite indicated that hydrophobic interaction chromatography was not able to separate the proteins of interest successfully. Fewer protein bands were obtained from the effluent and eluite from the hydrophobic-interaction chromatography (HIC) column in comparison to the bands found in the sample prior to separation by the hydrophobic interaction chromatography (Figure 6.8).

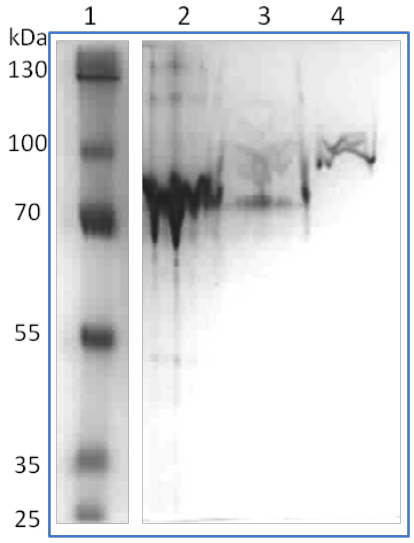

Figure 6.8: Native gel of protein samples obtained from hydrophobic-interaction chromatography (HIC). Lane 1 contained the PageRuler protein molecular weight marker, Lane 2 contained the protein sample from anion exchange chromatography that was loaded into the HIC column, Lane 3 contained protein sample from the effluent solution and Lane 4 contained the protein sample eluted from the HIC column.

The presence of fewer protein bands in the eluted sample suggested that a significant protein fraction had been lost after HIC. The loss of protein observed after the HIC indicated that the HIC was not an effective method for purification of the proteins obtained from anion exchange chromatography. The loss of proteins from HIC was also reported by Murakami et al., (2007), where there was no improvement in specific amylase activity after hydrophobic interaction chromatography and the amount of protein recovered was low. Hence, it was recommended that the hydrophobic interaction chromatography should be omitted from the purification regime in future work, and that other purification techniques should be explored to improve separation of the amylases and their yields.

“Frowning” of protein bands observed in the gels was probably due to high concentration of salts in the sample solution due to high concentration of salts in the mobile phase used to elute the proteins from the chromatography column matrix. The samples were

not diluted to reduce the salt concentration because the concentration of protein in the samples was low. Hence, dilution would have further reduce the concentration of proteins in the samples, making them difficult to detect. Alternatively, dialysis could have been used to remove the salts from the enzyme solution; however, this was difficult to achieve with the small sample size available.

The proteins eluted from the hydrophobic-interaction column (i.e. bound proteins) were further purified by size exclusion chromatography (SEC). Only one peak was obtained from the size exclusion column (Figure6.9).

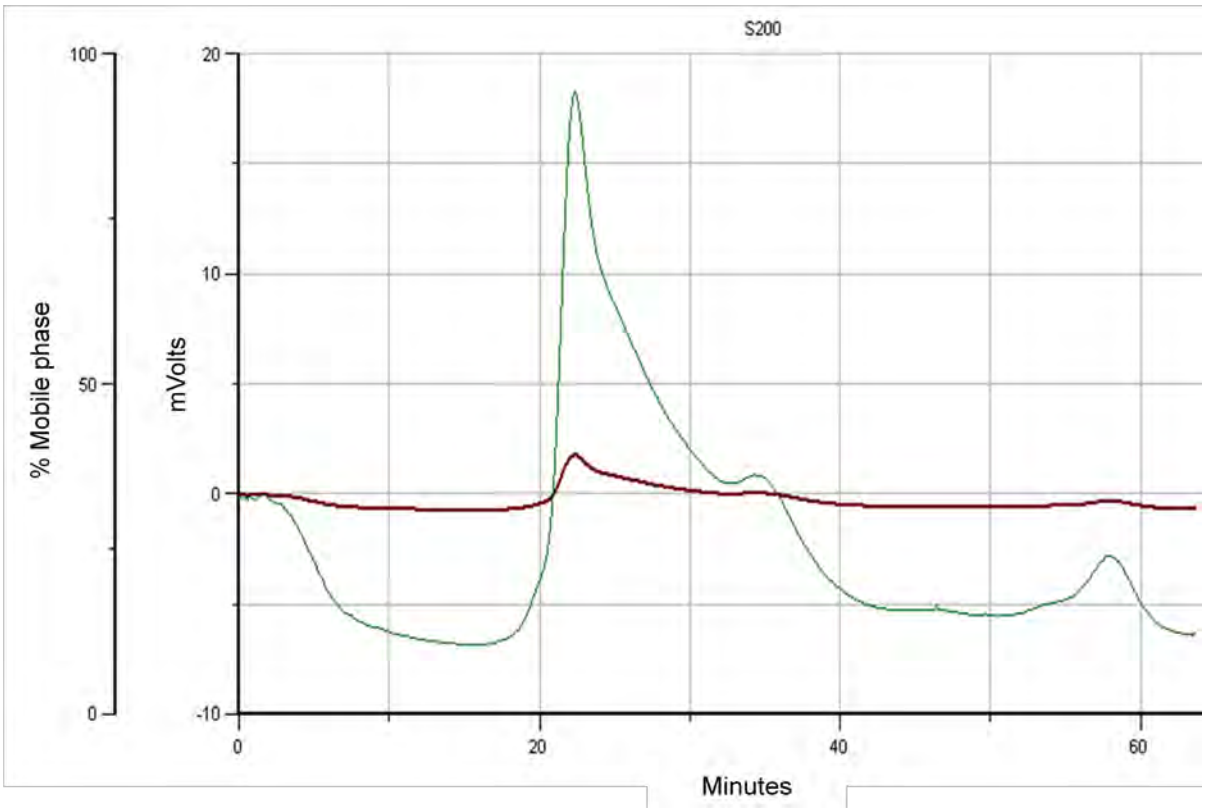

Figure 6.9: Chromatogram showing the protein peak obtained from size-exclusion chromatography of the protein sample eluted from the hydrophobic-interaction column. The red lines indicate the protein concentration measured by UV detection at 280 nm while the green line indicates the protein concentration measured by refractive index.

A starch-zymogram of the protein sample obtained after separation by SEC showed three faint bands with activity on starch, while no bands were observed in the native PAGE (Figure 6.10). The absence of protein bands in the native PAGE indicated that the protein concentration in the protein sample was very low.

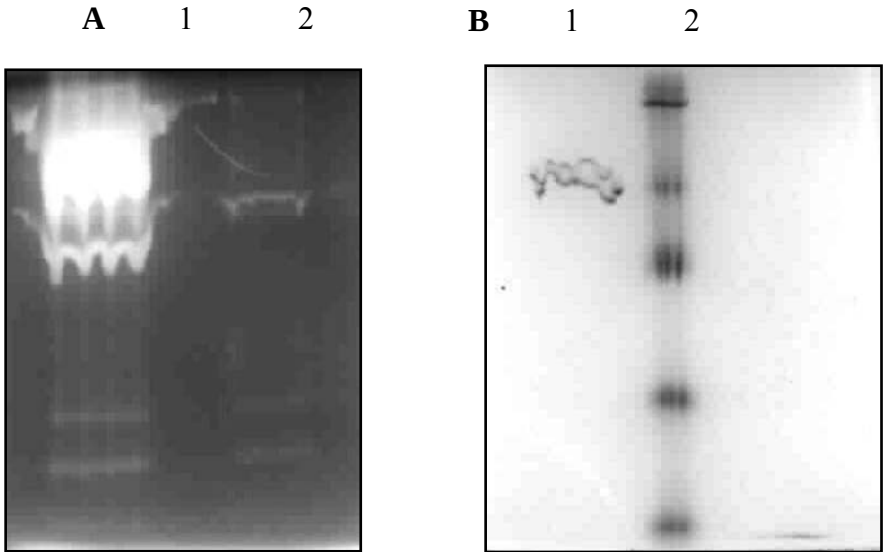

Figure 6.10: Zymogram (A) and native PAGE (B) of the protein samples obtained from Size-exclusion chromatography. Lane 1 contained protein sample before separation on SEC. Lane 2 contained the protein sample eluted from the gel filtration column.

In a typical protein-purification protocol, the specific activities of the protein of interest increases with each purification step, since unwanted proteins are removed (Berg et al., 2002). Some protein loss is expected in downstream processing; however, the amount of protein loss during the purification of amylases in the present study was unacceptably high (99%) as illustrated in Table 6.3. Poor protein and amylase recoveries, observed in the present study, were postulated to be due to protein denaturation and amylase inactivation. In the present study partial purification and separation of the amylases from *B. halodurans* Alk36 using the purification protocol adapted from Murakami et al. (2007) was unsuccessful. Even though Murakami et al. (2007) were able effectively purify and separate two amylases from *B. halodurans* 38C-1, using a similar protocol, the amount of activity recovered at the end of the purification was very low (4%).

Table 6.3: Protein recovery and amylase activities obtained at different purification stages.

Sample source	[Total protein] (g/L)	Sample volume (mL)	Total protein (mg)	Protein Yield (%)	Amylase activity (g/L/min)	Total Activity (mg/min)	Activity recovery (%)	Specific amylase activity (U/mg protein)*
Culture Supernatant	0.12	3500	420	100	5.55	19.42	100	46
Ammonium sulphate precipitate with 50 to 60% salt	3.69	35	129	31	188	6.58	34	51
AEC* Peak 1	0.58	5	2.90	2.2	Not analysed[b]			
AEC* Peak 2	0.59	4.5	2.66	2.1	Not analysed[b]			
AEC* Peak 3	1.58	4.5	7.11	4.9	231	1.04	16	146
Effluent of from HIC*	1.54	1.5	2.31	1.8	8.87	0.01	1.26	5.76
Protein from Peak 3 that bound the HIC*	0.08	1.5	0.12	0.09	6.69	0.01	1.0	83.62
SEC* of protein sample from Peak 3	0.06	1.5	0.09	0.07	Not analysed[b]			

* AEC – Anion-exchange chromatography, HIC – Hydrophobic interaction chromatography, SEC – Size exclusion chromatography

a - One unit of amylase activity is defined as the amount of enzyme that hydrolyses 1 mg starch per min under the assay conditions.

b - The samples were not analysed because the activity of the amylases was not observed in starch zymograms or the concentration of proteins and amylases in the sample was too low to perform the assays.

Hence, it was concluded that the purification protocol used was unsuitable for separation of amylases from *B. halodurans* Alk36 and further investigation should be done to determine a purification protocol that can effectively purify the amylases. Alternatively, a method to improve amylase yield and recovery through the use of protein stabilizing agents should be investigated.

6.4. Effect of buffer solutions on stability of amylases

The low activities observed in samples obtained from the chromatography could have been due to instability of the amylases in the buffer solution used for chromatography (Tris/Cl buffer). Hence, the stability of amylases in the buffer solutions used for growth and storage (phosphate and Tris/Cl buffers) was investigated by determining the amylase activity at different days. The activity of the enzyme solution decreased by about 20% in two days, when the enzyme solution obtained from ammonium sulphate precipitation was stored in 0.1 M phosphate buffer(K_2HPO_4/KH_2PO4 at pH 8.5) at 4°Cas illustrated in Table 6.4.

Table 6.4: Effect of buffer solution on amylase activity and stability.

Time	Amylase activity (Units/mg protein)	
	Phosphate buffer	Tris buffer
Day 0	132 ± 4	62 ± 2
Day 2	106 ± 4	44 ± 8

* One unit of amylase activity is defined as the amount of enzyme that hydrolyses 1 mg starch per min under the assay conditions.

The decrease in amylase activity indicated that the amylases were unstable and the use of stabilizing agents should been investigated. Interestingly, when the activity of the amylase solution was determined using a sample diluted in 0.1 M Tris/HCl buffer at pH

8.5, the amylase activity was about two-times lower than that obtained with phosphate buffer (Table 6.4). The difference in observed activities indicated that Tris buffer may cause interference in the amylase activity assay. Several studies have reported interference effects of Tris buffer on the activity of alpha-amylase from *Bacillus* species (Ghalanbor et al., 2008; Bernhardsdotter et al., 2005). In these studies, the Tris molecule acted as a competitive inhibitor by competing with starch for the active site of the amylases. Protein degradation and the interference caused by Tris buffer could justify the low activities observed in protein purification (Table 6.3),since Tris buffer was used for all liquid chromatography procedures. Tris buffer was used instead of phosphate buffer during chromatography because the Tris buffer does not interact with the chromatography matrix. On the other hand, the phosphate ions in phosphate buffer are known to interfere with chromatographic purification by binding to the column matrix and hence, limit the interactions available for protein binding. Therefore, it was suggested that buffer exchange should have been done to remove the Tris molecules in enzyme solution prior determination of amylase activity. Alternatively, further studies should be done to determine a suitable buffer solution that can be used for chromatography without interfering with the amylase activity. Further, the identification of stabilizers that can prevent degradation of the amylases should also be investigated.

6.5 Characterisation of *B. halodurans* Alk36 amylases

The purification protocol used in the present study provided insufficient purification of the potential amylases produced by *B. halodurans* Alk36 for all the potential amylases (proteins with the ability to degrade starch as seen in the zymograms above)to be identified by PMF. Further, the characteristics of the individual amylases could not be determined. Since the starch-zymograms have shown that most of the observed amylase activity was due to one amylase i.e. the alpha amylase G-6, it was assumed that the activity based on the polysugar-degrading amylases was negligible. Hence, the concentrated enzyme solution was characterised to determine the pH and temperature range for optimal activity of alpha amylase G-6.The enzyme solution was obtained from the culture supernatant of *B. halodurans* Alk36 grown in EnBase® medium at 45˚Cand

pH 8.5, with dextrin or maltose as the carbon source. The amylases were partially purified and concentrated by ammonium sulphate precipitation, at 50% to 60% salt saturation, as discussed in Section 6.2.

6.5.1 Optimal temperature for amylase activity

The temperature range for optimal amylase activity was investigated by determining the amylase activity of the enzyme solution at 30˚C, 40˚C, 45˚C, 50˚C, 55˚C and 60˚C in phosphate buffer at pH 8.5 as described in Section 3.2.2.5. The amylase activities increased with increase in temperature from 30˚C to 50˚C, and then decreased rapidly as shown in Figure 6.11. The highest activity was obtained at 50˚C, for both cultures; 158 ± 8 U/µg protein for the culture grown on maltose and 78 ± 3 U/µg protein for the culture grown on dextrin (where 1 Unit of enzyme activity was equivalent to 1 mg of starch hydrolysed per minute at the given temperature and pH 8.5).

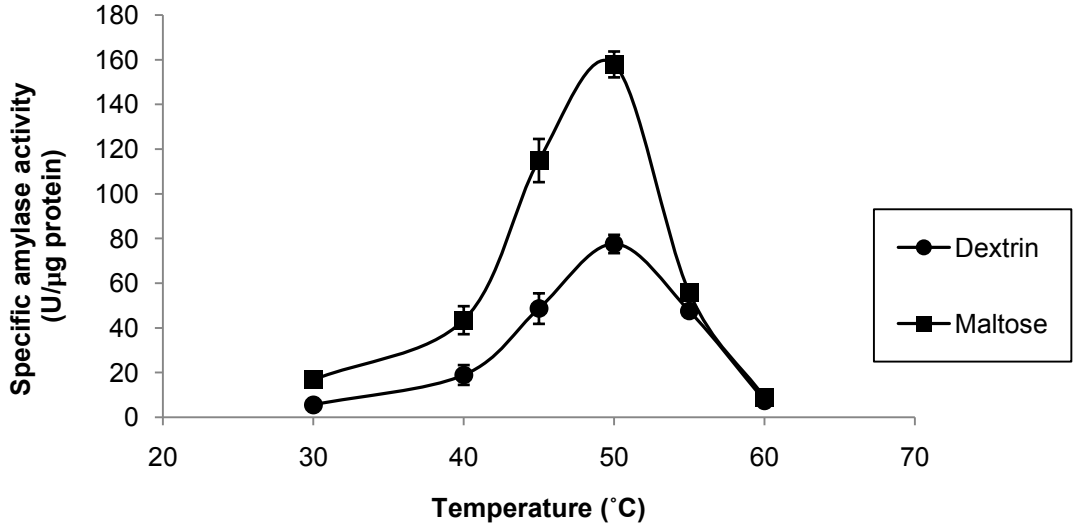

Figure 6.11: **Effect of temperature on amylase activity of the protein sample concentrated from the culture supernatant of *B. halodurans* Alk36 grown on EnBase® medium at 45°C with dextrin or maltose as the carbon source. The values presented were obtained from replicate experiments and the error bars were derived from the standard error of the mean.**

The optimal temperature (50˚C) for the activity of *B. halodurans* Alk36 amylases was similar to the optimal temperature reported by Hashim et al., (2005) and Murakami et al., (2007 & 2008) i.e. 50 - 60 °C. Furthermore, the optimal temperature for amylase activity, determined in the present study, was similar to the optimal growth temperature described in Section 5.5 i.e. 50°C . It was suggested that the amylases from *B. halodurans* Alk36 are thermotolerant since their optimal activity was at 50 ˚C.

6.5.2 Optimal pH for amylase activity

The optimal pH for amylase activity was investigated by determining the activities of amylases from *B. halodurans* Alk36 in buffer solutions at different pH. The enzyme solution was obtained from the culture supernatant of *B. halodurans* Alk36 grown on EnBase medium at 45°C and pH 8.5. The amylase assays were done at 50˚C in phosphate buffer at pH 7 to 10, as described in Section 3.2.2.3. The activity of *B. halodurans* amylases between pH 7, 8 and 8.5 were similar, but decreased substantially above pH 8.5 as shown in Figure 6.12.

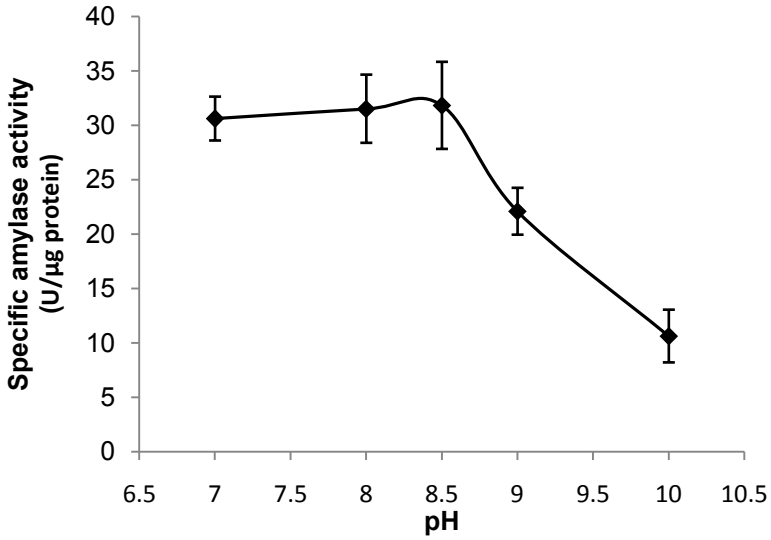

Figure 6.12: **Effect of pH on amylase activity of the protein sample concentrated from the culture supernatant of *B. halodurans* Alk36 grown on EnBase® medium at 45°C with Dextrin as the carbon source. The graph represents values obtained from replicate experiments and the error bars were derived from the standard error of the mean.**

The highest activity was obtained at pH 8.5 (31.81 ± 5.66 U/µg protein), while the activity at pH 8 was 31.50 ± 4.43 U/µg protein and that at pH 7 was 30.60 ± 2.58 U/µg protein (where 1Unit of enzyme activity is equivalent to 1 g of starch hydrolysed per minute at 50˚C and the given pH). The error bars given in Figure 6.12 were determined from replicate experiments conducted on different days, rather than replicate samples within the same experiment. Hence the large error bars represent inter-experiment error and may be attributable to the decrease in activity with time, since the amylases were shown to be unstable in the storage buffer (Section 6.4). The optimal pH for amylase activity obtained in the present study was similar to the optimal pH for growth of *B. halodurans* Alk36, but it was lower than that reported from other *B. halodurans* strains, which had an optimal activity at pH 10 (Hashim et al., 2005; Murakami et al., 2007; Murakami et al., 2008). The observed differences may be due to the different *B. halodurans* strains used in these studies, particularly since the strain used in the present study (*B. halodurans* strain Alk36), failed to grow in pH above pH 9. Consequently, future investigations should include the determination of the activity of *B. halodurans*Alk36 amylases at pH values lower than 7, to establish whether the amylases are alkaliphilic or alkali-tolerant.

The enzyme solution used to determine the optimal pH and temperature for amylase activity was obtained from cultures in exponential phase, since the growth experiment at 45°C was terminated prematurely due to oxygen limitation. Hence, the obtained activities did not represent the optimal amylase activity of *B. halodurans* Alk36 because the specific amylase activity of the exponential phase culture was shown to be lower than that of the early stationary phase culture (Section 4.7). However, the obtained pH and temperature profiles would have been similar to that of enzyme solution obtained from an early stationary phase culture because the same types of amylases were produced during the exponential and stationary phase, as illustrated in Section 4.7.It is recommended that further studies should be done to determine the optimal activity of the enzyme solution obtained from early-stationary phase cultures grown under optimal growth condition i.e. 45˚C to 50˚C and pH 7 to 8.5, with maltose as the carbon source. The activity obtained from the culture grown under optimal conditions would enable accurate assessment of improvements made by using optimal conditions for growth and production of amylases by *B. halodurans* Alk36.

6.6 Conclusions

The protocol used in the present study for purification of alkaliphilic amylases from *B. halodurans*Alk36 was inefficient and a more effective protocol should be established. Protein purification and concentration by ammonium sulphate precipitation recovered 41% of the amylase activity. However, the liquid chromatography regime used in this study for purification of amylases was not effective in purifying and separating the amylases. It was recommended that the use of protein stabilizers and different buffer systems for chromatography should be investigated to enable effective purification and separation of the amylases produced by *B. halodurans* Alk36.

The optimal temperature and pH for the activity of *B. halodurans* Alk36 amylases were 50˚C and pH 8.5, indicating that amylases from *B. halodurans* Alk36 could be thermotolerant and alkaliphilic or alkali-tolerant. These amylases performed appropriately in alkaphilic cultivation using starch-based media and are appropriate for moderately alkaphilic applications. Since the activity of the amylases from *B. halodurans* Alk36 decreased rapidly in pH above pH 8.5, these amylases may not be suitable in detergent formulations whose pH is above 9.

Chapter Seven

Conclusions

Amylases have many applications, particularly in industrial processes requiring starch hydrolysis and in detergent formulations. Alkaline amylases are preferable for application in detergent formulations where they are used for removal of starch stains. *B. halodurans* Alk36 produces alkaline amylases that enable it to grow on starch as the carbon source. The present study was carried out to determine the types of amylases produced by *B. halodurans* Alk36 and the optimal growth conditions for improved growth and amylase production, in addition to characterising the amylases produced, to assess their application in detergent formulations.

7.1 Types of amylases produced by *B. halodurans* Alk36

Using amylolytic activity on starch zymographs to discern the amylases, the present study has demonstrated that *B. halodurans* Alk36 produced six proteins with potential amylase activity. Two of the six proteins were confirmed to be amylases by Peptide Mass Fingerprinting analysis. The two proteins were identified as a 107 kDa alpha-amylase G-6 and a 37 kDa polysugar-degrading amylase. The amino acid sequence of the alpha-amylase G-6was comparable to amylases from other *B. halodurans* strains i.e. C-125, 38C-2-1, MS-2-5 and LBK 34,and*B. clausii*, demonstrating 99 to 10% identity, while the polysugar-degrading amylase showed reduced similarity.

From the zymographs, the alpha-amylase G-6 showed higher amylase activity than the polysugar-degrading amylase, such that most of the observed activity was due to the alpha-amylase G-6. Since the rate of starch hydrolysis by *B. halodurans* Alk36 amylases was higher than the rate of release of reducing sugars, the amylases from *B. halodurans* Alk36 were postulated to be endo-acting.

7.2 Validation of small-vessels for bioprocess optimisation

In the present study, the 24-well plates and shake flasks were characterised based on oxygen transfer rates (OTR) and the volumetric mass transfer coefficient (k_La) to select the appropriate vessel and operating conditions for the optimisation studies. The oxygen transfer rates (OTR) attained in the multiwell plates under normal operating conditions (10% filling volume and 200 rpm shaking frequency) were about ten-fold lower than that attained in the bioreactor and two-fold lower than that attained in the shake flasks. Thus, shake flasks were used for the optimisation studies at small scale.

Shake-flasks and multiwell plates provided a platform for performing multiple experiments in parallel while using small culture volumes. They were unable to deliver as much oxygen to the system as the stirred-tank bioreactor. Further, optimal conditions could not be maintained in the dynamic shake-flask or multiwall plate environment e.g. changes in pH were recorded. Hence, the small scale vessels could not effectively determine the difference in final end-products (i.e. the biomass and amylase activities) under the examined growth conditions. Therefore the growth rate, instead of the biomass concentration or amylase activity, was used as a measure for determining the optimal growth conditions for *B. halodurans* Alk36 in EnBase® medium. The optimal growth conditions were also shown to represent the optimal conditions for amylase production since growth of *B. halodurans* Alk36 in EnBase® medium was dependent on the production of endogenous amylase/s.

7.3 Optimal conditions for growth of *B. halodurans* Alk36

B. halodurans Alk36 was considered to be a moderate thermophile since its optimal growth temperature was between at 45°C to 50˚C. The optimal pH for growth of *B. halodurans* Alk36 (pH 7 to 8.5) suggested that *B. halodurans* Alk36 could be a facultative alkaliphile. Unlike other *B. halodurans* strains, *B. halodurans* Alk36 could not grow above pH 9.

The growth of *B. halodurans* Alk36 in EnBase® medium while using dextrin as the carbon source, led to improved biomass production compared to growth using maltose

as the carbon source. However, the amylase activity of the protein solution obtained from culture grown on maltose was slightly higher than that from the culture grown on dextrin. Improved amylase activity in presence of maltose was thought to be due to the mode of action of the amylases that made hydrolysis of starch more favourable than that of maltose. Under this conditions, the bacterium may produce more enzyme and hence the amount of amylase in medium containing maltose would be higher than that in medium containing dextrin.

7.4 Characteristics of amylases from *B. halodurans* Alk36

The amylases from *B. halodurans* Alk36 were active at the pH range between 7 to 10, and temperature range between 30°C and 60˚C. The optimal activity was observed between pH 7 ando8.5 and between45°C and50˚C. The amylase activity decreased rapidly above pH 8.5 and 55°C,while that below pH 7 and 30C was not determined . Based on the characteristics reported in the present study, amylases from *B. halodurans* Alk36 have potential for application with the EnBase® medium for growing moderately alkaliphilic bacteria and for starch hydrolysis under moderately alkaphilic conditions. However, these amylases are not expected to perform optimally in detergent formulations with pH above 8.5.

The amylases were not stable in phosphate buffer at 4˚C, demonstrated by a decrease in activity with increase in storage-time. The decrease in stability was thought to be due to removal of stabilizing agent subsequent to concentration by ammonium sulphate precipitation.

7.5 Recommendations:

Based on the findings of this study, several recommendations were made. These include:

- The purity of protein samples that showed amylase activity on starch-zymography should be improved by two-dimensional gel electrophoresis, to enable identification by PFM analysis or determination of amino acid sequence of the amylases or both.

- Since the activities obtained in Tris buffer were 2-fold lower than those obtained in phosphate buffer at the same pH, different buffer solutions should be explored to identify buffers that enable effective purification by liquid chromatography without loss of activity. Alternatively, buffer exchange should be used to remove the Tris molecules prior determination of amylase activity, depending on whether Tris buffer affects the activity demonstrated or the protein stability.
- Different methods for partial purification and concentration of the amylases should be investigated to determine methods with improved amylase yield since the yields obtained using ammonium sulphate were less than 40% of the activity in the culture supernatant.
- Amylase stabilising agents should be explored to prevent rapid protein denaturation of the amylases with time and hence, maintain high amylase activities upon storage.
- The activity and productivity of the amylases from cultures grown under the optimal conditions identified should be determined.
- The types of hydrolysis products formed from starch hydrolysis by *B. halodurans* Alk36 amylase should be determined to confirm that the mode of action of these amylases is endo-acting.
- The variety of substrates that can be hydrolysed by *B. halodurans* Alk36 amylases should be determined to enable the extension of the potential applications of the amylases.

References

1. AEB Africa (Pty) Ltd, Product information. Retrieved: March 26, 2014, from http://www.aebafrica.co.za/beer/enzymes.html.

2. Aehle, W. (2008). Amylases. In *Enzymes in Industry.* (3rd ed.,) John Wiley & Sons. 168. Retrieved April 11, 2014, from http://www.books.google.com

3. Aiyer, P.V. 2005. Amylases and their applications. *African Journal of Biotechnology.* 4(13):1525-1529.

4. Alcalde, M., Ferrer, M., Plou, F.J. & Ballesteros, A. 2006. Environmental biocatalysis: from remediation with enzymes to novel green processes. *Trends in Biotechnology.* 24(6):281-287.

5. Andrews, P. 1964. Estimation of the molecular weights of proteins by Sephadex gel-filtration. *The Biochemical Journal.* 91(2): 222-233.

6. Anantharaman, V. & Aravind, L. 2003. Evolutionary history, structural features and biochemical diversity of the NlpC/P60 superfamily of enzymes. *Genome Biology.* 4(2):R11.

7. Annamalai, N., Thavasi, R., Vijayalakshmi, S. & Balasubramanian, T. 2011. Extraction, purification and characterization of thermostable, alkaline tolerant α-amylase from *Bacillus cereus*. *Indian Journal of Microbiology.*51(4): 424-429.

8. Arikan, B. 2008. Highly thermostable, thermophilic, alkaline, SDS and chelator resistant amylase from a thermophilic *Bacillus sp*. isolate A3-15. *Bioresource Technology.* 99(8):3071-3076.

9. Aygan, A., Arikan, B., Korkmaz, H., Dinçer, S. & Çolak, Ö. 2008. Highly thermostable and alkaline α-amylase from a halotolerant-alkaliphilic *Bacillus* sp. AB68. *Brazilian Journal of Microbiology.* 39(3):547-553.

10. Ayrapaa, T. & Nihlen, H. 1954. Investigation on barley malt amylases and related proteins. *Acta Chemica Scandanica.* 8:88-105.

11. Bailey, J.S. 2009. *Biochemical Engineering.* CBS Publishers & Distributors. 470 – 494.

12. Baldwin, R., Bear, R. & Rundle, R. 1944. The Relation of Starch—Iodine Absorption Spectra to the Structure of Starch and Starch Components1. *Journal of the American Chemical Society.* 66(1):111-115.

13. Bandaiphet, C. & Prasertsan, P. 2006. Effect of aeration and agitation rates and scale-up on oxygen transfer coefficient k_La in exopolysaccharide production from *Enterobacter cloacae* WD7. *Carbohydrate Polymers.* 66(2):216-228.

14. Bernfeld, P. 1955. Amylases, alpha and beta. *Methods in Enzymology I.*:149-158.

15. Bernhardsdotter, E.C., Ng, J.D., Garriott, O.K. & Pusey, M.L. 2005. Enzymic properties of an alkaline chelator-resistant α-amylase from an alkaliphilic *Bacillus* sp. isolate L1711. *Process Biochemistry.* 40(7): 2401-2408.

16. Berg, J. M., Tymoczko J. L., Stryer L. Biochemistry. 5th edition. New York: W H Freeman; 2002. Section 4.1, The purification of proteins is an essential first step in understanding their function. Retrieved on April 1st, Available from: http://www-ncbi-nlm-nih-gov.ezproxy.uct.ac.za/books/NBK22410/

17. bcc Research Market Forecasting March, 2012. *Global market for enzymes in Industrial application.* Retrieved April 11, 2014 from http://www.bccresearch.com/market-research/biotechnology/enzymes-industrial-applications-markets-bio030g.html.

18. Biedendieck, R., Yang, Y., Deckwer, W., Malten, M. & Jahn, D. 2007. Plasmid system for the intracellular production and purification of affinity-tagged proteins in *Bacillus megaterium*. *Biotechnology and Bioengineering.* 96(3):525-537.

19. Bijttebier, A., Goesaert, H. & Delcour, J.A. 2008. Amylase action pattern on starch polymers. *Biologia.* 63(6):989-999.

20. Bradford, M.M. 1976. A rapid and sensitive method for the quantitation of microgram quantities of protein utilizing the principle of protein-dye binding. *Analytical Biochemistry.* 72(1): 248-254.

21. Bravo Rodríguez, V., Jurado Alameda, E., Martínez Gallegos, J.F., Reyes Requena, A., García López, A.I., Sampaio Cabral, J.M., Fernandes, P. & Pina da Fonseca, Luis Joaquim 2006. Modification of the activity of an alpha-amylase from *Bacillus licheniformis* by several surfactants. *Electronic Journal of Biotechnology.* 9(5). DOI: 10.2225/vol9-issue5-fulltext-16

22. Brown, R.E., Jarvis, K.L. & Hyland, K.J. 1989. Protein measurement using bicinchoninic acid: elimination of interfering substances. *Analytical Biochemistry.* 180(1): 136-139.

23. Bruijn, J. & Jennings, R. 1968. Enzymatic hydrolysis of starch in cane juice. *Proceedings of the South Africa Sugar Technology Ass.* 45.

24. Bryant, J. 1977. The characterization of mixing in fermenters. In *Advances in Biochemical Engineering, Volume 5.* Springer. 101-123.

25. Büchs, J. 2001. Introduction to advantages and problems of shaken cultures. *Biochemical Engineering Journal.* 7(2):91-98.

26. Buchs, J. & Zoels, B. 2001. Evaluation of maximum to specific power consumption ratio in shaking bioreactors. *Journal of Chemical Engineering of Japan.* 34(5):647-653.

27. Çalík, P., Çalík, G. & Özdamar, T.H. 1998. Oxygen transfer effects in serine alkaline protease fermentation by *Bacillus licheniformis* use of citric acid as the carbon source. *Enzyme and Microbial Technology.* 23(7):451-461.

28. Chaplin, M.F. & Bucke, C. 1990. *Enzyme Technology* (139 -141). CUP Archive.

29. Cherry, J.R. & Fidantsef, A.L. 2003. Directed evolution of industrial enzymes: an update. *Current Opinion in Biotechnology.* 14(4):438-443.

30. Chick, H. & Martin, C.J. 1913. The Precipitation of Egg-Albumin by Ammonium Sulphate. A Contribution to the Theory of the "Salting-out" of Proteins. *The Biochemical Journal.* 7(4):380-398.

31. Clark, G.J. & Bushell, M.E. 1995. Oxygen limitation can induce microbial secondary metabolite formation: investigations with miniature electrodes in shaker and bioreactor culture. *Microbiology.* 141(3):663-669.

32. Clarke, J.T. 1964. Simplified “disc”(polyacrylamide gel) electrophoresis*. *Annals of the New York Academy of Sciences.* 121(2):428-436.

33. Compton, S.J. & Jones, C.G. 1985. Mechanism of dye response and interference in the Bradford protein assay. *Analytical Biochemistry.* 151(2):369-374.

34. Congdon, R.W., Muth, G.W. & Splittgerber, A.G. 1993. The binding interaction of Coomassie blue with proteins. *Analytical Biochemistry.* 213(2):407-413.

35. Crampton, M., Berger, E., Reid, S. & Louw, M. 2007. The development of a flagellin surface display expression system in a moderate thermophile, *Bacillus halodurans* Alk36. *Applied Microbiology and Biotechnology.* 75(3):599-607.

36. Csonka, L.N. 1989. Physiological and genetic responses of bacteria to osmotic stress. *Microbiological Reviews.* 53(1): 121-147.

37. Cuatrecasas, P. 1970. Protein purification by affinity chromatography. Derivatizations of agarose and polyacrylamide beads. *The Journal of Biological Chemistry.* 245(12): 3059-3065.

38. Das, K., Doley, R. & Mukherjee, A.K. 2004. Purification and biochemical characterization of a thermostable, alkaliphilic, extracellular α-amylase from *Bacillus subtilis* DM-03, a strain isolated from the traditional fermented food of India. *Biotechnology and Applied Biochemistry.* 40(3):291-298.

39. Davie, E.W. & Neurath, H. 1955. Identification of a peptide released during autocatalytic activation of trypsinogen. *The Journal of Biological Chemistry.* 212(2):515-529.

40. Del Valle, E.M. 2004. Cyclodextrins and their uses: a review. *Process Biochemistry.* 39(9):1033-1046.

41. Doig, S.D., Pickering, S.C., Lye, G.J. & Baganz, F. 2005. Modelling surface aeration rates in shaken microtitre plates using dimensionless groups. *Chemical Engineering Science.* 60(10):2741-2750.

42. Doran, P.M. 1995. *Bioprocess Engineering Principles.* Academic Press. 190 - 217

43. Ducros, E., Ferrari, M., Pellegrino, M., Raspanti, C. & Bogni, C. 2009. Effect of aeration and agitation on the protease production by *Staphylococcus aureus* mutant RC128 in a stirred tank bioreactor. *Bioprocess and Biosystems Engineering.* 32(1):143-148.

44. Duedahl-Olesen, L., Haastrup Pedersen, L. & Lambertsen Larsen, K. 2000. Suitability and limitations of methods for characterisation of activity of malto-oligosaccharide-forming amylases. *Carbohydrate Research.* 329(1):109-119.

45. Duetz, W.A., Rüedi, L., Hermann, R., O'Connor, K., Büchs, J. & Witholt, B. 2000. Methods for intense aeration, growth, storage, and replication of bacterial strains in microtiter plates. *Applied and Environmental Microbiology.* 66(6):2641-2646.

46. Duetz, W.A. & Witholt, B. 2001. Effectiveness of orbital shaking for the aeration of suspended bacterial cultures in square-deepwell microtiter plates. *Biochemical Engineering Journal.* 7(2):113-115.

47. Duetz, W.A. & Witholt, B. 2004. Oxygen transfer by orbital shaking of square vessels and deepwell microtiter plates of various dimensions. *Biochemical Engineering Journal.* 17(3):181-185.

48. Dunker, A.K. & Rueckert, R.R. 1969. Observations on molecular weight determinations on polyacrylamide gel. *The Journal of Biological Chemistry.* 244(18):5074-5080.

49. Eadie, G.S. 1926. The Effect of Substrate Concentration on the Hydrolysis of Starch by the Amylase of Germinated Barley. *The Biochemical Journal.* 20(5):1016-1023.

50. El-Fallal, A., Dobara, M.A., El-Sayed, A. & Omar, N. 2012. Starch and Microbial α-Amylases: From Concepts to Biotechnological Applications. Carbohydrates - Comprehensive Studies on Glycobiology and Glycotechnology. ed. C Chang. Retrieved: March 19, 2014 from http://www.intechopen.com/books/carbohydrates-comprehensive-studies-on-glycobiology-and-glycotechnology/starch-and-microbial-amylases-from-concepts-to-biotechnological-applications.

51. Enfors, S. & Häggström, L. 2000. *Bioprocess technology: fundamentals and applications.* Royal Institute of Technology. 79 – 94.

52. Feng, Y., He, Z., Ong, S.L., Hu, J., Zhang, Z. & Ng, W.J. 2003. Optimization of agitation, aeration, and temperature conditions for maximum β-mannanase production. *Enzyme and Microbial Technology.* 32(2):282-289.

53. Forouchi, E. & Gunn, D. 1983. Some effects of metal ions on the estimation of reducing sugars in biological media. *Biotechnology and Bioengineering.* 25(7):1905-1911.

54. Foster, P., Dunnill, P. & Lilly, M. 1971. Salting-out of enzymes with ammonium sulphate. *Biotechnology and Bioengineering.* 13(5):713-718.

55. French, D. 1973. Chemical and physical properties of starch. *Journal of animal science.* 37(4):1048-1061.

56. Funke, M., Buchenauer, A., Mokwa, W., Kluge, S., Hein, L., Muller, C., Kensy, F. & Buchs, J. 2010. Bioprocess control in microscale: scalable fermentations in disposable and user-friendly microfluidic systems. *Microbial Cell Factories.* 9:86-2859-9-86.

57. Fuwa, H. 1954. A new method for microdetermination of amylase activity by the use of amylose as the substrate. *Journal of Biochemistry.* 41(5):583-603.

58. Garcia-Ochoa, F. & Gomez, E. 2009. Bioreactor scale-up and oxygen transfer rate in microbial processes: an overview. *Biotechnology Advances.* 27(2):153.

59. Ghalanbor, Z., Ghaemi, N., Marashi, S., Amanlou, M., Habibi-Rezaei, M., Khajeh, K. & Ranjbar, B. 2008. Binding of Tris to *Bacillus licheniformis* α-amylase can affect its starch hydrolysis activity. *Protein and Peptide Letters.* 15(2): 212-214.

60. Gjessing, E.T. & Lee, G.F. 1967. Fractionation of organic matter in natural waters on Sephadex columns. *Environmental Science & Technology.* 1(8): 631-638.

61. Glazyrina, J., Krause, M., Junne, S., Glauche, F., Strom, D. & Neubauer, P. 2012. Glucose-limited high cell density cultivations from small to pilot plant scale using an enzyme-controlled glucose delivery system. *New Biotechnology.* 29(2):235-242.

62. Gonçalves, C., Rodriguez-Jasso, R.M., Gomes, N., Teixeira, J.A. & Belo, I. 2010. Adaptation of dinitrosalicylic acid method to microtiter plates. *Analytical Methods.* 2(12):2046-2048.

63. Grimm, T., Grimm, M., Klat, R., Neubauer, A., Palela, M. & Neubauer, P. 2012. Enzyme-based glucose delivery as a high content screening tool in yeast-based whole-cell biocatalysis. *Applied Microbiology and Biotechnology.* 94(4):931-937.

64. Grist, S.M., Chrostowski, L. & Cheung, K.C. 2010. Optical oxygen sensors for applications in microfluidic cell culture. *Sensors.* 10(10):9286-9316.

65. Gupta, R., Gigras, P., Mohapatra, H., Goswami, V.K. & Chauhan, B. 2003a. Microbial α-amylases: a biotechnological perspective. *Process Biochemistry.* 38(11):1599-1616.

66. Gupta, R., Gigras, P., Mohapatra, H., Goswami, V.K. & Chauhan, B. 2003b. Microbial α-amylases: a biotechnological perspective. *Process Biochemistry.* 38(11):1599-1616.

67. Hagihara, H., Igarashi, K., Hayashi, Y., Endo, K., Ikawa-Kitayama, K., Ozaki, K., Kawai, S. & Ito, S. 2001. Novel α-Amylase that is highly resistant to chelating reagents and chemical oxidants from the alkaliphilic *Bacillus* isolate KSM-K38. *Applied and Environmental Microbiology.* 67(4):1744-1750.

68. Harms, P., Kostov, Y. & Rao, G. 2002. Bioprocess monitoring. *Current Opinion in Biotechnology.* 13(2):124-127.

69. Hashim, S.O., Delgado, O.D., Martínez, M.A., Kaul, R., Mulaa, F.J. & Mattiasson, B. 2005. Alkaline active maltohexaose-forming α-amylase from *Bacillus halodurans* LBK 34. *Enzyme and Microbial Technology.* 36(1):139-146.

70. Hermann, R., Lehmann, M. & Büchs, J. 2003. Characterization of gas–liquid mass transfer phenomena in microtiter plates. *Biotechnology and Bioengineering.* 81(2):178-186.

71. Hermann, R., Walther, N., Maier, U. & Büchs, J. 2001. Optical method for the determination of the oxygen-transfer capacity of small bioreactors based on sulfite oxidation. *Biotechnology and Bioengineering.* 74(5):355-363.

72. Holmes, W., Smith, R. & Bill, R. 2006. Evaluation of antifoams in the expression of a recombinant FC fusion protein in shake flask cultures of Saccharomyces cerevisiae & Pichia pastoris. *Microbial Cell Factories.* 5(Suppl 1):P30.

73. Horikoshi, K. 1999. Alkaliphiles: some applications of their products for biotechnology. *Microbiology and Molecular Biology Previews.* 63(4):735-750.

74. Horton, H.R., Rawn, J.D., Scrimgeour, K.G., Moran, L. & Ochs, R. 1993. *Principles of Biochemistry.* N. Patterson Publishers. 129 – 132.

75. Hortsch, R. & Weuster-Botz, D. 2011. Growth and recombinant protein expression with *Escherichia coli* in different batch cultivation media. *Applied Microbiology and Biotechnology.* 90(1):69-76.

76. Huggins, C. & Russell, P.S. 1948. Colorimetric Determination of Amylase. *Annals of Surgery.* 128(4):668-678.

77. Hunter & Burstone, 1960. The zymogram as a tool for the characterization of enzyme substrate specificity. *The Journal of Histochemistry and Cytochemistry : Official Journal of the Histochemistry Society.* 8:58-62.

78. Hwang, J.W., Yang, Y.K., Hwang, J.K., Pyun, Y.R. & Kim, Y.S. 1999. Effects of pH and dissolved oxygen on cellulose production by *Acetobacter xylinum* BRC5 in agitated culture. *Journal of Bioscience and Bioengineering.* 88(2):183-188.

79. Igarashi, K., Hatada, Y., Hagihara, H., Saeki, K., Takaiwa, M., Uemura, T., Ara, K., Ozaki, K. 1998. Enzymatic properties of a novel liquefying alpha-amylase from an

alkaliphilic *Bacillus* isolate and entire nucleotide and amino acid sequences. *Applied and Environmental Microbiology.* 64(9):3282-3289.

80. Islam, R., Tisi, D., Levy, M. & Lye, G. 2008. Scale-up of Escherichia coli growth and recombinant protein expression conditions from microwell to laboratory and pilot scale based on matched kLa. *Biotechnology and Bioengineering.* 99(5):1128-1139.

81. John, G.T., Klimant, I., Wittmann, C. & Heinzle, E. 2003. Integrated optical sensing of dissolved oxygen in microtiter plates: a novel tool for microbial cultivation. *Biotechnology and Bioengineering.* 81(7):829-836.

82. Kareem, S., Akpan, I., Popoola, T. & Sanni, L. 2011. Activated Charcoal—A Potential Material in Glucoamylase Recovery. *Enzyme Research.* 2011.

83. Kenney, A.C. 1992. Ion-exchange chromatography of proteins. In *Practical Protein Chromatography.* Springer. 249-258.

84. Kensy, F., Zimmermann, H.F., Knabben, I., Anderlei, T., Trauthwein, H., Dingerdissen, U. & Büchs, J. 2005. Oxygen transfer phenomena in 48-well microtiter plates: Determination by optical monitoring of sulfite oxidation and verification by real-time measurement during microbial growth. *Biotechnology and Bioengineering.* 89(6):698-708.

85. Kirk, O., Borchert, T.V. & Fuglsang, C.C. 2002. Industrial enzyme applications. *Current opinion in Biotechnology.* 13(4):345-351

86. Kim, T.U., Gu, B.G., Jeong, J.Y., Byun, S.M. & Shin, Y.C. 1995. Purification and Characterization of a Maltotetraose-Forming Alkaline (alpha)-Amylase from an alkalophilic *Bacillus* strain, GM8901. *Applied and Environmental Microbiology.* 61(8):3105-3112.

87. Klein, B., Foreman, J.A. & Searcy, R.L. 1970. New chromogenic substrate for determination of serum amylase activity. *Clinical Chemistry.* 16(1):32-38.

88. Korz, D., Rinas, U., Hellmuth, K., Sanders, E. & Deckwer, W. 1995. Simple fed-batch technique for high cell density cultivation of *Escherichia coli*. *Journal of Biotechnology.* 39(1):59-65.

89. Krause, M., Ukkonen, K., Haataja, T., Ruottinen, M., Glumoff, T., Neubauer, A., Neubauer, P. & Vasala, A. 2010. A novel fed-batch based cultivation method provides

high cell-density and improves yield of soluble recombinant proteins in shaken cultures. *Microbial Cell Factories.* 9(1):11.

90. Kruger, N.J. 2009. The Bradford method for protein quantitation. In *The Protein Protocols Handbook.* Springer. 17-24.

91. Krulwich, T.A. & Guffanti, A.A. 1989. Alkalophilic bacteria. *Annual Reviews in Microbiology.* 43(1):435-463.

92. Kumar, C.G.P. 2003. Activated charcoal: a versatile decolorization agent for the recovery and purification of alkaline protease. *World Journal of Microbiology and Biotechnology.* 19(3):243-246.

93. Kumar, D., Savitri, N.T., Verma, R. & Bhalla, T.C. 2008. Microbial proteases and application as laundry detergent additive. *Research Journal of Microbiology.* 3:661-672.

94. Kumar, S., Tsai, C. & Nussinov, R. 2002. Maximal stabilities of reversible two-state proteins. *Biochemistry.* 41(17): 5359-5374.

95. Laemmli, U.K. 1970. Cleavage of structural proteins during the assembly of the head of bacteriophage T4. *Nature.* 227(5259):680-685.

96. Lam, K., Chow, K. & Wong, W. 1998. Construction of an efficient *Bacillus subtilis* system for extracellular production of heterologous proteins. *Journal of Biotechnology.* 63(3):167-177.

97. Lawrence, J. & Maier, S. 1977. Correction for the inherent error in optical density readings. *Applied and Environmental Microbiology.* 33(2):482-484.

98. Layne, E. 1957. [73] Spectrophotometric and turbidimetric methods for measuring proteins. *Methods in Enzymology.* 3447-454.

99. Lin, W. & Lee, D. 1997. Micromixing effects in aerated stirred tank. *Chemical Engineering Science.* 52(21):3837-3842.

100. Lin, L., Lo, H., Chiang, W., Hu, H., Hsu, W. & Chang, C. 2003. Replacement of methionine 208 in a truncated *Bacillus* sp. TS-23 α-amylase with oxidation-resistant leucine enhances its resistance to hydrogen peroxide. *Current Microbiology.* 46(3):0211-0216.

101. Lin, L., Chyau, C. & Hsu, W. 1998. Production and properties of a raw-starch-degrading amylase from the thermophilic and alkaliphilic Bacillus sp. TS-23. *Biotechnology and Applied Biochemistry.* 28(1):61-68.

102. Lorentz, K. 2000. Routine α-amylase assay using protected 4-nitrophenyl-1, 4-α-D-maltoheptaoside and a novel α-glucosidase. *Clinical Chemistry.* 46(5):644-649.

103. Losen, M., Frölich, B., Pohl, M. & Büchs, J. 2004. Effect of oxygen limitation and Medium composition on *Escherichia coli* fermentation in shake-flask cultures. *Biotechnology Progress.* 20(4):1062-1068.

104. Louw, M.E., Reid, S.J. & Watson, T. 1993. Characterization, cloning and sequencing of a thermostable endo-(1, 3–1, 4) β-glucanase-encoding gene from an alkalophilic *Bacillus brevis*. *Applied Microbiology and Biotechnology.* 38(4):507-513.

105. Lowry, O.H., Rosebrough, N.J., Farr, A.L. & Randall, R.J. 1951. Protein measurement with the Folin phenol reagent. *Journal of Biological Chemistry.* 193(1): 265-275.

106. Maier, U. & Büchs, J. 2001. Characterisation of the gas–liquid mass transfer in shaking bioreactors. *Biochemical Engineering Journal.* 7(2):99-106.

107. Maier, U., Losen, M. & Büchs, J. 2004. Advances in understanding and modeling the gas–liquid mass transfer in shake flasks. *Biochemical Engineering Journal.* 17(3):155-167.

108. Mamo, G., Hatti-Kaul, R. & Mattiasson, B. 2006. A thermostable alkaline active endo-β-1-4-xylanase from *Bacillus halodurans* S7: Purification and characterization. *Enzyme and Microbial Technology.* 39(7):1492-1498.

109. Manners, D. 1979. The enzymic degradation of starches. In *Polysaccharides in food.* Butterworth London. 75-91.

110. Margaritis, A. & Wallace, J.B. 1984. Novel bioreactor systems and their applications. *Nature Biotechnology.* 2(5): 447-453.

111. Maurer, H.R. 1978. *Disc electrophoresis and related techniques of polyacrylamide gel electrophoresis.* Walter de Gruyter & Co, Berlin. 1 – 30.

112. McDaniel, L. & Bailey, E. 1969. Effect of shaking speed and type of closure on shake flask cultures. *Applied Microbiology.* 17(2):286-290.

113. McTigue, M., Kelly, C.T., Doyle, E.M. & Fogarty, W.M. 1995. The alkaline amylase of the alkaliphilic *Bacillus* sp. IMD 370. *Enzyme and Microbial Technology.* 17(6):570-573.

114. McDaniel, L., Bailey, E. & Zimmerli, A. 1965. Effect of Oxygen-Supply Rates on Growth of Escherichia coli I. Studies in Unbaffled and Baffled Shake Flasks. *Applied Microbiology.* 13(1):109-114.

115. Micheletti, M., Barrett, T., Doig, S., Baganz, F., Levy, M., Woodley, J. & Lye, G. 2006. Fluid mixing in shaken bioreactors: Implications for scale-up predictions from microlitre-scale microbial and mammalian cell cultures. *Chemical Engineering Science.* 61(9):2939-2949.

116. Miller, G.L. 1959. Use of dinitrosalicylic acid reagent for determination of reducing sugar. *Analytical Chemistry.* 31(3):426-428.

117. Mori, S. & Barth, H.G. 1999. *Size exclusion chromatography.* Springer.

118. Mueller, J.A., Boyle, W.C. & Lightfoot, E.N. 1967. Effect of the response time of a dissolved oxygen probe on the oxygen uptake rate. *Applied Microbiology.* 15(3):674-676.

119. Murakami, S., Nishimoto, H., Toyama, Y., Shimamoto, E., Takenaka, S., Kaulpiboon, J., Prousoontorn, M., Limpaseni, T. 2007. Purification and Characterization of Two Alkaline, Thermotolerant. ALPHA.-Amylases from *Bacillus halodurans* 38C-2-1 and Expression of the Cloned Gene in Escherichia coli. *Bioscience, Biotechnology, and Biochemistry.* 71(10):2393-2401.

120. Murakami, S., Nagasaki, K., Nishimoto, H., Shigematu, R., Umesaki, J., Takenaka, S., Kaulpiboon, J., Prousoontorn, M. 2008. Purification and characterization of five alkaline, thermotolerant, and maltotetraose-producing α-amylases from *Bacillus halodurans* MS-2-5, and production of recombinant enzymes in *Escherichia coli*. *Enzyme and Microbial Technology.* 43(4):321-328.

121. Murphy, J.B. & Kies, M.W. 1960. Note on spectrophotometric determination of proteins in dilute solutions. *Biochimica Et Biophysica Acta.* 45382-384.

122. Nelson, N. 1944. A photometric adaptation of the Somogyi method for the determination of glucose. *Journal of Biological Chemistry.* 153(2): 375-379.

123. Nigam, P. & Singh, D. 1995. Enzyme and microbial systems involved in starch processing. *Enzyme and Microbial Technology.* 17(9):770-778.

124. Narang, A. & Pilyugin, S.S. 2007. Bacterial gene regulation in diauxic and non-diauxic growth. *Journal of Theoretical Biology.* 244(2): 326-348.

125. Noble, J.E. & Bailey, M.J. 2009. Quantitation of protein. *Methods in Enzymology.* 46373-95.

126. Norouzian, D., Akbarzadeh, A., Scharer, J.M. & Moo Young, M. 2006. Fungal glucoamylases. *Biotechnology Advances.* 24(1):80-85.

127. O'Farrell, P. 1996. Hydrophobic Interaction Chromatography. In *Protein Purification Protocols.* Springer. 151-155.

128. Ornstein, L. 1964. Disc electrophoresis-I background and theory*. *Annals of the New York Academy of Sciences.* 121(2):321-349.

129. Ortiz-Ochoa, K., Doig, S.D., Ward, J.M. & Baganz, F. 2005. A novel method for the measurement of oxygen mass transfer rates in small-scale vessels. *Biochemical Engineering Journal.* 25(1):63-68.

130. Osváth, A Szilágyi J Kardos S & Závodszky, L.B.P. 2007. 10 Protein folding. *Handbook of neurochemistry and molecular neurobiology: Neural protein Metabolism and Function.* 3.

131. Özbek, B. & Gayik, S. 2001. The studies on the oxygen mass transfer coefficient in a bioreactor. *Process Biochemistry.* 36(8):729-741.

132. Padan, E., Bibi, E., Ito, M. & Krulwich, T.A. 2005. Alkaline pH homeostasis in bacteria: new insights. *Biochimica et Biophysica acta (BBA)-Biomembranes.* 1717(2):67-88.

133. Pappin, D., Hojrup, P. & Bleasby, A. 1993. Rapid identification of proteins by peptide-mass fingerprinting. *Current biology.* 3(6):327-332.

134. Panula-Perälä, J., Å iurkus, J., Vasala, A., Wilmanowski, R., Casteleijn, M.G. & Neubauer, P. 2008. Enzyme controlled glucose auto-delivery for high cell density cultivations in microplates and shake flasks. *Microbial Cell Factories.* 731.

135. Pimstone, N. 1964. A study of the starch-iodine complex: a modified colorimetric micro determination of amylase in biologic fluids. *Clinical Chemistry.* 10(10):891-906.

136. Porath, J. 1962. Cross-linked dextrans as molecular sieves. *Adv.Protein Chem.* 17209.

137. Porath, J. & Flodin, P. 1959. Gel filtration: a method for desalting and group separation. *Nature.* 183(4676): 1657-1659.

138. Power, D.A. & Johnson, J.A. 2009. Manual of Microbiological Culture Media. Difco™ & BBL™ Manual. 2nd ed. Maryland, USA.

139. *Prescott, L.M, Harley J.P, and Klein D.A.2005. Microbiology-6th ed.* McGraw-Hill Higher Education .New York. 109 - 131.

140. Reynders, M., Rawlings, D. & Harrison, S. 1996. Studies on the growth, modelling and pigment production by the yeast *Phaffia rhodozyma* during fed-batch cultivation. *Biotechnology Letters.* 18(6):649-654.

141. Roohi, R., Kuddus, M. & Saima, S. 2013. Cold-active detergent-stable extracellular α-amylase from *Bacillus cereus* GA6: Biochemical characteristics and its perspectives in laundry detergent formulation. *Journal of Biochemical Technology.* 4(4):636-644.

142. Rozzell, J.D. 1999. Commercial scale biocatalysis: myths and realities. *Bioorganic & Medicinal Chemistry.* 7(10):2253-2261.

143. Rundle, R., Foster, J.F. & Baldwin, R. 1944. On the nature of the starch—iodine complex1. *Journal of the American Chemical Society.* 66(12):2116-2120.

144. Saenger, W. 1984. The structure of the blue starch-iodine complex. *Naturwissenschaften.* 71(1):31-36.

145. Sakaguchi, H., Sharyo, M. & Shimoto, H. 1999. Deinking of starch-coated printed paper by treatment with starch degrading enzyme*. U.S. Patent No. 5,879*,509.

146. Sarethy, I.P., Saxena, Y., Kapoor, A., Sharma, M., Sharma, S.K., Gupta, V. & Gupta, S. 2011. Alkaliphilic bacteria: applications in industrial biotechnology. *Journal of Industrial Microbiology & Biotechnology.* 38(7):769-790.

147. Sarethy, I.P., Saxena, Y., Kapoor, A., Sharma, M., Seth, R., Sharma, H., Sharma, S.K. & Gupta, S. 2012. Amylase produced by *Bacillus* sp. SI-136 isolated from soda-alkaline soil for efficient starch desizing. *Journal of Biochemical Technology.* 4(2).

148. Saxena, R.K., Dutt, K., Agarwal, L. & Nayyar, P. 2007. A highly thermostable and alkaline amylase from a *Bacillus* sp. PN5. *Bioresource Technology.* 98(2):260-265.

149. Schallmey, M., Singh, A. & Ward, O.P. 2004. Developments in the use of *Bacillus* species for industrial production. *Canadian Journal of Microbiology.* 50(1):1-17.

150. Schmidt, F. 2004. Recombinant expression systems in the pharmaceutical industry. *Applied Microbiology and Biotechnology.* 65(4):363-372.

151. Scholtz, J.M., Qian, H., Robbins, V.H. & Baldwin, R.L. 1993. The energetics of ion-pair and hydrogen-bonding interactions in a helical peptide. *Biochemistry.* 32(37): 9668-9676.

152. Schultz, J.S. & Gaden, E.L. 1956. Sulfite oxidation as a measure of aeration effectiveness. *Industrial & Engineering Chemistry.* 48(12):2209-2212.

153. Scopes, R.K. 1994. *Protein purification: principles and practice.* Springer.

154. Sezonov, G., Joseleau-Petit, D. & D'Ari, R. 2007. *Escherichia coli* physiology in Luria-Bertani broth. *Journal of Bacteriology.* 189(23):8746-8749.

155. Simonen, M. & Palva, I. 1993. Protein secretion in *Bacillus* species. *Microbiological Reviews.* 57(1):109-137.

156. Šiurkus, J., Panula-Perälä, J., Horn, U., Kraft, M., Rimšeliene, R. & Neubauer, P. 2010. Novel approach of high cell density recombinant bioprocess development: Optimisation and scale-up from microlitre to pilot scales while maintaining the fed-batch cultivation mode of *E. coli* cultures. *Microbial Cell Factories.* 9(1):35.

157. Smith, P., Krohn, R.I., Hermanson, G., Mallia, A., Gartner, F., Provenzano, M., Fujimoto, E., Goeke, N. et al. 1985. Measurement of protein using bicinchoninic acid. *Analytical Biochemistry.* 150(1): 76-85.

158. Smithies, O. 1955. Zone electrophoresis in starch gels: group variations in the serum proteins of normal human adults. *The Biochemical Journal.* 61(4):629-641.

159. Souza, P.M.d. 2010a. Application of microbial α-amylase in industry-A review. *Brazilian Journal of Microbiology.* 41(4):850-861.

160. Souza, P.M.d. 2010b. Application of microbial α-amylase in industry-A review. *Brazilian Journal of Microbiology.* 41(4):850-861.

161. Swanson, M.A. 1948. Studies on the structure of polysaccharides; relation of the iodine color to the structure. *The Journal of Biological Chemistry.* 172(2): 825-837.

162. Taylor, R.F. & Schultz, J.S. 1996. *Handbook of chemical and biological sensors.* CRC Press. 419 – 434.

163. Terpe, K. 2006. Overview of bacterial expression systems for heterologous protein production: from molecular and biochemical fundamentals to commercial systems. *Applied Microbiology and Biotechnology.* 72(2):211-222.

164. Teixeira, R.S.S., da Silva, A.S., Ferreira-Leitão, V.S. & Bon, Elba Pinto da Silva. 2012. Amino acids interference on the quantification of reducing sugars by the 3, 5-dinitrosalicylic acid assay mislead carbohydrate activity measurements. *Carbohydrate Research.* 363:33-37.

165. Toma, M., Ruklisha, M., Vanags, J., Zeltina, M., Lelte, M., Galinine, N., Viesturs, U. & Tengerdy, R. 1991. Inhibition of microbial growth and metabolism by excess turbulence. *Biotechnology and Bioengineering.* 38(5):552-556.

166. Tribe, L., Briens, C. & Margaritis, A. 1995. Determination of the volumetric mass transfer coefficient (k_La) using the dynamic “gas out–gas in” method: Analysis of errors caused by dissolved oxygen probes. *Biotechnology and Bioengineering.* 46(4):388-392.

167. Underkofler, L., Barton, R. & Rennert, S. 1958. Production of microbial enzymes and their applications. *Applied Microbiology.* 6(3):212.

168. Van Der Maarel, Marc JEC, Van Der Veen, B., Uitdehaag, J.C., Leemhuis, H. & Dijkhuizen, L. 2002. Properties and applications of starch-converting enzymes of the a-amylase family. *Journal of Biotechnology.* 94(2):137-156.

169. Van Hung, P., 2008. Characteristics of starch and starch-based food products-Roles of amylose and amylopectin. In *Food Chemistry Research Developments*. K.N. Papadopoulos, Ed. New York. Nova Publishers. 141-150.

170. Villadsen, J., Nielsen, J. & Lidâen, G. 2011. *Bioreaction engineering principles.* 3rd edition. New York. Springer.

171. Virolle, M., Morris, V.J. & Bibb, M.J. 1990. A simple and reliable turbidimetric and kinetic assay for alpha-amylase that is readily applied to culture supernatants and cell extracts. *Journal of Industrial Microbiology.* 5(5):295-301.

172. Warmoeskerken, M. & Smith, J.M. 1985. Flooding of disc turbines in gas-liquid dispersions: A new description of the phenomenon. *Chemical Engineering Science.* 40(11):2063-2071.

173. Weber, K. & Osborn, M. 1969. The reliability of molecular weight determinations by dodecyl sulfate-polyacrylamide gel electrophoresis. *The Journal of Biological Chemistry.* 244(16):4406-4412.

174. Wedemeyer, W.J., Welker, E., Narayan, M. & Scheraga, H.A. 2000. Disulfide bonds and protein folding. *Biochemistry.* 39(15):4207-4216.

175. Wong, S. 1995. Advances in the use of *Bacillus subtilis* for the expression and secretion of heterologous proteins. *Current Opinion in Biotechnology.* 6(5):517-522.

176. Woodley, J.M. 2008. New opportunities for biocatalysis: making pharmaceutical processes greener. *Trends in Biotechnology.* 26(6):321-327.

177. Xiao, Z., Storms, R. & Tsang, A. 2006. A quantitative starch–iodine method for measuring alpha-amylase and glucoamylase activities. *Analytical Biochemistry.* 351(1):146-148.

178. Xu, B., Jahic, M., Blomsten, G. & Enfors, S. 1999. Glucose overflow metabolism and mixed-acid fermentation in aerobic large-scale fed-batch processes with *Escherichia coli*. *Applied microbiology and Biotechnology.* 51(5):564-571.

179. Yamamoto, S., Nakanishi, K. & Matsuno, R. 1988. *Ion-exchange chromatography of proteins.* CRC Press.

180. Yang, H., Liu, L., Li, J., Du, G. & Chen, J. 2011. Heterologous expression, biochemical characterization, and overproduction of alkaline a-amylase from *Bacillus alcalophilus* in *Bacillus subtilis. Microbial Cell Factories.* 1077.

181. Zimmermann, H.F., John, G.T., Trauthwein, H., Dingerdissen, U. & Huthmacher, K. 2003. Rapid evaluation of oxygen and water permeation through microplate sealing tapes. *Biotechnology Progress.* 19(3):1061-1063.

APPENDIX

Appendix 1: Amylase production in *B. halodurans Alk36*

Appendix 1.1: Growth of *B. halodurans Alk36* in shake flasks

Bacillus halodurans Alk36 were cultured in shake flasks as described in Section 3.1.4.3. The bacterial growth was measured by spectrophotometry at 600 nm as described in Section 3.3.1.1. The optical densities and pH of the cultures are presented in Table 1.1.1 and Table 1.1.2 respectively. The growth rate was calculated from the slope of the plot of ln(OD) as a function of time between t_0 and t_6.

Table 1.1.1: The optical densities (OD) of *B. halodurans* Alk36 culture growing on LB medium in shake flaks at 30˚C.

Time	OD1	OD2	OD3	average OD	Standard deviation	relative error	LN OD	standard deviation	Growth rate*
0	0.236	0.239	0.233	0.236	0.003	0.424	-1.44	0.61	0.394
3	0.927	0.922	0.927	0.925	0.003	0.692	-0.08	0.05	
6	2.550	2.460	2.540	2.517	0.049	0.691	0.92	0.64	
9	4.670	4.630	4.670	4.657	0.023	0.601	1.54	0.92	
12	6.080	6.100	6.000	6.060	0.053	0.459	1.80	0.83	
15	6.230	6.250	6.350	6.277	0.064	0.562	1.84	1.03	
24	6.480	6.450	6.510	6.480	0.030	0.698	1.87	1.30	

* The growth rate was calculated from the slope of the plot of LN (OD) versus time between t_0 and t_6.

Table 1.1.2: The pH of *B. halodurans* Alk36 culture growing on LB medium in shake flaks at 30˚C.

time	pH	pH	pH	average	Standard deviation
0	8.35	8.37	8.36	8.36	0.01
3	7.81	7.83	7.80	7.81	0.02
6	7.86	7.85	7.84	7.85	0.01
9	8.16	8.15	8.15	8.15	0.01
12	8.51	8.53	8.48	8.51	0.03
15	8.65	8.64	8.60	8.63	0.03
24	8.80	8.77	8.78	8.78	0.02

Table 1.1.3: The optical densities (OD) of *B. halodurans* Alk36 culture growing on EnBase® medium in shake flaks at 30˚C

Time	OD1	OD2	OD3	average OD	standard deviation	relative error	LN OD	standard deviation	Growth rate*
0	0.212	0.221	0.210	0.214	0.006	0.027	-1.54	0.04	0.264
3	0.417	0.423	0.415	0.418	0.004	0.010	-0.87	0.01	
6	1.080	1.110	1.130	1.107	0.025	0.023	0.10	0.00	
9	2.160	2.180	2.210	2.183	0.025	0.012	0.78	0.01	
12	2.920	2.870	2.950	2.913	0.040	0.014	1.07	0.01	
15	3.620	3.650	3.600	3.623	0.025	0.007	1.29	0.01	
24	4.470	4.420	4.500	4.463	0.040	0.009	1.50	0.01	

* The growth rate was calculated from the slope of the plot of LN (OD) versus time between t_0 and t_9.

Table 1.1.4: The pH of *B. halodurans* Alk36 culture growing on EnBase® medium in shake flaks at 30˚C

time	pH	pH	pH	average	Standard deviation
0	8.4	8.37	8.36	8.38	0.02
3	8.12	8.08	8.11	8.10	0.02
6	7.67	7.69	7.69	7.68	0.01
9	7.63	7.60	7.60	7.61	0.02
12	7.50	7.49	7.47	7.49	0.02
15	7.31	7.28	7.30	7.30	0.02
24	6.87	6.87	6.86	6.87	0.01

Appendix 1.2: Determination of bacterial dry cell weight (DCW)- optical density correlation

Bacillus halodurans Alk36 were cultured in shake flasks as described in Section 3.1.4.3. The culture samples were taken at two hours intervals and the optical density of the culture was measured by spectrophotometry at 600 nm as described in Section 3.3.1.1. The biomass concentration was determined gravimetrically as described in Section 3.3.1.2. The bacterial dry cell weight (DCW) and the optical density (OD) values used to determine the DCW-OD correlation are presented on Table 1.2.1 and 1.2.2.

Table 1.2.1: The bacterial dry cell weight (DCW) and the optical density (OD) values used to determine the DCW-OD correlation for *B. halodurans* Alk36 cultures grown in LB medium

Time	weight (g/L)	weight (g/L)	weight (g/L)	average weight (g/L)	Blank corrected	Standard deviation	average OD_{600}
0							0.10
2	0.40	0.45	0.40	0.42	0.34	0.02	0.68
4	0.82	0.75	0.70	0.76	0.68	0.03	1.79
6	1.05	1.05	1.05	1.05	0.97	0.00	2.48
8	1.25	1.15	1.20	1.20	1.12	0.03	3.02
10	1.65	1.50	1.58	1.58	1.50	0.04	3.55
12	1.7	1.85	1.72	1.76	1.68	0.05	4.61
24	1.4	1.35	1.25	1.33	1.25	0.04	3.85

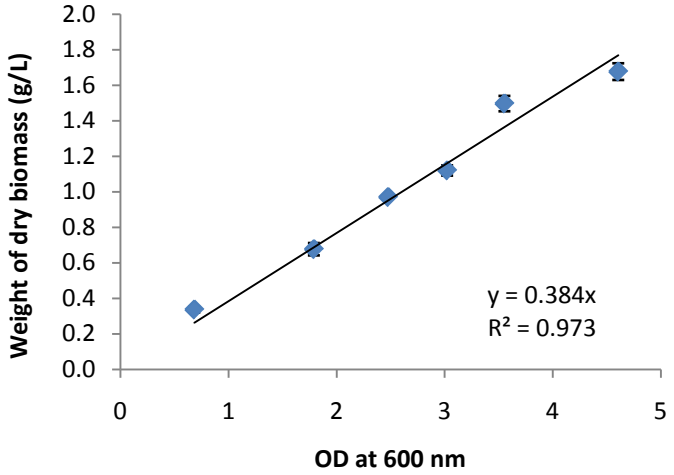

Figure 1.2.1: The dry cell weight (DCW) –optical density (OD)correlation in LB medium.

Table 1.2.2: The bacterial dry cell weight (DCW) and the optical density (OD) values used to determine the DCW-OD correlation of *B. halodurans* Alk36 cultures grown in EnBase® medium

Time	weight (g/L)	weight (g/L)	weight (g/L)	average weight (g/L)	Blank corrected	Standard deviation	average OD_{600}
0							0.10
2	0.75	0.80	0.85	0.80	0.72	0.03	0.48
4	1.40	1.45	1.55	1.47	1.39	0.04	1.88
6	2.03	2.05	1.95	2.01	1.93	0.03	3.37
8	2.10	2.15	2.18	2.14	2.06	0.02	3.95
10	2.02	1.95	2.15	2.04	1.96	0.06	3.63
12	1.8	1.2	1.9	1.63	1.55	0.22	3.55
24	1.8	1.6	1.4	1.60	1.52	0.12	3.18

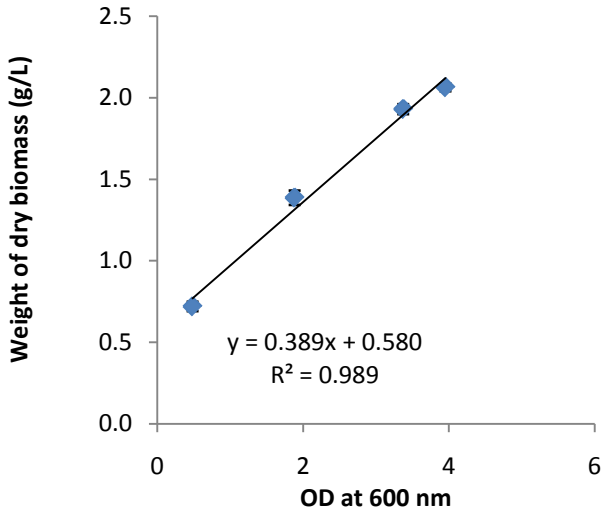

Figure 1.2.2: The dry cell weight (DCW) –optical density (OD) correlation in EnBase® medium.

Appendix 1.3: Growth of *B. halodurans* Alk36 in the bioreactor

Bacillus halodurans Alk36 was cultured in shake flasks as described in Section 3.1.4.1. The bacterial growth was measured by spectrometry at 600 nm as described in Section 3.3.1.1. The optical densities (OD) of *B. halodurans* Alk36 culture growing in the bioreactor using LB and EnBase medium are presented on Table 1.3.1 to 1.3.4.

Table 1.3.1: The optical densities (OD) of *B. halodurans* Alk36 culture growing on LB medium in the bioreactor at 30˚C and pH 8.5.

time	OD1	OD2	Average OD	LN OD 1	LN OD 2	Average LN OD	Standard deviation	Biomass 1	Biomass 2	Average biomass	Standard deviation	Growth rate (h^{-1})
0	0.139	0.133	0.136	-1.973	-2.021	-2.00	0.024	0.054	0.051	0.052	0.001	0.52*
2	0.243	0.293	0.268	-1.417	-1.229	-1.32	0.094	0.093	0.113	0.103	0.010	
4	0.776	1.038	0.907	-0.254	0.037	-0.11	0.145	0.299	0.399	0.349	0.050	
6	2.020	2.120	2.070	0.703	0.751	0.73	0.024	0.778	0.816	0.797	0.019	
8	3.305	3.520	3.413	1.195	1.258	1.23	0.032	1.272	1.355	1.314	0.041	
10	3.645	3.745	3.695	1.293	1.320	1.31	0.014	1.403	1.442	1.423	0.019	
12	4.505	4.420	4.463	1.505	1.486	1.50	0.010	1.734	1.702	1.718	0.016	
14	4.515	4.595	4.555	1.507	1.525	1.52	0.009	1.738	1.769	1.754	0.015	
24	4.430	4.495	4.463	1.488	1.503	1.50	0.007	1.706	1.731	1.718	0.013	

* The growth rate was calculated from the slope of the plot of LN (OD) versus time between t_0 and t_8.

Table 1.3.2: The optical densities (OD) of *B. halodurans* Alk36 culture growing on EnBase® medium in the bioreactor at 30˚C and pH 8.5.

time	OD1	OD2	Average OD	LN OD 1	LN OD 2	Average LN OD	Standard deviation	Biomass 1	Biomass 2	Average biomass	Standard deviation	Growth rate (h^{-1})
0	0.114	0.114	0.114	-2.176	-2.176	-2.18	0.000	0.644	0.644	0.644	0.000	0.41*
2	0.282	0.310	0.296	-1.266	-1.173	-1.22	0.047	0.710	0.721	0.715	0.005	
4	0.653	0.667	0.660	-0.426	-0.406	-0.42	0.010	0.855	0.860	0.857	0.003	
6	1.385	1.567	1.476	0.326	0.449	0.39	0.062	1.140	1.211	1.176	0.035	
8	3.140	3.552	3.346	1.144	1.268	1.21	0.062	1.825	1.985	1.905	0.080	
10	5.115	5.357	5.236	1.632	1.678	1.66	0.023	2.595	2.689	2.642	0.047	0.23*
12	8.180	7.897	8.039	2.102	2.066	2.08	0.018	3.790	3.680	3.735	0.055	
14	12.050	10.787	11.419	2.489	2.378	2.43	0.055	5.300	4.807	5.053	0.246	
16	15.400	13.817	14.609	2.734	2.626	2.68	0.054	6.606	5.989	6.297	0.309	
24	22.250	20.417	21.334	3.102	3.016	3.06	0.043	9.278	8.563	8.920	0.357	

* The growth rate was calculated from the slope of the plot of LN (OD) versus time between t_0 - t_8 and t_8 – t_{16}.

Table 1.3.3: The optical densities (OD) of *B. halodurans* Alk36 culture growing on EnBase® medium (without booster) in the bioreactor at 30˚C and pH 8.5.

time (hrs)	offline pH	OD1	OD2	OD3	average OD	standard deviation	Ln OD	Ln OD	Ln OD	Average Ln OD	standard deviation	Growth rate (h^{-1})
0	8.42	0.112	0.115	0.114	0.114	0.002	-2.189	-2.163	-2.172	-2.175	0.013	0.265*
2	8.51	0.289	0.275	0.280	0.281	0.007	-1.241	-1.291	-1.273	-1.268	0.025	
4	8.40	0.645	0.661	0.655	0.654	0.008	-0.439	-0.414	-0.423	-0.425	0.012	
6	8.60	1.430	1.340	1.390	1.387	0.045	0.358	0.293	0.329	0.327	0.033	
8	8.60	3.130	3.150	3.110	3.130	0.010	1.141	1.147	1.135	1.141	0.006	
10	8.58	4.710	5.520	4.980	5.070	0.405	1.550	1.708	1.605	1.621	0.081	
12	8.53	7.870	8.490	8.130	8.163	0.310	2.063	2.139	2.096	2.099	0.038	
14	8.54	13.300	11.800	12.100	12.400	0.750	2.588	2.468	2.493	2.516	0.063	
16	8.61	16.200	15.100	15.700	15.667	0.550	2.785	2.715	2.754	2.751	0.035	
24	8.75	23.600	22.900	23.000	23.167	0.350	3.161	3.131	3.135	3.143	0.016	

* The growth rate was calculated from the slope of the plot of LN (OD) versus time between $t_0$and t_{16}.

Table 1.3.4: The optical densities (OD) and pH of *B. halodurans* Alk36 culture growing on EnBase® medium (without booster) in the bioreactor at 30˚C and pH 8.5.

Time	OD1	OD 2	OD3	average OD	biomass equivalent	standard deviation	ln od	Ln OD	Ln OD	Average Ln OD	standard deviation	growth rate (h^{-1})
0	0.140	0.137	0.142	0.140	0.05	0.00	-1.966	-1.988	-1.952	-1.969	0.018	0.260*
4	0.417	0.420	0.423	0.420	0.16	0.00	-0.875	-0.868	-0.860	-0.868	0.007	
7	0.866	0.870	0.861	0.866	0.33	0.00	-0.144	-0.139	-0.150	-0.144	0.005	
9	1.730	1.750	1.770	1.750	0.67	0.02	0.548	0.560	0.571	0.560	0.011	
12	4.660	4.600	4.620	4.627	1.78	0.03	1.539	1.526	1.530	1.532	0.007	
15	7.450	7.390	7.430	7.423	2.86	0.03	2.008	2.000	2.006	2.005	0.004	
18	15.700	15.200	15.500	15.467	5.95	0.25	2.754	2.721	2.741	2.739	0.016	
24	17.900	18.000	18.500	18.133	6.98	0.32	2.885	2.890	2.918	2.898	0.018	

* The growth rate was calculated from the slope of the plot of LN (OD) versus time between t_0 and t_{16}.

Appendix 1.4: Carbon-source utilization in *B. halodurans* Alk36 cultures grown in EnBase® medium at 30°C and pH 8.5.

The starch-iodine and the DNS assays were used to determine the concentration of residual starch and reducing sugars in the medium, respectively. The assays were done as described in Section 3.3.2.

Table 1.4.1: Starch standards for Starch-Iodine assay

(g/L)	A580	A580	A580	Average OD	standard deviation
0	0.000	0.000	0.000	0.000	0.000
0.2	0.037	0.040	0.037	0.038	0.001
0.4	0.064	0.060	0.055	0.060	0.003
0.6	0.096	0.091	0.099	0.095	0.002
0.8	0.127	0.129	0.134	0.130	0.002
1.0	0.152	0.169	0.168	0.155	0.006

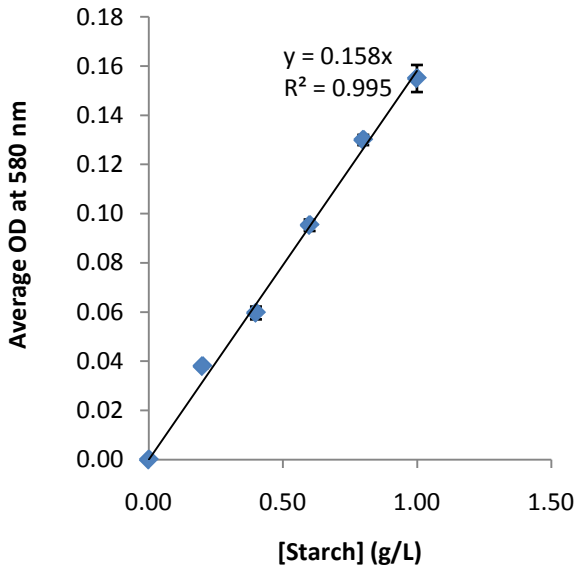

Figure 1.4.1: The starch standard curve used with the starch-iodine assay.

Table 1.4.2: Concentration of starch in cultures grown on EnBase® medium without booster

time	Absorbance at 580	Absorbance at 580	Absorbance at 580	Average absorbency	Standard deviation	blank corrected	[starch] g/L	x dil. factor
0	0.506	0.497	0.511	0.505	0.007	0.431	2.726	27.26
4	0.501	0.496	0.494	0.497	0.004	0.423	2.677	26.77
7	0.494	0.508	0.494	0.499	0.008	0.425	2.688	26.88
9	0.455	0.453	0.432	0.447	0.013	0.373	2.359	23.59
12	0.346	0.36	0.377	0.361	0.016	0.287	1.816	18.16
15	0.295	0.302	0.291	0.296	0.006	0.222	1.405	14.05
18	0.155	0.15	0.152	0.152	0.003	0.078	0.496	4.96

Table 1.4.3: Concentration of starch in cultures grown on EnBase® medium with booster

samples time	A580	A580	A580	Average OD	OD standard deviation	starch (µg)	x dilution factor [starch] (g/l)
0	0.185	0.180	0.193	0.186	0.005	1.18	23.54
2	0.179	0.171	0.178	0.176	0.003	1.11	22.28
4	0.190	0.185	0.188	0.188	0.002	1.19	23.76
6	0.155	0.163	0.148	0.155	0.005	0.98	19.66
8	0.185	0.186	0.188	0.186	0.001	1.18	23.59
10	0.163	0.165	0.174	0.167	0.004	1.06	21.18
12	0.097	0.098	0.100	0.098	0.001	0.62	12.45
14	0.070	0.069	0.070	0.070	0.000	0.44	8.82
24	0.060	0.061	0.061	0.061	0.000	0.38	7.68

Table 1.4.3: Glucose standards for the DNS assay

A575	A575	A575	average OD	Standard deviation	blank corrected	[glucose] (g/l)
0.031	0.034	0.029	0.031	0.003	0.000	0.0
0.085	0.082	0.081	0.083	0.002	0.052	0.2
0.148	0.148	0.144	0.147	0.002	0.116	0.4
0.211	0.21	0.206	0.209	0.003	0.178	0.6
0.278	0.28	0.28	0.279	0.001	0.248	0.8
0.349	0.345	0.344	0.346	0.003	0.315	1.0

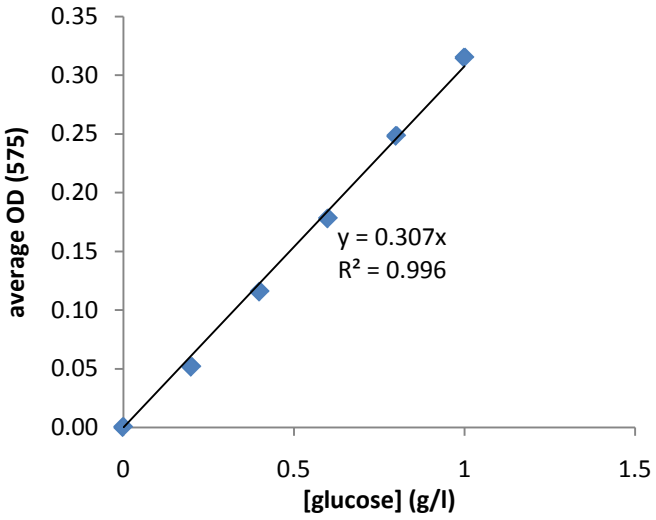

Figure 1.4.2: The glucose standard curve used with the DNS assay.

Table 1.4.4: Concentration of glucose in cultures grown on EnBase® medium without booster

time (hrs)	A575	A575	A575	average OD	standard deviation	relative error	[glucose] (g/l)	x dilution factor	standard deviation
0	0.121	0.121	0.125	0.122	0.002	0.019	0.397	3.974	0.075
4	0.167	0.167	0.169	0.168	0.001	0.007	0.545	5.447	0.038
7	0.152	0.154	0.152	0.153	0.001	0.008	0.496	4.960	0.038
9	0.117	0.121	0.115	0.118	0.003	0.026	0.382	3.823	0.099
17	0.100	0.103	0.099	0.101	0.002	0.021	0.327	3.271	0.068
20	0.062	0.063	0.061	0.062	0.001	0.016	0.201	2.014	0.032
24	0.060	0.057	0.058	0.058	0.002	0.026	0.190	1.895	0.050
32	0.035	0.034	0.035	0.035	0.001	0.017	0.113	1.126	0.019

Table 1.4.5: Concentration of glucose in cultures grown on EnBase® medium with booster

Sample time	A580	A580	A580	Average OD	OD standard deviation	relative error	[glucose]	x dilution factor	standard deviation
0	0.135	0.128	0.130	0.131	0.004	0.03	0.68	3.39	0.09
2	0.096	0.097	0.095	0.096	0.001	0.01	0.50	2.48	0.03
4	0.090	0.085	0.098	0.091	0.007	0.07	0.47	2.35	0.17
6	0.076	0.079	0.081	0.079	0.003	0.03	0.41	2.03	0.07
8	0.094	0.086	0.088	0.089	0.004	0.05	0.46	2.31	0.11
10	0.090	0.088	0.089	0.089	0.001	0.01	0.46	2.30	0.03
12	0.176	0.169	0.170	0.172	0.004	0.02	0.89	4.44	0.10
14	0.100	0.106	0.102	0.103	0.003	0.03	0.53	2.65	0.08
24	0.001	0.001	0.000	0.001	0.001	0.87	0.00	0.02	0.01

Appendix 1.5: Determination of sugars and organic acids by HPLC analysis

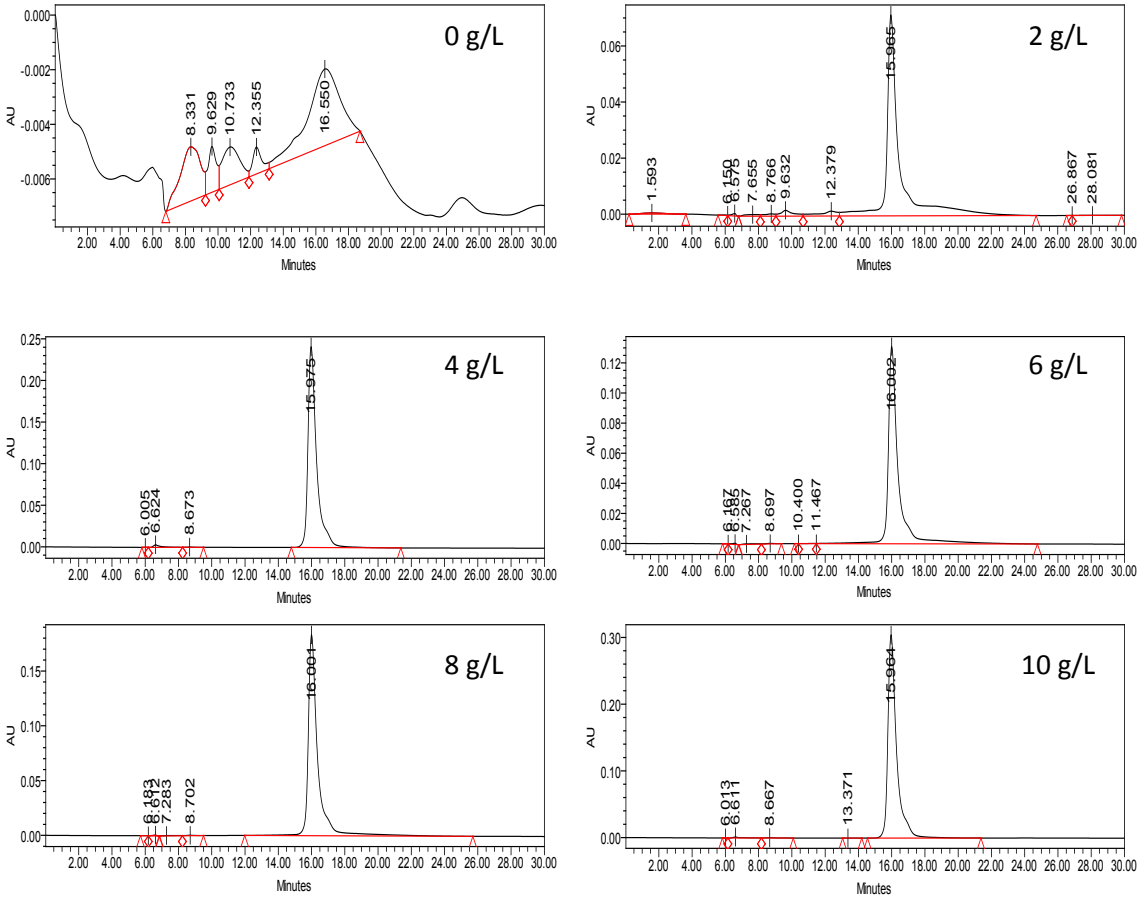

Figure 1.5.1: Peaks obtained from the chromatograms of acetic acid standards at different concentrations using Aminex HPX-87 column.

Table 1.5.1: The peak areas of acetic acid standards used for the determination of organic acids by HPLC

[Acetic acid] (g/L)	Retention time	Peak area	Blank corrected (x10^6)
0	16.55	593,122	0.00
2	15.96	2,748,422	2.16
4	16.00	5,469,924	4.88
6	16.00	7,284,272	6.69
8	15.98	8,795,766	8.20
10	15.96	11,098,813	10.51

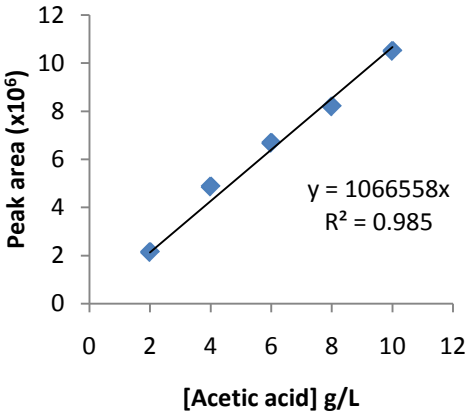

Figure 1.5.2: Acetic acid standard curve used to calculate the concentration of organic acids in the HPLC samples.

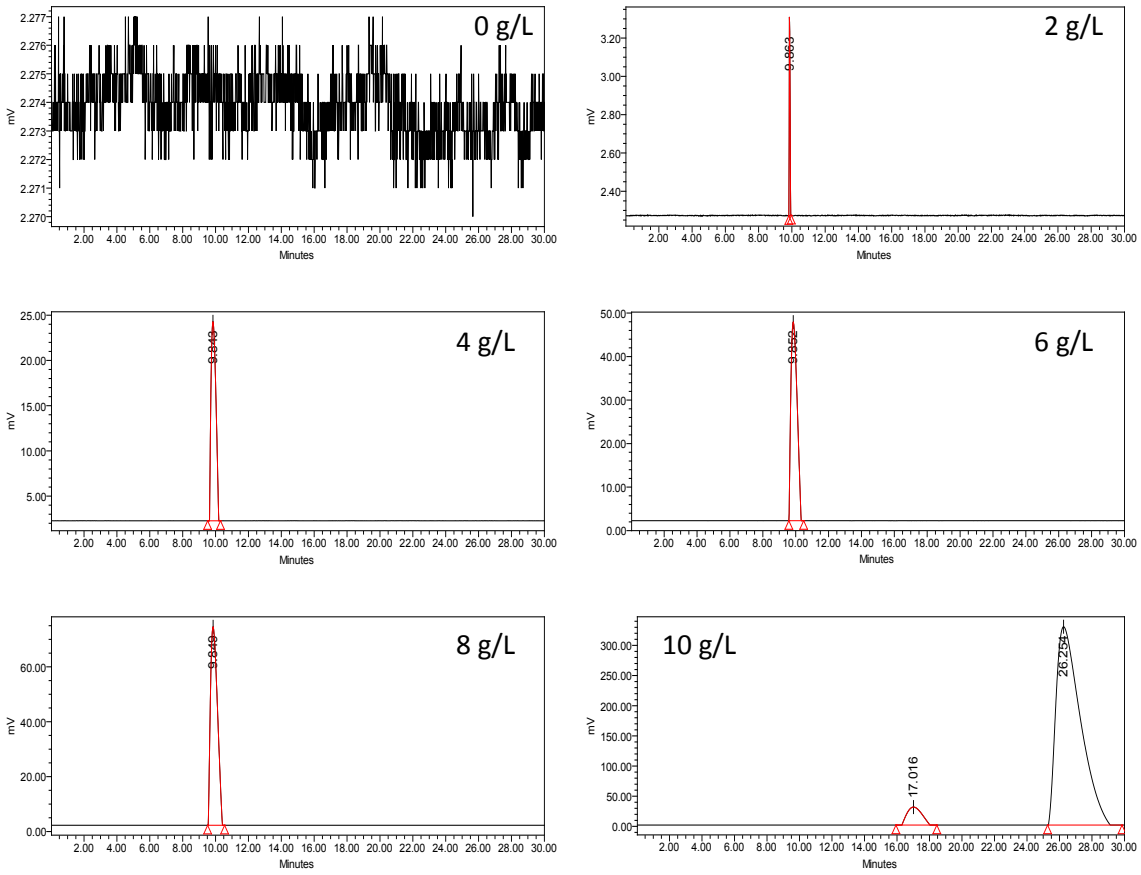

Figure 1.5.3: Peaks obtained from the chromatograms of glucose standards at different concentrations using Aminex HPX-87 column.

Table 1.5.2: The peak areas of Glucose standards used for analysis of sugars by HPLC.

[Glucose] (g/L)	Retention time	Peak area	Blank corrected (x10^6)
0	9.35	637	0.00
2	9.44	4,954,851	0.39
4	9.44	7,956,539	0.96
6	9.44	12,777,343	1.61
8	9.44	16,589,851	2.14
10	9.44	21,368,008	0.00

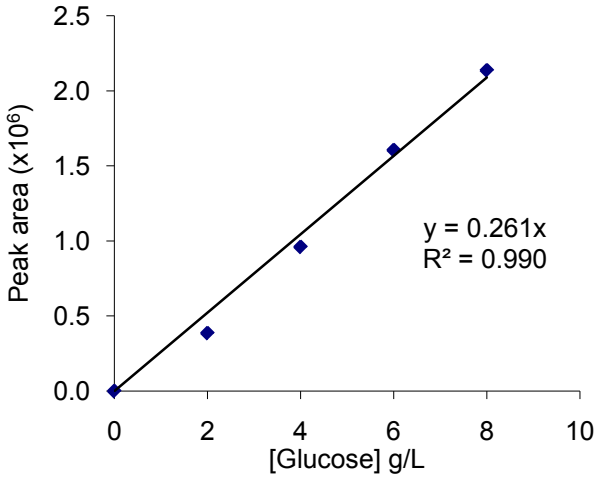

Figure 1.5.4: Glucose standard curve used for determination of the concentration of sugars in the culture samples by the HPLC analysis.

Table 1.5.3: The concentration of glucose in the culture medium at different time points during growth of *B. halodurans Alk36* as determined by HPLC analysis.

Time (h)	Retention time	Peak area	[glucose] (g/L)	[glucose]x dilution factor(g/L)	Average [glucose] (g/L)	standard deviation
0	9.10	476,960	1.83	3.65	3.72	0.06
	9.12	491,111	1.88	3.76		
	9.11	491,614	1.88	3.77		
2	9.10	559,500	2.14	4.28	4.20	0.12
	9.11	533,201	2.04	4.08		
	9.11	561,812	2.15	4.30		
4	9.09	501,840	1.92	3.84	3.75	0.25
	9.08	514,067	1.97	3.94		
	9.08	452,489	1.73	3.47		
6	9.08	350,932	1.34	2.69	2.68	0.01
	9.08	349,082	1.34	2.67		
	9.08	348,901	1.34	2.67		
8	9.07	170,401	0.65	1.31	1.18	0.17
	9.08	164,623	0.63	1.26		
	9.07	128,314	0.49	0.98		

Appendix 1.6: Determination of yields obtained from LB and EnBase® medium

The biomass yields with respect to the medium used were calculated by determining the amount of carbon present in the biomass and that present in the substrate.

1.6.1. Yields based on the amount of carbon added into the medium

For cultures grown in LB broth

- LB medium contains 10 g/L tryptone and 5 g/L yeast extract
- The amount of carbon present in tryptone and yeast extract was determined from the total free carbohydrate content and the carbohydrate provided by the amino acids (assuming that the carbohydrate was glucose).
- The amount of carbon in the amino acids present in tryptone and yeast extract was calculated as indicated in Table 1.6..1 and 1.6.2.2 and presented as the amino carbon content.
- The amount of carbohydrate and amino acids in tryptone and yeast extract was determined from the Difco™ & BBL™ Manual of Microbiological Culture Media (Power & Johnson, 2009).

- Amount of amino carbon in the medium = Amino carbon content of YE x amount of yeast extract

  = 0.24 g Carbon per g yeast extract x 5 g/L y/extract

  = 1.2 g/L Carbon

- Total carbohydrate present in yeast extract = 163.3 mg/g yeast extract

  Amount of carbohydrate in the medium = 0.1633 g carbohydrate per g yeast extract x 5 g/L

  Total carbohydrate in the medium = 0.816 g/L

  Assuming the carbohydrate is glucose, the mass fraction of carbon in glucose is 0.4

  Thus, the amount of carbon in carbohydrate present = 0.816 g/L x 0.4

  = 0.33 g/L

- Total carbon due to amino acids and carbohydrate = 0.33 + 1.2

  = 1.53 g/L

- Total carbon present in LB broth = 1.53 + 3.72 = 5.25 g/L

$$= \frac{5.25\ \text{g/L carbon}}{12\ \text{g/Mole carbon}}$$

= 0.44 Moles/L carbon

Table 1.6.1: Amount of Carbon in amino acid present in yeast extract

Amino acids present	Molecular formula	% of amino acids in tryptone	Weight (g)	molecular mass of	#C	mass fraction	amount of carbon present
Alanine	C3H7NO2	5.6	0.056	89.09	3	0.40	0.02
Arginine	C6H14N4O2	2.6	0.026	174.20	6	0.41	0.01
Asparagine	C4H8N2O3	1	0.01	132.12	4	0.36	0.00
Aspartic acid	C4H7NO4	5.3	0.053	133.11	4	0.36	0.02
Cysteine	C3H7NO2S	0.2	0.002	121.16	3	0.30	0.00
Glutamic acid	C5H9NO4	9.4	0.094	147.13	5	0.41	0.04
Glutamine	C5H10N2O3	0.2	0.002	146.14	5	0.41	0.00
Glycine	C2H5NO2	3	0.03	75.07	2	0.32	0.01
Histidine	C6H9N3O2	1.3	0.013	155.15	6	0.46	0.01
Isoleucine	C6H13NO2	3	0.03	131.17	6	0.55	0.02
Leucine	C6H13NO2	4.1	0.041	131.17	6	0.55	0.02
Lysine	C6H14N2O2	4.6	0.046	146.19	6	0.49	0.02
Methione	C5H11NO2S	0.8	0.008	149.21	5	0.40	0.00
Pheynylalanine	C9H11NO2	2.6	0.026	165.19	9	0.65	0.02
Proline	C5H9NO2	2	0.02	115.13	5	0.52	0.01
Serine	C3H7NO3	1.6	0.016	105.09	3	0.34	0.01
Threonine	C4H9NO3	1.6	0.016	119.12	4	0.40	0.01
Tryptophan	C11H12N2O2	0.5	0.005	204.23	11	0.65	0.00
Tyrosine	C9H11NO3	1.2	0.012	181.19	9	0.60	0.01
Valine	C5H11NO2	3.5	0.035	117.15	5	0.51	0.02
Total amount of amino carbon present in g of yeast extract							0.24

Table 1.6.2: Amount of Carbon in amino acid present in tryptone

Amino acids Present	Molecular Formula	% of amino acids in tryptone	Weight (g)	molecular mass of	#C	mass fraction	amount of carbon present
Alanine	C3H7NO2	3.2	0.032	89.09	3	0.40	0.01
Arginine	C6H14N4O2	5	0.05	174.20	6	0.41	0.02
Asparagine	C4H8N2O3	0.6	0.006	132.12	4	0.36	0.00
Aspartic acid	C4H7NO4	5.2	0.052	133.11	4	0.36	0.02
Cysteine	C3H7NO2S	0.3	0.003	121.16	3	0.30	0.00
Glutamic acid	C5H9NO4	15.1	0.151	147.13	5	0.41	0.06
Glutamine	C5H10N2O3	0.1	0.001	146.14	5	0.41	0.00
Glycine	C2H5NO2	1.7	0.017	75.07	2	0.32	0.01
Histidine	C6H9N3O2	1.9	0.019	155.15	6	0.46	0.01
Isoleucine	C6H13NO2	5.5	0.055	131.17	6	0.55	0.03
Leucine	C6H13NO2	7.5	0.075	131.17	6	0.55	0.04
Lysine	C6H14N2O2	6.2	0.062	146.19	6	0.49	0.03
Methione	C5H11NO2S	2.1	0.021	149.21	5	0.40	0.01
Pheynylalanine	C9H11NO2	5.2	0.052	165.19	9	0.65	0.03
Proline	C5H9NO2	6.6	0.066	115.13	5	0.52	0.03
Serine	C3H7NO3	2.2	0.022	105.09	3	0.34	0.01
Threonine	C4H9NO3	1.8	0.018	119.12	4	0.40	0.01
Tryptophan	C11H12N2O2	0.8	0.008	204.23	11	0.65	0.01
Tyrosine	C9H11NO3	1.3	0.013	181.19	9	0.60	0.01
Valine	C5H11NO2	5.9	0.059	117.15	5	0.51	0.03
Total amino carbon content present in g of tryptone							0.37

- Amount of amino carbon in the medium = Total amino carbon content x amount of tryptone used

  = 0.37 g Carbon per g tryptone x 10 g/L tryptone

  = 3.7 g/L Carbon

- Total carbon due to amino acids and carbohydrate = 0.0172 + 3.7

  = 3.72 g/L

For cultures grown in EnBase medium

- The amount of carbon present in the medium = 30 g/L starch
  = 30 g/L glucose
  $= \frac{30\ \mathrm{g/L}}{180\ \mathrm{g/Mole}}$ = 0.17 Moles/L glucose
  = 0.17 Moles/L x 6 Moles C/Mole glucose
  = 1.00 Moles/L Carbon
- The amount of carbon in booster
  - Amount of tryptone added = concentration x dilution factor
    = 120 g/L x 0.02
    = 2.4 g/L

    Amount of carbohydrate present in tryptone = 4.3 mg/g
    = 4.3mg/g x amount of tryptone added
    = 4.3 mg/g x 2.4 g/L
    = 10.32 mg/L carbohydrate

    Amount of carbon from carbohydrate present in tryptone= 10.32 mg/L x 0.4
    = 4.13 mg/L Carbon

    Amount of amino carbon present in tryptone (from Table 4.1) = 0.37 g/g tryptone
    Amount of amino carbon in the medium = 0.37 x 2.4 g/L tryptone
    = 0.888 g/L Carbon
    Total carbon due to amino acids and carbohydrate = 4.13+ 0.89
    = 5.02 g/L
  - Amount of yeast extract added = concentration x dilution factor
    = 240 g/L x 0.02
    = 4.8 g/L

    Amount of carbohydrate present in yeast extract = 163 mg/g
    = 163mg/g x amount y.e added
    = 163 mg/g x 4.8 g/L
    = 782.4 mg/L carbohydrate

    Amount of amino carbon present in y.e (from Table 4.2) = 0.37 g/g yeast extract

Amount of amino carbon in the medium = 0.24 x 4.8 g/L tryptone

= 1.15 g/L Carbon

Total carbon due to amino acids and carbohydrate = 1.15+ 0.78

= 1.93 g/L

- Total amount of carbon in the booster = carbon in yeast extract + carbon in tryptone

  = 1.93 g/L + 5.02 g/L

  = 6.95 g/L carbon

  $= \frac{6.95\ \mathrm{g/L}}{12\ \mathrm{g/Mole}}$

  = 0.56 Moles/L Carbon

Total amount of carbon in EnBase medium (with booster) = 1.00 + 0.56 = 1.56 M Carbon

Total amount of carbon in EnBase medium (without booster) = 1.00 M Carbon

- Carbon content in biomass

  Formula of biomass = $CH_{1.8}O_{0.5}N_{0.2}$ (Bailey &Ollis, 1986)

  Molecular weight of biomass = 12 + 1.8 + (0.5 x16) + (0.2 x14)

  = 24.6 g/Mole biomass

  Concentration of dry biomass = 1.72 g/L

  $= \frac{1.72\ \mathrm{g/L}}{24.6\ \mathrm{g/Mole}}$ = 0.07 Moles biomass/L

  [carbon] in biomass = 0.07 Moles biomass /L x 1 Mole carbon/ Mole Biomass

  = 0.07 Moles Carbon/L

  Yield on LB $= \frac{\text{concentration of carbon in biomass}}{\text{concentration of carbon in LB}}$

  $= \frac{0.07\ \text{Moles Carbon /L}}{0.44\ \text{Moles Carbon /L}}$

  = 0.16

Yield on EnBase (with booster) $= \frac{\text{concentration of carbon in biomas s}}{\text{concentration of carbon in EnBase}}$

$= \frac{0.37 \text{ Moles Carbon /L}}{1.56 \text{Moles Carbon /L}}$

= 0.24

Yield on EnBase (without booster) $= \frac{\text{concentration of carbon in biomass}}{\text{concentration of carbon in EnBase}}$

$= \frac{0.28 \text{ Moles Carbon /L}}{1.00 \text{ Moles Carbon /L}}$

= 0.28

Yields based on the measured carbon content

For culture grown in EnBase medium with booster (based on values from Table 1.3.3, 1.4.3 and 1.4.4 in Appendix 1.3 and 1.4)

- The amount of carbon-source present in the medium due to starch at t_0 = 23.54 ± 0.59 g/L starch
  The amount of carbon-source present in the medium due to glucose at t_0 = 3.39 ± 0.09 g/L glucose
  Total amount of carbon-source present in the medium at t_0 = 26.93 ± 1.39 g/L

  The amount of carbon present in the medium at $t_0 = \frac{26.93 \text{ g/L}}{180 \text{ g/Mole}}$ = 0.15 Moles/L glucose

  = 0.15 Moles glucose/L x 6 Moles C/Mole glucose

  = 0.90 ± 0.05 Moles/L carbon

  Total amount of carbon in the booster = 0.56 Moles/L Carbon
  Total amount of carbon at t_0 = 1.46 ± 0.05 moles/L Carbon
- The amount of carbon-source present in the medium due to starch at t_{24} = 7.68 ± 0.05 g/L starch
  The amount of carbon-source present in the medium due to glucose at t_{24} = 0.02 ± 0.01 g/L glucose

Total amount of carbon-source present in the medium at t_{24} = 7.70 ±0.51 g/L

The amount of carbon present in the medium at t_{24} = $\frac{7.7\ \text{g/L}}{180\ \text{g/Mole}}$ = 0.043 Moles/L glucose

= 0.043 Moles glucose/L x 6 Moles C/Mole glucose

= 0.26± 0.02 Moles/L carbon

- Carbon content in biomass

  Formula of biomass = $CH_{1.8}O_{0.5}N_{0.2}$ (Bailey &Ollis, 1986)

  Molecular weight of biomass = 12 + 1.8 + (0.5 x16) + (0.2 x14)

  = 24.6 g/Mole biomass

  Concentration of dry biomass at t_{24} = 8.92 ± 0.36 g/L

  = $\frac{8.92\ \text{g/L}}{24.6\ \text{g/Mole}}$ = 0.36 ± 0.01 Moles biomass/L

  [carbon] in biomass = 0.36 Moles biomass /L x 1 Mole carbon/ Mole Biomass

  = 0.36 ± 0.01 Moles Carbon/L

- Yield on EnBase (with booster) = $\frac{\text{concentration of carbon in biomass}}{\text{concentration of carbon in EnBase}}$

  = $\frac{0.36\ \text{Moles Carbon /L}}{(1.46-0.26)\ \text{Moles Carbon /L}}$

  = 0.3 Moles in biomass per mole in substrate

For culture grown in EnBase medium without booster (based on values from Table 1.3.4, 1.4.2 and 1.4.3 in Appendix 1.3 and 1.4)

- The amount of carbon-source present in the medium due to starch at t_0 = 27.26 ± 0.38 g/L starch
  The amount of carbon-source present in the medium due to glucose at t_0 = 3.97 ± 0.08 g/L glucose
  Total amount of carbon-source present in the medium at t_0 = 31.23 ± 0.03 g/L

The amount of carbon present in the medium at t_0= $\frac{31.23\ \mathrm{g/L}}{180\ \mathrm{g/Mole}}$ = 0.17 Moles/L glucose

= 0.17 Moles glucose/L x 6 Moles C/Mole glucose

= 1.04 ± 0.00 Moles/L carbon

- The amount of carbon-source present in the medium due to starch at t_{24} = 4.96 ± 0.08 g/L starch

  The amount of carbon-source present in the medium due to glucose at t_{24} = 1.90 ± 0.05 g/L glucose

  Total amount of carbon-source present in the medium at t_{24} = 6.86 ±0.04 g/L

  The amount of carbon present in the medium at t_{24} = $\frac{6.86\ \mathrm{g/L}}{180\ \mathrm{g/Mole}}$ = 0.038 Moles/L glucose

  = 0.038 Moles glucose/L x 6 Moles C/Mole glucose

  = 0.23± 0.00 Moles/L carbon

  - Carbon content in biomass

    Formula of biomass = $CH_{1.8}O_{0.5}N_{0.2}$ (Bailey &Ollis, 1986)

    Molecular weight of biomass = 12 + 1.8 + (0.5 x16) + (0.2 x14)

    = 24.6 g/Mole biomass

    Concentration of dry biomass at t_{24} = 7.49 ± 0.18 g/L

    = $\frac{7.49\ \mathrm{g/L}}{24.6\ \mathrm{g/Mole}}$= 0.30 ± 0.01 Moles biomass/L

    [carbon] in biomass = 0.30 Moles biomass /L x 1 Mole carbon/ Mole Biomass

    = 0.30 ± 0.01 Moles Carbon/L

- Yield on EnBase (with booster) = $\frac{\text{concentration of carbon in biomass}}{\text{concentration of carbon in EnBase}}$

  = $\frac{0.30\ \text{Moles Carbon /L}}{(1.04-0.23)\ \text{Moles Carbon /L}}$

  = 0.37 Moles in biomass per mole in substrate

Appendix 1.7: Determination of the oxygen transfer rate (OTR) and the oxygen utilization rate (OUR) of *B. halodurans Alk36* culture grown in EnBase medium at 30°C and pH 8.5.

Table 1.7.1: The dissolved oxygen concentration used to determine the OUR of *B. halodurans Alk36* culture at 30°C and pH 8.5 with 3 L/min aeration and 1000 rpm agitation.

time (s)	dO2	dO2	dO2	$[O_2]$ mMols/L	$[O_2]$ mMols/L	$[O_2]$ mMols/L	average $[O_2]$ mMols/L	standard deviation
0	22.2	27.6	28.7	0.053	0.066	0.069	0.063	0.006
30	42.6	40.7	48.0	0.102	0.098	0.115	0.105	0.006
60	60.4	61.1	62.2	0.145	0.147	0.149	0.147	0.002
90	66.7	67.9	67.9	0.160	0.163	0.163	0.162	0.001
120	68.6	69.9	69.5	0.165	0.168	0.167	0.166	0.001

The OUR was calculated from the slope of the average oxygen concentration versus time as shown in Figure 1.6.1.

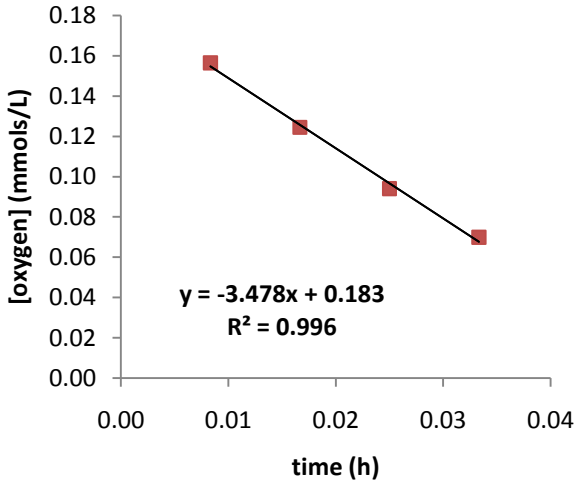

Figure 1.7.1: The rate of decrease of the dissolved oxygen concentration in *B. halodurans* Alk36 cultures growing on EnBase® medium at pH 8.5 and 30°C. The slope of the liner line represents the oxygen utilization rate.

The volumetric mass transfer coefficient (k_La) was determined using the dissolved oxygen concentration and the oxygen utilization rate as illustrated in the following equation:

$$C_L = \frac{-1}{k_L a}\left(\frac{dC_L}{dt} + OUR\right) + C_{sat}$$

Where $\mathbf{C_L}$ is the dissolved oxygen concentration and $\mathbf{C_{sat}}$is the concentration of oxygen at saturation

Thus the reciprocal of the slope of the line obtained from plotting C_L versus $\left(\frac{dC_L}{dt} + OUR\right)$ represents the k_La as illustrated in Figure 1.5.2.

Table 1.7.2: The dissolved oxygen concentration used to calculate the k_La of the bioreactor system used to grown the *B. halodurans* Alk36 cultures on EnBase® medium at 30˚C, pH 8.5.

time (s)	average [O2] mMols/L	C_{L1}-C_{L2}	dC_L/dt	dC_L/dt +OUR	k_La (h^{-1})
0	0.063				
30	0.105	0.042	5.069	8.549	
60	0.147	0.042	5.030	8.510	227
90	0.162	0.015	1.805	5.285	
120	0.166	0.004	0.528	4.008	

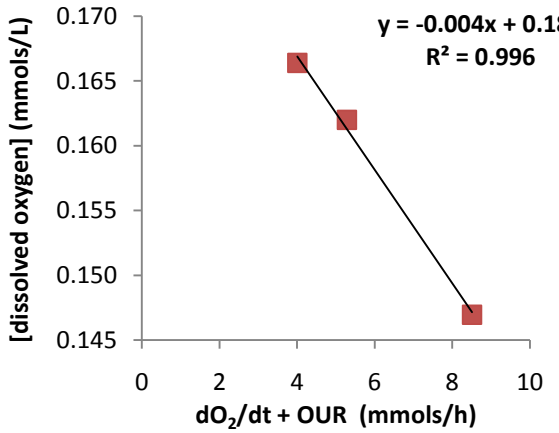

Figure 1.7.2: The k_La value obtained in *B. halodurans Alk36* cultures growing on EnBase® medium at pH 8.5 and 30˚C. The slope of the liner line represents the reciprocal of the k_La value.

Table 1.7.3: The dissolved oxygen concentration used to determine the OTR of the NewBrunswick bioreactor system at 30°C, 3 L/min aeration and agitation between 400 rpm and 1000 rpm.

Agitation: 400rpm					
time (s)	dO2	[O2] mmols/L	Csat - Ct	ln (Csat - Ct)	tsat– t
0	0.0	0.000	0.231	-1.47	300
20	15.5	0.037	0.193	-1.64	280
40	30.5	0.073	0.157	-1.85	260
60	47.6	0.114	0.116	-2.15	240
80	58.2	0.140	0.091	-2.40	220
100	67.5	0.162	0.069	-2.68	200
120	70.6	0.169	0.061	-2.79	180
140	77.9	0.187	0.044	-3.13	160
160	80.6	0.193	0.037	-3.29	140
180	86.0	0.206	0.024	-3.72	120
200	88.2	0.212	0.019	-3.97	100
220	91.8	0.220	0.010	-4.57	80
240	93.4	0.224	0.006	-5.04	60
260	94.0	0.226	0.005	-5.29	40
280	96.1	0.231	0.000		20
300	96.1	0.231	0.000		0

Agitation: 600 rpm					
time (s)	dO2	[O2] mmols/L	Csat - Ct	ln (Csat - Ct)	tsat - t
0	0.0	0.000	0.240	-1.43	140
20	29.7	0.071	0.169	-1.78	120
40	51.7	0.124	0.116	-2.15	100
60	74.7	0.179	0.061	-2.80	80
80	88.0	0.211	0.029	-3.55	60
100	95.2	0.228	0.012	-4.46	40
120	98.9	0.237	0.003	-5.94	20
140	100.0	0.240	0.000		0

Continuation of Table 1.6.3

Table 1.7.3: The dissolved oxygen concentration used to determine the OTR of the NewBrunswick bioreactor system at 30 °C, 3 L/min aeration and agitation between 400 rpm and 1000 rpm.

Agitation: 800 rpm					
time (s)	dO2	[O_2] mmols/L	C_{sat}- C_t	ln (C_{sat}- C_t)	t_{sat}- t
0	0.0	0.000	0.240	-1.43	100
20	30.7	0.074	0.166	-1.79	80
40	69.9	0.168	0.072	-2.63	60
60	89.4	0.215	0.025	-3.67	40
80	97.4	0.234	0.006	-5.08	20
100	100.0	0.240	0.000		0

Agitation: 1000 rpm					
time (s)	dO2	[O_2] mmols/L	C_{sat}- C_t	ln (C_{sat}- C_t)	t_{sat}– t
0	0.0	0.000	0.240	-1.43	120
20	26.1	0.063	0.177	-1.73	100
40	68.6	0.165	0.075	-2.59	80
60	88.7	0.213	0.027	-3.61	60
80	96.4	0.231	0.009	-4.75	40
100	99.4	0.239	0.001	-6.54	20
120	100.0	0.240	0.000		0

The OTR was calculated from the slope of the plot of [Ln (C_{sat} – C_L)] versus (t_{sat} – t_L) (Figure 1.7.3).

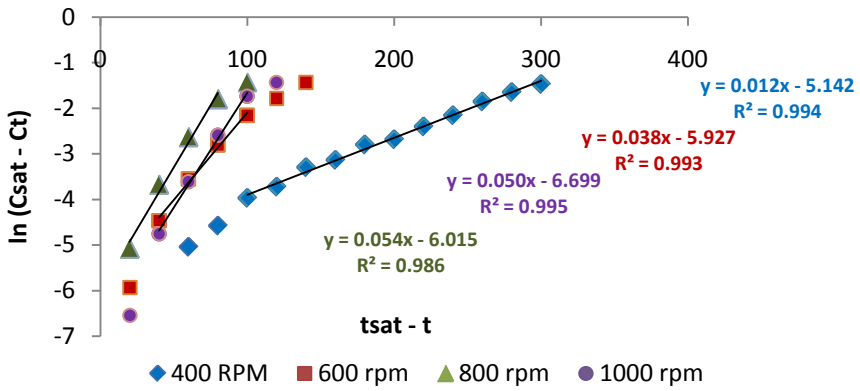

Figure 1.7.3: Determination of the OTR in the NewBrunswick bioreactor at 30 °C and 3 L/min aeration. Slopes of the liner curves represent the OTR.

Appendix 1.8: Effect of addition of ammonium salt *in B. halodurans* Alk36 cultures grown at 30°C and pH 8.5.

Table 1.8.1: The optical densities (OD) and pH of *B. halodurans* Alk36 culture growing on EnBase® medium at pH 8.5 and 30˚C without addition of ammonium salt.

Culture time	OD_{600}	OD_{600}	OD_{600}	Average OD	standard deviation	LN OD	growth rate (h^{-1})	pH
0	0.227	0.228	0.226	0.227	0.001	-1.483		8.52
4	0.391	0.393	0.392	0.392	0.001	-0.936	0.137	8.67
7	0.814	0.816	0.818	0.816	0.002	-0.203	0.244	8.61
15	3.980	3.960	4.010	3.983	0.025	1.382	0.198	8.45
19	9.790	9.750	9.740	9.760	0.026	2.278	0.224	8.46
23.5	18.20	18.100	18.200	18.167	0.058	2.900	0.138	8.57
25.5	18.600	18.500	18.600	18.567	0.058	2.921	0.011	8.24
31	19.400	19.400	19.300	19.367	0.058	2.964	0.008	8.76

Table 1.8.2: The optical densities (OD) and pH of *B. halodurans Alk36* culture growing on EnBase® medium at pH 8.5 and 30˚C with addition of ammonium salt.

Culture time	OD_{600}	OD_{600}	OD_{600}	Average OD	standard deviation	LN OD	growth rate (h^{-1})	pH
0	0.233	0.231	0.234	0.233	0.002	-1.458		8.63
3	0.401	0.403	0.398	0.401	0.003	-0.915	0.181	8.37
6	0.787	0.792	0.789	0.789	0.003	-0.237	0.226	8.48
14	3.822	3.819	3.820	3.820	0.002	1.340	0.197	8.37
18	6.760	6.757	6.762	6.760	0.003	1.911	0.143	8.24
22.5	17.600	17.500	17.600	17.567	0.058	2.866	0.212	8.19
26.5	15.700	15.700	15.600	15.667	0.058	2.752	-0.029	8.58
30	11.800	11.900	12.000	11.900	0.100	2.477	-0.079	8.23

Appendix 1.9: Determination of the assay to be used for determination of the activity of *B. halodurans* Alk36 amylases.

Table 1.9.1: Maltose standards for DNS assay

[maltose] mg/L	A575	A575	A575	Average absorbance	standard deviation	blank corrected
0.0	0.052	0.053	0.055	0.053	0.002	0.000
0.2	0.264	0.267	0.266	0.266	0.002	0.213
0.4	0.543	0.545	0.546	0.545	0.002	0.492
0.6	0.749	0.742	0.748	0.746	0.004	0.693
0.8	0.913	0.914	0.89	0.906	0.014	0.853

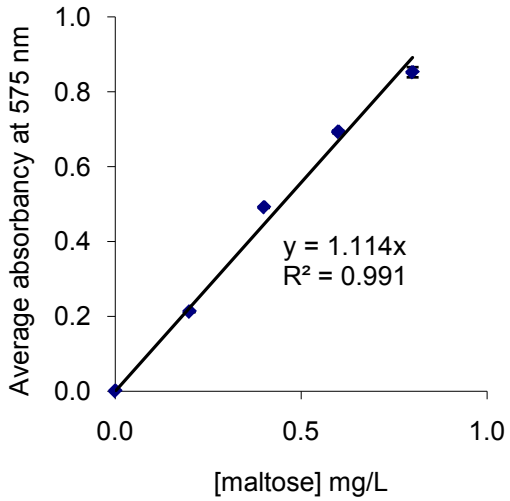

Figure 1.9.1: Maltose standard curve used with the DNS assay for determination of amylase activities of commercial amylase from *B. licheniformis.*

Table 1.9.2: The starch hydrolysis profile used for determination of the activity of commercial amylase from *B .licheniformis* using DNS assay and 1U/ mg of the enzyme

Given unit: 1 U/mL									
A575	A575	A575	Average absorbance	standard deviation	relative error	blank corrected	[maltose] mg/L	x dilution factor	Time (mins)
0.254	0.274	0.264	0.264	0.010	0.038	0.000	0.000	0.000	0
0.272	0.270	0.262	0.268	0.005	0.020	0.004	0.004	0.036	1
0.280	0.294	0.278	0.284	0.009	0.031	0.020	0.018	0.179	2
0.312	0.318	0.320	0.317	0.004	0.013	0.053	0.047	0.473	3
0.350	0.350	0.342	0.347	0.005	0.013	0.083	0.075	0.748	4
0.386	0.378	0.372	0.379	0.007	0.019	0.115	0.103	1.029	5
					0.133				

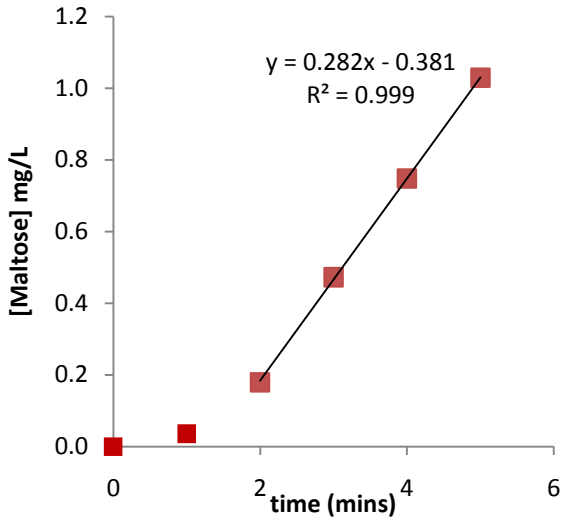

Figure 1.9.2: The rate of release of Maltose from starch hydrolysis by *B. licheniformis*amylase when using 1U/mg of the enzyme.

$$Amylaseactivity = \frac{0.2824(mg.L^{-1}.min^{-1})\ x\ 3}{1\ (mg.L^{-1})} = 0.85\ (U.mg^{-1}\ protein)$$

Table 1.9.3: The starch hydrolysis profile used for determination of the activity of commercial amylase from *B .licheniformis* using DNS assay with 5 U/ mg of the enzyme

Given unit: 5 U/mL									
A575	A575	A575	Average absorbance	standard deviation	relative error	blank corrected	[maltose] mg/L	x dilution factor	Time (mins)
0.260	0.246	0.242	0.249	0.009	0.038	0.000	0.000	0.003	0
0.436	0.440	0.400	0.425	0.022	0.052	0.176	0.158	1.582	1
0.576	0.598	0.580	0.585	0.012	0.020	0.336	0.301	3.012	2
0.730	0.758	0.746	0.745	0.014	0.019	0.496	0.445	4.448	3
0.898	0.912	0.902	0.904	0.007	0.008	0.655	0.588	5.878	4
0.946	0.958	0.964	0.956	0.009	0.010	0.707	0.634	6.344	5
					0.146				

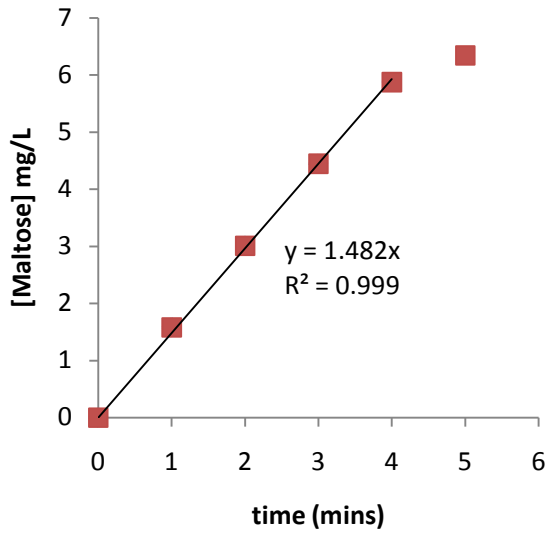

Figure 1.9.3: The rate of release of Maltose from starch hydrolysis by *B. licheniformis*amylasewhen using 5 U/ mg of the enzyme.

$$Amylaseactivity = \frac{1.482(mg.L^{-1}.min^{-1})\ x\ 3}{1\ (mg.L^{-1})} = 4.44\ (U.mg^{-1}\ protein)$$

Table 1.9.4: The starch hydrolysis profile used for determination of the activity of commercial amylase from *B .licheniformis* using DNS assay with 10 U/ mg of the enzyme

Given unit: 10 U/mL									
A575	A575	A575	Average absorbance	standard deviation	relative error	blank corrected	[maltose] mg/L	x dilution factor	Time (mins)
0.252	0.234	0.218	0.235	0.017	0.072	0.000	0.000	-0.003	0
0.572	0.572	0.574	0.573	0.001	0.002	0.338	0.303	3.030	1
0.978	1.006	0.98	0.988	0.016	0.016	0.753	0.676	6.757	2
1.306	1.292	1.278	1.292	0.014	0.011	1.057	0.948	9.485	3
1.376	1.368	1.342	1.362	0.018	0.013	1.127	1.011	10.113	4
					0.114				

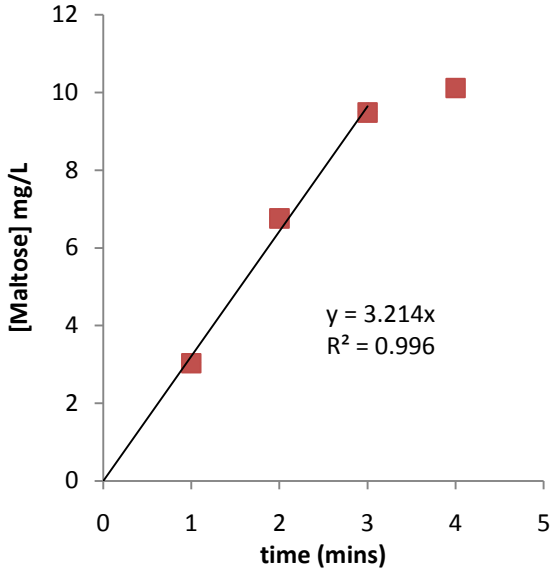

Figure 1.9.4: The rate of release of Maltose from starch hydrolysis by *B. licheniformis* amylase when using 5 U/ mg of the enzyme.

$$Amylaseactivity = \frac{3.2142(mg.L^{-1}.min^{-1})\ x\ 3}{1\ (mg.L^{-1})} = 9.64\ (U.mg^{-1}\ protein)$$

Table 1.9.5: Starch standards for the Starch-Iodine assay

[starch] mg/L	A580	A580	A580	Average absorbance	standard deviation	blank corrected
0	0.045	0.045	0.041	0.044	0.002	0.000
2	0.154	0.154	0.158	0.155	0.002	0.111
4	0.309	0.305	0.304	0.306	0.003	0.262
6	0.391	0.398	0.406	0.398	0.008	0.354
8	0.513	0.518	0.518	0.516	0.003	0.472
10	0.668	0.666	0.666	0.667	0.001	0.623

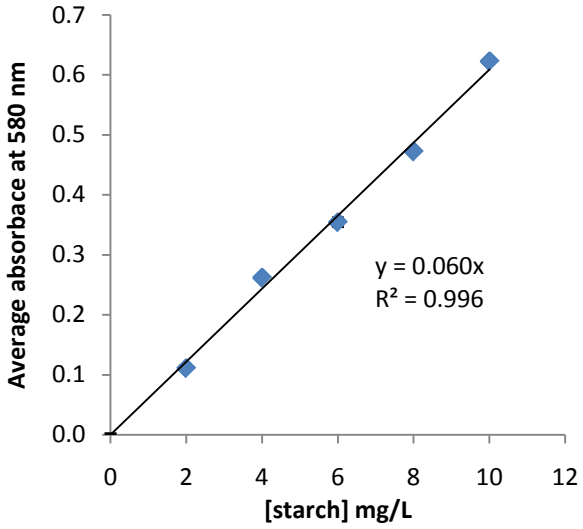

Figure 1.9.5: Starch standard curve used with the Starch-Iodine assay for determination of amylase activities of commercial amylase from *B. licheniformis.*

Table 1.9.6: The starch hydrolysis profile used for determination of the activity of commercial amylase from *B .licheniformis* using the Starch-Iodine assay and 1U/ mg of the enzyme

Given unit: 1 U/mL									
A580	A580	A580	Average absorbance	Standard deviation	relative error	blank corrected	[maltose] mg/L	x dilution factor	Time (mins)
0.254	0.274	0.264	0.264	0.010	0.038	0.000	0.000	0.000	0
0.272	0.270	0.262	0.268	0.005	0.020	0.004	0.004	0.036	1
0.280	0.294	0.278	0.284	0.009	0.031	0.020	0.018	0.179	2
0.312	0.318	0.320	0.317	0.004	0.013	0.053	0.047	0.473	3
0.350	0.350	0.342	0.347	0.005	0.013	0.083	0.075	0.748	4
0.386	0.378	0.372	0.379	0.007	0.019	0.115	0.103	1.029	5
					0.133				

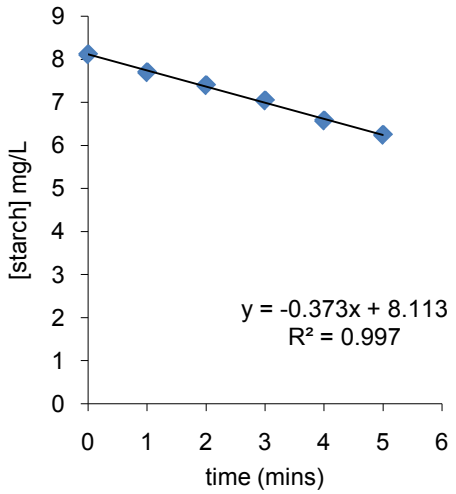

Figure 1.9.6: The rate of hydrolysis of starch by *B. licheniformis* amylase when using 1U/ mg of the enzyme.

$$Amylaseactivity = \frac{0.3731(mg.L^{-1}.min^{-1})\ x\ 3}{1\ (mg.L^{-1})} = 1.14\ (U.mg^{-1}\ protein)$$

Table 1.9.7: The starch hydrolysis profile used for determination of the activity of commercial amylase from *B .licheniformis* using the Starch-Iodine assay with 5 U/ mg of the enzyme

Given unit: 5 U/mL									
A580	A580	A580	Average absorbance	standard deviation	relative error	blank corrected	[maltose] mg/L	x dilution factor	Time (mins)
0.538	0.539	0.539	0.539	0.001	0.001	0.495	8.11	0	0.538
0.378	0.366	0.378	0.374	0.007	0.019	0.330	5.41	1	0.378
0.230	0.242	0.240	0.237	0.006	0.027	0.193	3.17	2	0.230
0.127	0.146	0.144	0.139	0.010	0.075	0.095	1.56	3	0.127
0.093	0.095	0.087	0.092	0.004	0.045	0.048	0.78	4	0.093
0.075	0.075	0.077	0.076	0.001	0.015	0.032	0.52	5	0.075
					0.182				

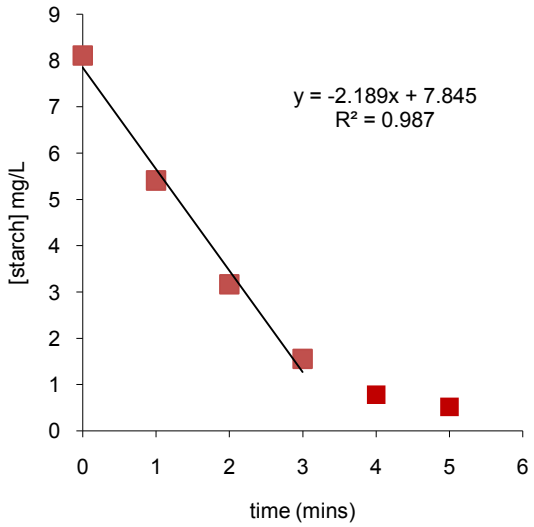

Figure 1.9.7: The rate of hydrolysis of starch by *B. licheniformis* amylase when using 5U/ mg of the enzyme.

$$Amylaseactivity = \frac{2.1896(mg.L^{-1}.min^{-1})\ x\ 3}{1\ (mg.L^{-1})} = 6.57\ (U.mg^{-1}\ protein)$$

Table 1.9.8: The starch hydrolysis profile used for determination of the activity of commercial amylase from *B .licheniformis* using the Starch-Iodine assay and 10 U/ mg of the enzyme

Given unit: 10 U/mL									
A580	A580	A580	Average absorbance	standard deviation	relative error	blank corrected	[maltose] mg/L	x dilution factor	Time (mins)
0.534	0.546	0.537	0.539	0.006	0.012	0.495	8.11	0	0.534
0.220	0.231	0.217	0.223	0.007	0.033	0.179	2.93	1	0.22
0.076	0.087	0.079	0.081	0.006	0.070	0.037	0.60	2	0.076
0.060	0.051	0.051	0.054	0.005	0.096	0.010	0.16	3	0.06
0.058	0.050	0.051	0.053	0.004	0.082	0.009	0.15	4	0.058
0.059	0.052	0.054	0.055	0.004	0.066	0.011	0.18	5	0.059
					0.359				

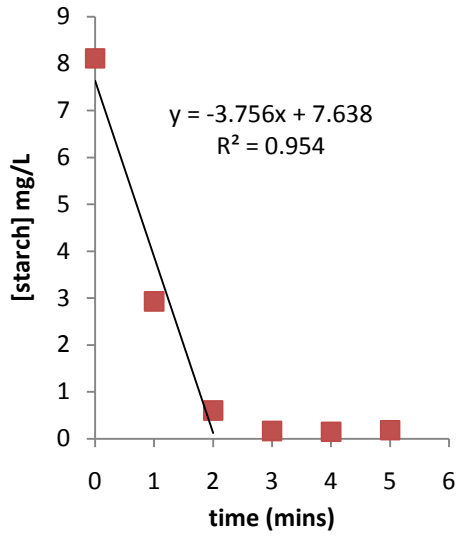

Figure 1.9.8: The rate of hydrolysis of starch by *B. licheniformis* amylase when using 10 U/ mg of the enzyme.

$$Amylaseactivity = \frac{3.7568(mg.L^{-1}.min^{-1})\ x\ 3}{1\ (mg.L^{-1})} = 11.27\ (U.mg^{-1}\ protein)$$

Table 1.9.9: The starch hydrolysis profile used for determination of the activity of commercial amylase from *B .licheniformis* using the Starch-Iodine assay and 10 U/ mg of the enzyme

Given unit: 10 U/mL									
A575	A575	A575	Average absorbance	standard deviation	relative error	blank corrected	[maltose] mg/L	x dilution factor	Time (mins)
0.252	0.234	0.218	0.235	0.017	0.072	0.000	0.000	-0.003	0
0.572	0.572	0.574	0.573	0.001	0.002	0.338	0.303	3.030	1
0.978	1.006	0.98	0.988	0.016	0.016	0.753	0.676	6.757	2
1.306	1.292	1.278	1.292	0.014	0.011	1.057	0.948	9.485	3
1.376	1.368	1.342	1.362	0.018	0.013	1.127	1.011	10.113	4
					0.114				

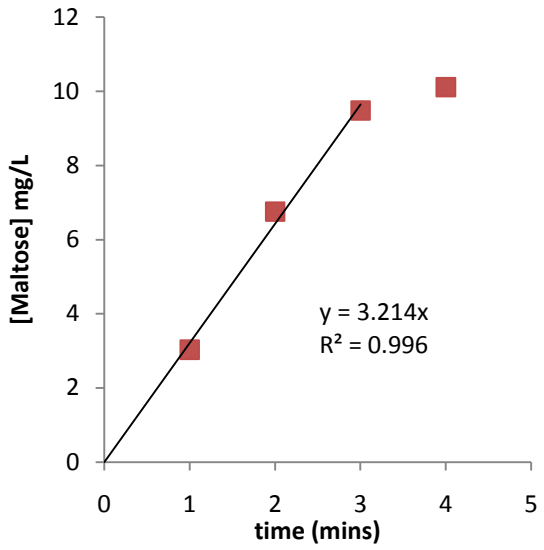

Figure 1.9.9: The rate of release of Maltose from hydrolysis by *B. licheniformis* amylase when using 5 U/ mg of the enzyme.

Table 1.9.10: The BSA standards used to determine the total protein concentration in *B. halodurans* Alk36 culture supernatant

OD1	OD2	OD3	average	error	blank corrected	[BSA] (mg/L)
0.841	0.873	0.853	0.856	0.016	0.000	0
0.971	0.981	0.989	0.980	0.009	0.124	20
1.039	1.093	1.079	1.070	0.028	0.214	40
1.159	1.165	1.204	1.176	0.024	0.320	60
1.287	1.281	1.289	1.286	0.004	0.430	80
1.295	1.304	1.326	1.308	0.016	0.452	100

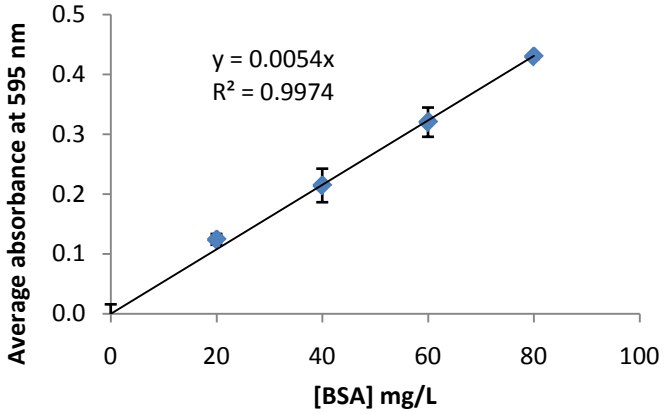

Figure 1.9.11: The BSA standard curve to determine the total protein concentration in *B. halodurans* Alk36 culture supernatant.

Table 1.9.11: The total protein concentration in *B. halodurans* Alk36 culture supernatant

OD1	OD2	OD3	average	error	blank corrected	[protein] (mg/L)	stdev
1.262	1.264	1.253	1.260	0.006	0.404	75	0.006
1.267	1.255	1.259	1.260	0.006	0.404	75	0.006
1.263	1.269	1.265	1.266	0.003	0.410	76	0.003
					average	75	0.00

Table 1.9.12: The glucose release profile used for determination of the activity of amylase from *B .halodurans Alk36* using the DNS assay

A575	A575	A575	average absorbance	standard deviation	blank corrected	Time (mins)	[glucose] g/L
0.065	0.065	0.062	0.064	0.002	0.000	0	0.00
0.247	0.249	0.248	0.248	0.001	0.184	3	0.27
0.303	0.301	0.296	0.300	0.004	0.236	6	0.34
0.328	0.327	0.334	0.330	0.004	0.266	9	0.39
0.362	0.366	0.223	0.317	0.081	0.253	12	0.37
0.383	0.386	0.381	0.383	0.003	0.319	15	0.46
0.390	0.379	0.390	0.386	0.006	0.322	18	0.47
0.420	0.399	0.402	0.407	0.011	0.343	21	0.50
0.391	0.391	0.388	0.390	0.002	0.326	24	0.47
0.408	0.415	0.415	0.413	0.004	0.349	27	0.51
0.404	0.41	0.427	0.414	0.012	0.350	30	0.51

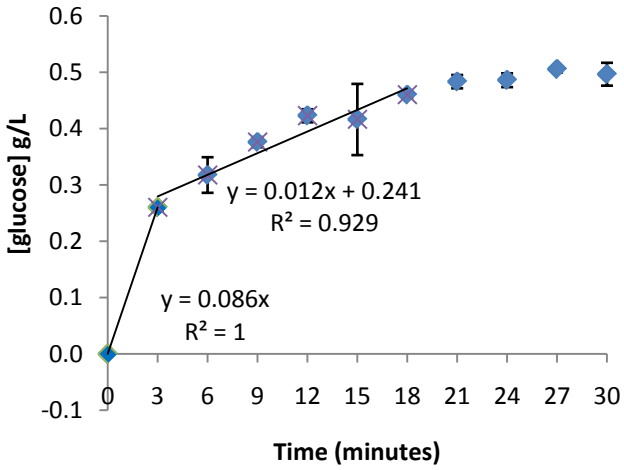

Figure 1.9.12: The rate of release of glucose from starch hydrolysis by amylase from *B .halodurans Alk36*.

$$Amylaseactivity = \frac{0.0867(mg.L^{-1}.min^{-1})\ x\ 10\ (dilution\ factor) x\ 1000\ \left(\frac{mg}{g}\right)}{75\ (mg.L^{-1})} = 11.56\ (U.mg^{-1}\ protein)$$

where 1U is equivalent to one mg of glucose released per minute.

Table 1.9.13: The starch hydrolysis profile used for determination of the activity of amylase from *B .halodurans Alk36* using the Starch-Iodine assay

A580	A580	A580	average	standard deviation	relative error	blank corrected	[starch] g/L	Time
1.293	1.259	1.256	1.269	0.021	0.016	1.229	9.662	0
1.015	1.068	1.043	1.042	0.027	0.025	0.951	8.023	3
0.833	0.821	0.848	0.834	0.014	0.016	0.769	6.523	6
0.677	0.680	0.666	0.674	0.007	0.011	0.613	5.123	9
0.525	0.511	0.507	0.514	0.009	0.018	0.461	3.900	12
0.389	0.370	0.360	0.373	0.015	0.039	0.325	2.769	15
0.293	0.295	0.289	0.292	0.003	0.010	0.229	2.223	18
0.255	0.260	0.250	0.255	0.005	0.020	0.191	1.923	21
0.214	0.209	0.206	0.210	0.004	0.019	0.150	1.585	24
0.192	0.188	0.184	0.188	0.004	0.021	0.128	1.415	27
0.171	0.168	0.165	0.168	0.003	0.018	0.107	1.269	30
					0.215			

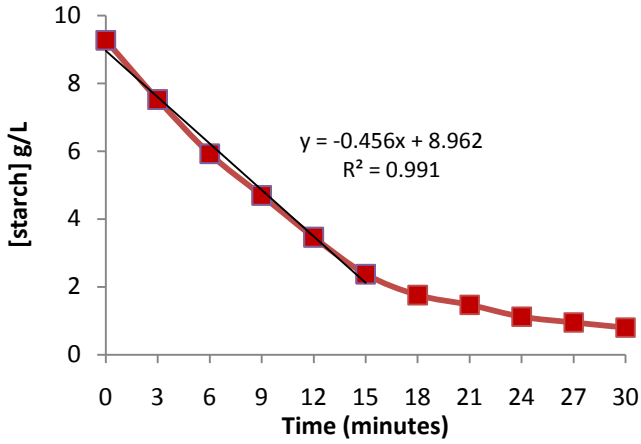

Figure 1.9.13: The rate of starch hydrolysis by *B. halodurans Alk36*amylase using the starch-iodine assay

$$Amylaseactivity = \frac{0.456(mg.L^{-1}.min^{-1})\ x\ 10\ (dilution\ factor) x\ \ 1000\ (\frac{mg}{g})}{75\ (mg.L^{-1})} = 60.8\ (U.mg^{-1}\ protein)$$

where 1U is equivalent to mg of starch hydrolysed per minute.

Appendix 1.10: Production of amylases in relation to growth cycle of *B. halodurans Alk36*

Table 1.10.1: BSA standards for the Bradford assay

A595	A595	A595	Average absorbance	standard deviation	blank corrected	[BSA] (mg/L)
0.607	0.608	0.605	0.607	0.002	0.009	0
0.693	0.692	0.687	0.691	0.003	0.093	2
0.759	0.762	0.761	0.761	0.002	0.163	4
0.861	0.851	0.847	0.853	0.007	0.255	6
0.839	0.962	0.912	0.904	0.062	0.306	8
0.959	0.965	0.973	0.966	0.007	0.368	10

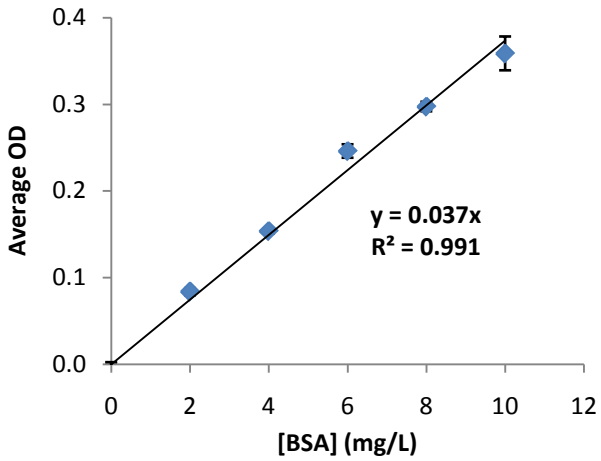

Figure 1.10.1: The BSA standard curve used with the Bradford assay.

Table 1.10.2: Total protein concentration in *B. halodurans* Alk36 culture supernatant at different time points during growth

A595	A595	A595	Average absorbance	standard deviation	blank corrected	[protein] (mg/L)	Dilution factor	X dilution factor	sample time
0.638	0.635	0.636	0.636	0.002	0.038	0.78	20	15.69	0
0.704	0.709	0.705	0.706	0.003	0.108	2.65	20	52.97	9
0.728	0.725	0.726	0.726	0.002	0.128	3.19	20	63.85	12
0.769	0.764	0.767	0.767	0.003	0.169	4.27	20	85.43	15
0.725	0.726	0.721	0.724	0.003	0.126	4.65	20	93.10	18
0.814	0.811	0.81	0.812	0.002	0.214	5.48	1	109.51	21

Table 1.10.3: Starch standards used for the determination of amylase activity in *B. halodurans* Alk36 culture supernatant grown in EnBase® medium

A580	A580	A580	average	standard deviation	black corrected	[starch]
0.061	0.062	0.065	0.063	0.002	0.000	0
0.353	0.338	0.312	0.334	0.021	0.271	0.2
0.555	0.472	0.498	0.508	0.042	0.445	0.4
0.755	0.668	0.680	0.701	0.047	0.638	0.6
0.943	0.915	0.840	0.899	0.053	0.836	0.8
1.120	1.022	1.043	1.062	0.052	0.999	1.0

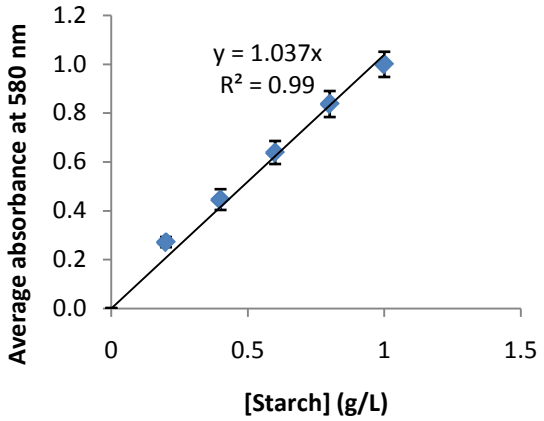

Figure 1.10.2: Starch standard curve used for the determination of amylase activity of *B. halodurans* Alk36 culture supernatant.

Table 1.10.4: The rate of starch hydrolysis upon hydrolysis by amylases from*B. halodurans* Alk36 culture supernatant at exponential phase

A580	A580	A580	Average absorbance	standard deviation	Relative error (%)	blank corrected	[starch] (g/L)	Time (h)
1.456	1.518	1.510	1.495	0.034	2.27	1.432	13.81	0
1.249	1.268	1.268	1.262	0.011	0.87	1.199	11.56	1
1.056	1.025	1.035	1.039	0.016	1.54	0.976	9.41	2
0.918	0.913	0.906	0.912	0.006	0.66	0.849	8.19	3
0.488	0.489	0.485	0.487	0.002	0.41	0.424	4.09	5

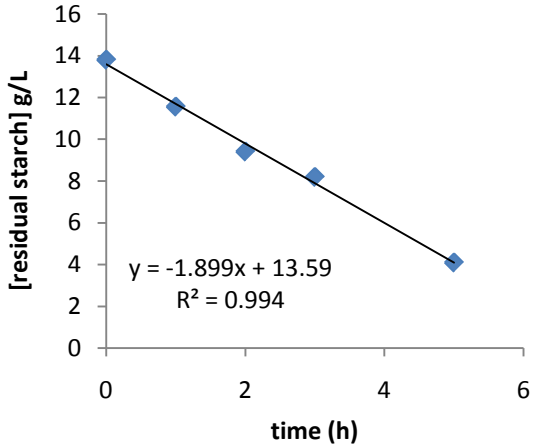

Figure 1.10.3: The rate of starch hydrolysis by *B. halodurans Alk36* amylase from exponential phase culture supernatant.

$$Amylaseactivity = \frac{1.8997(g.L^{-1}.h^{-1})\ x\ 5\ (dilution\ factor) x\ \ 10^3\ (mg/g)}{60\ (mins)\ x\ 63.85\ (mg.L^{-1}\ protein)} = 2.48\ \left(\frac{U}{mg} protein\right)$$

where 1U is equivalent to mg of starch hydrolysed per minute.

Table 1.10.5: Amylase activity of *B. halodurans* Alk36 culture supernatant at stationary phase

A580	A580	A580	Average absorbance	standard deviation	Relative error (%)	blank corrected	[starch]	time
1.197	1.198	1.190	1.195	0.004	0.335	1.136	10.95	0
1.035	1.038	1.033	1.035	0.003	0.290	0.976	9.41	2
0.806	0.807	0.802	0.805	0.003	0.373	0.746	7.19	4
0.706	0.700	0.704	0.703	0.003	0.427	0.644	6.21	5
0.589	0.595	0.593	0.592	0.003	0.507	0.533	5.14	6

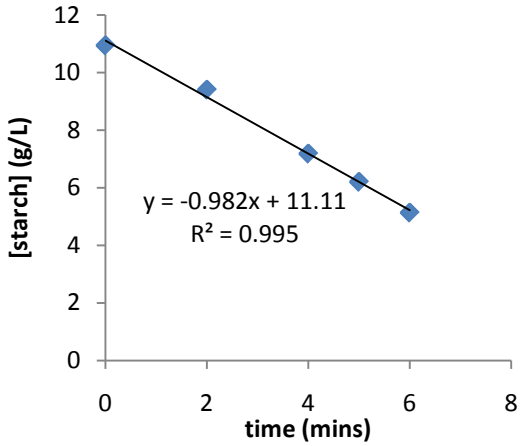

Figure 1.10.6: The rate of starch hydrolysis by *B. halodurans Alk36* amylase from stationary phase culture supernatant.

$$Amylaseactivity = \frac{0.982\ (g.L^{-1}.min^{-1})\ x\ 5\ (dilution\ factor) x\ 10^3\ (mg/g)}{110.15\ (mg.L^{-1}\ protein)} = 44.57\ (U.mg^{-1}\ protein)$$

where 1u is equivalent to mg of starch hydrolysed per minute.

Appendix 2: Optimisation of growth conditions

Appendix 2.1: Determination of the oxygen transfer rates in shake flasks and multiwell plates.

The sulphite oxidation method was used for the determination of the oxygen transfer rate in shake flasks and multiwell plates. Reagents and method used are described in Section 3.2.2.1.

The rate of oxidation of sulphite was determined by reacting the unoxidisedsulphite with iodine solution and then titrating the unreacted iodine with sodium thiosulphate solution. The amount of sodium thiosulphate used was used to determine the amount of Iodine that did not react with the sulphite solution and hence the amount of oxidized sulphite since the amount of sulphite added in the solution was known. The following stochiometry equations were used.

$$SO_3^{2-} + \frac{1}{2}O_2 \rightarrow \ SO_4^{2-} + \ H^+ \qquad Equation\ 1.1$$

$$I_2 + \ SO_3^{2-} + \ H_2O \ \rightarrow 2I^- + SO_4^{2-} + \ 2H^+ \qquad Equation\ 1.2$$

$$I_2 + \ 2S_2O_3^{2-} \ \rightarrow 2I + S_4O_6^{2-} \qquad Equation\ 1.3$$

The amount of thiosulphate used together with the calculated amounts of oxidized sulphite is shown in Table 2.1.1 and Table 2.1.2.

Table 2.1.1: Determination of the amount of sulphite that was oxidized in multiwell plates at different shaking frequencies and different filling volumes.

2 mL filling volume and 200 rpm shaking frequency										
Time	Volume of $Na_2S_2O_3$ used					A (mMols)	B (mMols)	C (mMols)	D (mMols)	relative standard deviation (%)
	vol1	vol2	vol3	Average	standard deviation					
0	20.8	20.4	20.7	20.6	1.009	1.032	0.516	0.984	0.000	0.025
4	22.1	22.2	21.9	22.1	0.692	1.103	0.552	0.948	0.036	0.017
8	24.0	23.8	24.2	24.0	0.833	1.200	0.600	0.900	0.084	0.021
11	25.5	25.1	25.7	25.4	1.201	1.272	0.636	0.864	0.120	0.030
3 mL filling volume and 200 rpm shaking frequency										
Time	Volume of $Na_2S_2O_3$ used					A (mMols)	B (mMols)	C (mMols)	D (mMols)	relative error (%)
	vol1	vol2	vol3	Average	Standard deviation					
0	20.8	20.4	20.7	20.6	1.009	1.032	0.516	0.984	0.000	0.025
4	21.7	21.4	21.2	21.4	1.174	1.072	0.536	0.964	0.020	0.029
8	22.4	22.8	22.5	22.6	0.922	1.128	0.564	0.936	0.048	0.023
11	23.2	23.0	23	23.1	0.433	1.155	0.578	0.923	0.062	0.011
2 mL filling volume and 250 rpm shaking frequency										
Time	Volume of $Na_2S_2O_3$ used					A (mMols)	B (mMols)	C (mMols)	D (mMols)	relative error (%)
	vol1	vol2	vol3	Average	Standard deviation					
0	20.8	20.4	20.7	20.6	1.009	1.032	0.516	0.984	0.000	0.025
4	23.2	22.6	22.8	22.9	1.336	1.143	0.572	0.928	0.056	0.033
8	26.0	25.6	25.8	25.8	0.775	1.290	0.645	0.855	0.129	0.019
11	27.0	27.6	27.3	27.3	1.099	1.365	0.683	0.818	0.167	0.027

A: Amount of $Na_2S_2O_3^{2-}$ reacted with the iodine solution, **B**: Amount of I_2 that reacted with thiosulphate solution

C: Amount of I2 that reacted with sulphite solution, **D**: Amount of sulphite that reacted with oxygen

Continuation of Table 2.1.1

Table 2.1.1: Determination of the amount of sulphite that was oxidized in multiwell plates at different shaking frequencies and different filling volumes.

3 mL filling volume and 250 rpm shaking frequency										
Time	Volume of $Na_2S_2O_3$ used					A (mMols)	B (mMols)	C (mMols)	D (mMols)	relative error (%)
	vol1	vol2	vol3	Average	Standard deviation					
0	20.8	20.4	20.7	20.6	1.009	1.032	0.516	0.984	0.000	0.025
4	22.0	22.1	22.2	22.1	0.452	1.105	0.553	0.948	0.037	0.011
8	23.4	24.2	24.0	23.9	1.744	1.193	0.597	0.903	0.081	0.044
11	24.6	25.4	25.3	25.1	1.737	1.255	0.628	0.873	0.112	0.043
2 mL filling volume and 300 rpm shaking frequency										
Time	Volume of $Na_2S_2O_3$ used					A (mMols)	B (mMols)	C (mMols)	D (mMols)	Relative error (%)
	vol1	vol2	vol3	Average	Standard deviation					
0	18.0	18.1	18.7	18.3	2.073	0.913	0.457	1.043	0.000	0.052
4	21.5	21.4	22.0	21.6	1.486	1.082	0.541	0.959	0.084	0.037
8	24.6	23.4	24.3	24.1	2.591	1.205	0.603	0.898	0.146	0.065
11	27.1	27.5	27.7	27.4	1.114	1.372	0.686	0.814	0.229	0.028
3 mL filling volume and 200 rpm shaking frequency										
Time	Volume of $Na_2S_2O_3$ used					A (mMols)	B (mMols)	C (mMols)	D (mMols)	relative standard deviation (%)
	vol1	vol2	vol3	Average	Standard deviation					
0	18.0	18.1	18.8	18.3	2.382	0.915	0.458	1.043	0.000	0.060
4	20.0	20.3	20.8	20.4	1.984	1.018	0.509	0.991	0.052	0.050
8	22.2	22.7	22.5	22.5	1.120	1.123	0.562	0.938	0.105	0.028
11	24.9	24.2	24.5	24.5	1.431	1.227	0.613	0.887	0.156	0.036

A: Amount of $Na_2S_2O_3^{2-}$ reacted with the iodine solution, **B**: Amount of I_2 that reacted with thiosulphate solution

C: Amount of I2 that reacted with sulphite solution, **D**: Amount of sulphite that reacted with oxygen

The rate of oxidation of sulphite was determined from the slope of the linear plots obtained from plotting the amount of sulphite that was oxidized versus time as illustrated in Figure 2.1.

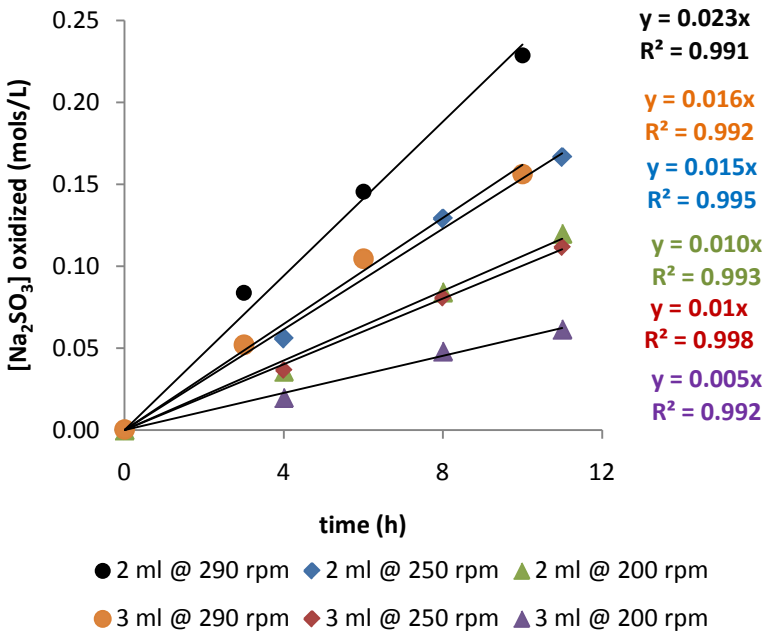

Figure 2.1.1: The rate of oxidation of sulphite solution by oxygen in 24-well multiwell plates at different filling volumes and shaking frequencies.Thevalues presented were calculated from the average of the triplicate and the standard deviation was ≤ 0.06.

The rate of oxidation of sulphite was used to calculate the OTR and hence the volumetric mass transfer coefficient $k_L a$ using the following equations:

$$OTR = \frac{Rate of oxidation of sulphite}{2} \quad Equation\ 1.4$$

$$\mathrm{OTR} = \mathrm{kLa}\ (\mathrm{C_{sat}} - \mathrm{C_L}) = k_L a . L_{O_2} . p_g since C_L \approx 0 \qquad Equation\ 1.5$$

Table 2.1.2: Determination of the amount of sulphite that was oxidized in shake flasks at 200 rpm shaking frequencies and different filling volumes.

100 mL filling volume										
time	Volume of $Na_2S_2O_3$ used					A (mMols)	B (mMols)	C (mMols)	D (mMols)	relative error (%)
	vol1	vol2	vol3	average	Standard deviation					
0	16	16.4	20.7	15.6	1.009	1.032	0.516	0.984	0.000	0.368
6	21.6	22.1	21.2	22.1	0.452	1.105	0.553	0.948	0.037	0.052
12	28.3	28.2	28.0	23.9	1.744	1.193	0.597	0.903	0.081	0.014
24	36.5	36.3	26.8	25.1	1.737	1.255	0.628	0.873	0.112	0.417
200 mL filling volume										
time	Volume of $Na_2S_2O_3$ used					A (mMols)	B (mMols)	C (mMols)	D (mMols)	relative error (%)
	vol1	vol2	vol3	average	Standard deviation					
0	18.0	18.1	18.7	18.3	2.073	0.913	0.457	1.043	0.000	0.041
4	21.5	21.4	22.0	21.6	1.486	1.082	0.541	0.959	0.084	0.035
8	24.6	23.4	24.3	24.1	2.591	1.205	0.603	0.898	0.146	0.118
11	27.1	27.5	27.7	27.4	1.114	1.372	0.686	0.814	0.229	0.009

A: Amount of $Na_2S_2O_3^{2-}$ reacted with the iodine solution, **B**: Amount of I_2 that reacted with thiosulphate solution

C: Amount of I2 that reacted with sulphite solution, **D**: Amount of sulphite that reacted with oxygen

Similarly to the multiwell plates, the rate of oxidation of sulphite was determined from the slope of the linear plots obtained from plotting the amount of sulphite that was oxidized versus time as illustrated in Figure 2.1.2.

The rate of oxidation of sulphite was used to calculate the OTR and hence the volumetric mass transfer coefficient k_La using the following Equation 1.4 and 1.5.

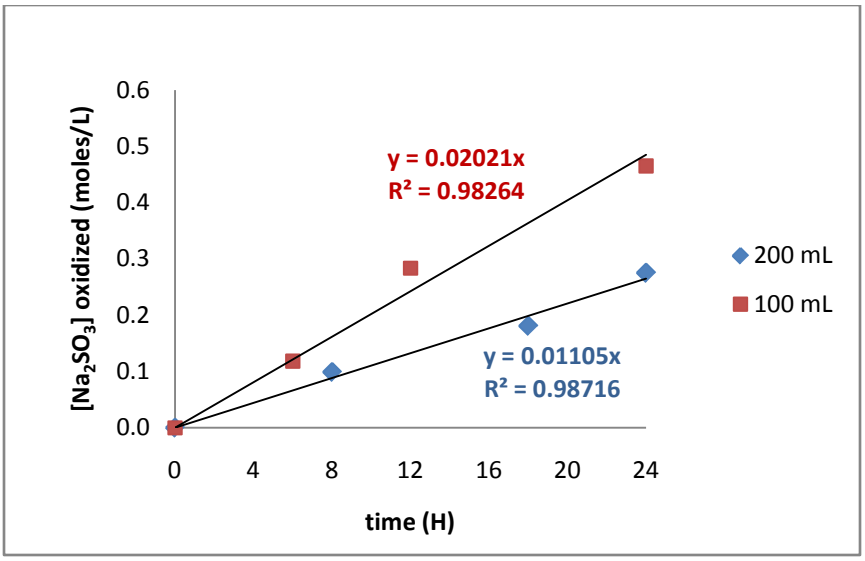

Figure 2.1.2: The rate of oxidation of sulphite solution by oxygen in shake flasks at different filling volumes 200 rpm shaking frequency.

Appendix 2.2: Determination of optimal pH for growth of *B. halodurans Alk36*

Bacillus halodurans Alk36 was cultured in EnBase® medium buffered at different pH as described in Section 3.2.2.2. The p\optical densities and pH of the culture was measured at different intervals throughout growth.

Table 2.2.1: Growth of *B. halodurans Alk36* in shake flasks using EnBase medium at different pH

time (hrs)	pH	pH	average pH	Absolute error	$OD_{600\ nm}$	$OD_{600\ nm}$	AVERAGE $OD_{600\ nm}$	Absolute error	Relative error	Ln OD	error	growth rate	biomass
0	7.10	7.13	7.11	0.02	0.112	0.104	0.108	0.005	0.047	-2.226	0.105		0.042
3	7.04	6.98	7.01	0.04	0.261	0.245	0.253	0.011	0.045	-1.374	0.061		0.097
6	6.96	6.81	6.88	0.11	0.631	0.604	0.617	0.019	0.030	-0.482	0.014		0.238
9	6.93	6.68	6.81	0.18	1.425	1.353	1.389	0.051	0.036	0.329	0.012	0.28	0.535
12	7.04	6.91	6.98	0.09	2.500	2.163	2.332	0.238	0.102	0.847	0.086		0.898
15	6.88	6.86	6.87	0.02	2.960	2.853	2.907	0.075	0.026	1.067	0.028		1.119
24	6.80	6.34	6.57	0.33	3.915	3.910	3.913	0.004	0.001	1.364	0.001		1.506
time	average pH	average pH	average	standard deviation	OD1	OD2	Average OD	Absolute error	Relative error	Ln OD	Error	growth rate	biomass
0	7.96	7.89	7.93	0.05	0.108	0.121	0.114	0.009	0.081	-2.172	0.175		0.044
3	7.58	7.52	7.55	0.05	0.259	0.228	0.243	0.022	0.089	-1.414	0.125		0.094
6	7.82	7.56	7.69	0.19	0.811	0.669	0.740	0.100	0.136	-0.302	0.041		0.285
9	7.63	7.58	7.60	0.04	1.545	1.315	1.430	0.163	0.114	0.358	0.041	0.28	0.551
12	7.76	7.49	7.62	0.19	3.150	3.195	3.173	0.032	0.010	1.155	0.012		1.221
15	7.83	7.35	7.59	0.34	4.230	4.570	4.400	0.240	0.055	1.482	0.081		1.694
24	7.30	7.05	7.17	0.17	4.650	4.715	4.683	0.046	0.010	1.544	0.015		1.803

Continuation of Table 2.2.1...

Table 2.2.1: Growth of *B. halodurans Alk36* in shake flasks using EnBase medium at different pH

time (hrs)	pH	pH	average pH	Absolute error	OD1	OD2	Average OD	Absolute error	Relative error	Ln OD	LN OD error	growth rate	biomass
0	8.52	8.55	8.53	0.02	0.104	0.104	0.104	0.000	0.000	-2.263	0.000		0.040
3	8.42	8.29	8.36	0.09	0.227	0.272	0.250	0.032	0.128	-1.388	0.177		0.096
6	8.29	8.53	8.41	0.17	0.753	0.701	0.727	0.037	0.051	-0.319	0.016		0.280
9	8.42	8.36	8.39	0.04	1.515	1.420	1.468	0.067	0.046	0.384	0.018	0.294	0.565
12	8.01	8.21	8.11	0.14	2.900	2.760	2.830	0.099	0.035	1.040	0.036		1.090
15	7.90	8.11	8.01	0.15	4.530	4.313	4.422	0.153	0.035	1.487	0.052		1.702
24	7.31	7.36	7.34	0.04	4.315	4.267	4.291	0.034	0.008	1.456	0.012		1.652
time (hrs)	pH	pH	average pH	Absolute error	OD1	OD2	Average OD	Absolute error	Relative error	Ln OD	Ln OD error	growth rate	biomass
0	9.00	9.00	9.00	0.00	0.103	0.099	0.101	0.003	0.030	-2.294	0.070		0.039
3	9.11	9.10	9.11	0.01	0.151	0.125	0.138	0.018	0.131	-1.982	0.259		0.053
6	9.02	9.08	9.05	0.04	0.241	0.225	0.233	0.012	0.050	-1.457	0.072		0.090
9	8.94	8.98	8.96	0.03	0.490	0.455	0.473	0.025	0.052	-0.749	0.039	0.195	0.182
12	8.81	8.84	8.83	0.02	1.035	0.788	0.911	0.175	0.192	-0.093	0.018		0.351
15	8.72	8.72	8.72	0.00	1.500	1.347	1.423	0.108	0.076	0.353	0.027		0.548
24	8.57	8.57	8.57	0.00	2.585	2.303	2.444	0.199	0.081	0.894	0.073		0.941

Table 2.2.2: Growth of *B .halodurans Alk36* in the Sixfors reactors using EnBase® medium at different pH.

time (hrs)	OD1	OD2	OD3	Average OD	standard deviation	Ln OD	PH
0	0.245	0.243	0.247	0.245	0.002	-1.406	11.11
3	0.186	0.182	0.188	0.185	0.003	-1.686	11.18
6	0.177	0.175	0.170	0.174	0.004	-1.749	11.28
9	0.179	0.176	0.177	0.177	0.002	-1.730	11.35
12	0.151	0.156	0.154	0.154	0.003	-1.873	11.37
15	0.194	0.198	0.196	0.196	0.002	-1.630	11.40
24	0.280	0.277	0.278	0.278	0.002	-1.279	11.42
28	0.330	0.336	0.333	0.333	0.003	-1.100	11.40
32	0.702	0.696	0.695	0.698	0.004	-0.360	11.42
time (hrs)	OD1	OD2	OD3	Average OD	standard deviation	Ln OD	PH
0	0.185	0.181	0.188	0.185	0.004	-1.689	10.33
3	0.199	0.202	0.196	0.199	0.003	-1.614	10.07
6	0.170	0.175	0.178	0.174	0.004	-1.747	10.16
9	0.193	0.190	0.187	0.190	0.003	-1.661	10.32
12	0.146	0.142	0.144	0.144	0.002	-1.938	10.36
15	0.156	0.157	0.154	0.156	0.002	-1.860	10.24
24	0.216	0.220	0.225	0.220	0.005	-1.513	10.36
28	0.396	0.397	0.397	0.397	0.001	-0.925	10.37
32	1.410	1.420	1.420	1.417	0.006	0.348	10.37
time (hrs)	OD1	OD2	OD3	Average OD	standard deviation	Ln OD	pH
0	0.189	0.187	0.191	0.189	0.002	-1.666	9.36
3	0.320	0.321	0.321	0.321	0.001	-1.137	9.09
6	0.539	0.535	0.537	0.537	0.002	-0.622	9.14
9	1.380	1.390	1.370	1.380	0.010	0.322	9.25
12	2.500	2.500	2.530	2.510	0.017	0.920	9.27
15	4.720	4.680	4.640	4.680	0.040	1.543	9.12
24	9.280	9.310	9.320	9.303	0.021	2.230	9.20
28	13.300	12.700	13.100	13.033	0.306	2.568	9.21
32	14.400	14.200	14.300	14.300	0.100	2.660	9.19

Continuation of Table 2.2.2...

Table 2.2.2: Growth of *B. halodurans Alk36* in the Sixfors reactors using EnBase® medium at different pH

time (hrs)	OD1	OD2	OD3	Average OD	standard deviation	Ln OD	pH
0	0.186	0.178	0.195	0.186	0.009	-1.680	8.82
3	0.511	0.505	0.509	0.508	0.003	-0.677	8.41
6	1.550	1.500	1.560	1.537	0.032	0.430	8.23
9	3.130	3.160	3.150	3.147	0.015	1.146	8.45
12	6.690	6.700	6.700	6.697	0.006	1.902	8.31
15	8.920	8.940	8.960	8.940	0.020	2.191	8.18
24	15.320	15.300	15.450	15.357	0.081	2.732	8.09
28	20.500	20.300	20.600	20.467	0.153	3.019	8.65
32	15.070	15.100	15.100	15.090	0.017	2.714	8.47
time (hrs)	OD1	OD2	OD3	Average OD	standard deviation	Ln OD	pH
0	0.220	0.224	0.221	0.222	0.002	-1.507	7.57
3	0.636	0.625	0.628	0.630	0.006	-0.463	7.38
6	2.310	2.290	2.300	2.300	0.010	0.833	7.32
9	3.690	3.650	3.720	3.687	0.035	1.305	7.70
12	6.850	6.900	6.890	6.880	0.026	1.929	7.77
15	9.530	9.510	9.470	9.503	0.031	2.252	7.80
24	17.020	17.060	17.040	17.040	0.020	2.836	7.43
28	15.150	15.170	15.110	15.143	0.031	2.718	7.38
32	11.200	11.100	11.100	11.133	0.058	2.410	7.08

Appendix 2.3: Determination of the optimal temperature for growth of *Bacillus halodurans* Alk36

Bacillus halodurans Alk36 was cultured in EnBase® medium at different temperatures as described in Section 3.2.2.5. The evaporation rate of water, from the shake flasks, was determined enable addition of the evaporated water as described in Section 3.2.2.4.

Table 2.3.1: Evaporation rate of water in shake flasks incubated at different temperatures with 200rpm shaking

Temperature: 30˚C					
weight of flask with water (g)	Weight of flask (g)	Weight of water (g)	Volume of water (mL)	Time (h)	evaporation rate
190.1325	141.8941	48.2384	48.2384	0	0.0661mL/h
190.0173	141.8941	48.1232	48.1232	3	
189.8253	141.8941	47.9312	47.9312	6	66.1µl/h
189.5360	141.8941	47.6419	47.6419	9	
Temperature: 37˚C					
weight of flask with water (g)	Weight of flask (g)	Weight of water (g)	Volume of water (mL)	Time (h)	evaporation rate
189.1050	140.9807	48.1243	48.1243	0	0.111 mL/h
188.8193	140.9807	47.8386	47.8386	3	
188.4957	140.9807	47.5150	47.5150	6	111 µl/h
188.1029	140.9807	47.1222	47.1222	9	
Temperature: 42˚C					
weight of flask with water (g)	Weight of flask (g)	Weight of water (g)	Volume of water (mL)	Time (h)	evaporation rate
193.0475	144.9836	48.0639	48.0639	0	0.113 mL/h
192.5920	144.9836	47.6084	47.6084	3	
192.2629	144.9836	47.2793	47.2793	6	113 µl/h
191.6650	144.9836	46.6814	46.6814	12	

Continuation of Table 2.3.1

Table 2.3.1: Evaporation rate of water in shake flasks incubated at different temperatures with 200rpm shaking

Temperature: 50˚C					
weight of flask with water(g)	Weight of flask(g)	Weight of water(g)	Volume of water (mL)	Time (h)	evaporation rate
250.0000	201.9836	48.0164	48.0164	0	0.2196 mL/h
249.4000	201.9836	47.4164	47.4164	3	
248.8000	201.9836	46.8164	46.8164	5	
248.4000	201.9836	46.4164	46.4164	7	220 µl/h
248.0000	201.9836	46.0164	46.0164	9	
247.4000	201.9836	45.4164	45.4164	12	

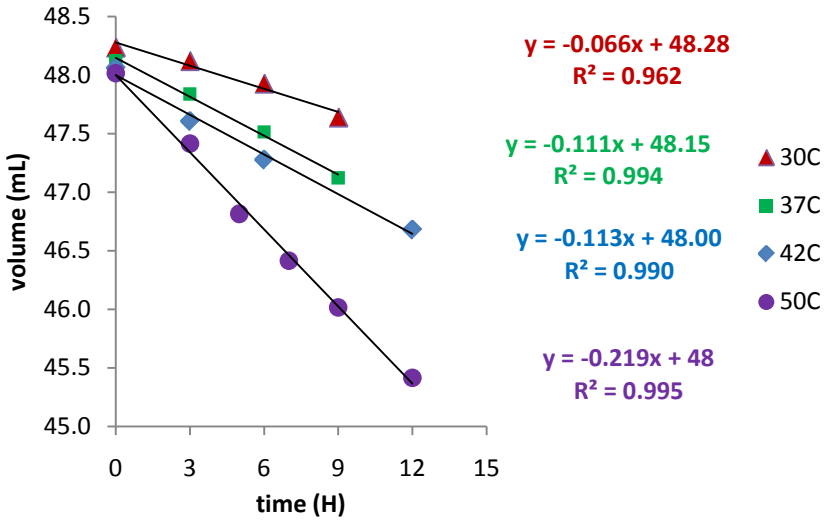

Figure 2.3.1: Evaporation rate of water in shake flasks incubated at different temperatures with 200rpm shaking.

Table 2.3.2: Growth of *B. halodurans Alk36* in shake flasks with EnBase media at 30˚C with 200 rpm shaking

Time	OD1	OD2	average	standard deviation	Relative error	LN OD	Error in Ln OD	pH1	pH2	average pH	Absolute error
0	0.214	0.219	0.217	0.004	0.016	-1.530	0.025	8.64	8.65	8.65	0.007
2	0.372	0.375	0.374	0.002	0.006	-0.985	0.006	8.61	8.61	8.61	0.000
4	0.720	0.840	0.780	0.085	0.109	-0.248	0.027	8.53	8.49	8.51	0.028
6	1.490	1.450	1.470	0.028	0.019	0.385	0.007	8.36	8.35	8.36	0.007
8	2.550	2.490	2.520	0.042	0.017	0.924	0.016	8.10	8.11	8.11	0.007
12	3.170	3.380	3.380	0.148	0.044	1.218	0.054				

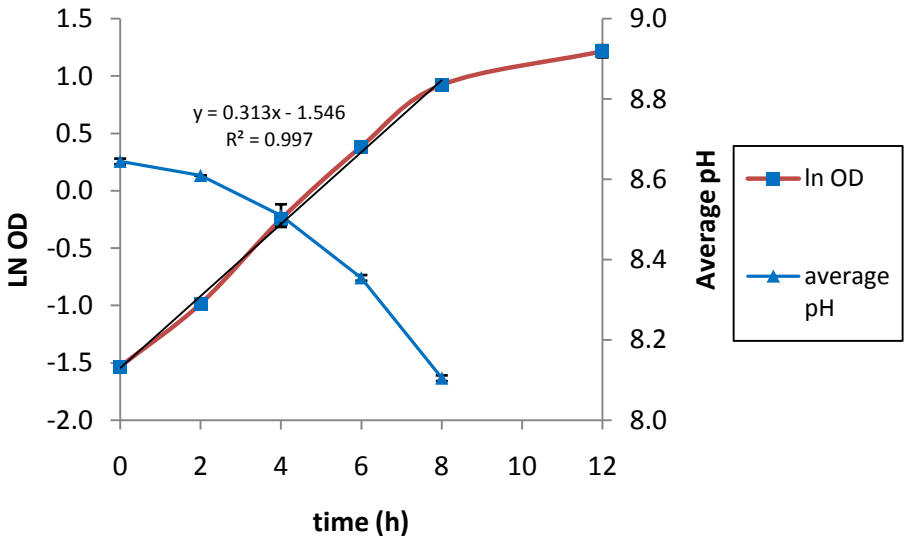

Figure 2.3.2: Growth of *B. halodurans* Alk36 in shake flasks with EnBase media at 30˚C with 200 rpm shaking.

Table 2.3.4: Growth of *B. halodurans Alk36* in shake flasks with EnBase media at 37˚C with 200 rpm shaking

time	OD1	OD2	average	Standard deviation	Relative error	LN OD	Error in Ln OD	PH1	PH2	average PH	standard deviation
0	0.248	0.254	0.251	0.004	0.017	-1.382	0.023	8.64	8.63	8.64	0.007
2	0.501	0.502	0.502	0.001	0.001	-0.690	0.001	8.61	8.61	8.61	0.000
4	1.000	1.030	1.015	0.021	0.021	0.015	0.000	8.42	8.40	8.41	0.014
6	1.690	1.720	1.705	0.021	0.012	0.534	0.007	8.20	8.17	8.19	0.021
8	3.190	3.290	3.240	0.071	0.022	1.176	0.026	8.09	8.10	8.10	0.007
12	3.740	3.860	3.860	0.085	0.022	1.351	0.030				

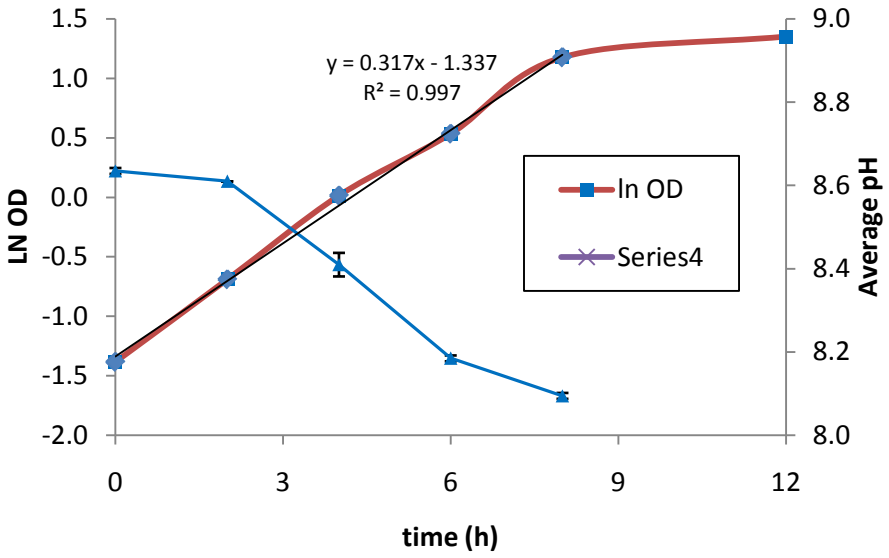

Figure 2.3.3: Growth of *B. halodurans* Alk36 in shake flasks with EnBase media at 37˚C with 200 rpm shaking.

Table 2.3.5: Growth of *B. halodurans Alk36* in shake flasks with EnBase media at 42˚C with 200 rpm shaking

Time	OD1	OD2	OD3	average	Standard deviation	Relative error	Ln OD	PH1	PH2	PH	average PH	standard deviation
0	0.283	0.282	0.279	0.281	0.003	0.010	-1.269	8.59	8.58	8.59	8.59	0.006
2	0.685	0.689	0.690	0.688	0.004	0.005	-0.375	8.52	8.48	8.50	8.50	0.020
4.5	2.050	2.060	2.060	2.055	0.007	0.003	0.720	8.02	8.03	8.01	8.02	0.010
6	3.290	3.260	3.270	3.280	0.014	0.004	1.188	8.41	8.46	8.47	8.45	0.032
8	4.310	4.280	4.230	4.273	0.057	0.013	1.452	8.11	8.10	8.10	8.10	0.006
12	4.53	4.55	4.5	4.527	0.021	0.005	1.510					

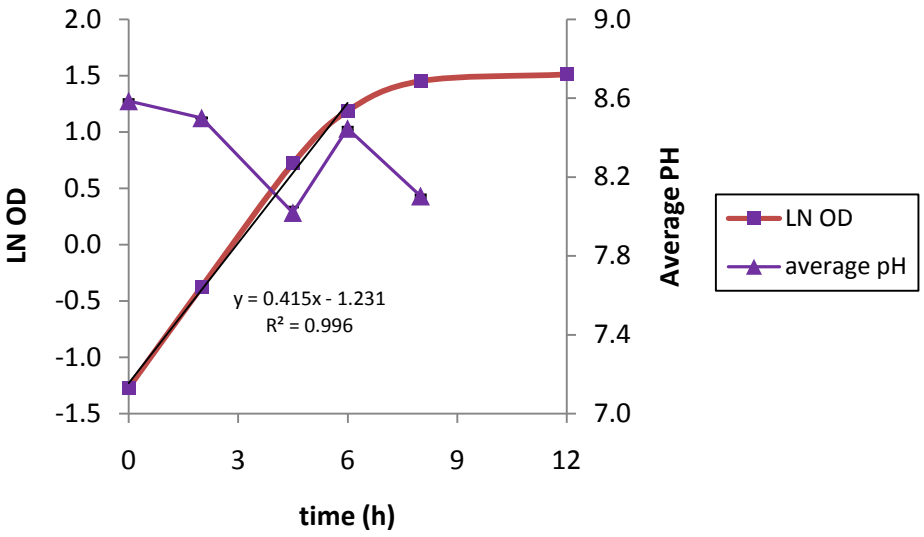

Figure 2.3.4: Growth of *B. halodurans* Alk36 in shake flasks with EnBase media at 42˚C with 200 rpm shaking

Table 2.3.6: Growth of *B. halodurans Alk36* in shake flasks with EnBase media at 45˚C with 200 rpm shaking

Time	OD1	OD2	OD3	average	Standard deviation	Relative error	Ln OD	PH1	PH2	PH3	average PH	standard deviation
0	0.218	0.221	0.219	0.219	0.001	0.003	-1.521	8.59	8.58	8.59	8.59	0.006
2	0.629	0.634	0.630	0.630	0.001	0.001	-0.463	8.52	8.48	8.50	8.50	0.020
4.5	1.840	1.860	1.820	1.830	0.014	0.008	0.604	8.02	8.03	8.01	8.02	0.010
6	3.240	3.200	3.220	3.230	0.014	0.004	1.172	8.41	8.46	8.47	8.45	0.032
8	3.890	3.860	3.980	3.910	0.064	0.016	1.364	8.11	8.10	8.10	8.10	0.006
12	5.250	5.270	5.180	5.233	0.049	0.009	1.655					

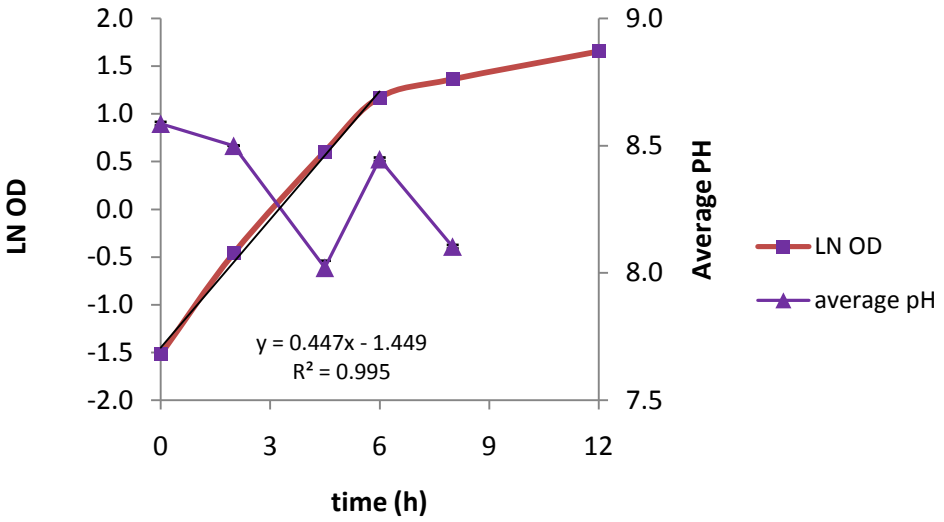

Figure 2.3.5: Growth of *B. halodurans* Alk36 in shake flasks with EnBase media at 45˚C with 200 rpm shaking

Table 2.3.7: Growth of *B. halodurans Alk36* in shake flasks with EnBase media at 50˚C with 200 rpm shaking

time	OD1	OD2	OD3	Average	Standard deviation	Relative error	LN OD	PH1	PH2	PH3	average PH	standard deviation
0	0.230	0.222	0.218	0.224	0.008	0.038	-1.496	8.32	8.40	8.32	8.35	0.046
2	0.555	0.573	0.630	0.593	0.053	0.090	-0.523	7.81	7.80	7.77	7.79	0.021
4	1.520	1.550	1.480	1.500	0.028	0.019	0.405	7.61	7.53	7.55	7.56	0.042
6	3.100	2.910	2.990	3.045	0.078	0.026	1.114	8.38	8.36	8.39	8.38	0.015
8	3.980	4.020	4.010	4.003	0.021	0.005	1.387	8.02	8.04	8.03	8.03	0.010
12	3.920	4.030	3.980	3.977	0.042	0.011	1.380					

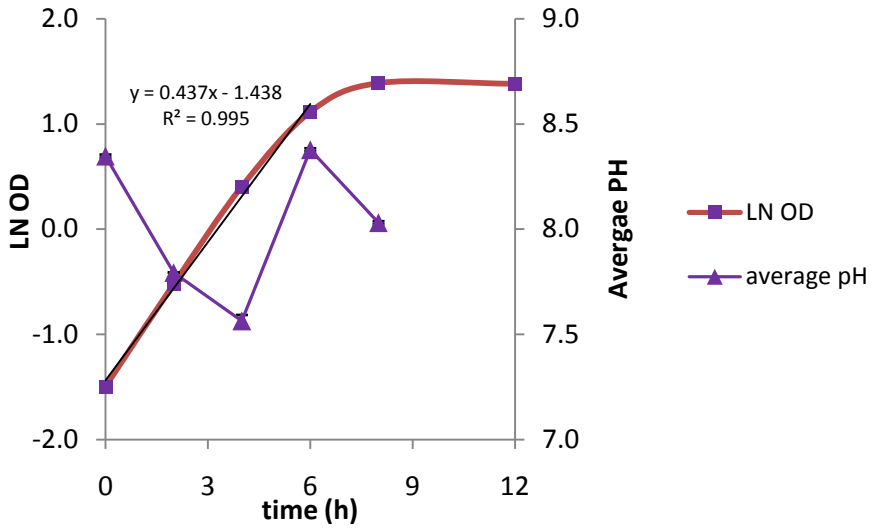

Figure 2.3.6: Growth of *B. halodurans*Alk 36 in shake flasks with EnBase media at 50˚C with 200 rpm shaking.

Appendix 2.4: Determination of the effect of the carbon source on amylase production

To determine the effect of carbon source on growth and amylase production, B. halodurans Alk36 was grown on EnBase medium containing dextrin, maltose or starch as the carbon source as described on Section

Table 2.4.1: Growth of *B. halodurans* Alk36 in the bioreactor at 45˚C with EnBase® medium containing dextrin as the carbon source.

Time	OD1	OD2	OD3	Average	standard deviation	relative error	LN OD	Error in Ln OD	average PH
0	0.167	0.159	0.165	0.164	0.004	0.025	-1.81	0.05	8.66
2	0.290	0.281	0.284	0.285	0.005	0.016	-1.26	0.02	8.95
4	1.360	1.410	1.400	1.390	0.026	0.019	0.33	0.01	8.76
6	2.550	2.560	2.550	2.553	0.006	0.002	0.94	0.00	8.51
9	3.820	3.760	3.750	3.777	0.038	0.010	1.33	0.01	8.15
12	4.960	4.970	5.010	4.980	0.026	0.005	1.61	0.01	7.62

Time	OD1	OD2	OD3	Average	standard deviation	relative error	LN OD	standard deviation	average PH
0	0.143	0.140	0.145	0.143	0.02	0.126	-1.95	0.24	8.66
2	0.285	0.291	0.295	0.290	0.02	0.056	-1.24	0.07	8.95
4	1.340	1.340	1.340	1.340	0.02	0.013	0.29	0.00	8.76
6	2.470	2.470	2.470	2.470	0.07	0.029	0.90	0.03	8.51
9	3.870	3.870	3.870	3.870	0.17	0.045	1.35	0.06	8.15
12	4.850	4.850	4.850	4.850	0.10	0.020	1.58	0.03	7.62
Time	OD1	OD2	OD3	Average	standard deviation	relative error	LN OD	standard deviation	average PH
0	0.165	0.158	0.169	0.164	0.01	0.086	-1.81	0.16	8.68
2	0.322	0.315	0.319	0.319	0.01	0.020	-1.14	0.02	8.56
4	1.410	1.420	1.370	1.400	0.04	0.025	0.34	0.01	8.02
6	2.390	2.350	2.450	2.397	0.09	0.038	0.87	0.03	7.83
9	4.040	4.060	4.040	4.047	0.01	0.002	1.40	0.00	8.25
12	4.720	4.680	4.750	4.717	0.13	0.027	1.55	0.04	7.97

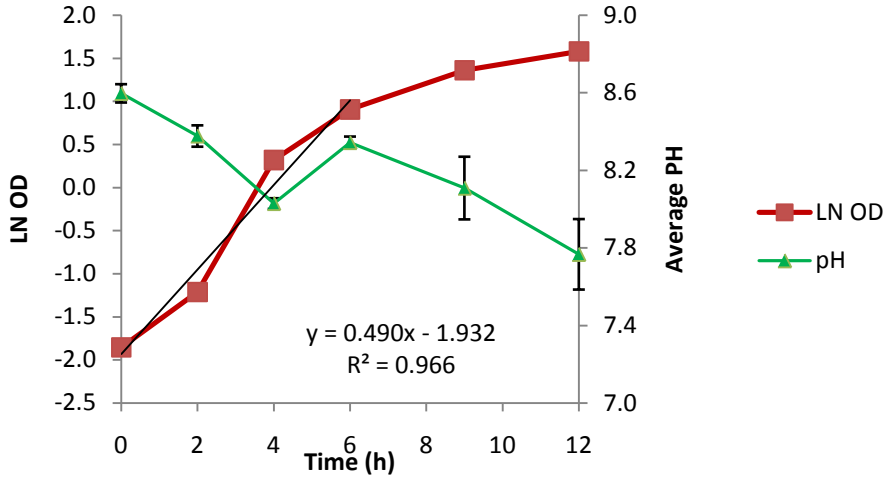

Figure 2.4.1: Growth of *B. halodurans* Alk36 in the bioreactor at 45˚C with EnBase® medium containing dextrin as the carbon source.

Table 2.4.2: Growth of *B. halodurans* Alk36 in shake flasks at 45˚C with EnBase® medium containing maltose as the carbon source.

time	OD1	OD2	OD3	average	standard deviation	relative error	LnOD	standard deviation	average PH
0	0.127	0.133	0.137	0.13	0.01	0.04	-2.02	0.08	8.65
2	0.359	0.360	0.357	0.36	0.00	0.00	-1.03	0.00	8.35
4	0.870	0.866	0.873	0.87	0.00	0.00	-0.14	0.00	8.01
6	1.910	1.900	1.930	1.91	0.02	0.01	0.65	0.01	8.35
9	3.210	3.190	3.200	3.20	0.01	0.00	1.16	0.00	8.24
12	4.080	4.180	4.140	4.13	0.05	0.01	1.42	0.02	8.16
time	OD1	OD2	OD3	average	standard deviation	relative error	LnOD	standard deviation	average PH
0	0.110	0.109	0.130	0.12	0.01	0.10	-2.15	0.22	8.59
2	0.392	0.401	0.397	0.40	0.00	0.01	-0.92	0.01	8.25
4	1.150	1.180	1.140	1.16	0.02	0.02	0.15	0.00	8.13
6	2.180	2.200	2.170	2.18	0.02	0.01	0.78	0.01	8.33
9	2.880	2.960	3.130	2.99	0.13	0.04	1.10	0.05	7.95
12	4.010	3.940	4.110	4.02	0.09	0.02	1.39	0.03	7.81
time	OD1	OD2	OD3	average	standard deviation	relative error	LnOD	standard deviation	average PH
0	0.132	0.129	0.125	0.13	0.00	0.03	-2.05	0.06	8.70
2	0.495	0.505	0.509	0.50	0.01	0.01	-0.69	0.01	8.59
4	1.330	1.350	1.310	1.33	0.02	0.02	0.29	0.00	8.41
6	2.260	2.250	2.220	2.24	0.02	0.01	0.81	0.01	8.25
9	3.250	3.210	3.350	3.27	0.07	0.02	1.18	0.03	7.91
12	4.200	4.160	4.250	4.20	0.05	0.01	1.44	0.02	7.84

Table 2.4.3: Growth of *B. halodurans* Alk36 in shake flasks at 45˚C with EnBase® medium containing soluble starch as the carbon source.

time	OD 1	OD 2	OD 3	average	standard deviation	relative error	LN OD	standard deviation	average PH
0	0.145	0.147	0.152	0.148	0.00	0.02	-1.91	0.05	8.55
2	0.270	0.266	0.271	0.269	0.00	0.01	-1.31	0.01	8.33
4	0.743	0.738	0.741	0.741	0.00	0.00	-0.30	0.00	8.15
6	1.110	1.100	1.080	1.097	0.02	0.01	0.09	0.00	8.38
9	1.360	1.380	1.430	1.390	0.04	0.03	0.33	0.01	8.25
12	1.910	2.100	1.970	1.993	0.10	0.05	0.69	0.03	8.07
time	OD 1	OD 2	OD 3	average	standard deviation	relative error	LN OD	standard deviation	average PH
0	0.160	0.161	0.158	0.16	0.00	0.01	-1.83	0.02	8.57
2	0.330	0.329	0.333	0.33	0.00	0.01	-1.11	0.01	8.28
4	0.804	0.890	0.814	0.84	0.05	0.06	-0.18	0.01	8.01
6	0.990	1.060	1.100	1.05	0.06	0.05	0.05	0.00	8.42
9	1.350	1.260	1.240	1.28	0.06	0.05	0.25	0.01	8.27
12	2.200	2.120	2.160	2.16	0.04	0.02	0.77	0.01	7.98
time	OD 1	OD 2	OD 3	average	standard deviation	relative error	LN OD	standard deviation	average PH
0	0.125	0.132	0.128	0.13	0.00	0.03	-2.05	0.06	8.53
2	0.322	0.360	0.320	0.33	0.02	0.07	-1.10	0.07	8.30
4	0.705	0.710	0.713	0.71	0.00	0.01	-0.34	0.00	8.10
6	0.831	0.828	0.831	0.83	0.00	0.00	-0.19	0.00	8.33
9	0.965	0.967	0.970	0.97	0.00	0.00	-0.03	0.00	8.14
12	1.150	1.150	1.150	1.15	0.00	0.00	0.14	0.00	7.07

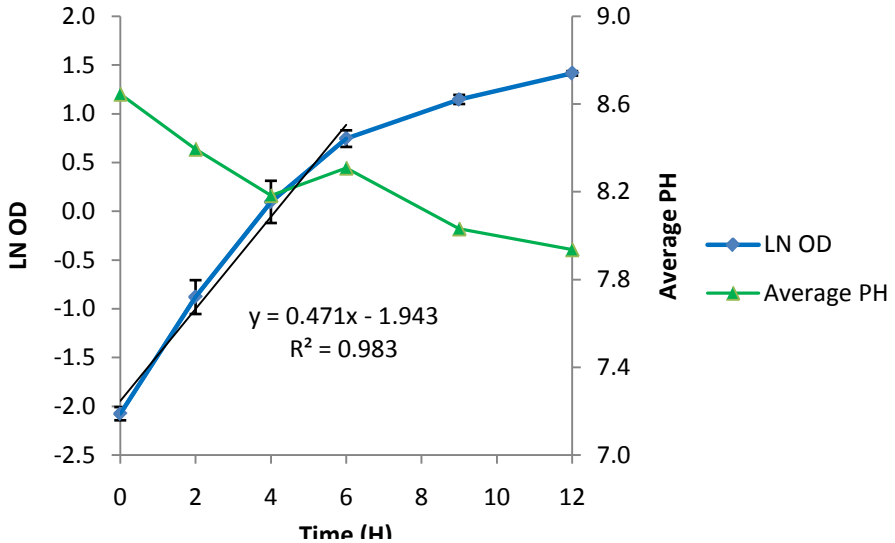

Figure 2.4.2: Growth of *B. halodurans* Alk36 in the bioreactor at 45˚C with EnBase® medium containing maltose as the carbon source.

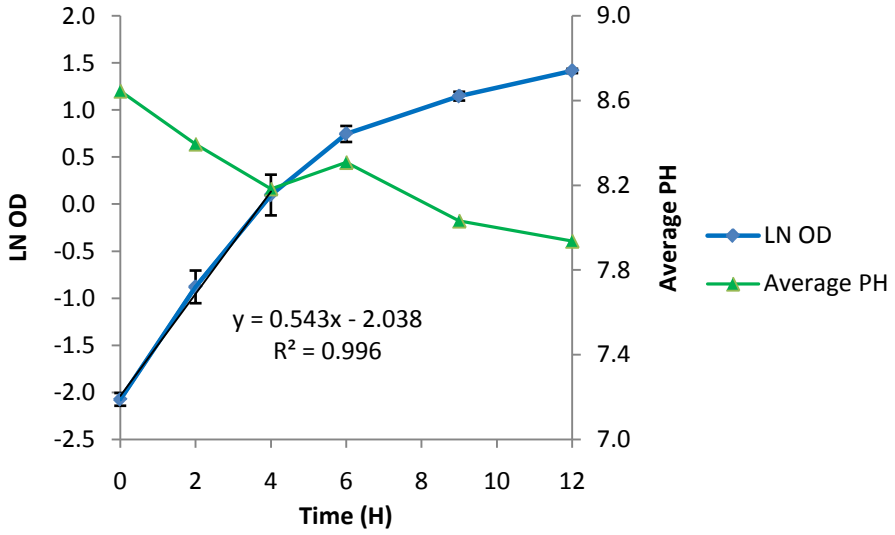

Figure 2.4.3: Growth of *B. halodurans* Alk36 in the bioreactor at 45˚C with EnBase® medium containing soluble starch as the carbon source.

Appendix 3: Partial purification and characterization of amylases from *Bacillus halodurans Alk36*

Appendix 3.1: Determination of the concentration of ammonium sulphate required for partial purification and concentration of amylases

Preliminary studies were done to determine the concentration of ammonium sulphate required to partially purify *B. halodurans* Alk36 amylases as described in Section 3.2.3.2. The concentration of protein and the amylase activity of the obtained fractions are presented in Table 3.1.2.

Table 3.1.1: BSA standard used for determination of total protein concentration (using Bradford assay) in protein recovered from ammonium sulphate precipitation.

OD_{595nm}	OD_{595nm}	OD_{595nm}	average	Standard deviation	blank corrected	[BSA] g/L
1.061	1.066	1.058	1.062	0.004	0.000	0.00
1.167	1.172	1.173	1.171	0.003	0.109	0.02
1.258	1.249	1.263	1.257	0.007	0.195	0.04
1.380	1.383	1.379	1.381	0.002	0.319	0.06
1.472	1.475	1.470	1.472	0.003	0.410	0.08
1.579	1.578	1.581	1.579	0.002	0.517	0.10

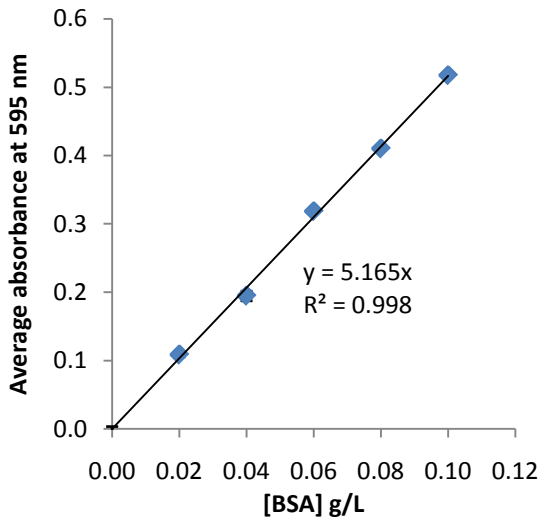

Figure 3.1.1: BSA standard curve obtained from Bradford assay

Table 3.1.2: Total protein concentration of fractions obtained from ammonium sulphate precipitation at different saturation

OD_{595nm}	OD_{595nm}	OD_{595nm}	Average	standard deviation	relative error	blank corrected	[protein] g/L	X dilution factor	Sample	Ammonium sulphate used for protein extraction	[protein] mg/L
0.428	0.422	0.425	0.425	0.003	0.007	0.425	0.082	0.82	F1	20 – 30 %	822.05
0.442	0.444	0.438	0.441	0.003	0.007	0.441	0.085	0.85	F2	30 – 40 %	853.64
0.647	0.62	0.632	0.633	0.014	0.021	0.633	0.122	1.22	F3	40 – 50 %	1224.37
0.388	0.389	0.393	0.391	0.003	0.007	0.391	0.076	3.78	F4	50 – 60 %	3781.43
0.475	0.467	0.489	0.478	0.016	0.033	0.478	0.092	4.62	F5	60 – 70 %	4622.82
0.215	0.214	0.213	0.214	0.001	0.005	0.214	0.041	2.07	F6	70 – 80%	2069.63
0.589	0.599	0.605	0.598	0.008	0.014	0.598	0.116	0.12	SPNT*	none	2587.04

* Culture supernatant prior precipitation

Table 3.1.2: Total protein recovered from ammonium sulphate precipitation at different saturation

sample	Ammonium sulphate used for protein extraction	[protein] g/L	Sample volume (mL)	Amount of protein (mg)	Protein recovery
F1	20 – 30 %	0.82	24	20	5 %
F2	30 – 40 %	0.85	20	17	4 %
F3	40 – 50 %	1.22	29	35	8 %
F4	50 – 60 %	3.78	35	132	31 %
F5	60 – 70 %	4.62	18	83	20 %
F6	70 – 80%	2.07	10	21	5 %
SPNT*	None	0.12	3500	420	100 %

Table 3.1.3: Amylase activity of protein samples obtained from fractions obtained from ammonium sulphate precipitation at different salt saturation.

F1- Protein fraction obtained from ammonium sulphate precipitation using 20 – 30 % salt							
A580	A580	A580	average	standard deviation	blank corrected	[starch] g/l	Time
0.996	0.994	0.992	0.994	0.002	0.950	9.50	0
0.861	0.879	0.882	0.874	0.011	0.830	8.30	2
0.744	0.745	0.8	0.773	0.039	0.729	7.29	4
0.631	0.641	0.649	0.640	0.009	0.596	5.96	6
0.511	0.502	0.504	0.506	0.005	0.462	4.62	8
0.396	0.388	0.391	0.392	0.004	0.348	3.48	10

F2- Protein fraction obtained from ammonium sulphate precipitation using 30 – 40 % salt							
A580	A580	A580	average	standard deviation	blank corrected	[starch] g/l	Time
1.007	1.002	1.006	1.005	0.003	0.961	9.61	0
0.843	0.862	0.857	0.854	0.010	0.810	8.10	2
0.789	0.783	0.781	0.782	0.001	0.738	7.38	4
0.706	0.705	0.707	0.706	0.001	0.662	6.62	6
0.581	0.596	0.594	0.590	0.008	0.546	5.46	8
0.427	0.439	0.437	0.434	0.006	0.390	3.90	10

Continuation of Table 3.1.3…

Table 3.1.3: Amylase activity of protein samples obtained from fractions obtained from ammonium sulphate precipitation at different salt saturation.

F3- Protein fraction obtained from ammonium sulphate precipitation using 40 – 50 % salt							
A580	A580	A580	average	standard deviation	blank corrected	[starch] g/l	Time
1.454	1.455	1.455	1.455	0.001	1.411	10.85	0
1.116	1.11	1.123	1.116	0.007	1.072	9.75	2
1.059	1.053	1.043	1.048	0.007	1.004	9.13	4
0.988	0.988	0.988	0.988	0.000	0.944	8.58	6
0.932	0.931	0.935	0.933	0.002	0.889	8.08	8
0.801	0.792	0.796	0.796	0.005	0.752	6.84	10
F4- Protein fraction obtained from ammonium sulphate precipitation using 20 – 30 % salt							
A580	A580	A580	A580	A580	A580	A580	A580
1.112	1.116	1.118	1.115	0.003	1.071	9.74	0
0.87	0.901	0.905	0.892	0.019	0.848	7.71	2
0.783	0.814	0.805	0.810	0.006	0.766	6.96	4
0.585	0.598	0.578	0.587	0.010	0.543	4.94	6
0.379	0.381	0.378	0.379	0.002	0.335	3.05	8
0.275	0.257	0.265	0.266	0.009	0.222	2.02	10

F5- Protein fraction obtained from ammonium sulphate precipitation using 30 – 40 % salt							
A580	A580	A580	average	standard deviation	blank corrected	[starch] g/l	time
0.841	0.844	0.819	0.835	0.014	0.791	6.08	0
1.185	1.188	1.187	1.187	0.002	1.143	8.79	2
1.07	1.077	1.064	1.070	0.007	1.026	7.89	4
0.969	0.967	0.951	0.962	0.010	0.918	7.06	6
0.722	0.753	0.737	0.737	0.016	0.693	5.33	8
0.584	0.568	0.578	0.577	0.008	0.533	4.10	10

Continuation of Table 3.1.3

Table 3.1.3: Amylase activity of protein samples obtained from fractions obtained from ammonium sulphate precipitation at different salt saturation

F6- Protein fraction obtained from ammonium sulphate precipitation using 40 – 50 % salt							
A580	A580	A580	average	standard deviation	blank corrected	[starch] g/l	time
0.759	0.77	0.794	0.774	0.018	0.730	5.62	0
1.16	1.202	1.205	1.189	0.025	1.145	8.81	2
0.963	1.107	1.101	1.104	0.004	1.060	8.15	4
1.033	1.021	1.001	1.018	0.016	0.974	7.49	6
0.885	0.869	0.879	0.878	0.008	0.834	6.41	8
0.766	0.746	0.736	0.749	0.015	0.705	5.43	10

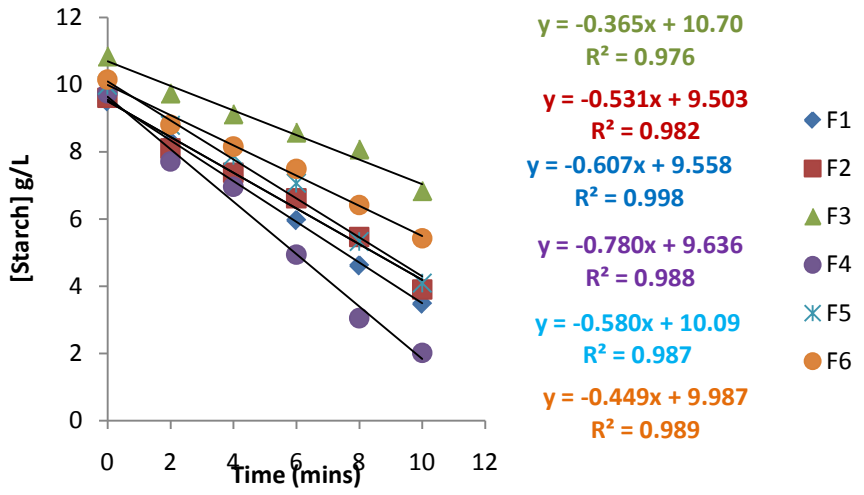

Figure 3.1.2: Rate of starch hydrolysis by amylases recovered from ammonium sulphate precipitation at different salt concentration.

Table 3.1.4: Amylase activity of culture supernatant prior ammonium sulphate precipitation.

A580	A580	A580	average	Standard deviation	blank corrected	[starch] g/l	Time
1.033	1.028	1.061	1.041	0.018	0.997	9.06	2
0.896	0.912	0.885	0.898	0.014	0.854	7.76	4
0.779	0.818	0.781	0.793	0.022	0.749	6.81	6
0.668	0.693	0.653	0.671	0.020	0.627	5.70	8
0.542	0.541	0.546	0.543	0.003	0.499	4.54	10

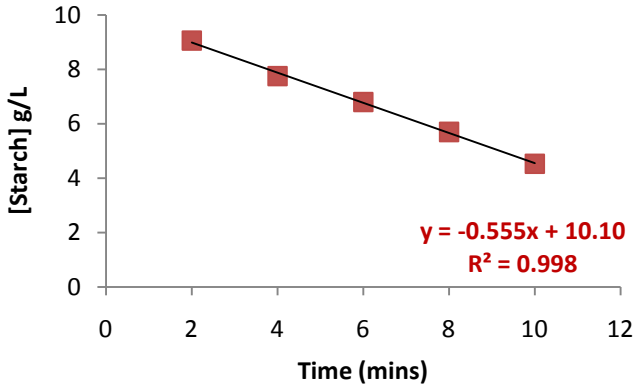

Figure 3.1.3: Rate of starch hydrolysis by amylases from *B. halodurans* culture supernatant.

Table 3.1.5: Amylase activity of protein fractions obtained from ammonium sulphate precipitation using different salt concentration.

Sample	Ammonium sulphate used for protein extraction	[protein] g/L	Rate of starch hydrolysis (g/L/min)	Dilution rate	x dilution rate	Specific amylase activity (U/mg protein)*
F1	20 – 30 %	0.82	0.6070	5	3.04	5.01
F2	30 – 40 %	0.85	0.5315	5	2.66	3.13
F3	40 – 50 %	1.22	0.3659	100	36.59	29.99
F4	50 – 60 %	3.78	0.7804	200	156.08	41.27
F5	60 – 70 %	4.62	0.5801	100	58.01	12.56
F6	70 – 80%	2.07	0.4494	100	44.94	21.71
SPNT*	None	0.12	0.5553	10	5.55	46.25

* The specific amylase activity was calculated using the following formula:

$$Amylaseactivity(U.mg^{-1}\,protein) = \frac{Slope\ (g.L^{-1}.min^{-1})\ x\ \ 10^3\ (\frac{mg}{g})}{[ptotein]\ (mg.L^{-1}\,protein)}$$

where 1 U is equivalent to one mg of starch hydrolyzed per minute under assay conditions.

Appendix 3.2.1: Comparison of protein recovery from ammonium sulphate precipitation and activated charcoal fractionation

The amount of protein and amylase activity of the protein samples were determined using the Bradford assay and the starch-iodine assay, respectively.

Table 3.2.1: BSA standard used for determination of total protein concentration by Bradford assay

A_{595nm}	A_{595nm}	A_{595nm}	Average absorbance	standard deviation	blank corrected	[BSA] g/L
0.841	0.873	0.853	0.856	0.016	0.000	0
0.971	0.981	0.989	0.980	0.009	0.124	20
1.039	1.093	1.079	1.070	0.028	0.214	40
1.159	1.165	1.204	1.176	0.024	0.320	60
1.287	1.281	1.289	1.286	0.004	0.430	80
1.295	1.304	1.326	1.308	0.016	0.452	100

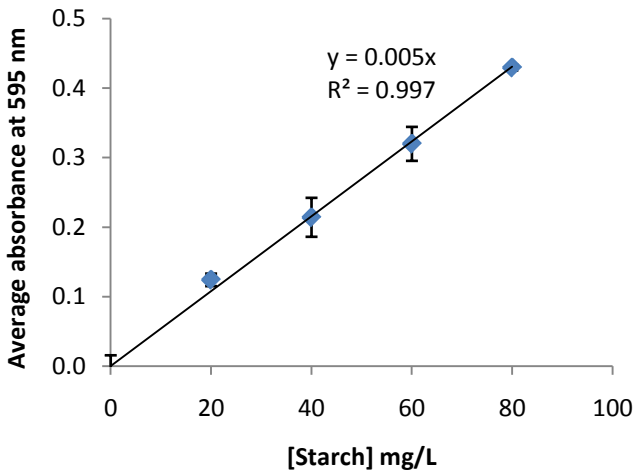

Figure 3.2.1: BSA standard curve obtained from Bradford assay.

Table 3.2.2: Total protein recovered from ammonium sulphate and activated charcoal fractionation

Sample	A_{595}	A_{595}	A_{595}	Average absorbance	standard deviation	Blank corrected	[protein] (mg/L)	Dilution factor	[protein] mg/L x dilution factor	volume	Total protein	Protein recovery
Culture supernatant	1.265	1.263	1.259	1.262	0.003	0.406	75	2	150	1 L	150	100 %
AC filtrate	1.325	1.325	1.338	1.329	0.008	0.473	88	1	88	1 L	88	59 %
AS precipitate	1.261	1.317	1.328	1.302	0.036	0.462	54	50	2700	18 mL	49	32 %

* The protein concentration was calculated using standard curve with equation (y = 0.0047x)

Table 3.2.3: Starch standards used for generation of standard curve for determination of amylase activity of protein sample recovered from ammonium sulphate and activated charcoal fractionation

A_{580}	A_{580}	A_{580}	average	standard deviation	blank corrected	[starch]
0.054	0.055	0.049	0.053	0.003	0.000	0
0.214	0.218	0.215	0.216	0.002	0.163	2
0.438	0.436	0.433	0.436	0.003	0.383	4
0.608	0.603	0.606	0.606	0.003	0.553	6
0.783	0.780	0.785	0.783	0.003	0.730	8
0.951	0.955	0.952	0.953	0.002	0.900	10

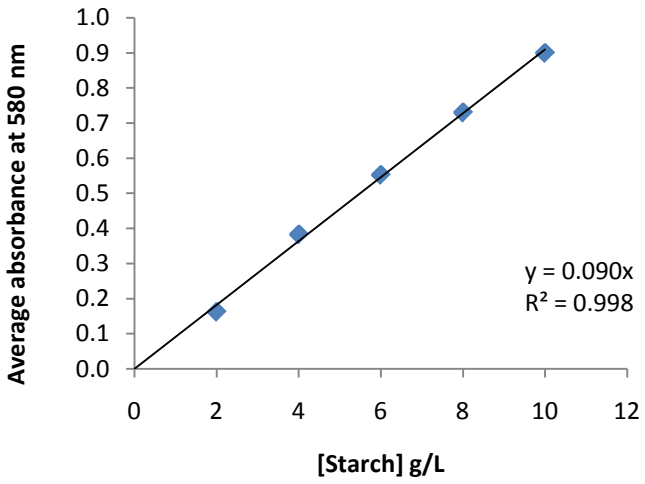

Figure 3.2.1: Starch standard curve obtained from the starch-iodine assay

Table 3.2.4: Rate of starch hydrolysis by amylases in culture supernatant

A_{580}	A_{580}	A_{580}	Average absorbance	standard deviation	blank corrected	[starch] g/L	Time
0.172	0.170	0.162	0.168	0.005	0.124	10	0
0.913	0.933	0.926	0.924	0.010	0.880	9	3
0.780	0.779	0.792	0.784	0.007	0.740	7	6
0.635	0.631	0.635	0.634	0.002	0.590	6	9
0.529	0.531	0.533	0.531	0.002	0.487	5	12
0.478	0.485	0.475	0.479	0.005	0.435	4	15

Table 3.2.5: Rate of starch hydrolysis by amylases in protein samples obtained from activated charcoal fractionation

A_{580}	A_{580}	A_{580}	Average Absorbance	standard deviation	blank corrected	[starch] g/L	Time
1.423	1.379	1.450	1.417	0.036	1.373	10	0
1.043	1.056	1.087	1.062	0.023	1.018	8	3
0.930	0.942	0.956	0.943	0.013	0.899	7	6
0.745	0.755	0.772	0.757	0.014	0.713	6	9
0.651	0.659	0.668	0.659	0.009	0.615	5	12
0.565	0.587	0.577	0.576	0.011	0.532	4	15

Table 3.2.6: Rate of starch hydrolysis by amylases in samples obtained from ammonium sulphate precipitation

A_{580}	A_{580}	A_{580}	Average Absorbance	standard deviation	blank corrected	[starch] g/L	Time
1.347	1.404	1.410	1.387	0.035	1.343	10	0
1.135	1.158	1.160	1.151	0.014	1.107	8	3
0.874	0.899	0.896	0.890	0.014	0.846	6	6
0.736	0.750	0.749	0.745	0.008	0.701	5	9
0.558	0.587	0.566	0.570	0.015	0.526	4	12
0.439	0.437	0.439	0.438	0.001	0.394	3	15

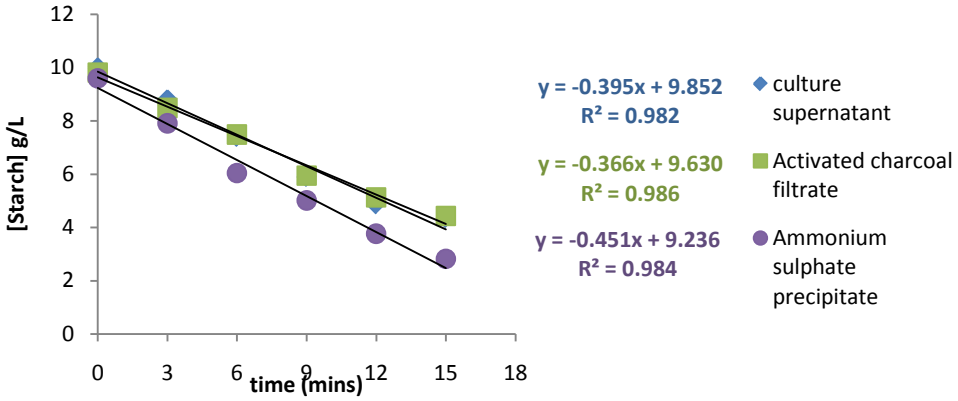

Figure 3.2.2: Rate of starch hydrolysis by amylases from *B. halodurans* culture supernatant, protein sample from activated charcoal fractionation and ammonium sulphate precipitation.

Table 3.2.7: Rate of starch hydrolysis by amylases in samples obtained from ammonium sulphate precipitation

Sample	[protein] Mg	Rate of starch hydrolysis (g/L/min)	Dilution rate	Rate of starch hydrolysis x dilution rate	Sample volume	Total Activity (µMols/min)	Activity recovery	Specific amylase activity (U/mg protein)*
Culture supernatant	150	0.3955	10	3.96	1 L	22,000	100 %	147
Activated charcoal fraction	88	0.3655	10	3.66	1 L	20,333	92 %	231
Ammonium sulphate precipitate	24	0.4510	100	45.1	18 mL	4510	21 %	188

* The specific amylase activity was calculated using the following formula:

$$Amylaseactivity\ (U.mg^{-1}\ protein) = \frac{Slope\ (g.L^{-1}.min^{-1})\ x\ 10^3\ (mg/g)}{[ptotein]\ (mg.L^{-1}\ protein)}$$

where 1 U is equivalent to one mg of starch hydrolyzed per minute under assay conditions.

Appendix 3.3: Protein recovery and amylase activities obtained from different stages of purification by liquid chromatography

Table 3.3.1: BSA standards used to generate a standard curve for the determination of protein concentration samples from different purification stages.

A_{595}	A_{595}	A_{595}	average	standard deviation	blank corrected	[BSA] g/L
0.890	0.885	0.887	0.887	0.003	0.000	0.00
0.973	0.972	0.989	0.978	0.010	0.091	0.02
1.079	1.072	1.081	1.077	0.005	0.190	0.04
1.171	1.179	1.175	1.175	0.004	0.288	0.06
1.256	1.255	1.252	1.254	0.002	0.367	0.08
1.323	1.320	1.317	1.320	0.003	0.433	0.10

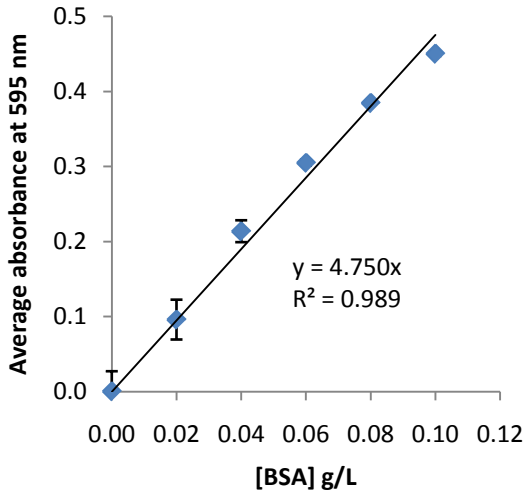

Figure 3.3.1: BSA standard curve obtained from Bradford assay

Table 3.3.1: Protein concentration of samples obtained from different purification stages

Sample source	A_{595}	A_{595}	A_{595}	Average absorbance	standard deviation	blank corrected	[Total protein] g/L	dilution factor	x dilution factor
Culture Supernatant	1.143	1.158	1.199	1.167	0.029	0.297	0.062	2	0.12
Ammonium sulphate precipitate	1.175	1.216	1.226	1.221	0.007	0.351	0.074	50	3.69
AEC* peak 1	1.139	1.155	1.144	1.146	0.008	0.276	0.058	10	0.58
AEC* peak 2	1.125	1.158	1.161	1.148	0.020	0.278	0.059	10	0.59
AEC* peak 3	1.034	1.008	1.019	1.020	0.013	0.150	0.032	50	1.58
Flow out from HIC*	1.002	1.029	1.019	1.017	0.014	0.147	0.031	50	1.54
Bound protein from HIC*	1.254	1.271	1.216	1.247	0.028	0.377	0.079	1	0.08
Gel filtration	0.995	1.026	1.004	1.008	0.016	0.138	0.029	2	0.06

* AEC – Anion exchange chromatography& HIC – Hydrophobic interaction chromatography

Table 3.3.2: Protein yield from the purification stages

Sample source	[Total protein] g/L	Sample volume (mL)	Total protein (mg)	Protein Yield
Culture Supernatant	0.12	3500	420	100 %
Ammonium sulphate precipitate	3.69	35	129	31 %
AEC* peak 1	0.58	5	2.90	2.2 %
AEC* peak 2	0.59	4.5	2.66	2.1 %
AEC* peak 3	1.58	4.5	7.11	4.9 %
Effluent from HIC*	1.54	1.5	2.31	1.8 %
Bound protein from HIC*	0.08	1.5	0.12	0.09 %
Gel filtration	0.06	1.5	0.09	0.07 %

Table 3.3.3: Starch standards used to generate a standard curve for the determination of amylase activity of samples from different purification stages

A_{580}	A_{580}	A_{580}	Average absorbance	standard deviation	blank corrected	[starch] g/L
0.045	0.046	0.052	0.048	0.004	0.000	0
0.511	0.500	0.502	0.504	0.006	0.456	2
0.818	0.824	0.820	0.821	0.003	0.773	4
1.112	1.116	1.115	1.114	0.002	1.066	6
1.504	1.505	1.512	1.507	0.004	1.459	8
1.857	1.841	1.852	1.850	0.008	1.802	10

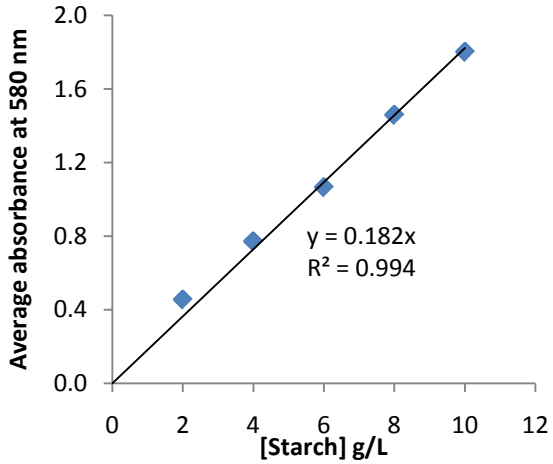

Figure 3.3.2: Starch standard curve obtained from Starch-Iodine assay

Table 3.3.3: Amylase activities of samples obtained from different purification stages

Sample	A_{580}	A_{580}	A_{580}	average	standard deviation	blank corrected	[starch]	Time
Culture supernatant	1.752	1.748	1.747	1.749	0.003	1.701	9.336	0
	1.607	1.587	1.665	1.620	0.041	1.572	8.626	2
	1.389	1.434	1.385	1.403	0.027	1.355	7.435	4
	1.246	1.269	1.263	1.259	0.012	1.211	6.648	6
	1.197	1.139	1.136	1.157	0.034	1.109	6.089	8
	1.021	1.018	1.014	1.018	0.004	0.970	5.322	10
Ammonium sulphate precipitate	A_{580}	A_{580}	A_{580}	average	standard deviation	blank corrected	[starch]	Time
	1.729	1.718	1.713	1.720	0.008	1.672	9.177	0
	1.608	1.594	1.592	1.598	0.009	1.550	8.507	2
	1.455	1.45	1.454	1.453	0.003	1.405	7.711	4
	1.349	1.348	1.351	1.349	0.002	1.301	7.142	6
	1.166	1.17	1.169	1.168	0.002	1.120	6.149	8
	1.041	1.038	1.047	1.042	0.005	0.994	5.456	10

Continuation of Table 3.3.3

Table 3.3.3: Rate of starch hydrolysis by amylases from samples obtained from different purification stages

	A_{580}	A_{580}	A_{580}	average	standard deviation	blank corrected	[starch]	time
Peak 3 from anion-exchange chromatography	1.644	1.611	1.607	1.621	0.020	1.573	8.632	0
	1.431	1.433	1.462	1.442	0.017	1.394	7.651	2
	1.301	1.365	1.338	1.335	0.032	1.287	7.062	4
	1.141	1.161	1.158	1.153	0.011	1.105	6.067	6
	0.919	0.919	0.915	0.918	0.002	0.870	4.773	8
	0.769	0.801	0.806	0.792	0.020	0.744	4.083	10
Effluent from hydrophobic interaction column	A_{580}	A_{580}	A_{580}	average	standard deviation	blank corrected	[starch]	time
	0.939	0.991	0.914	0.948	0.039	0.900	9.879	0
	0.808	0.803	0.879	0.830	0.043	0.782	8.584	2
	0.655	0.544	0.597	0.599	0.056	0.551	6.045	4
	0.476	0.434	0.412	0.441	0.033	0.393	4.310	6
	0.292	0.262	0.367	0.307	0.054	0.259	2.843	8
	0.163	0.179	0.18	0.174	0.010	0.126	1.383	10
Protein eluted from the hydrophobic interaction column	A580	A580	A580	average	standard deviation	blank corrected	[starch]	time
	0.796	0.8	0.797	0.798	0.002	0.750	10.286	0
	0.722	0.726	0.728	0.725	0.003	0.677	9.294	2
	0.624	0.636	0.643	0.634	0.010	0.586	8.045	4
	0.539	0.554	0.546	0.546	0.008	0.498	6.838	6
	0.442	0.438	0.439	0.440	0.002	0.392	5.374	8
	0.339	0.327	0.34	0.335	0.007	0.287	3.943	10

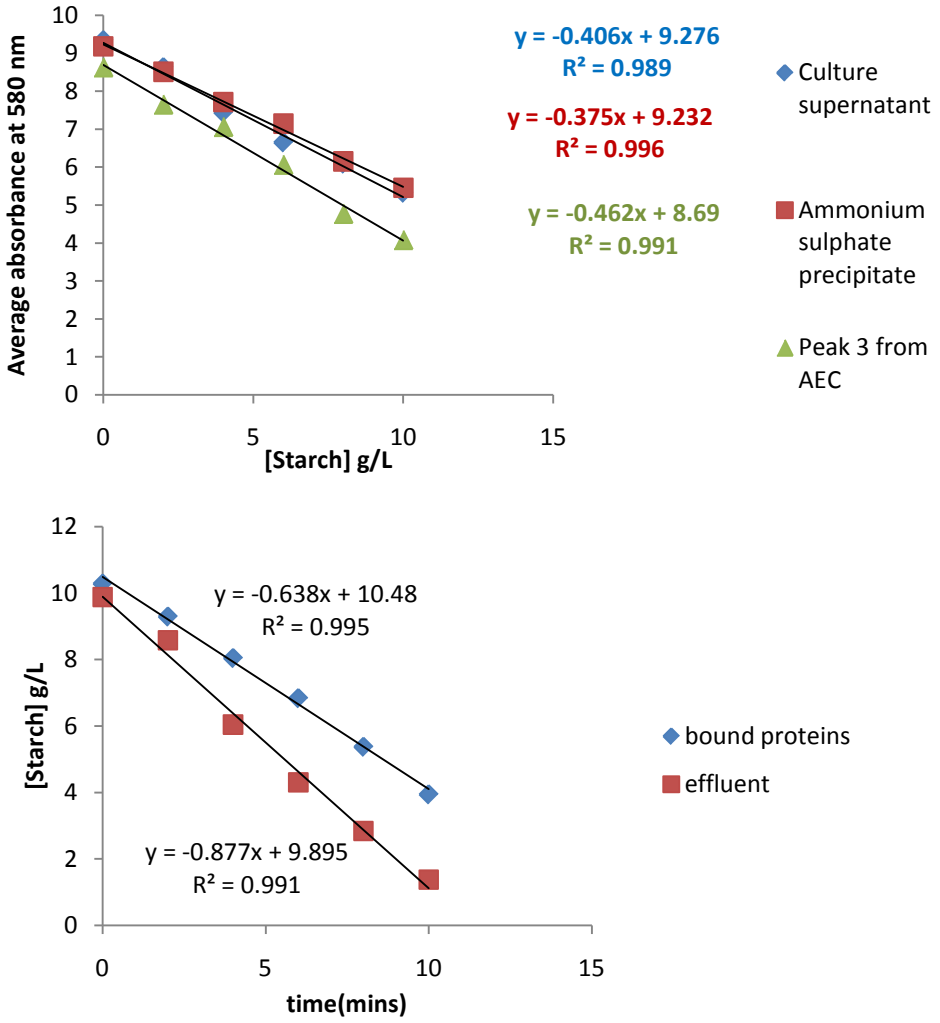

Figure 3.3.3: Rate of protein hydrolysis by amylases recovered from different purification stages.

Table 3.3.4: Amylase activities of samples obtained from different purification stages

Sample source	[protein] mg	Rate of starch hydrolysis (g/L/min)	Dilution rate	Amylase activity (g/L/min)	Sample volume	Total Activity (µMols/min)	Activity recovery	Specific amylase activity (U/mg protein)*
Culture Supernatant	420	0.4067	10	4.07	3.5 L	79,081	100 %	147
Ammonium sulphate precipitate	129	0.3750	500	188	35 mL	36,458	92 %	231
Peak 3 from AEC*	7.11	0.4624	500	231	4.5 mL	5,775	16 %	812
Flow out from HIC*	2.31	0.8777	10	8.77	1.5 mL	73.08	1.26 %	32
Eluted protein from HIC*	0.12	0.6384	10	6.38	1.5 mL	53.2	0.1%	443

***** AEC – Anion exchange chromatography & HIC – Hydrophobic interaction chromatography

The specific amylase activity was calculated using the following formula:

$$Amylaseactivity\ (U.mg^{-1}\ protein) = \frac{Slope\ (g.L^{-1}.min^{-1})\ x\ \ 10^3\ (\frac{mg}{g})}{[ptotein]\ (mg.L^{-1}\ protein)}$$

where 1 U is equivalent to mg of starch released per minute under assay conditions

Appendix 3.4: Effect of buffer solutions on the activity of *B. halodurans* Alk36 amylases

The effect of phosphate and tris buffer solutions on amylase activity was determined by performing activity assays using the two buffers solutions.

Table 3.4.1: Starch standards in different buffers

Starch standards in phosphate buffer						
A_{580}	A_{580}	A_{580}	average	standard deviation	blank corrected	[starch]
0.057	0.057	0.057	0.057	0.000	0.000	0
0.344	0.343	0.342	0.343	0.001	0.286	2
0.568	0.567	0.567	0.567	0.001	0.510	4
0.788	0.788	0.779	0.785	0.005	0.728	6
1.056	1.053	1.053	1.054	0.002	0.997	8
1.213	1.215	1.212	1.213	0.002	1.156	10
Starch standards in Tris buffer						
A_{580}	A_{580}	A_{580}	average	standard deviation	blank corrected	[starch]
0.054	0.058	0.055	0.056	0.002	0.000	0
0.339	0.331	0.336	0.335	0.004	0.279	2
0.604	0.605	0.604	0.604	0.001	0.548	4
0.792	0.797	0.799	0.796	0.004	0.740	6
0.993	0.995	0.997	0.995	0.002	0.939	8
1.096	1.092	1.09	1.093	0.003	1.037	10
Starch standards in Triethanolacetate buffer						
A_{580}	A_{580}	A_{580}	average	standard deviation	blank corrected	[starch]
0.058	0.057	0.056	0.057	0.001	0.000	0
0.354	0.359	0.355	0.356	0.003	0.299	2
0.536	0.532	0.532	0.533	0.002	0.476	4
0.697	0.701	0.698	0.699	0.002	0.642	6
0.982	0.9836	0.9821	0.983	0.001	0.926	8
1.197	1.199	1.21	1.202	0.007	1.145	10

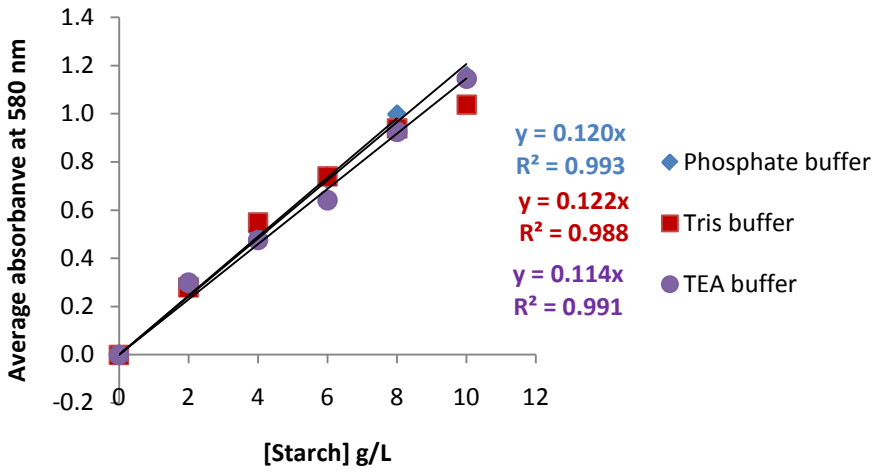

Figure 3.4.1: Starch standard curves obtained when using different buffer solutions.

Appendix 3.5: The stability of amylases in phosphate buffer

The amylase activity assays were done on different days to determine the stability of *B. halodurans* Alk36 amylases.

Table 3.5.1: Rate of starch hydrolysis with amylase from culture supernatant diluted in 0.1 M phosphate buffer at pH 8.5 at day 0

A_{580}	A_{580}	A_{580}	average	standard deviation	blank corrected	[starch]	time
1.079	1.078	1.073	1.077	0.003	1.033	9.388	0
0.954	0.945	0.944	0.948	0.006	0.904	8.215	2
0.761	0.764	0.773	0.766	0.006	0.722	6.564	4
0.669	0.671	0.675	0.672	0.003	0.628	5.706	6
0.503	0.499	0.504	0.502	0.003	0.458	4.164	8
0.457	0.446	0.453	0.452	0.006	0.408	3.709	10
A_{580}	A_{580}	A_{580}	average	standard deviation	blank corrected	[starch]	time
1.117	1.117	1.121	1.118	0.002	1.074	9.767	0
0.982	0.978	0.979	0.980	0.002	0.936	8.506	2
0.78	0.778	0.773	0.777	0.004	0.733	6.664	4
0.674	0.678	0.683	0.678	0.005	0.634	5.767	6
0.505	0.49	0.488	0.494	0.009	0.450	4.094	8
0.415	0.412	0.414	0.414	0.002	0.370	3.361	10

Continuation of Table 3.5.1…

Table 3.5.1: Rate of starch hydrolysis with amylase from culture supernatant diluted in 0.1 M phosphate buffer at pH 8.5 at day 0

A_{580}	A_{580}	A_{580}	average	standard deviation	blank corrected	[starch]	time
1.122	1.124	1.121	1.122	0.002	1.078	9.803	0
0.996	0.988	0.998	0.994	0.005	0.950	8.636	2
0.877	0.882	0.884	0.881	0.004	0.837	7.609	4
0.673	0.666	0.682	0.674	0.008	0.630	5.724	6
0.531	0.529	0.534	0.531	0.003	0.487	4.430	8
0.276	0.271	0.276	0.274	0.003	0.230	2.094	10

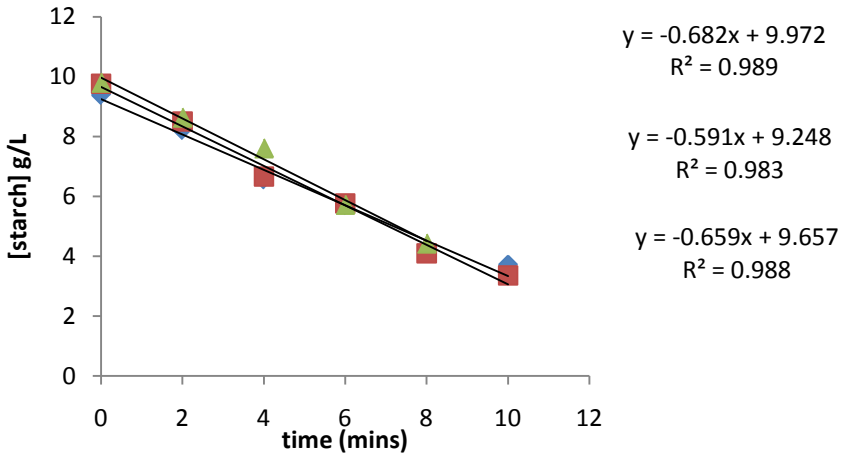

Figure 3.5.1: Rate of starch hydrolysis obtained with phosphate buffer solution at day 0.

Table 3.5.2: Amylase activity of culture supernatant diluted in 0.1 M phosphate buffer at pH 8.5 (day 0)

Rate of starch hydrolysis	Dilution factor	Amylase activity(g/L/min)
0.6829	100	68.29
0.5915	100	59.15
0.6595	100	65.95
Average amylase activity		64.45 ± 4.75

Table 3.5.3: Rate of starch hydrolysis with amylase from culture supernatant diluted in 0.1 M Tris buffer at pH 8.5 (day 0)

A_{580}	A_{580}	A_{580}	average	standard deviation	blank corrected	[starch]	time
1.214	1.156	1.189	1.186	0.029	1.142	9.325	0
1.08	1.082	1.091	1.084	0.006	1.040	8.493	3
1.016	1.022	1.013	1.017	0.005	0.973	7.943	5
0.918	0.937	0.945	0.933	0.014	0.889	7.260	7
0.847	0.875	0.855	0.859	0.014	0.815	6.653	10
0.791	0.804	0.806	0.800	0.008	0.756	6.174	12
A580	A580	A580	average	standard deviation	blank corrected	[starch]	time
1.195	1.17	1.206	1.190	0.018	1.146	9.396	0
1.084	1.106	1.085	1.092	0.012	1.048	8.587	3
1.016	1.03	1.032	1.026	0.009	0.982	8.049	5
0.945	0.948	0.942	0.945	0.003	0.901	7.385	7
0.833	0.834	0.829	0.832	0.003	0.788	6.459	10
0.790	0.804	0.808	0.801	0.009	0.757	6.202	12

Continuation of Table 3.5.3

Table 3.5.3: Rate of starch hydrolysis with amylase from culture supernatant diluted in 0.1 M Tris buffer at pH 8.5 (day 0)

A_{580}	A_{580}	A_{580}	average	standard deviation	blank corrected	[starch]	time
1.213	1.215	1.218	1.215	0.003	1.171	9.562	0
1.083	1.079	1.076	1.079	0.004	1.035	8.452	3
1.019	0.977	1.016	1.004	0.023	0.960	7.837	5
0.95	0.961	0.971	0.961	0.011	0.917	7.483	7
0.829	0.829	0.832	0.830	0.002	0.786	6.416	10
0.803	0.806	0.803	0.804	0.002	0.760	6.204	12

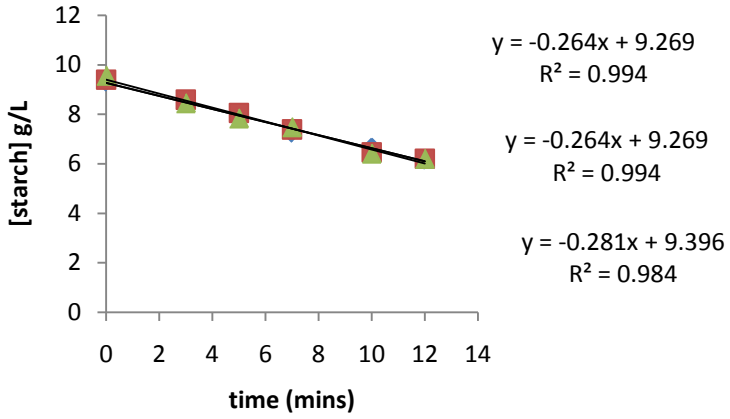

Figure 3.5.2: Rate of starch hydrolysis obtained with Tris buffer at day 0.

Table 3.5.4: Amylase activity of culture supernatant diluted in 0.1 M Tris buffer at pH 8.5 (day 0)

Rate of starch hydrolysis	Dilution factor	Amylase activity (g/L/min)
0.264	100	26.4
0.264	100	26.4
0.282	100	28.2
Average activity		27.0 ± 1.0

Table 3.5.5: Rate of starch hydrolysis with amylase from culture supernatant diluted in 0.1 M Phosphate buffer at pH 8.5 (day 2)

A_{580}	A_{580}	A_{580}	average	standard deviation	blank corrected	[starch]	Time
0.911	0.9	0.923	0.911	0.012	0.853	7.08	0
0.961	0.971	0.967	0.966	0.005	0.908	7.54	2
0.846	0.864	0.876	0.862	0.015	0.804	6.67	4
0.725	0.715	0.717	0.719	0.005	0.661	5.49	6
0.602	0.602	0.603	0.602	0.001	0.544	4.52	8
0.472	0.473	0.466	0.470	0.004	0.412	3.42	10

A580	A580	A580	average	standard deviation	blank corrected	[starch]	Time
1.007	1.021	1.023	1.017	0.009	0.959	7.96	0
0.969	0.983	0.956	0.969	0.014	0.911	7.56	2
0.881	0.869	0.874	0.875	0.006	0.817	6.78	4
0.719	0.722	0.73	0.724	0.006	0.666	5.52	6
0.586	0.583	0.575	0.581	0.006	0.523	4.34	8
0.475	0.481	0.463	0.473	0.009	0.415	3.44	10

Continuation of Table 3.5.5…

Table 3.5.5 Rate of starch hydrolysis with amylase from culture supernatant diluted in 0.1 M Phosphate buffer at pH 8.5 (day 2)

A_{580}	A_{580}	A_{580}	average	standard deviation	blank corrected	[starch]	Time
1.094	1.095	1.098	1.096	0.002	1.038	8.61	0
0.987	0.985	0.978	0.983	0.005	0.925	7.68	2
0.907	0.896	0.892	0.898	0.008	0.840	6.97	4
0.758	0.761	0.751	0.757	0.005	0.699	5.80	6
0.588	0.59	0.573	0.584	0.009	0.526	4.36	8
0.526	0.536	0.529	0.530	0.005	0.472	3.92	10

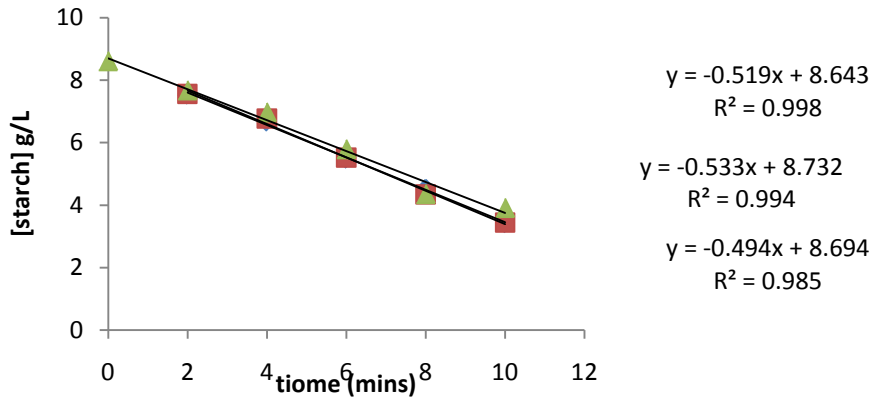

Figure 3.5.3: Rate of starch hydrolysis obtained with phosphate buffer solution (day 2).

Table 3.5.6: Amylase activity of culture supernatant diluted in 0.1 M phosphate buffer at pH 8.5 (day 2)

Rate of starch hydrolysis	Dilution factor	Amylase activity(g/L/min)
0.5194	100	51.94
0.5336	100	53.36
0.4941	100	49.41

Average amylase activity	51.57 ± 2.00

Table 3.5.7: Rate of starch hydrolysis with amylase from culture supernatant diluted in 0.1 M phosphate buffer at pH 8.5 at day 0

A_{580}	A_{580}	A_{580}	average	standard deviation	blank corrected	[starch]	Time
0.993	0.984	0.991	0.989	0.005	0.931	7.60	0
0.892	0.923	0.906	0.907	0.016	0.849	6.93	2
0.822	0.834	0.829	0.828	0.006	0.770	6.29	4
0.748	0.756	0.756	0.753	0.005	0.695	5.68	6
0.706	0.695	0.705	0.702	0.006	0.644	5.26	8
0.641	0.638	0.628	0.636	0.007	0.578	4.72	10
A580	A580	A580	average	standard deviation	blank corrected	[starch]	Time
0.906	0.929	0.9	0.912	0.015	0.854	6.97	0
0.856	0.8	0.849	0.835	0.031	0.777	6.34	2
0.813	0.801	0.783	0.799	0.015	0.741	6.05	4
0.75	0.737	0.744	0.744	0.007	0.686	5.60	6
0.69	0.69	0.694	0.691	0.002	0.633	5.17	8
0.653	0.641	0.645	0.646	0.006	0.588	4.80	10
A_{580}	A_{580}	A_{580}	average	standard deviation	blank corrected	[starch]	Time
0.869	0.873	0.878	0.873	0.005	0.815	6.66	0
0.877	0.889	0.876	0.881	0.007	0.823	6.72	2
0.822	0.838	0.828	0.829	0.008	0.771	6.30	4
0.766	0.759	0.765	0.763	0.004	0.705	5.76	6
0.731	0.707	0.696	0.711	0.018	0.653	5.33	8
0.668	0.666	0.674	0.669	0.004	0.611	4.99	10

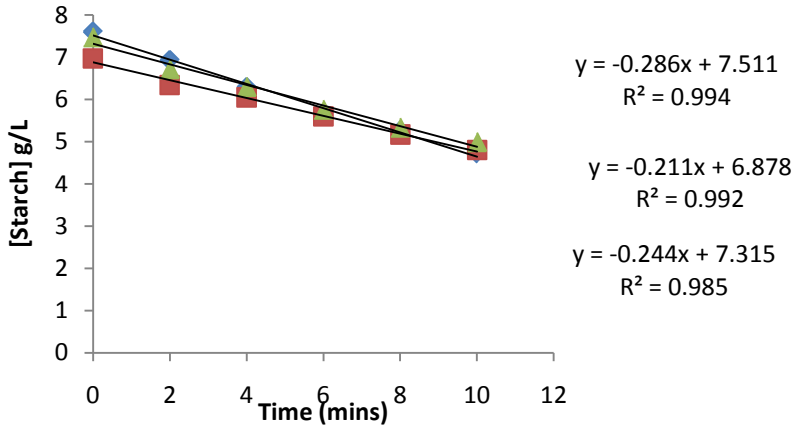

Figure 3.5.4: Rate of starch hydrolysis obtained with Tris buffer solution (day 2).

Table 3.5.8: Amylase activity of culture supernatant diluted in 0.1 M phosphate buffer at pH 8.5 (day 2)

Rate of starch hydrolysis	Dilution factor	Amylase activity(g/L/min)
0.2867	100	28.67
0.2114	100	21.14
0.2442	100	24.42
Average amylase activity		23.96 ± 4.11

Table 3.5.9: Rate of starch hydrolysis with amylase from culture supernatant diluted in 0.1 M Triethanolacetate (TEA) buffer at pH 8.5

A_{580}	A_{580}	A_{580}	average	standard deviation	blank corrected	[starch]	Time
0.945	0.945	0.946	0.945	0.001	0.887	7.74	0
0.91	0.913	0.918	0.914	0.004	0.856	7.47	2
0.841	0.845	0.843	0.843	0.002	0.785	6.85	4
0.819	0.815	0.814	0.816	0.003	0.758	6.61	6
0.791	0.796	0.793	0.793	0.003	0.735	6.42	8
0.731	0.724	0.722	0.726	0.005	0.668	5.83	10

Continuation of Table 3.5.9…

Table 3.5.9: Rate of starch hydrolysis with amylase from culture supernatant diluted in 0.1 M Triethanolacetate (TEA) buffer at pH 8.5

A_{580}	A_{580}	A_{580}	average	standard deviation	blank corrected	[starch]	Time
0.933	0.943	0.944	0.940	0.006	0.882	7.70	0
0.924	0.928	0.924	0.925	0.002	0.867	7.57	2
0.873	0.872	0.874	0.873	0.001	0.815	7.11	4
0.829	0.828	0.832	0.830	0.002	0.772	6.73	6
0.783	0.777	0.778	0.779	0.003	0.721	6.29	8
0.743	0.747	0.742	0.744	0.003	0.686	5.99	10
A_{580}	A_{580}	A_{580}	average	standard deviation	blank corrected	[starch]	Time
0.942	0.94	0.943	0.942	0.002	0.884	7.71	0
0.885	0.884	0.88	0.883	0.003	0.825	7.20	2
0.846	0.852	0.843	0.847	0.005	0.789	6.88	4
0.815	0.816	0.813	0.815	0.002	0.757	6.60	6
0.785	0.783	0.779	0.782	0.003	0.724	6.32	8
0.724	0.722	0.719	0.722	0.003	0.664	5.79	10

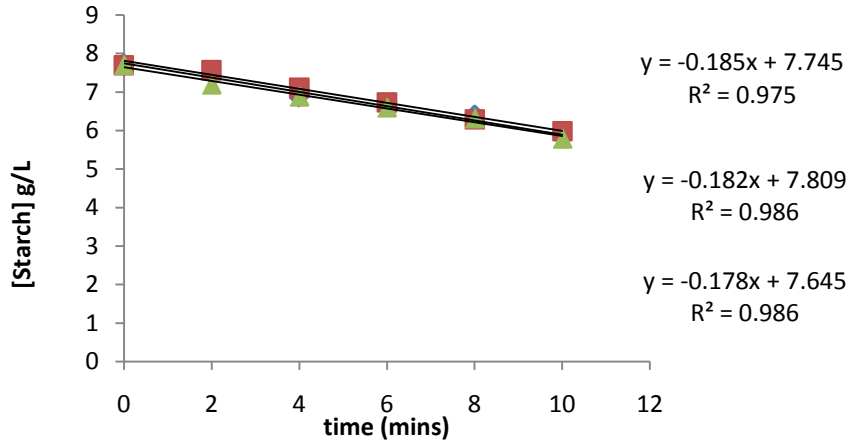

Figure 3.5.5: Rate of starch hydrolysis obtained with Tris buffer solution (day 2).

Table 3.5.10: Amylase activity of culture supernatant diluted in 0.1 M TEA buffer at pH 8.5 (day 0)

Rate of starch hydrolysis	Dilution factor	Amylase activity(g/L/min)
0.1853	100	18.53
0.1822	100	18.22
0.1788	100	17.88
Average amylase activity		18.21 ± 0.33